

Performance Analysis of Type-1 and Type-2 FLC based Shunt Active Filter Control Strategies for Power Quality Improvement

Ph.D. thesis submitted in partial fulfillment of the requirements for the degree of

Doctor of Philosophy
in
Electrical Engineering

Submitted by

Suresh Mikkili

Roll No: 510EE101

Under the Supervision of

Prof. Anup Kumar Panda



**Department of Electrical Engineering
National Institute of Technology, Rourkela**

July 2013

Performance Analysis of Type-1 and Type-2 FLC based Shunt Active Filter Control Strategies for Power Quality Improvement

Suresh Mikkili

Department of Electrical Engineering

National Institute of Technology, Rourkela.

Performance Analysis of Type-1 and Type-2 FLC based Shunt Active Filter Control Strategies for Power Quality Improvement

Ph.D. thesis submitted in partial fulfillment of the requirements for the degree of

Doctor of Philosophy
in
Electrical Engineering

Submitted by

Suresh Mikkili

Roll No: 510EE101

Under the Supervision of

Prof. Anup Kumar Panda

Professor



**Department of Electrical Engineering
National Institute of Technology, Rourkela**

July 2013

Declaration

I hereby declare that the work which is being presented in the thesis entitled, **“Performance Analysis of Type-1 and Type-2 FLC based Shunt Active Filter Control Strategies for Power Quality Improvement,”** in partial fulfillment of the requirements for the award of the degree of **DOCTOR OF PHILOSOPHY** submitted in the Department of Electrical Engineering of National Institute of Technology, Rourkela, is an authentic record of my own work under the supervision of Prof. Anup Kumar Panda, Department of Electrical Engineering. I have not submitted the matter embodied in this thesis for the award of any other degree or diploma of the university or any other institute.

Date: 08th July, 2013

Suresh Mikkili

Dedicated

To

All My Family Members

and

Well-Wishers

...Suresh Mikkili



DEPARTMENT OF ELECTRICAL ENGINEERING
NATIONAL INSTITUTE OF TECHNOLOGY, ROURKELA
ORISSA, INDIA – 769008

CERTIFICATE

This is to certify that the thesis titled “**Performance Analysis of Type-1 and Type-2 FLC based Shunt Active Filter Control Strategies for Power Quality Improvement,**” submitted to the National Institute of Technology, Rourkela by **Mr. Suresh Mikkili**, Roll No. **510EE101** for the award of **Doctor of Philosophy** in Electrical Engineering, is a bonafide record of research work carried-out by him under my supervision and guidance.

The candidate has fulfilled all the prescribed requirements.

The Thesis which is based on candidates own work, has not submitted elsewhere for a degree/diploma.

In my opinion, the thesis is of standard required for the award of a **Doctor of Philosophy** degree in **Electrical Engineering**.

ROURKELA

Prof. Anup Kumar Panda

Professor,

Department of Electrical Engineering,

National Institute of Technology,

Rourkela, India, 769008.

Email: akpanda@nitrkl.ac.in

BIO-DATA OF THE CANDIDATE

Name : Suresh Mikkili

Date of Birth : 05th August 1985

Permanent Address : S/O Kantha Rao,
Gudipudi (Post),
Bapatla (Mandal),
Guntur (District),
Andhra Pradesh - 522310, India.

Email : msuresh.ee@gmail.com,
mikkili.suresh@nitgoa.ac.in

ACADEMIC QUALIFICATION:

- ↻ Pursuing **Ph. D** in Electrical Engineering, National Institute of Technology, Rourkela.
- ↻ **M.Tech** in Electrical Engineering, National Institute of Technology, Rourkela.
- ↻ **B.Tech** in Electrical and Electronics Engineering (EEE) from S.I.T.E Tadepalligudem, JNTU, Andhra Pradesh.

PUBLICATIONS

JOURNALS: - 10 - Articles published in International Journals

- 1) Suresh Mikkili, Anup Kumar Panda, “Types-1 and -2 Fuzzy logic controllers-based shunt active filter I_d - I_q control strategy with different Fuzzy membership functions for power quality improvement using RTDS hardware,” **IET Power Electronics**, Vol. 6, Issue 4, pp. 818 – 833, **April 2013**.

- 2) Anup Kumar Panda, Suresh Mikkili, “FLC based shunt active filter control strategies for mitigation of harmonics with different Fuzzy MFs using MATLAB and real-time digital simulator,” **International Journal of Electrical Power and Energy Systems – Elsevier**, vol. 47, pp. 313-336, **May 2013**.
- 3) Suresh Mikkili, Anup Kumar Panda, “Performance analysis and real-time implementation of shunt active filter current control strategy with type-1 and type-2 FLC triangular M.F,” **International Transactions on Electrical Energy Systems - John Wiley & Sons Ltd**, DOI: 10.1002/etep.1698, **2013**.
- 4) Suresh Mikkili, Anup Kumar Panda, “Real-time implementation of PI and Fuzzy logic controllers based shunt active filter control strategies for power quality improvement,” **International Journal of Electrical Power and Energy Systems – Elsevier**, vol. 43, pp. 1114-1126, **Dec. 2012**.
- 5) Suresh Mikkili, Anup Kumar Panda, “RTDS hardware implementation and simulation of SHAF for mitigation of harmonics using p-q control strategy with PI and Fuzzy logic controllers,” **Frontiers of Electrical and Electronic Engineering– Springer**, Vol. 7, No.4, pp. 427–437, **Dec. 2012**.
- 6) Suresh Mikkili, A. K. Panda, “Simulation and real-time implementation of shunt active filter I_d - I_q control strategy for mitigation of harmonics with different Fuzzy membership functions,” **IET Power Electronics**, Vol. 5, No. 9, pp.1856 – 1872, **Nov. 2012**.
- 7) Anup Kumar Panda, Suresh Mikkili, “Fuzzy logic controller based Shunt Active Filter control strategies for Power quality improvement using different Fuzzy M.F.s,” **International Journal of Emerging Electric Power Systems: be press (Berkeley Electronics press)**, Vol. 13: Issue. 05, Article 2, **Nov. 2012**
- 8) Suresh Mikkili, Anup Kumar Panda, “Real-Time Implementation of Shunt Active Filter P-Q Control Strategy for Mitigation of Harmonics with different Fuzzy M.F.s,” **Journal**

of power Electronics (JPE) (KIPE- South Korea), Vol. 12, No. 5, , pp.821-829, Sept. 2012.

- 9) Suresh Mikkili, Anup Kumar Panda, "PI and Fuzzy Logic Controller based 3-Phase 4-Wire Shunt Active Filters for the Mitigation of Current Harmonics with the I_d - I_q Control Strategy," **Journal of power Electronics (JPE) (KIPE- South Korea)**, Vol. 11, No. 6, pp. 914-921, **Nov. 2011.**
- 10) Suresh Mikkili, Anup Kumar Panda, "RTDS Hardware implementation and Simulation of 3-ph 4-wire SHAF for Mitigation of Current Harmonics with p-q and I_d - I_q Control strategies using Fuzzy Logic Controller," **International Journal of Emerging Electric Power Systems: be press (Berkeley Electronics press)**, Vol. 12: No. 5, **Aug. 2011.**

CONFERENCES: - 10 Articles presented in International Conferences

(IEEE & IET)

- 11) Suresh Mikkili, Anup Kumar Panda, "Real-time implementation of power theory using FLC based shunt active filter with different Fuzzy M.F.s," **IECON 2012 - 38th Annual Conference on IEEE Industrial Electronics Society , Montreal, QC, Canada**, pp. 702 – 707, DOI : 10.1109/IECON.2012.6388666, **25-28 Oct. 2012.**
- 12) Suresh Mikkili, Anup Kumar Panda, "Fuzzy logic controller based 3-ph 4-wire SHAF for current harmonics compensation with I_d - I_q control strategy using simulation and RTDS hardware," **IEEE PEDS Singapore**, pp. 430-435, DOI: 10.1109/PEDS.2011.6147284, **07-10 Dec 2011.**
- 13) Mikkili Suresh, Anup Kumar Panda, S. S. Patnaik, S. Yellasiri, "Comparison of two compensation control strategies for shunt active power filter in three-phase four-wire system," **IEEE PES Innovative Smart Grid Technologies (ISGT), Hilton Anaheim, CA, USA**, pp.1-6, DOI:10.1109/ISGT.2011.5759126, **17 - 19 Jan. 2011.**

- 14) Suresh Mikkili, Anup Kumar Panda, "Type-1 and Type-2 FLC based Shunt active filter I_d - I_q control strategy for mitigation of harmonics with Triangular MF," **IEEE PEDES CPRI/IISC-Bangalore**, pp.1–6, DOI: 10.1109/PEDES.2012.6484308, **Dec. 16-19, 2012.**
- 15) Suresh Mikkili, Anup Kumar Panda, "Mitigation of Harmonics using Fuzzy Logic Controlled Shunt Active Power Filter with different Membership Functions by Instantaneous Power Theory," **IEEE SCES, MNNIT-ALLAHABAD**, pp.1–6, DOI: 10.1109/SCES.2012.6199103, **16-18, Marh 2012.**
- 16) Suresh Mikkili, Anup Kumar Panda, "PI controller based shunt active filter for mitigation of current harmonics with p-q control strategy using simulation and RTDS hardware," **IEEE-INDICON, BITS-PILANI HYD**, pp. 1-6, DOI: 10.1109/INDCON.2011.6139547, **16-18 Dec. 2011.**
- 17) Suresh Mikkili, Anup Kumar Panda, "Fuzzy logic controller based SHAF for current harmonics compensation with p-q control strategy using simulation and RTDS hardware," **IEEE - INDICON, BITS-PILANI HYD**, pp. 1-6, DOI: 10.1109/INDCON.2011.6139546, **16-18 Dec. 2011.**
- 18) Suresh Mikkili, Anup Kumar Panda, "Simulation and RTDS Hardware implementation of SHAF for current harmonics cancellation using I_d - I_q control strategy with PI and Fuzzy controllers," **IEEE ICPS- IIT MADRAS**, pp. 1-6, DOI: 10.1109/ICPES.2011.6156669, **20-24 Dec 2011.**
- 19) Suresh Mikkili, Anup Kumar Panda, " I_d - I_q control strategy for mitigation of current harmonics with PI and Fuzzy controllers," **IEEE ICPS - IIT-MADRAS**, pp. 1-6, DOI:10.1109/ICPES.2011.6156668, **20-24 Dec 2011.**
- 20) Suresh Mikkili, Anup Kumar Panda, "PI and Fuzzy controller based 3-ph 4-wire SHAF for current harmonics compensation using p-q control strategy," **IET-SEISCON**, pp. 299 – 303, DOI: 10.1049/cp.2011.0378, **20-22 July 2011.**

ACKNOWLEDGEMENT

It has been a pleasure for me to work on this dissertation. I hope the **reader** will find it not only interesting and useful, but also comfortable to read.

The research reported here has been carried out in the **Dept. of Electrical Engineering, National Institute of Technology Rourkela at the Power Electronics and Drives Laboratory**. I am greatly indebted to many persons for helping me complete this dissertation.

First and foremost, I would like to express my sense of gratitude and indebtedness to my supervisor **Prof. Anup Kumar Panda**, Professor, Department of Electrical Engineering, for his inspiring guidance, encouragement, and untiring effort throughout the course of this work. His timely help and painstaking efforts made it possible to present the work contained in this thesis. I consider myself fortunate to have worked under his guidance. Also, I am indebted to him for providing all official and laboratory facilities.

I express my heartfelt thanks to the **International Journal Reviewers** for giving their valuable comments on the published papers in different international journals, which helps to carry the research work in a right direction. I also thank to the **International Conference Organizers** for intensely reviewing the published papers.

I am grateful to my Doctoral Scrutiny Members, **Prof. K. B. Mohanty, Prof. U. C. Pati** and **Prof. G. K. Panda**, for their valuable suggestions and comments during this research work.

I am especially indebted to my colleagues in the power electronics group. First, I would like to thank Mr. **Y. Suresh**, who helped me in my research work. We shared each other a lot of knowledge in the field of power electronics. I would also like to thank other members of P.E Lab, Mr. **M. Mahesh**, Mr. **T. Ramesh** and Ms. **S. S. Patnaik** for extending their

technical and personal support. It has been a great pleasure to work with such a helpful, hardworking, and creative group. I would also thank my friends **Mr. N. Rajendra Prasad** and **Mr. G. Kiran Kumar** for their valuable thoughts in my research and personal career.

This section would remain incomplete if I don't thank the lab assistant **Mr. Rabindra Nayak** without him the work would have not progressed.

I express my deep sense of gratitude and reverence to my beloved father **Sri. KanthaRao**, Mother **Smt. Suvarna Pushpa**, my brother **Mr. Seshu babu** and my sister **Ms. Sowjanya** who supported and encouraged me all the time, no matter what difficulties I encountered. I would like to express my greatest admiration to **all my family members** and **relatives** for their positive encouragement that they showered on me throughout this research work. Without my family's sacrifice and support, this research work would not have been possible.

It is a great pleasure for me to acknowledge and express my appreciation to all **my well wishers** for their understanding, relentless supports, and encouragement during my research work. Last but not the least; I wish to express my sincere thanks to all those who helped me directly or indirectly at various stages of this work.

Above all, I would like to thank **The Almighty God** for the wisdom and perseverance that he has been bestowed upon me during this research work, and indeed, throughout my life.

Suresh Mikkili

CONTENTS

CHAPTER	TITLE	PAGE No.
	Abbreviations	vii
	Notations	x
	Abstract	xii
	List of Figures	xiv
	List of Tables	xxvi
CHAPTER -1		
Introduction		
CHAPTER -1	1.1 Research background	01
	1.2 Introduction to APF Technology	03
	1.3 Power Quality Issues	06
	<i>1.3.1 Main causes of poor Power Quality</i>	07
	<i>1.3.2 Power Quality Problems</i>	07
	1.3 Solutions For Mitigation of Harmonics	11
	<i>1.4.1 Classification of power filters</i>	12
	1.4.1.1 Passive Filters	13
	1.4.1.2 Active Filters	14
	1.4.1.3 Hybrid Filters	14
	<i>1.4.2 Active filters applications depending on PQ issues</i>	14
	<i>1.4.3 Selection of Power Filters</i>	15
1.5 Categorization of Active Power Filter	16	
<i>1.5.1 Converter based Categorization</i>	16	
<i>1.5.2 Topology based Categorization</i>	17	
<i>1.5.3 Supply System based Categorization</i>	19	
1.5.3.1 Two-Wire APFs	20	
1.5.3.2 Three-Wire APFs	20	
1.5.3.3 Four-Wire APFs	21	

	1.6 Selection considerations of APFs	23
	1.7 Technical and Economic considerations	24
	1.8 Introduction to Active Power Filter Control Strategies	25
	1.9 Motivation	28
	1.10 Dissertation Objectives	31
	1.11 Dissertation Structure	32
CHAPTER -2		
Shunt Active Filter Control Strategies and its Performance Analysis Using PI Controller		
CHAPTER -2	2.1 shunt active filter basic compensation principle	35
	2.2 Active Power Filter control strategies	37
	2.2.1 <i>Signal Conditioning</i>	38
	2.2.2. <i>Derivation of Compensating Signals</i>	38
	2.2.2.1 Compensation in Frequency Domain	40
	2.2.2.2 Compensation in Time Domain	40
	2.2.2.2.1 <i>Instantaneous Active and Reactive Power (P-Q) Control Strategy</i>	40
	2.2.2.2.2 <i>Instantaneous Active and Reactive Current (I_d-I_q) Control Strategy</i>	46
	2.2.3 <i>Current Control Techniques for derivation of Gating Signals</i>	50
	2.2.3.1 Generation of Gating Signals to the devices of the APF	51
	2.2.3.1.1 <i>Hysteresis Current Control Scheme</i>	51
	2.3 Introduction to Dc Link Voltage Regulation	54
	2.3.1. <i>Dc Link Voltage Regulation with PI Controller</i>	55
	2.4. System performance of p-q and I_d - I_q control strategies with PI controller using MATLAB.	56
	2.5 System performance of p-q and I_d - I_q control strategies with PI controller using Real-time digital simulator.	59

	2.6 Summary	63
CHAPTER -3		
Performance analysis of Shunt active filter control strategies using Type-1 FLC with different Fuzzy MFs		
CHAPTER -3	3.1. Type-1 Fuzzy logic controller	64
	3.1.1. Fuzzification	65
	3.1.2. Fuzzy Inference Systems	66
	3.1.2.1 Mamdani Max-min composition scheme	67
	3.1.2.2 Mamdani Max-prod composition scheme	68
	3.1.3. De-fuzzification	69
	3.1.3.1. Centroid of Area	70
	3.1.3.2. Bisector of Area	71
	3.1.3.3. Mean, Smallest, and Largest of Maximum	71
	3.1.4. Design of control rules:	71
	3.1.4.1. Trapezoidal membership function	72
	3.1.4.2. Triangular membership function	75
	3.1.4.3. Gaussian membership function	77
	3.1.5. Rule Base	78
	3.2. System Performance of Type-1 FLC based P-Q Control Strategy with different Fuzzy MFs using MATLAB	82
	3.3. System Performance of Type-1 FLC based I_d - I_q Control Strategy with different Fuzzy MFs using MATLAB.	86
	3.4. System Performance of Type-1 FLC based p-q Control Strategy with different Fuzzy MFs using Real-Time Digital Simulator	90
	3.5. System Performance of Type-1 FLC based I_d - I_q Control Strategy with different Fuzzy MFs using Real-Time Digital Simulator	94
	3.6. Comparative study	97
	3.7. Summary	101

CHAPTER -4		
Performance analysis of Shunt active filter control strategies using Type-2 FLC with different Fuzzy MFs		
CHAPTER -4	4.1 Introduction to Type-2 FLC	102
	<i>4.1.1 Why type-2 FLCs</i>	104
	4.2 The structure of Type-2 FLC	105
	4.3 Type-2 Fuzzy inference system with different Fuzzy MFs	108
	4.4 System Performance of Type-2 FLC based P-Q Control Strategy with different Fuzzy MFs using MATLAB	112
	4.5 System Performance of Type-2 FLC based I_d - I_q Control Strategy with different Fuzzy MFs using MATLAB	115
	4.6 Comparative Study	119
4.7 Summary	120	
CHAPTER -5		
RT-LAB and Steps involved for real-time implementation of shunt active filter control strategies		
	5.1 Introduction to RT-LAB	121
	<i>5.1.1 Why using real-time simulation?</i>	122
	<i>5.1.2 What is a real-time simulation?</i>	123
	5.2. Evolution of Real-Time Simulators	123
	5.3. RT-Lab Simulator Architecture	125
	<i>5.3.1. Block Diagram and Schematic Interface</i>	125
	<i>5.3.2 Inputs and Outputs (I/O)</i>	126
	<i>5.3.3 Simulator Configuration</i>	126
	5.4 How RT-LAB Works	127
	<i>5.4.1 Single Target Configuration</i>	128
	<i>5.4.2 Distributed Target Configuration</i>	129
<i>5.4.3 Simulator solvers</i>	130	

	<i>5.4.4 RT-LAB Simulation development Procedure</i>	131
CHAPTER -5	5.5 PCI OP5142 configuration	132
	<i>5.5.1 Key Features</i>	133
	<i>5.5.2 Technical Specifications</i>	137
	<i>5.5.3 Analog conversion interface</i>	137
	5.6 System Performance of Type-2 FLC based P-Q Control Strategy with Different Fuzzy MFs using real-time digital simulator	138
	5.7 System Performance of Type-2 FLC based I_d - I_q Control Strategy with different Fuzzy MFs using real-time digital simulators	142
	5.8 Comparative Study	146
5.9 Summary	147	
	CHAPTER -6 Conclusion and Future Scope	
CHAPTER -6	6.1 Conclusions	148
	6.2 Future Scope	153
	REFERENCES	155
	PUBLICATIONS	171

ABBREVIATIONS

APF	Active Power Filter
APLCs	Active Power Line Conditioners
APQCs	Active Power Quality Conditioners
ASDs	Adjustable Speed Drives
AMD	Advanced Micro Devices
ADC	Analog-to-Digital Converter
ARTEMIS	Advanced Real-Time Electro-Mechanical Transient Simulator
BJT	Bipolar Junction Transistor
BOA	Bisector of Area
COA	Centroid of Area
COTS	Commercial Off The Shelf
SC	Console Subsystem
CSI	Current Source Inverter
CTs	Current Transformers
DSP	Digital Signal Processor
DAC	Digital-to-Analog Converter
EEPROM	Electrically Erasable Programmable Read Only Memory
EMI	Electromagnetic Interference
EMT	Electromagnetic Transient
EMTP-RV	Electro Magnetic Transients Program - Restructured Version
FIS	Fuzzy Inference System
FLC	Fuzzy Logic Controller
FPGA	Field-Programmable Gate Array
FOU	Foot Point of Uncertainty
GTO	Gate-Turn-Off Thyristor
GUI	Graphical User Interface

HDL	Hardware Description Language
HIL	Hardware-In-The-Loop
HVDC	High-Voltage Direct Current
IRPCs	Instantaneous Reactive Power Compensators
p-q theory	Instantaneous Active and Reactive Power Theory
I_d-I_q theory	Instantaneous Active and Reactive Current Theory
IEEE	Institute of Electrical and Electronics Engineers
IGBT	Insulated Gate Bipolar Transistor
INTEL	Integrated Electronics
JTAG	Joint Test Action Group
LOM	Largest (Absolute) Value of Maximum
LMF	Lower Membership Function
SM	Master Subsystem
MATLAB	Matrix Laboratory
MOM	Mean Value of Maximum
MFs	Membership Functions
MOSFET	Metal-Oxide Semiconductor Field Effect Transistor
NB	Negative Big
NM	Negative Medium
NS	Negative Small
PCI-Express	Peripheral Component Interconnect - Express
PB	Positive Big
PM	Positive Medium
PS	Positive Small
PTs	Potential Transformers
PE	Power Electronics
PQ	Power Quality

PSB	Power System Block Set
PSCAD	Power Systems Computer Aided Design
PSS/E	Power System Simulator For Engineering
PI	Proportional Integral
PLCs	Programmable Logic Controllers
PWM	Pulse Width Modulation
RTOS	Real-Time Operating System
RTSI	Real-Time System Integration
RTW	Real-Time Workshop
SHAF	Shunt Active Filter
SS	Slave Subsystem
SOM	Smallest (Absolute) Value of Maximum
SIT	Static Induction Thyristor
SRF	Synchronous Reference Frame
THD	Total Harmonic Distortion
TCP/IP	Transmission Control Protocol / Internet Protocol
TNAs	Transient Network Analysers
Type-1 FLC	Type-1 Fuzzy Logic Controller (T1FLC)
Type-2 FLC	Type-2 Fuzzy Logic Controller (T2FLC)
UMF	Upper Membership Function
UPQC	Unified Power Quality Conditioners
UPS	Un-interruptible Power Supply
VSI	Voltage Source Inverter
ZE	Zero

NOTATIONS

A	Fuzzy set
\tilde{A}	Type-2 Fuzzy set
c	Centre
E	Error
ΔE	Change in Error
i_c	Compensation/Filter current
i_{ca}, i_{cb} and i_{cc}	Compensation/Filter currents of phase A, B and C
i_{cn}	Compensation/Filter current of neutral
i_{ca}^*, i_{cb}^* and i_{cc}^*	Reference current of phase A, B and C
$i_{c\alpha ref}$ (or) $i_{c\alpha}^*$	α - axis Reference current
$i_{c\beta ref}$ (or) $i_{c\beta}^*$	β - axis Reference current
i_{c0ref}	0- axis Reference current
i_l	Load current
i_{la}, i_{lb} and i_{lc}	Load current of phase A, B and C
i_{ln}	Load current of neutral
i_{ld}	d- axis load current
i_{lq}	q- axis load current
$i_{l\alpha}$	α - axis load current
$i_{l\beta}$	β - axis load current
i_s	Source current
i_{sa}, i_{sb} and i_{sc}	Source current of phase A, B and C

i_{sn}	Source current of neutral
i_0	Zero- axis load current
i_{0p} and i_{0q}	Instantaneous zero-sequence active and reactive current
$i_{\alpha p}$ and $i_{\alpha q}$	Instantaneous active and reactive current on α -axis
$i_{\beta p}$ and $i_{\beta q}$	Instantaneous active and reactive current on β -axis
m	Fuzzification factor
P_0	zero-sequence instantaneous real power
$P_{\alpha\beta}$	Instantaneous real power due to '+ve and '-ve sequence components
i_{Ld1h} and i_{Lq1h}	Fundamental frequency component of i_{id} and i_{iq}
σ	Width
$\mu_A(x)$	Membership function
$\mu_A^{\sim}(x,u)$	Type-2 membership function
V_a, V_b and V_c	Voltages across phase A, B, C to neutral
V_{dc}	Actual DC link voltage
V_{dc-ref}	Reference DC link voltage
V_{dc1} and V_{dc2}	DC link voltages of splitted capacitors 1 and 2
v_{α}	α - axis voltage
v_{β}	β - axis voltage
X	Universe of discourse

ABSTRACT

In recent years electrical power quality has been an important and growing problem because of the proliferation of nonlinear loads such as power electronic converters in typical power distribution systems. Particularly, voltage harmonics and power distribution equipment problems result from current harmonics produced by nonlinear loads. The electronic equipments like; computers, battery chargers, electronic ballasts, variable frequency drives, and switch mode power supplies, generate perilous harmonics and cause enormous economic loss every year. Problems caused by power quality have great adverse economic impact on the utilities and customers. Due to that both power suppliers and power consumers are concerned about the power quality problems and compensation techniques.

Issue of harmonics are of a greater concern to engineers and building designers because harmonics can do more than distort voltage waveforms, they can overheat the building wiring, causes nuisance tripping, overheat transformer units, and cause random end-user equipment failures. Thus power quality (PQ) has become more and more serious with each passing day. As a result active power filter (APF) gains much more attention due to excellent harmonic and reactive power compensation in two-wire (single phase), three-wire (three-phase without neutral), and four-wire (three-phase with neutral) ac power networks with nonlinear loads. The APF technology has been under research and development for providing compensation for harmonics, reactive power, and/or neutral current in ac networks. Current harmonics are one of the most common power quality problems and are usually resolved by the use of shunt active filters.

In this research work, the performance of the shunt active filter control strategies has been evaluated in terms of harmonic mitigation and DC link voltage regulation. Three-phase reference current waveforms generated by proposed scheme are tracked by the three-phase voltage source converter in a hysteresis band control scheme. This research presents different

topologies and controllers with enhanced performance of shunt active filter for power quality improvement by mitigating the harmonics and maintaining dc link voltage constant.

For extracting the three-phase reference currents for shunt active power filters, we have developed shunt active filter Instantaneous active and reactive power “ $p-q$ ” and Instantaneous active and reactive current “ I_d-I_q ” control strategies. For regulating and maintaining the DC link capacitor voltage constant, the active power flowing into the active filter needs to be controlled. In order to maintain DC link voltage constant and to generate the compensating reference currents, we have developed *PI Controller, Type-1 and Type-2 Fuzzy logic controller with different Fuzzy MFs (Trapezoidal, Triangular and Gaussian)*. The proposed APF is verified through *MATLAB/SIMULINK*. The detailed real-time results using *Real-time digital simulator* are presented to support the feasibility of proposed control strategy.

LIST OF FIGURES

Fig. No.	Title	Page Number
CHAPTER - 1		
Fig. 1.1	Classifications of Power Filters	12
Fig. 1.2	Classifications of Hybrid Filters	13
Fig. 1.3	Current-fed-type APF	17
Fig. 1.4	Voltage-fed-type APF	17
Fig. 1.5	Series-type APF	18
Fig. 1.6	Unified power quality conditioner (UPQC) as universal APF	19
Fig. 1.7	Two-wire shunt APF with current source inverter	20
Fig. 1.8	Three-phase three-wire APF	21
Fig. 1.9	Three-phase four-wire four-pole Shunt APF	22
Fig. 1.10	Three-phase four-wire Capacitor midpoint Shunt APF	23
CHAPTER - 2		
Fig. 2.1	Basic architecture of three-phase four-wire shunt active filter	35
Fig. 2.2	Basic Compensation Principle	36
Fig. 2.3	Compensation Principle of a Shunt Active power filter	36
Fig. 2.4	Reference current extraction with p-q control strategy using PI controller	41
Fig. 2.5	Reference current extraction with p-q control strategy using Fuzzy logic controller	41
Fig. 2.6	Control method for Shunt current compensation based on p-q control strategy.	42
Fig. 2.7	Control method for Shunt current compensation based on I_d - I_q control strategy	46
Fig. 2.8	Instantaneous voltage and current vectors	49

Fig. 2.9	Reference current extraction with I_d - I_q control strategy with PI controller	49
Fig. 2.10	Reference current extraction with I_d - I_q control strategy with Fuzzy logic controller	50
Fig. 2.11	(a) Details of voltage and current wave with hysteresis band current controller.	52
	(b) Details of hysteresis band current controller	52
	(c) Typical Hysteresis Current Controller	53
Fig. 2.12	Conventional PI Controller	55
Fig. 2.13	SHAF response using p-q control strategy with PI controller using MATLAB under (a) <i>Balanced Sinusoidal</i> (b) <i>Un-balanced and</i> (c) <i>Non-Sinusoidal</i> .	57
	(i) Source Voltage (ii) Load Current (iii) Compensation current (iv) Source Current with filter (v) DC Link Voltage (vi) THD of Source current	
Fig. 2.14	SHAF response using I_d - I_q control strategy with PI controller using MATLAB under (a) <i>Balanced Sinusoidal</i> (b) <i>Un-balanced and</i> (c) <i>Non-Sinusoidal</i> .	58
	(i) Source Voltage (ii) Load Current (iii) Compensation current (iv) Source Current with filter (v) DC Link Voltage (vi) THD of Source current	
Fig. 2.15	Real-time implementation of Shunt active filter control strategies using OPAL – RT	59
Fig. 2.16	SHAF response using p-q control strategy with PI controller using Real-time digital simulator under (a) <i>Balanced Sinusoidal</i> (b) <i>Un-balanced and</i> (c) <i>Non-Sinusoidal</i> .	60
	(i) Source Voltage (ii) Load Current (Scale 20A/div) (iii) Compensation current (Scale 20A/div) (iv) Source Current (Scale 30A/div) with filter (v) DC Link Voltage (vi) THD of Source current	
Fig. 2.17	SHAF response using I_d - I_q control strategy with PI controller using Real-time digital simulator under (a) <i>Balanced Sinusoidal</i> (b) <i>Un-balanced and</i> (c) <i>Non-Sinusoidal</i> .	61
	(i) Source Voltage (ii) Load Current (Scale 20A/div) (iii) Compensation current (Scale 20A/div) (iv) Source Current (Scale 30A/div) with filter (v) DC	

	Link Voltage (vi) THD of Source current	
Fig. 2.18	THD of Source Current for p-q and I_d - I_q control strategies with PI Controller Using MATLAB and Real-time digital simulator	62
CHAPTER - 3		
Fig. 3.1	Proposed Fuzzy logic Controller	65
Fig. 3.2	Block Diagram of Fuzzy Logic Controller (FLC)	66
Fig. 3.3	Block diagram of Fuzzy Inference system	67
Fig. 3.4	The Mamdani Fuzzy inference system using max-min composition	68
Fig. 3.5	The Mamdani Fuzzy inference system using max-prod composition	68
Fig. 3.6	Defuzzification	69
Fig. 3.7	Defuzzification methods	70
Fig. 3.8	(a) Trapezoidal MF	73
	(b) Input Variable Error 'E' Trapezoidal MF 3x3	73
	(c) Input Change in Error Normalized Trapezoidal MF 3x3	73
	(d) Output I_{max} Normalized Trapezoidal MF 3x3	73
	(e) Input Variable Error 'E' Trapezoidal MF 5x5	74
	(f) Input Change in Error Normalized Trapezoidal MF 5x5	74
	(g) Output I_{max} Normalized Trapezoidal MF 5x5	74
	(h) Input Variable Error 'E' Trapezoidal MF 7x7	74
	(i) Input Change in Error Normalized Trapezoidal MF 7x7	75
	(j) Output I_{max} Normalized Trapezoidal MF 7x7	75
Fig. 3.9	(a) Triangular MF	76
	(b) Input Variable Error 'E' Triangular MF 7x7	76
	(c) Input Change in Error Normalized Triangular MF 7x7	76
	(d) Output I_{max} Normalized Triangular MF 7x7	76
Fig. 3.10	(a) Gaussian MF	77
	(b) Input Variable Error 'E' Gaussian MF 7x7	77

	(c) Input Change in Error Normalized Gaussian MF 7x7	77
	(d) Output I_{\max} Normalized Gaussian MF 7x7	78
Fig. 3.11	(a) Fuzzy Inference System with Trapezoidal MF 7x7	80
	(b) Fuzzy Inference System with Triangular MF 7x7	81
	(c) Fuzzy Inference System with Gaussian MF 7x7	82
Fig. 3.12	SHAF response using p-q control strategy with Type-1 FLC (Trapezoidal, Triangular and Gaussian MF) under balanced Sinusoidal condition using MATLAB <i>(a) Source Voltage (b) Load Current (c) Compensation current using Trapezoidal MF (d) Source Current with filter using Trapezoidal MF (e) DC Link Voltage using Trapezoidal MF (f) Compensation current using Triangular MF (g) Source Current with filter using Triangular MF (h) DC Link Voltage using Triangular MF (i) Compensation current using Gaussian MF (j) Source Current with filter using Gaussian MF (k) DC Link Voltage using Gaussian MF (l) THD of Source current with Trapezoidal MF (m) THD of Source current with Triangular MF (n) THD of Source current with Gaussian MF</i>	83
Fig. 3.13	SHAF response using p-q control strategy with Type-1 FLC (Trapezoidal, Triangular and Gaussian MF) under un-balanced Sinusoidal condition using MATLAB <i>(a)Source Voltage (b)Load Current (c)Compensation current using Trapezoidal MF (d)Source Current with filter using Trapezoidal MF (e)DC Link Voltage using Trapezoidal MF (f)Compensation current using Triangular MF (g)Source Current with filter using Triangular MF (h)DC Link Voltage using Triangular MF (i)Compensation current using Gaussian MF (j)Source Current with filter using Gaussian MF (k)DC Link Voltage using Gaussian MF (l)THD of Source current with Trapezoidal MF (m)THD of Source current with Triangular MF (n)THD of Source current with Gaussian MF</i>	84
Fig. 3.14	SHAF response using p-q control strategy with Type-1 FLC (Trapezoidal, Triangular and Gaussian MF) under Non-Sinusoidal condition using MATLAB <i>(a)Source Voltage (b)Load Current (c)Compensation current using Trapezoidal MF (d)Source Current with filter using Trapezoidal MF (e)DC Link Voltage using Trapezoidal MF (f)Compensation current using Triangular MF (g)Source Current with filter using Triangular MF (h)DC Link Voltage using Triangular MF (i)Compensation current using Gaussian MF (j)Source Current with filter using Gaussian MF (k)DC Link Voltage using Gaussian MF (l)THD of Source current with Trapezoidal MF (m)THD of Source current with Triangular MF (n)THD of Source current with</i>	85

	<i>Gaussian MF</i>	
Fig. 3.15	<p>SHAF response using I_d-I_q control strategy with Type-1 FLC (Trapezoidal, Triangular and Gaussian MF) under balanced Sinusoidal condition using MATLAB</p> <p>(a)Source Voltage (b)Load Current (c)Compensation current using Trapezoidal MF (d)Source Current with filter using Trapezoidal MF (e)DC Link Voltage using Trapezoidal MF (f)Compensation current using Triangular MF (g)Source Current with filter using Triangular MF (h)DC Link Voltage using Triangular MF (i)Compensation current using Gaussian MF (j)Source Current with filter using Gaussian MF (k)DC Link Voltage using Gaussian MF (l)THD of Source current with Trapezoidal MF (m)THD of Source current with Triangular MF (n)THD of Source current with Gaussian MF</p>	87
Fig. 3.16	<p>SHAF response using I_d-I_q control strategy with Type-1 FLC (Trapezoidal, Triangular and Gaussian MF) under un-balanced Sinusoidal condition using MATLAB</p> <p>(a)Source Voltage (b)Load Current (c)Compensation current using Trapezoidal MF (d)Source Current with filter using Trapezoidal MF (e)DC Link Voltage using Trapezoidal MF (f)Compensation current using Triangular MF (g)Source Current with filter using Triangular MF (h)DC Link Voltage using Triangular MF (i)Compensation current using Gaussian MF (j)Source Current with filter using Gaussian MF (k)DC Link Voltage using Gaussian MF (l)THD of Source current with Trapezoidal MF (m)THD of Source current with Triangular MF (n)THD of Source current with Gaussian MF</p>	88
Fig. 3.17	<p>SHAF response using I_d-I_q control strategy with Type-1 FLC (Trapezoidal, Triangular and Gaussian MF) under Non-Sinusoidal condition using MATLAB</p> <p>(a)Source Voltage (b)Load Current (c)Compensation current using Trapezoidal MF (d)Source Current with filter using Trapezoidal MF (e)DC Link Voltage using Trapezoidal MF (f)Compensation current using Triangular MF (g)Source Current with filter using Triangular MF (h)DC Link Voltage using Triangular MF (i)Compensation current using Gaussian MF (j)Source Current with filter using Gaussian MF (k)DC Link Voltage using Gaussian MF (l)THD of Source current with Trapezoidal MF (m)THD of Source current with Triangular MF (n)THD of Source current with Gaussian MF</p>	89
Fig. 3.18	<p>SHAF response using p-q control strategy with Type-1 FLC (Trapezoidal, Triangular and Gaussian MF) under balanced Sinusoidal condition using real-time digital simulator</p> <p>(a)Source Voltage (b)Load Current (Scale 20A/div) (c)Compensation current (Scale 20A/div) using Trapezoidal MF (d)Source Current (Scale 30A/div) with filter using</p>	91

	<p>Trapezoidal MF (e)DC Link Voltage using Trapezoidal MF (f)Compensation current using Triangular MF (g)Source Current with filter using Triangular MF (h)DC Link Voltage using Triangular MF(i)Compensation current using Gaussian MF (j)Source Current with filter using Gaussian MF (k)DC Link Voltage using Gaussian MF (l)THD of Source current with Trapezoidal MF (m)THD of Source current with Triangular MF (n)THD of Source current with Gaussian MF</p>	
Fig. 3.19	<p>SHAF response using p-q control strategy with Type-1 FLC under un-balanced Sinusoidal condition using real-time digital simulator</p> <p>(a)Source Voltage (b)Load Current (Scale 20A/div) (c)Compensation current (Scale 20A/div) using Trapezoidal MF (d)Source Current (Scale 30A/div) with filter using Trapezoidal MF (e)DC Link Voltage using Trapezoidal MF (f)Compensation current using Triangular MF (g)Source Current with filter using Triangular MF (h)DC Link Voltage using Triangular MF(i)Compensation current using Gaussian MF (j)Source Current with filter using Gaussian MF (k)DC Link Voltage using Gaussian MF (l)THD of Source current with Trapezoidal MF (m)THD of Source current with Triangular MF (n)THD of Source current with Gaussian MF</p>	92
Fig. 3.20	<p>SHAF response using p-q control strategy with Type-1 FLC (Trapezoidal, Triangular and Gaussian MF) under Non-Sinusoidal condition using real-time digital simulator</p> <p>(a)Source Voltage (b)Load Current (Scale 20A/div) (c)Compensation current (Scale 20A/div) using Trapezoidal MF (d)Source Current (Scale 30A/div) with filter using Trapezoidal MF (e)DC Link Voltage using Trapezoidal MF (f)Compensation current using Triangular MF (g)Source Current with filter using Triangular MF (h)DC Link Voltage using Triangular MF(i)Compensation current using Gaussian MF (j)Source Current with filter using Gaussian MF (k)DC Link Voltage using Gaussian MF (l)THD of Source current with Trapezoidal MF (m)THD of Source current with Triangular MF (n)THD of Source current with Gaussian MF</p>	93
Fig. 3.21	<p>SHAF response using I_d-I_q control strategy with Type-1 FLC (Trapezoidal, Triangular and Gaussian MF) under balanced Sinusoidal condition using real-time digital simulator</p> <p>(a)Source Voltage (b)Load Current (Scale 20A/div) (c)Compensation current (Scale 20A/div) using Trapezoidal MF (d)Source Current (Scale 30A/div) with filter using Trapezoidal MF (e)DC Link Voltage using Trapezoidal MF (f)Compensation current using Triangular MF (g)Source Current with filter using Triangular MF (h)DC Link Voltage using Triangular MF(i)Compensation current using Gaussian MF (j)Source Current with filter using Gaussian MF (k)DC Link Voltage using Gaussian MF (l)THD of Source current with Trapezoidal MF (m)THD of Source current with Triangular MF (n)THD of Source current with Gaussian MF</p>	94
Fig. 3.22	<p>SHAF response using I_d-I_q control strategy with Type-1 FLC (Trapezoidal, Triangular and Gaussian MF) under un-balanced</p>	95

	<p>Sinusoidal condition using real-time digital simulator</p> <p>(a)Source Voltage (b)Load Current (Scale 20A/div) (c)Compensation current (Scale 20A/div) using Trapezoidal MF (d)Source Current (Scale 30A/div) with filter using Trapezoidal MF (e)DC Link Voltage using Trapezoidal MF (f)Compensation current using Triangular MF (g)Source Current with filter using Triangular MF (h)DC Link Voltage using Triangular MF(i)Compensation current using Gaussian MF (j)Source Current with filter using Gaussian MF (k)DC Link Voltage using Gaussian MF (l)THD of Source current with Trapezoidal MF (m)THD of Source current with Triangular MF (n)THD of Source current with Gaussian MF</p>	
Fig. 3.23	<p>SHAF response using I_d-I_q control strategy with Type-1 FLC (Trapezoidal, Triangular and Gaussian MF) under Non-Sinusoidal condition using real-time digital simulator</p> <p>(a)Source Voltage (b)Load Current (Scale 20A/div) (c)Compensation current (Scale 20A/div) using Trapezoidal MF (d)Source Current (Scale 30A/div) with filter using Trapezoidal MF (e)DC Link Voltage using Trapezoidal MF (f)Compensation current using Triangular MF (g)Source Current with filter using Triangular MF (h)DC Link Voltage using Triangular MF(i)Compensation current using Gaussian MF (j)Source Current with filter using Gaussian MF (k)DC Link Voltage using Gaussian MF (l)THD of Source current with Trapezoidal MF (m)THD of Source current with Triangular MF (n)THD of Source current with Gaussian MF</p>	96
Fig. 3.24	THD of Source Current for p-q method using PI controller and Type-1 FLC with different Fuzzy MFs using MATLAB	98
Fig. 3.25	THD of Source Current for I_d - I_q method using PI controller and Type-1 FLC with different Fuzzy MFs using MATLAB	98
Fig. 3.26	THD of Source Current for p-q method using PI controller and Type-1 FLC with different Fuzzy MFs using real-time digital simulator	98
Fig. 3.27	THD of Source Current for I_d - I_q method using PI controller and Type-1 FLC with different Fuzzy MFs using real-time digital simulator	99
Fig. 3.28	The amount of THD reduced for PI controller and Type-1 FLC with different Fuzzy MFs using p-q control strategy with MATLAB	99
Fig. 3.29	The amount of THD reduced for PI controller and Type-1 FLC with different Fuzzy MFs using I_d - I_q control strategy with MATLAB	99
Fig. 3.30	The amount of THD reduced for PI controller and Type-1 FLC with different Fuzzy MFs using p-q control strategy with real-time digital simulator	100
Fig. 3.31	The amount of THD reduced for PI controller and Type-1 FLC with	100

	different Fuzzy MFs using I_d - I_q control strategy with real-time digital simulator	
	CHAPTER - 4	
Fig. 4.1	The Architecture of Type 1 FLC	105
Fig. 4.2	The Architecture of Type-2 FLC	105
Fig. 4.3	(a) Membership Function of Type-1 FLC	106
	(b) Membership Function of Type-2 FLC	106
Fig. 4.4	(a) Type-2 Fuzzy Inference System with Trapezoidal MF 7×7	109
	(b) Type-2 Fuzzy Inference System with Triangular MF 7×7	110
	(c) Type-2 Fuzzy Inference System with Gaussian MF 7×7	111
Fig. 4.5	SHAF response using p-q control strategy with Type-2 FLC under balanced Sinusoidal condition using MATLAB <i>(a) Balanced Sinusoidal (b) Un-balanced and (c) Non-Sinusoidal.</i> (i) Source Voltage (ii) Load Current (iii) Compensation current (iv) Source Current with filter (v) DC Link Voltage (vi) THD of Source current	112
Fig. 4.6	SHAF response using p-q control strategy with Type-2 FLC under un-balanced Sinusoidal condition using MATLAB <i>(a) Balanced Sinusoidal (b) Un-balanced and (c) Non-Sinusoidal.</i> (i) Source Voltage (ii) Load Current (iii) Compensation current (iv) Source Current with filter (v) DC Link Voltage (vi) THD of Source current	113
Fig. 4.7	SHAF response using p-q control strategy with Type-2 FLC under Non-Sinusoidal condition using MATLAB <i>(a) Balanced Sinusoidal (b) Un-balanced and (c) Non-Sinusoidal.</i> (i) Source Voltage (ii) Load Current (iii) Compensation current (iv) Source Current with filter (v) DC Link Voltage (vi) THD of Source current	114
Fig. 4.8	SHAF response using I_d - I_q control strategy with Type-2 FLC under balanced Sinusoidal condition using MATLAB <i>(a) Balanced Sinusoidal (b) Un-balanced and (c) Non-Sinusoidal.</i> (i) Source Voltage (ii) Load Current (iii) Compensation current (iv) Source Current with filter (v) DC Link Voltage (vi) THD of Source current	116
Fig. 4.9	SHAF response using I_d - I_q control strategy with Type-2 FLC under Un-balanced Sinusoidal condition using MATLAB	117

	<p><i>(a) Balanced Sinusoidal (b) Un-balanced and (c) Non-Sinusoidal.</i></p> <p>(i) Source Voltage (ii) Load Current (iii) Compensation current (iv) Source Current with filter (v) DC Link Voltage (vi) THD of Source current</p>	
Fig. 4.10	<p>SHAF response using I_d-I_q control strategy with Type-2 FLC under Non-Sinusoidal condition using MATLAB</p> <p><i>(a) Balanced Sinusoidal (b) Un-balanced and (c) Non-Sinusoidal.</i></p> <p>(i) Source Voltage (ii) Load Current (iii) Compensation current (iv) Source Current with filter (v) DC Link Voltage (vi) THD of Source current</p>	118
Fig. 4.11	The Bar Graph indicating the THD of Source Current for p-q control strategy using PI controller, Type-1 FLC and Type-2 FLC with different Fuzzy MFs using MATLAB	119
Fig. 4.12	The Bar Graph indicating the THD of Source Current for I_d - I_q control strategy using PI controller, Type-1 FLC and Type-2 FLC with different Fuzzy MFs using MATLAB	119
CHAPTER - 5		
Fig. 5.1	Evolution of RT-LAB Simulator	124
Fig. 5.2	Speed, Cost and Size of RT-LAB Simulators	125
Fig. 5.3	RT-LAB Simulator Architecture	127
Fig. 5.4	RT-LAB Simulator with Single Target system	128
Fig. 5.5	RT-LAB Simulator with Single Target system and HIL	128
Fig. 5.6	RT-LAB Simulator with Distributed target system	129
Fig. 5.7	RT-LAB Simulator with Distributed target system and HIL	129
Fig. 5.8	OP5142 Layout	133
Fig. 5.9	<p>SHAF response using p-q control strategy with Type-2 FLC (Trapezoidal, Triangular and Gaussian MF) under balanced Sinusoidal condition using real-time digital simulator</p> <p><i>(a)Source Voltage (b)Load Current (Scale 20A/div)(c)Compensation current (Scale 20A/div) using Trapezoidal MF(d)Source Current (Scale 30A/div with filter using Trapezoidal MF (e)DC Link Voltage using Trapezoidal MF (f)Compensation current using Triangular MF (g)Source Current with filter using Triangular MF (h)DC Link Voltage using Triangular MF(i)Compensation current using Gaussian MF (j)Source Current with filter using Gaussian MF (k)DC Link Voltage using Gaussian MF (l)THD of Source current with Trapezoidal MF (m)THD of Source current with Triangular MF</i></p>	139

	<i>(n)THD of Source current with Gaussian MF</i>	
Fig. 5.10	<p>SHAF response using p-q control strategy with Type-2 FLC (Trapezoidal, Triangular and Gaussian MF) under un-balanced Sinusoidal condition using real-time digital simulator</p> <p><i>(a)Source Voltage (b)Load Current (Scale 20A/div) (c)Compensation current (Scale 20A/div) using Trapezoidal MF (d)Source Current (Scale 30A/div) with filter using Trapezoidal MF (e)DC Link Voltage using Trapezoidal MF (f)Compensation current using Triangular MF (g)Source Current with filter using Triangular MF (h)DC Link Voltage using Triangular MF(i)Compensation current using Gaussian MF (j)Source Current with filter using Gaussian MF (k)DC Link Voltage using Gaussian MF (l)THD of Source current with Trapezoidal MF (m)THD of Source current with Triangular MF (n)THD of Source current with Gaussian MF</i></p>	140
Fig. 5.11	<p>SHAF response using p-q control strategy with Type-2 FLC (Trapezoidal, Triangular and Gaussian MF) under Non-Sinusoidal condition using real-time digital simulator</p> <p><i>(a)Source Voltage (b)Load Current (Scale 20A/div) (c)Compensation current (Scale 20A/div) using Trapezoidal MF (d)Source Current (Scale 30A/div) with filter using Trapezoidal MF (e)DC Link Voltage using Trapezoidal MF (f)Compensation current using Triangular MF (g)Source Current with filter using Triangular MF (h)DC Link Voltage using Triangular MF(i)Compensation current using Gaussian MF (j)Source Current with filter using Gaussian MF (k)DC Link Voltage using Gaussian MF (l)THD of Source current with Trapezoidal MF (m)THD of Source current with Triangular MF (n)THD of Source current with Gaussian MF</i></p>	141
Fig. 5.12	<p>SHAF response using I_d-I_q control strategy with Type-2 FLC (Trapezoidal, Triangular and Gaussian MF) under balanced Sinusoidal condition using real-time digital simulator</p> <p><i>(a)Source Voltage (b)Load Current (Scale 20A/div) (c)Compensation current (Scale 20A/div) using Trapezoidal MF (d)Source Current (Scale 30A/div) with filter using Trapezoidal MF (e)DC Link Voltage using Trapezoidal MF (f)Compensation current using Triangular MF (g)Source Current with filter using Triangular MF (h)DC Link Voltage using Triangular MF(i)Compensation current using Gaussian MF (j)Source Current with filter using Gaussian MF (k)DC Link Voltage using Gaussian MF (l)THD of Source current with Trapezoidal MF (m)THD of Source current with Triangular MF (n)THD of Source current with Gaussian MF</i></p>	143
Fig. 5.13	<p>SHAF response using I_d-I_q control strategy with Type-2 FLC (Trapezoidal, Triangular and Gaussian MF) under un-balanced Sinusoidal condition using real-time digital simulator</p> <p><i>(a)Source Voltage (b)Load Current (Scale 20A/div) (c)Compensation current (Scale 20A/div) using Trapezoidal MF (d)Source Current (Scale 30A/div) with filter using</i></p>	144

	<i>Trapezoidal MF (e)DC Link Voltage using Trapezoidal MF (f)Compensation current using Triangular MF (g)Source Current with filter using Triangular MF (h)DC Link Voltage using Triangular MF(i)Compensation current using Gaussian MF (j)Source Current with filter using Gaussian MF (k)DC Link Voltage using Gaussian MF (l)THD of Source current with Trapezoidal MF (m)THD of Source current with Triangular MF (n)THD of Source current with Gaussian MF</i>	
Fig. 5.14	SHAF response using I_d - I_q control strategy with Type-2 FLC (Trapezoidal, Triangular and Gaussian MF) under Non-Sinusoidal condition using real-time digital simulator <i>(a)Source Voltage (b)Load Current (Scale 20A/div) (c)Compensation current (Scale 20A/div) using Trapezoidal MF (d)Source Current (Scale 30A/div) with filter using Trapezoidal MF (e)DC Link Voltage using Trapezoidal MF (f)Compensation current using Triangular MF (g)Source Current with filter using Triangular MF (h)DC Link Voltage using Triangular MF(i)Compensation current using Gaussian MF (j)Source Current with filter using Gaussian MF (k)DC Link Voltage using Gaussian MF (l)THD of Source current with Trapezoidal MF (m)THD of Source current with Triangular MF (n)THD of Source current with Gaussian MF</i>	145
Fig. 5.15	The Bar Graph indicating the THD of Source Current for p-q control strategy using PI controller, Type-1 FLC and Type-2 FLC with different Fuzzy MFs using real-time digital simulator	146
Fig. 5.16	The Bar Graph indicating the THD of Source Current for I_d - I_q control strategy using PI controller, Type-1 FLC and Type-2 FLC with different Fuzzy MFs using real-time digital simulator	146
CHAPTER - 6		
Fig. 6.1	The Line Graph indicating the amount of THD reduced for PI controller, Type-1 FLC and Type-2 FLC with different Fuzzy MFs using p-q control strategy with MATLAB	149
Fig. 6.2	The Line Graph indicating the amount of THD reduced for PI controller, Type-1 FLC and Type-2 FLC with different Fuzzy MFs using I_d - I_q control strategy with MATLAB	149
Fig. 6.3	The Line Graph indicating the amount of THD reduced for PI controller, Type-1 FLC and Type-2 FLC with different Fuzzy MFs using p-q control strategy with Real-time digital simulator	150
Fig. 6.4	The Line Graph indicating the amount of THD reduced for PI controller, Type-1 FLC and Type-2 FLC with different Fuzzy MFs using I_d - I_q control strategy with Real-time digital simulator	150

LIST OF TABLES

Table No.	Title	Page Number
Table 1.1	Description, Causes and Consequences of Power Quality Issues	08
Table 1.2	Active Power Filter Applications depending on PQ issues	15
Table 1.3	Selection of APFs for Specific Application Considerations	24
Table.2.1	Classification of Harmonic Detection methods	39
Table 2.2	System parameters	62
Table 3.1	Rule base 3x3	78
Table 3.2	Rule base 5x5	78
Table 3.3	Rule base 7x7	79
Table 5.1	Description of components in OP5142 Layout (OPAL-RT)	134

Chapter - 1

Introduction

Research background

Introduction to APF Technology

Power Quality Issues

Solutions For Mitigation of Harmonics

Categorization of Active Power Filter

Selection Considerations of APFs

Technical and Economic Considerations

Introduction to Active power filter Control Strategies

Motivation

Dissertation Objectives

Dissertation Structure

CHAPTER – 1

1.1 RESEARCH BACKGROUND

The electronic equipment like; computers, battery chargers, electronic ballasts, variable frequency drives, and switch mode power supplies, generate perilous harmonics and cause enormous economic loss every year. Due to that both power suppliers and power consumers are concerned about the power quality problems and compensation techniques. Harmonics surfaced as a buzz word from 1980's which always threaten the normal operation of power system and user equipment. Issue of Harmonics are of a greater concern to engineers and building designers because harmonics can do more than distort voltage waveforms, they can overheat the building wiring, causes nuisance tripping, overheat transformer units, and cause random end-user equipment failures. Thus power quality (PQ) has become more and more serious with each passing day. As a result, active power filter (APF) gains much more attention due to excellent harmonic and reactive power compensation in two-wire (single phase), three-wire (three-phase without neutral), and four-wire (three-phase with neutral) ac power networks with nonlinear loads.

Active power filters have been under research and development for more than three decades and have found successful industrial applications with varying configurations, control strategies, and solid-state devices. However, this is still a technology under development, and many new contributions and new control topologies have been reported in the last few years. It is aimed at providing a broad perspective on the status of APF technology to researchers and application engineers dealing with power quality issues.

***In this research work,** the performance of the shunt active filter current control strategies has been evaluated in terms of harmonic mitigation and DC link voltage regulation. This research presents different control strategies and controllers with enhanced performance of shunt active filter for power quality improvement by mitigating the harmonics and maintaining DC link*

voltage constant. Three-phase reference current waveforms generated by proposed schemes are tracked by the three-phase voltage source converter in a hysteresis band control scheme.

For extracting the three-phase reference currents for shunt active power filters, we have developed instantaneous active and reactive power “ $p-q$ ” and Instantaneous active and reactive current “ I_d-I_q ” control strategies. For regulating and maintaining the DC link capacitor voltage constant, the active power flowing into the active filter needs to be controlled. In order to maintain DC link voltage constant and to generate the compensating reference currents, we have developed PI, Type-1 and Type-2 Fuzzy logic controllers with different Fuzzy MFs (Trapezoidal, Triangular and Gaussian). The proposed APF is verified through Real-time digital simulator. The detailed real-time results are presented to support the feasibility of proposed control strategies.

When the supply voltages are balanced and sinusoidal, the two control strategies; Instantaneous active and reactive Power ($p-q$) control strategy and Instantaneous active and reactive current (I_d-I_q) control strategy are converging to the same compensation characteristics but, when the supply voltages are distorted and/or un-balanced sinusoidal, these control strategies result in different degrees of compensation in harmonics. The $p-q$ control strategy is unable to yield an adequate solution, when source voltages are not ideal. Under unbalanced/non-sinusoidal condition, $p-q$ control strategy is not succeeded in compensating harmonic currents, notches are observed in the source current. The main reason behind the notches is that the controller failed to track the current correctly and thereby APF fails to compensate completely. So to avoid the difficulties occur with $p-q$ control strategy, we have considered I_d-I_q control strategy.

This chapter is organized as follows: section 1.2 introduces the importance of active power filters and solid state devices, section 1.3 deals with the power quality issues, section 1.4 provides the solutions for mitigation of harmonics, section 1.5 provides the classifications of active power

filter, section 1.6 provides the details of selection considerations of APFs, section 1.7 provides the details of technical and economic considerations, section 1.8 provides the introduction to active power filter control strategies and finally motivation, dissertation objectives and dissertation structure are clearly outlined in section 1.9, 1.10, and section 1.11 respectively.

1.2 INTRODUCTION TO APF TECHNOLOGY

The growing number of power electronics-based equipments has produced significant impact on the quality of electric power supply. Both high power industrial loads and domestic loads cause harmonics [1] in the network voltages. At the same time, much of the equipments causing the disturbances are quite sensitive to deviations from the ideal sinusoidal line voltage. Therefore, power quality problems may originate in the system or may be caused by the consumer itself. Moreover, in the last years the growing concern related to power quality comes from:

- ↳ Consumers that are becoming gradually aware of the power quality issues [2] and being more informed about the consequences of harmonics, interruptions, voltage sags, switching transients, etc. Motivated by deregulation, they are challenging the energy suppliers to improve the quality of the power delivered.
- ↳ The proliferation of load equipment with microprocessor based controllers and power electronic devices which are sensitive to many types of power quality disturbances.
- ↳ Emphasis on increasing overall process productivity, which has led to the installation of high-efficiency equipment, such as adjustable speed drives and power factor correction equipment. This in turn has resulted in an increase in harmonics injected into the power system, causing concern about their impact on the system behavior.

For an increasing number of applications, conventional equipment is proving insufficient for mitigation of power quality problems. Harmonic distortion has traditionally been dealt

with the use of passive LC filters. However, the application of passive filters [3] for harmonic reduction may result in parallel resonances with the network impedance, over compensation of reactive power at fundamental frequency, and poor flexibility for dynamic compensation of different frequency harmonic components.

The increased severity of power quality in power networks has attracted the attention of power engineers to develop dynamic and amendable solutions to the power quality problems. Such equipment, generally known as active power filters [4], are also called active power line conditioners, and are able to compensate current and voltage harmonics, reactive power, regulate terminal voltage, suppress flicker, and to improve voltage balance in three-phase systems. The advantage of active filtering is that it automatically adapts to changes in the network and load fluctuations. They can compensate for several harmonic orders, and are not affected by major changes in network characteristics, eliminating the risk of resonance between the filter and network impedance. Another advantage is that they take up very little space compared with traditional passive compensators.

The demand from the electricity customers for good quality of power supply is ever rising due to the increase of sensitive loads. This is often a stimulating task. Solid state control of ac power using thyristors and other semiconductor switches is widely employed to feed controlled electric power to electrical loads, such as adjustable speed drives (ASDs) [5], furnaces, computer power supplies, etc. Such controllers are also used in HVDC systems and renewable electrical power generation. As non-linear loads, these solid-state converters draw harmonic and reactive power components of current from ac mains. In three-phase systems, they could also cause unbalance and draw excessive neutral currents. The injected harmonics, reactive power burden, unbalance, and excessive neutral currents cause low system efficiency and poor power factor. They also cause disturbance to other consumers and interference in

nearby communication networks. The increased severity of harmonic pollution in power networks has attracted the attention of power electronics and power system engineers to develop dynamic and adjustable solutions to the power quality problems. Such equipment, generally known as active power filters (APFs) [1-65], are also called active power line conditioners (APLCs), instantaneous reactive power compensators (IRPCs), and active power quality conditioners (APQCs). In recent years, many publications have also appeared on harmonics [6-9, 12-16, 26, 47, 50, 60, 65], reactive power, load balancing and neutral current compensation associated with linear and non-linear loads [27, 32, 60].

The active power filter (APF) [1-65] technology has been under research and development for providing compensation for harmonics, reactive power, and/or neutral current in ac networks. APFs are also used to eliminate harmonics, to regulate terminal voltage, to suppress voltage flicker, and to improve voltage balance in three-phase systems. This wide range of objectives is achieved either individually or in combination, depending upon the requirements and control strategy [7, 26, 36, 48, 50, 61, 63, 65] and configuration which have to be selected appropriately.

One of the major factors in advancing the APF technology is the advent of fast self-commutating solid-state devices. In the initial stages, thyristors, bipolar junction transistors (BJTs) [4] and power MOSFETs were used for APF fabrication; later, static induction thyristors (SITs) and gate-turn-off thyristors (GTOs) were employed to develop APFs. With the introduction of insulated gate bipolar transistors (IGBTs), the APF technology got a real enhancement and, at present, they are considered as ideal solid-state devices for APFs. The improved sensor technology has also contributed to the enhanced performance of the APF. The availability of Hall-effect sensors and isolation amplifiers at reasonable cost and with adequate ratings has improved the APF performance.

The next breakthrough in APF development has resulted from the micro-electronics revolution. Starting from the use of discrete analog and digital components [5, 6], the progression has been to micro-processors, micro-controllers, and digital signal processors (DSPs) [6]. Now, it is possible to implement complex algorithms on-line for the control of the APF at reasonable cost. This development has made it possible to use different controllers such as, proportional integral (PI) [7, 26], variable-structure control, Fuzzy logic controller [7, 11-13, 26, 50, 54, 62, 65], and neural networks [15-21] for improving the dynamic and steady-state performance of the APF. With these improvements, the APFs [1-65] are capable of providing fast corrective action, even with dynamically changing non-linear loads.

1.3 POWER QUALITY ISSUES

The Power Quality (PQ) issue is defined as “Any power problem manifested in voltage, current, or frequency deviations those results in damage, upset, failure or mis-operation of customer equipment.” Almost all PQ issues [8] are closely related with power electronics in almost every aspect of commercial, domestic, and industrial application. Equipments using power electronic devise are residential appliances like TVs, PCs etc.; business and office equipment like copiers, printers etc.; industrial equipment like programmable logic controllers (PLCs), adjustable speed drives (ASDs), rectifiers, inverters, CNC tools and etc. The PQ problem can be detected from one of the following several symptoms depending on the type of issue involved.

Power electronics (PE) has three aspects in power distribution:

- (a) Power electronics introduces valuable industrial and domestic equipment;
- (b) Power electronics are the most important cause of harmonics; interharmonics, notches, and neutral currents.
- (c) Power electronics helps to solve those PQ problems.

1.3.1 Main causes of poor Power Quality

The main causes of PQ issues are Non-linear loads, Adjustable-speed drives, Traction drives, Start of large motor loads, Arc furnaces, Intermittent loads transients, Lightning, Switching transients and Faults.

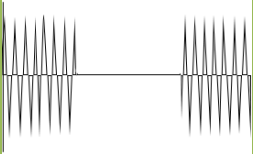
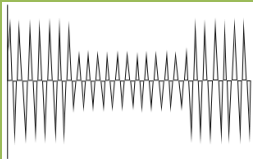
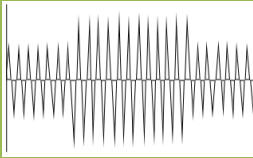
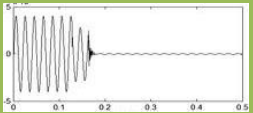
1.3.2 Power Quality Problems

The PQ problems [7] are Short-duration Voltage Variations (Voltage Interruption, Voltage Sag and Voltage Swell); Long-duration Voltage Variations (Under Voltage and Over Voltage); Voltage Flicker; Voltage Notching; Transient Disturbance and Harmonic Distortion. The descriptions, causes and consequences of Power Quality Issues are given in **Table 1.1**.

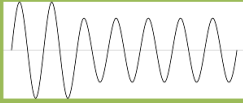
The Harmonics [9] are produced by rectifiers, ASDs, soft starters, electronic ballast for discharge lamps, switched-mode power supplies, and HVAC using ASDs. Equipment affected by harmonics includes transformers, motors, cables, interrupters, and capacitors (resonance). Notches are produced mainly by converters, and they principally affect the electronic control devices. Neutral currents are produced by equipment using switched-mode power supplies, such as PCs, printers, photocopiers, and any triplet's generator. Neutral currents seriously affect the neutral conductor temperature and transformer capability. Inter-harmonics are produced by static frequency converters, cyclo-converters, induction motors & arcing devices.

Equipment presents different levels of sensitivity to PQ issues, depending on the type of both the equipment and the disturbance. Furthermore, the effect on the PQ of electric power systems, due to the presence of PE, depends on the type of PE utilized. The maximum acceptable values of harmonic contamination are specified in IEEE standard in terms of total harmonic distortion (THD).

Table.1.1 Description, Causes and Consequences of Power Quality Issues

Power Quality Issues	Description, Causes and Consequences
<p>Very short Interruptions</p> 	<p>Description: Total interruption of electrical supply for duration from few milliseconds to less than 1 minute.</p> <p>Causes: Caused by mainly due to the opening and automatic reclosure of protection devices to decommission a faulty section of the network. The main fault causes are insulation failure, lightning and insulator flashover.</p> <p>Consequences: Tripping of protection devices, loss of information and malfunction of data processing equipment. Stoppage of sensitive equipment, such as ASDs, PCs, PLCs, if they're not prepared to deal with this situation.</p>
<p>Voltage sag (or dip)</p> 	<p>Description: It is a reduction in the rms voltage in the range of 10% and 90% for duration greater than half a mains cycle and less than 1 minute.</p> <p>Causes: Caused by faults on the transmission or distribution network. Faults in consumer's installation. Connection of increased load demand (heavy loads) and start-up of large motors.</p> <p>Consequences: Malfunction of information technology equipment, namely microprocessor-based control systems (PCs, PLCs, ASDs, etc.) that may lead to a process stoppage. Tripping of contactors and Electro-mechanical relays. Disconnection and loss of efficiency in electric rotating machines.</p>
<p>Voltage swell</p> 	<p>Description: Momentary increase of the voltage, at the power frequency, outside the normal tolerances, with duration of more than one cycle and typically less than a 1 minute.</p> <p>Causes: Caused by Start/stop of heavy loads, badly dimensioned power sources, badly regulated transformers (mainly during off-peak hours), system faults, load switching and capacitor switching.</p> <p>Consequences: Data loss, flickering of lighting and screens, stoppage or damage of sensitive equipment, if the voltage values are too high.</p>
<p>Long interruptions</p> 	<p>Description: Total interruption of electrical supply for duration more than 1 to 2 minutes.</p> <p>Causes: Caused by equipment failure in the power system network, storms and objects (trees, cars, etc.) striking lines or poles, fire, human error, bad coordination or failure of protection devices.</p> <p>Consequences: Stoppage of all the equipment.</p>

Under Voltage

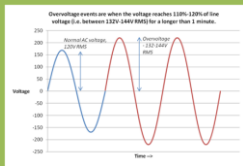


Description: It is a decrease in the rms ac voltage to less than 90% at the power frequency for a duration longer than 1 min.

Causes: Caused by switching on a large load or switching off a large capacitor bank.

Consequences: The flickering of lighting and screens, giving the impression of unsteadiness of visual perception.

Over voltage

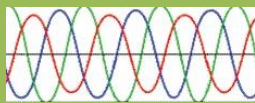


Description: It is an increase in the rms ac voltage to a level greater than 110% at the power frequency for a duration longer than 1 min.

Causes: Caused by switching off a large load or energizing a capacitor bank. Incorrect tap settings on transformers can also cause under voltages and over voltages.

Consequences: The flickering of lighting and screens, stoppage or damage of sensitive equipment, if the voltage values are too high.

Voltage Unbalance

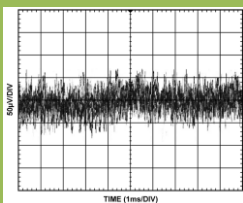


Description: A voltage variation in a three-phase system in which the three voltage magnitudes or the phase angledifferences between them are not equal.

Causes: Large single-phase loads (induction furnaces, traction loads), incorrect distribution of all single-phase loads by the three phases of the system (this may be also due to a fault).

Consequences: Unbalanced systems imply the existence of a negative sequence that is harmful to all three phase loads. The most affected loads are three-phase induction machines.

Noise

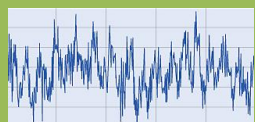


Description: Superimposing of high frequency signals on the waveform of the power-system frequency.

Causes: Electromagnetic interferences provoked by Hertzian waves such as microwaves, television diffusion, and radiation due to welding machines, arc furnaces, and electronic equipment. Improper grounding may also be a cause.

Consequences: Disturbances on sensitive electronic equipment, usually not destructive, data loss and data processing errors.

Voltage Flicker



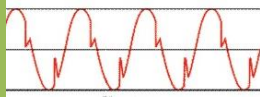
Description: A waveform may exhibit voltage flicker if its amplitude is modulated at frequencies less than 25 Hz, which the human eye can detect as a variation in the lamp intensity of a standard bulb.

Causes: Caused by an arcing condition on the power system, arc furnaces, and frequent start/stop of electric motors and oscillating loads.

Consequences: The flickering of lighting and screens, giving the impression

of unsteadiness of visual perception.

Voltage Notching

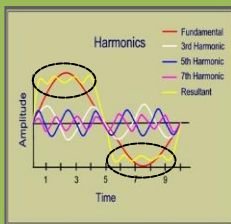


Description: Very fast variation of the voltage value for durations from a several microseconds to few milliseconds. These variations may reach thousands of volts, even in low voltage. It is an effect that can raise PQ issues in any facility where solid-state rectifiers are used.

Causes: Caused by lightning, switching of lines or power factor correction capacitors, disconnection of heavy loads, the commutation of power electronic rectifiers.

Consequences: Destruction of components and of insulation materials, data processing errors or data loss, electromagnetic interference.

Harmonic Distortion



Description: Harmonics are periodic sinusoidal distortions of the supply voltage or load current caused by non-linear loads. Harmonics are measured in integer multiples of the fundamental supply frequency. Voltage or current waveforms assume non-sinusoidal shape.

Classic sources: Electric machines working above the knee of the magnetization curve (magnetic saturation), arcs (Arc furnaces, fluorescent lights), welding machines, rectifiers (Microprocessors, motor drives, any electronic load), and DC brush motors.

Modern sources: all non-linear loads such as power electronics equipment including ASDs, switched mode power supplies, data processing equipment, high efficiency lighting.

Consequences: Transformers to overheat, neutral overload in 3-phase systems, overheating of all cables and equipment, transformer secondary voltage distortion, power system losses to increase, loss of efficiency in electric machines, electro-magnetic interference with communication systems, protective relays to fail, capacitors to explode, increased probability in occurrence of resonance, errors in measures when using average reading meters, nuisance tripping of thermal protections.

Harmonics have frequencies that are integer multiples of the waveform's fundamental frequency. For example, given a 50Hz fundamental waveform, the 2nd, 3rd, 4th and 5th harmonic components will be at 100Hz, 150Hz, 200Hz and 250Hz respectively. Thus, harmonic distortion is the degree to which a waveform deviates from its pure sinusoidal

values as a result of the summation of all these harmonic elements. The ideal sine wave has zero harmonic components. In that case, there is nothing to distort this perfect wave.

Total Harmonic Distortion [10] of a signal is a measurement of the harmonic distortion present and is defined as the ratio of the summation of all harmonic components of the voltage or current waveform compared to the fundamental component of the voltage or current wave. THD [11] of source current is a measure of the effective value of harmonic distortion and can be calculated as per (1.1 and 1.2) in which i_1 is the RMS value of fundamental frequency component of current and i_n represents the RMS value of n^{th} order harmonic component of current as follows:

$$THD = \frac{\sqrt{(i_2^2 + i_3^2 + i_4^2 + \dots + i_n^2)}}{i_1} \quad (1.1)$$

$$THD = \frac{\sqrt{\sum_{n=2}^{\infty} i_n^2}}{i_1} \quad (1.2)$$

1.4 SOLUTIONS FOR MITIGATION OF HARMONICS

There are two methodologies to the mitigation of power quality problems. The first methodology is called load conditioning, which ensures that the equipment is made less sensitive to power disturbances, allowing the operation even under significant voltage distortion. The other methodology is to install line-conditioning systems that suppress or counteract the power system disturbances.

Passive filters have been most commonly used to limit the flow of harmonic currents in distribution systems. They are usually custom designed for the application. However, their performance is restricted to a few harmonics, and they can introduce resonance in the power system. Among the different new technical preferences available to improve power quality, active power filters have proved to be an important and flexible alternative to compensate for

current and voltage disturbances in power distribution systems. The idea of active filters is relatively old, but their practical development was made possible with the new improvements in power electronics and microcomputer control strategies as well as with cost reduction in electronic components. Active power filters [12] are becoming a viable alternative to passive filters and are gaining market share speedily as their cost becomes competitive with the passive variety. Through power electronics, the active filter introduces current or voltage components, which cancel the harmonic components of the nonlinear loads [13] or supply lines, respectively.

1.4.1 Classification of power filters

Classifications of Power Filters [7] and hybrid filters are shown in **Fig 1.1** and **Fig. 1.2**. Power Filters are classified as Passive Filters, Active Filters and Hybrid Filters. Passive and active filters are again categorised as Series Filters (Passive or Active), Shunt Filters (Passive or Active), Combination of Series and Shunt Filters (Passive or Active).

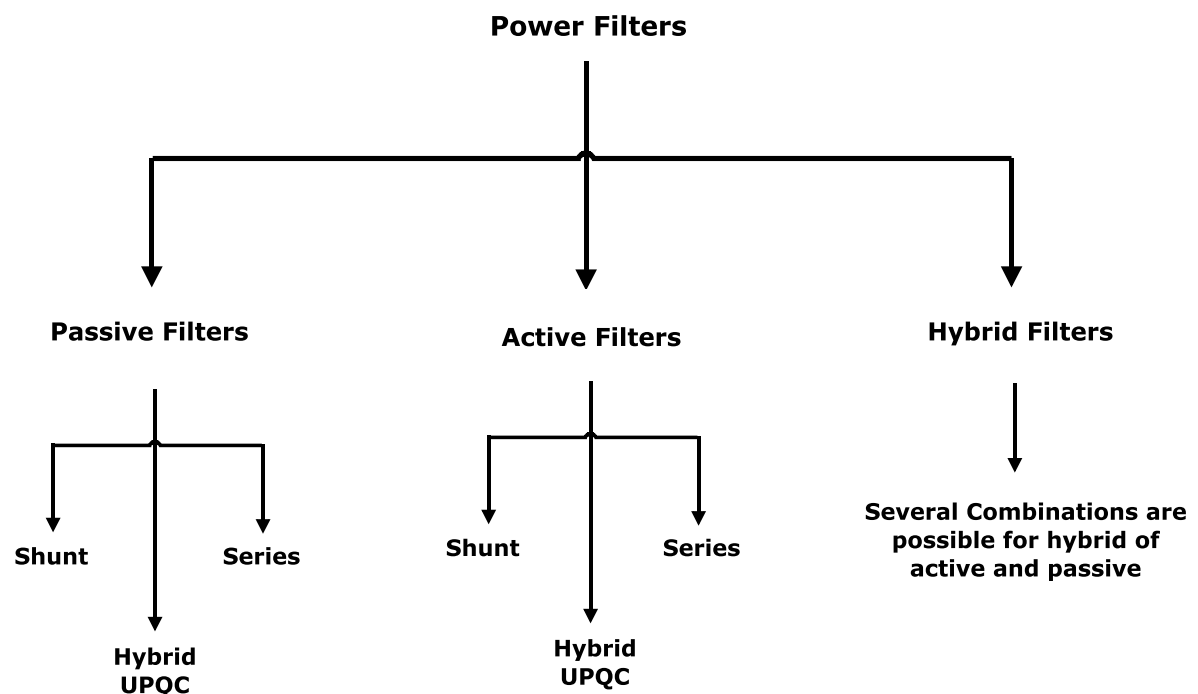


Fig.1.1. Classifications of Power Filters

Hybrid filters are used in single-phase, three-phase three-wire and three-phase four-wire systems and they are classified as Series passive – Shunt Passive filters, Series active – Shunt active filters, Series passive – Shunt active filters and Series active – Shunt passive filters

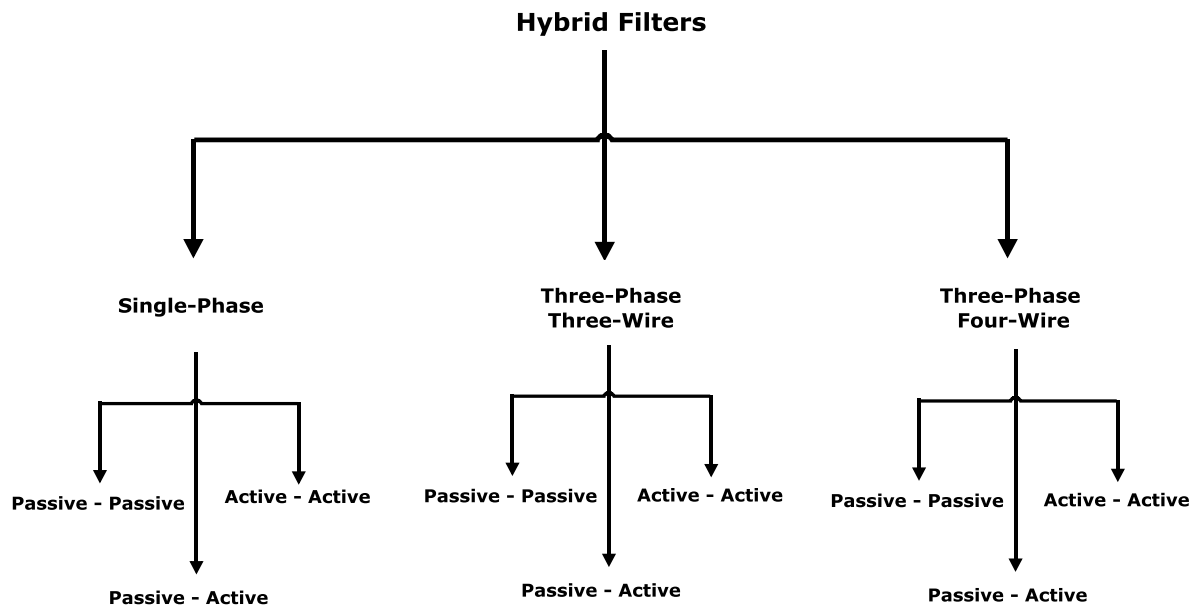


Fig.1.2. Classifications of Hybrid Filters

1.4.1.1 Passive Filters: It Provide a low-impedance path to ground for the harmonic frequencies.

Advantages:

- ✓ Harmonic reduction is possible.
- ✓ Undesirable harmonics are absent.
- ✓ Reactive power compensation is possible.

Disadvantages:

- x Resonance with line impedance occurs.
- x Tuning frequency is less accurate and requires a lot of calculations.
- x It cannot be used when harmonic components vary randomly.
- x Heavy and bulky.

1.4.1.2 Active Filters: It inject equal and opposite harmonics onto the power system to cancel those generated by other equipment [26].

Advantages:

- ✓ Cancel out harmonics.
- ✓ Block resonance.
- ✓ Reactive power management.
- ✓ Small Size.
- ✓ Tuning is easy and accurate.
- ✓ It can be used when harmonic components vary randomly.

Disadvantages:

- x Costly.
- x Chance to develop inherent harmonics (Because of power electronic devices).

1.4.1.3 Hybrid Filters

Advantages:

- ✓ Cancel out both Voltage and current harmonics.
- ✓ Block resonance.
- ✓ Reactive power management.
- ✓ Cheap.

1.4.2 Active filters applications depending on PQ issues

Shunt active filters [7, 9-15, 22, 24, 26, 36, 48, 50, 61] are used for reactive power compensation, voltage regulation, unbalance current compensation (for 3-phase systems), and neutral current compensation (for 3-phase 4-wire systems). **Series active filters** [3, 28, 57] are used for reactive power compensation, voltage regulation, compensation for voltage sag and swell, and unbalance voltage compensation (for 3-phase systems).

Table.1.2 Active Power Filter Applications depending on PQ issues

Active Filter Connection	Load Effect on AC Supply	AC Supply Effect on Load
Shunt Active Filter	<ul style="list-style-type: none"> • Unbalance current compensation • Reactive power compensation • Voltage Regulation • Neutral Current Compensation 	
Series Active Filter	<ul style="list-style-type: none"> • Unbalance voltage compensation • Reactive Power Compensation • Voltage Regulation • Compensation for Voltage sag and Swell 	<ul style="list-style-type: none"> • Voltage sag/swell • Voltage unbalance • Voltage distortion • Voltage interruption • Voltage flicker • Voltage notching
Series-Shunt Active Filter	<ul style="list-style-type: none"> • Unbalance current compensation • Unbalance voltage compensation • Reactive Power Compensation • Voltage Regulation • Compensation for Voltage sag and swell • Neutral Current Compensation 	<ul style="list-style-type: none"> • Voltage sag/swell • Voltage unbalance • Voltage distortions • Voltage interruptions • Voltage flicker • Voltage notching

Series-Shunt Active Filters [8, 17, 54] are used for reactive power compensation, voltage regulation, compensation for voltage sag and swell, unbalance compensation for current and voltage (for 3-phase systems), and neutral current compensation (for 3-phase 4-wire systems). Active filters applications depending on PQ issues are given in **Table. 1.2**

1.4.3 Selection of Power Filters

The selection of power filters [7, 26, 50] is based on the following factors:

- ↳ Nature of Load (Voltage Fed, Current Fed or Mixed).

- ↪ Type of Supply System (single-phase, three-phase three-wire, three-phase four-wire).
- ↪ Pattern of loads (fixed, variable, fluctuating).
- ↪ Compensation required in current (harmonics, reactive power, balancing, neutral current) or voltage (harmonics, flicker, unbalance, regulation, sag, swell, spikes, notches).
- ↪ Level of compensation required (THD, Individual harmonic reduction meeting specific standard, and etc.).
- ↪ Environmental factors (ambient temperature, altitude, pollution, humidity, and etc.).
- ↪ Cost, size, weight.
- ↪ Efficiency.
- ↪ Reliability.

1.5 CATEGORIZATION OF ACTIVE POWER FILTER

APFs can be classified based on converter topology, type, and the number of phases. The topology can be shunt, series, or a combination of both. The converter type can be either CSI or VSI bridge structure. The third classification is based on the number of phases, such as two-wire (single phase) [15, 22, 27] and three or four-wire three-phase systems [23-26, 35-41, 45-50, 61, 63, 71].

1.5.1 Converter based categorization

In the development of APFs [7, 26, 50, 63] two types of converters are used, they are Current-fed-type APF and Voltage-fed-type APF. **Fig. 1.3** shows the current-fed pulse width modulation (PWM) inverter bridge structure. It behaves as a non-sinusoidal current source to meet the harmonic current requirement of the non-linear load. A diode is used in series with the self-commutating device (IGBT) [29] for reverse voltage blocking. However, GTO-based configurations do not need the series diode, but they have restricted frequency of switching.

They are considered sufficiently reliable, but have higher losses and require higher values of parallel ac power capacitors. Moreover, they cannot be used in multilevel or multistep modes to improve performance in higher ratings.

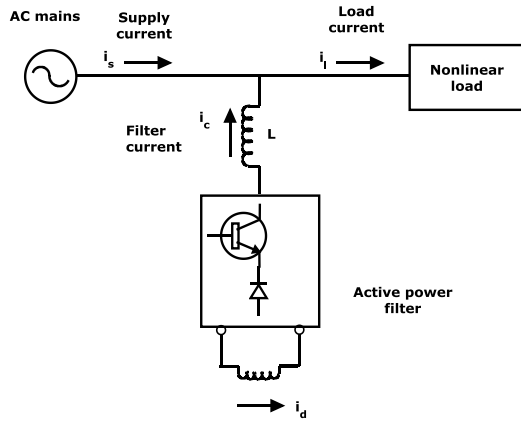


Fig.1.3. Current-fed-type APF

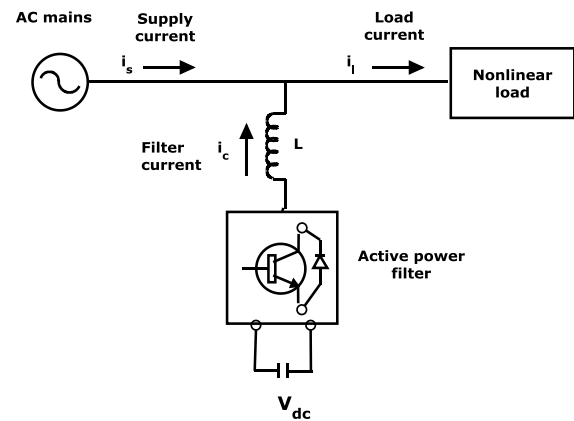


Fig.1.4 Voltage-fed-type APF

The other converter used as an APF is a voltage-fed PWM [57] inverter structure, as shown in **Fig.1.4**. It has a self-supporting dc voltage bus with a large dc capacitor. It has become more dominant, since it is lighter, cheaper, and expandable to multilevel and multistep versions, to enhance the performance with lower switching frequencies. It is more popular in UPS based applications, because in the presence of mains, the same inverter bridge can be used as an APF to eliminate harmonics of critical non-linear loads.

1.5.2 Topology based categorization

APFs can be classified based on the topology [7, 26, 50, 54] used as Series-type APF, Shunt-type APF, Unified power quality conditioners (UPQC) and Hybrid filters. **Fig. 1.5** shows the basic block of a stand-alone series APF [5]. It is connected before the load in series with the mains, using a matching transformer, to eliminate voltage harmonics, and to balance and regulate the terminal voltage of the load or line. It has been used to reduce negative-sequence voltage and regulate the voltage on three-phase systems. It can be installed by

electric utilities to compensate voltage harmonics [26] and to damp out harmonic propagation caused by resonance with line impedances and passive shunt compensators.

Fig.1.3 and **Fig.1.4** are examples of shunt active filter [5, 7, 9, 11-14, 22, 26, 36, 48, 50], which is most widely used to eliminate current harmonics, reactive power compensation, and balancing un-balanced currents. It is mainly used at the load end, because current harmonics are injected by non-linear loads. It injects equal compensating currents, opposite in phase, to cancel harmonics and/or reactive components of the non-linear load current at the point of connection. It can also be used as a static var generator in the power system network for stabilizing and improving the voltage profile [9, 22].

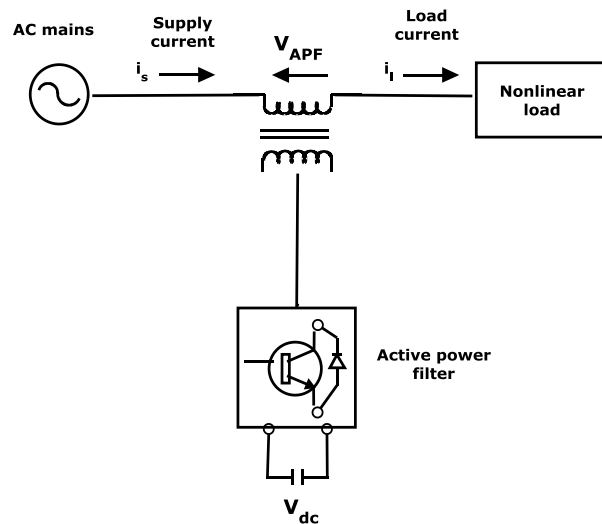


Fig.1.5 Series-type APF

Fig.1.6 shows a unified power quality conditioner [8, 17, 54] (also known as a universal APF), which is a combination of active series and active shunt filters. The dc-link storage element (either inductor or dc-bus capacitor) is shared between two current source or voltage-source bridges operating as active series and active shunt compensators [17]. It is used in single-phase as well as three-phase configurations. It is considered an ideal APF which eliminates voltage and current harmonics and is capable of giving clean power to critical and harmonic-prone loads, such as computers, medical equipment, etc. It can balance and regulate

terminal voltage and eliminate negative-sequence currents. Its main drawbacks are its large cost and control complexity because of the large number of solid-state devices involved [54].

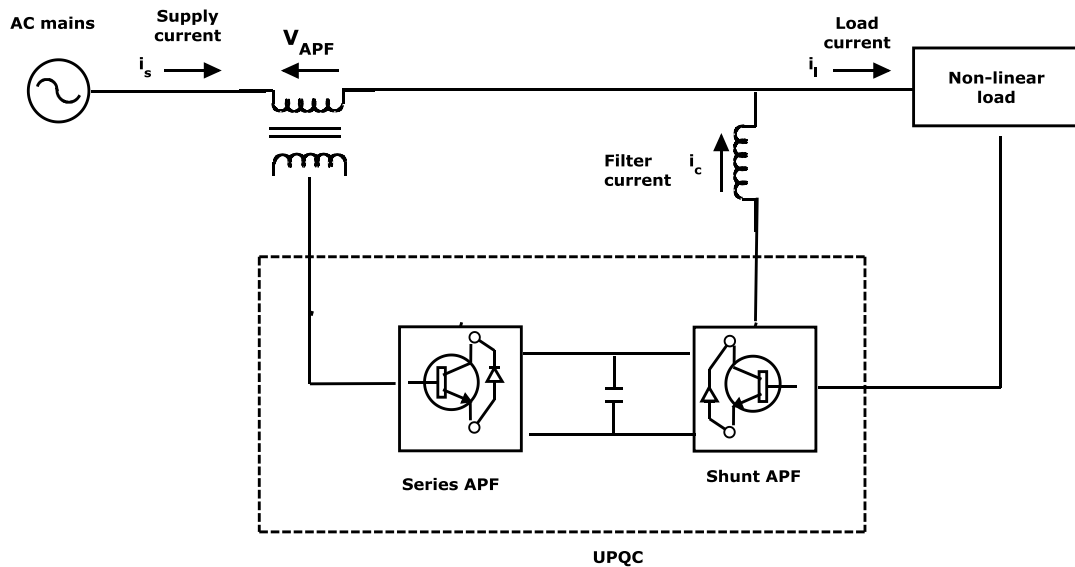


Fig.1.6 Unified power quality conditioner (UPQC) as universal APF

The hybrid filter [3, 34] is a combination of series filters (either active or passive) and shunt filter (either active or passive). It is quite popular because the solid-state devices used in the active series part can be of reduced size and cost (about 5% of the load size) and a major part of the hybrid filter is made of the passive shunt L-C filter used to eliminate lower order harmonics [34]. It has the capability of reducing voltage and current harmonics at a reasonable cost. There are many more hybrid configurations, but for the sake of brevity, they are not discussed here, however, details can be found in the respective references.

1.5.3 Supply system based categorization

Supply system based classification of APFs is based on the supply and/or the load system. They are Single-phase Two-wire APF, Three-phase Three-wire APF and Three-phase Four-wire APF. There are many non-linear loads, such as domestic appliances, connected to single-phase supply systems. Some three-phase non-linear loads are without neutral, such as ASDs, fed from three-wire supply systems. There are many non-linear single-phase loads

distributed on three-phase four-wire supply systems [7, 25, 46-48, 50, 61, 63], such as computers [27], commercial lighting, and etc.

1.5.3.1 Two-Wire APFs:

Fig.1.7 shows a two-wire shunt APF with current source inverter two-wire (single-phase) [15, 22, 27]. APFs are used in all three modes as active series active shunt, and a combination of both as unified line conditioners.

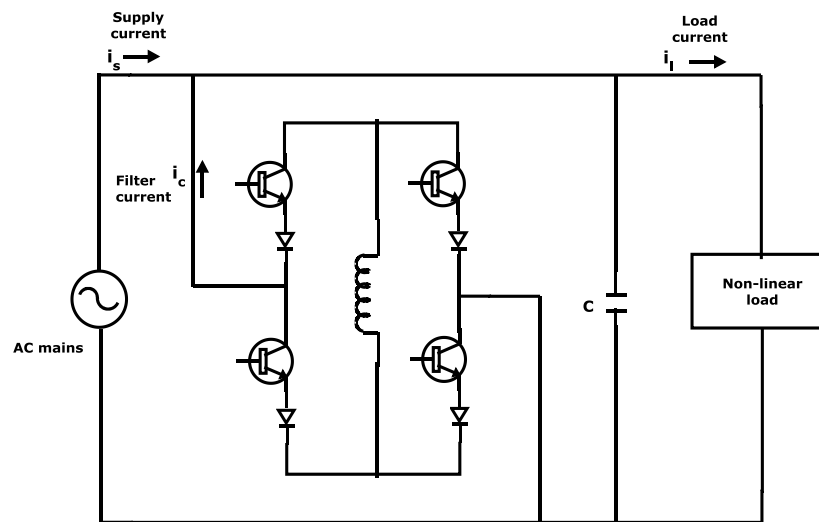


Fig.1.7 Two-wire shunt APF with current source inverter

Both converter configurations, current-source PWM bridge with inductive energy storage element and voltage-source PWM bridge with capacitive dc-bus energy storage elements, are used to form two-wire APF circuits [22]. In some cases, active filtering is included in the power conversion stage to improve input characteristics at the supply end. The series APF is normally used to eliminate voltage harmonics, spikes, sags, notches, etc., while the shunt APF is used to eliminate current harmonics and reactive power compensation [27].

1.5.3.2 Three-Wire APFs:

Fig.1.8 shows Three-phase three-wire APF [23, 24, 35, 39- 41, 45]. Three-phase three-wire non-linear loads, such as ASDs, are major applications of solid-state power converters and, lately, many ASDs, etc., incorporate APFs in their front-end design. A large number of

publications have appeared on three-wire APFs [23] with different configurations. Active shunt APFs are developed in the current-fed type (**Fig. 1.3**) or voltage fed type with single-stage (**Fig.1.4**) or multistep/multilevel and multi series [57] configurations. Active shunt APFs are also designed with three single-phase APFs with isolation transformers for proper voltage matching, independent phase control, and reliable compensation with un-balanced systems. Active series filters are developed for stand-alone mode (**Fig. 1.5**) or hybrid mode with passive shunt filters.

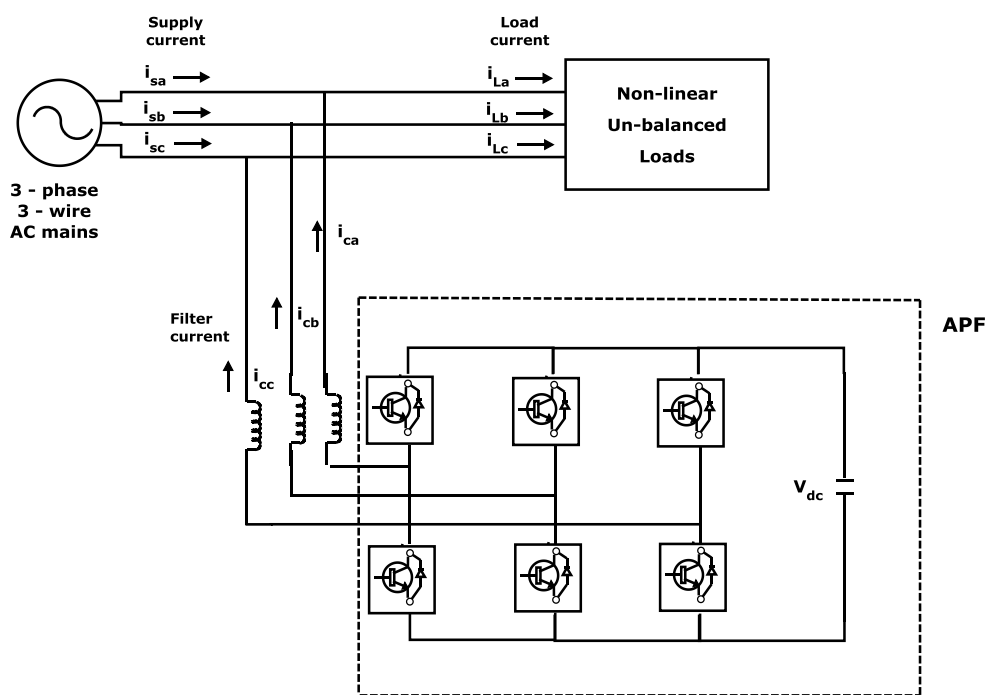


Fig.1.8 Three-phase three-wire APF

1.5.3.3 Four-Wire APFs:

A large number of single-phase loads may be supplied from three-phase mains with neutral conductor [7, 25, 46-48, 50, 61, 63], (**Fig.1.9**). They cause excessive neutral current [23, 24], harmonic and reactive power burden, and unbalance. To reduce these problems, four-wire APFs have been attempted. They have been developed as active shunt mode with current fed and voltage fed, active series mode and hybrid form with active series and passive shunt mode.

To employ APFs in three-phase four-wire systems, two types of configurations are possible;

- (a) Three-phase four-wire four-pole Shunt APF
- (b) Three-phase four-wire Capacitor midpoint Shunt APF

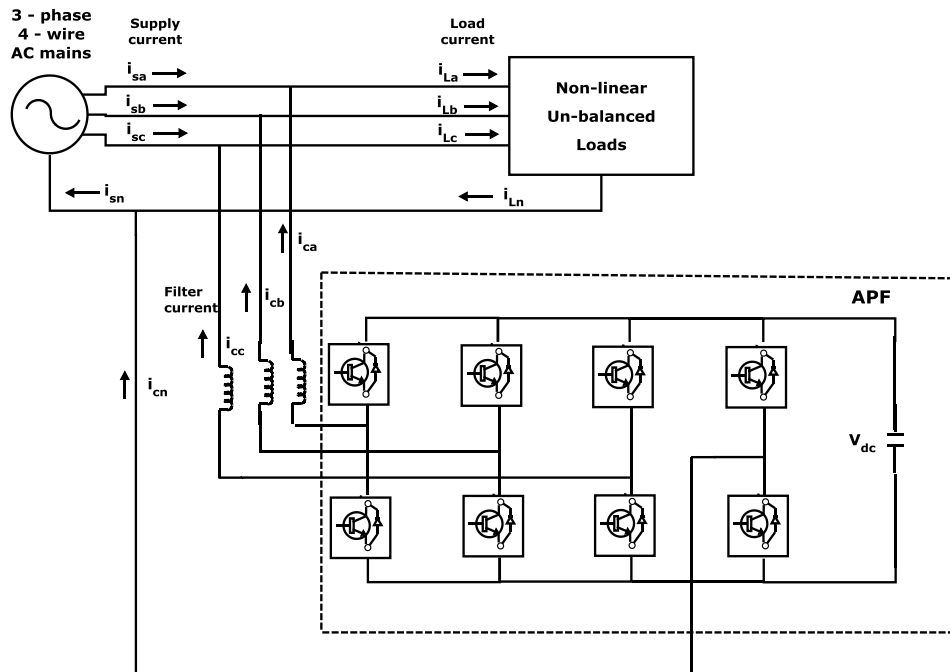


Fig.1.9 Three-phase four-wire four-pole Shunt APF

Three-phase four-wire [7, 25, 46-48, 50, 61, 63], four-pole Shunt APF is a four-leg structure, where a fourth leg is provided exclusively for neutral current compensation (**Fig.1.9**) and three-phase four-wire capacitor midpoint Shunt APF is a three-leg structure with the neutral conductor being connected to midpoint of dc-link capacitor (**Fig.1.10**). The four-leg eight-switch APF topology is preferred to be implemented as many researchers have appointed this configuration as the most proficient alternative to be used in shunt APF [26]. The three-leg six-switch split-capacitor configuration of shunt APF suffers from several shortcomings viz.

- ↪ Control circuit is somewhat complex
- ↪ Voltages of the two capacitors of split-capacitor need to be properly balanced
- ↪ Large dc-link capacitors are required.

Despite the fact, three-phase four-wire capacitor midpoint [26, 50] Shunt APF topology is preferred owing to less number of switching devices and lower switching losses compared to the eight-switch topology [4]. However, the higher order harmonics generated in the eight switch configuration due to frequent switching of semiconductor devices can be eliminated by the use of RC high-pass filter and switching losses occurring in the VSI can also be minimized by the use of DC-link voltage regulator.

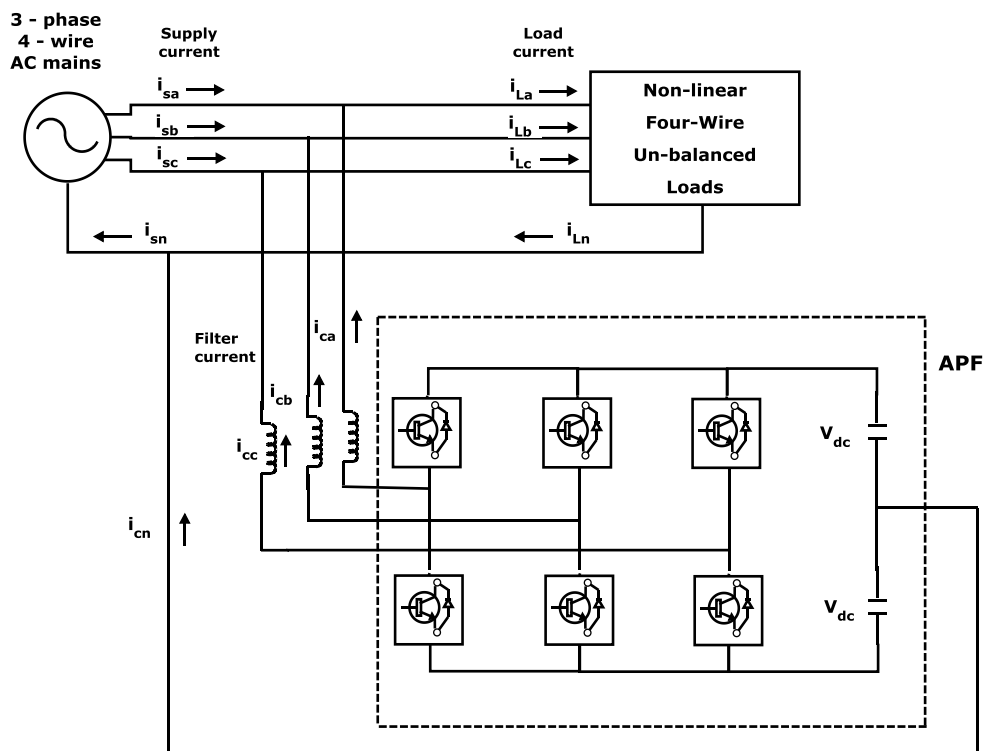


Fig.1.10 Three-phase four-wire Capacitor midpoint Shunt APF

1.6 SELECTION CONSIDERATIONS OF APFs

Selection of the APF for a particular application is an important task for end users and application engineers. There are widely varying application requirements, such as single-phase or three-phase, three-wire and four wire systems, requiring current or voltage-based compensation [1-65]. **Table 1.3** gives brief guidelines for the proper selection of APFs suited to the needs of individual (Current-based compensation, voltage-based compensation and voltage and current based compensation) requirements.

Table 1.3 - Selection of APFs for Specific Application Considerations

SELECTION OF APF'S FOR SPECIFIC APPLICATION CONSIDERATIONS				
Compensation for Specific Application	Active Series	Active Shunt	Hybrid of Active Series and Passive Shunt	Hybrid of Active Shunt and Active Series
> A. Current Harmonics		**	***	*
> B. Reactive Power		***	**	*
> C. Load Balancing		*		
> D. Neutral Current		**	*	
> E. Voltage Harmonics	***		**	*
> F. Voltage Regulation	***	*	**	*
> G. Voltage Balancing	***		**	*
> H. Voltage Flicker	**	***		*
> I. Voltage Sag&Dips	***	*	**	*
> J. (A + B)		***	**	*
> K. (A+B+C)		**		*
> L. (A+B+C+D)		*		
> M. (E+F)	**			*
> N. (E+F+H+I)	**			*
> O. (A+E)			**	*
> P. (A+B+E+F)			*	**
> Q. (F+G)	**		*	
> R. (B+C)		*		
> S. (B+C+D)		*		
> T. (A+B+G)		**	*	
> U. (A+C)		*		
> V. (A+D+G)		*	**	

1.7 TECHNICAL AND ECONOMIC CONSIDERATIONS

Technical literature on the APFs has been reported since 1971 [55] and, in the last two decades, has boomed. Around 1990, many commercial development projects were completed [28, 56, 57] and put into practice. A number of configurations discussed earlier have been investigated, but could not be developed commercially because of cost and complexity

considerations. Initially reported configurations were quite general and the rating of solid-state devices involved was substantial, which resulted in high cost. Due to these reasons, the technology could not be translated to field applications. Later on, the rating of active filtering was reduced by the introduction of supplementary passive filtering [57], without deteriorating the overall filter performance.

Moreover, modern APFs are capable of compensating quite high orders of harmonics (typically, the 25th now a days it is up to 50th) dynamically. However, as high-order harmonics are small, they are compensated by using a passive ripple filter. This approach has given a boost to field applications. Another major attempt has been to separate out various compensation aspects of the APFs to reduce the size and cost. However, additional features get included on specific demand. Economic considerations were the hindrance at the initial stages of APF development [58], but now they are becoming affordable due to a reduction in the cost of the devices used. With the harmonic pollution in present-day power systems, the demand for the APF is increasing. Recommended standards such as IEEE-519 [59] will result in the increased use of APFs in the coming years.

1.8 INTRODUCTION TO ACTIVE POWER FILTER CONTROL STRATEGIES

For a long time one of the main concerns related to electric equipment was power factor correction, which could be done by using capacitor banks or, in some cases reactors. For all situations, the load acted as a linear circuit drawing a sinusoidal current from a sinusoidal voltage source. Hence, the conventional power theory based on active, reactive and apparent power definitions was sufficient for design and analysis of power systems. Nevertheless, some papers were published in the 1920's, showing that the concept of reactive and apparent power losses its usefulness in non-sinusoidal conditions [66]. Then, two important approaches to power definitions under non-sinusoidal conditions were introduced by

Budeanu [67, 68], in 1927 and *Fryze* [69] in 1932. Fryze defined power in the *time domain*, whereas Budeanu did it in the frequency domain. At that time, non-linear loads were negligible, and little attention was paid to this matter for a long time.

Since *power Electronics (PE)* was introduced in the late 1960's, *non-linear loads* that consume non-sinusoidal current have increased significantly. In some cases, they represent a very high percentage of the total loads. Today, it is common to find a house without linear loads such as conventional incandescent lamps. In most cases these lamps have been replaced by electronically controlled fluorescent lamps. In industrial applications, an induction motor that can be considered as a linear load in a steady state is now equipped with a rectifier and inverter for the purpose of achieving adjustable speed control. The induction motor together with its drive is no longer a linear load.

The power theories presented by Budeanu and Fryze had basic concerns related to the calculation of average power or rms values of voltage and current. The development of PE technology has brought new conditions to power theories. Exactly speaking, the new conditions have not emerged from the proliferation of power converters using power semiconductor devices such as diodes, thyristors, IGBT's, GTO's, and so on. Although these power converters have a quick response in controlling their voltages and/or currents, they may draw reactive power as well as harmonic current from power networks. This has made it clear that conventional power theories based on average and/or rms values of voltages and/or currents are not applicable to the analysis and design of power converters and power networks. This problem has become more serious during comprehensive analysis and design of active filters intended for *reactive power compensation* as well as *harmonic compensation*.

From the end of 1960's to the beginning of 1970's, *Erlicki* and *Emmanuel Eigeles* [70], *Sasaki* and *Machida* [71], and *Fukao*, *Iida*, and *Miyairi* [72] published their pioneer papers

presenting what can be considered as a basic principle of controlled reactive power compensation. For instance, Erlicki and Emmanuel Eigeles [70] presented some basic ideas like “compensation of distortive power is unknown to date.” They also determined that “a non-linear resistor behaves like a reactive power generator while having no energy storage elements,” and presented the very first approach to active power factor control. Fukao, Iida, and Miyairi [72] stated that “by connecting a reactive power source in parallel with the load, and by controlling it in such a way as to supply reactive power to the load, the power network will only supply active power to the load. Therefore ideal power transmission would be possible.”

In 1976, Gyugyi and pelly [73] presented the idea that reactive power could be compensated by a naturally commutated cyclo-converter without energy storage elements. This idea was explained from a physical point of view. However, no specific mathematical proof was presented. In 1976, Harashima, Inaba, and Tsuboi [74] presented, probably for the first time, the term “*instantaneous reactive power*” for a single phase circuit. In that same year (1976), Gyugyi and strycula [75] used the term “*active ac power filters*” for the first time. A few years later, in 1981, Takahashi, Fuziwara, and Nabae published two papers [76, 77] giving a hint of the emergence of the instantaneous power theory or “*p-q theory*.” The *p-q* theory in its first version was first published in the *Japanese language* in 1982 [78] in a local conference, and 1983 in *Transactions of the Institute of Electrical Engineers of Japan* by H. Akagi, Y. Kanazawa and Nabae [79]. With a minor time lag, a paper was published in English in an international conference in 1983 [37], showing the possibility of compensating for instantaneous reactive power without energy storage elements by H. Akagi, Y. Kanazawa and Nabae. Then, a more complete paper including experimental verifications was published in the *IEEE Transactions on Industry Applications* in 1984 [39] by H. Akagi et al.

The p - q theory defines a set of instantaneous powers in the time domain. Since no restrictions are imposed on voltage or current behaviours, it is applicable to *three-phase systems with or without neutral conductors*, as well as to generic voltage and current waveforms. Thus it is valid not only in steady states, but also during transient states. Contrary to other traditional power theories treating three-phase systems as three single-phase circuits, the p - q theory deals with all the *three phases at the same time*, as a unity system. Therefore, this theory always considers three-phase systems together, *not* as a superposition or *sum of three single phase circuits*. It was defined by using the “ $\alpha\beta$ -transformation,” also known as *Clarke transformation* [80], which consists of a real matrix that transforms three phase voltages and currents into $\alpha\beta$ -stationary reference frame currents.

In 1997, Vasco Soares, Pedro Verdelho and Gil D. Marques, published a paper “Active Power Filter Control Circuit Based on the Instantaneous Active and Reactive Current I_d - I_q Method,” in IEEE Power Electronics Specialists Conference. Later in 2000, Vasco Soares, Pedro Verdelho and Gil D. Marques, published a paper “An Instantaneous Active and Reactive Current Component Method for Active Filters,” in *IEEE Trans. Power Electronics*.

I_d - I_q control strategy is also known as synchronous reference frame (SRF) [7, 26, 43-50]. Here, the reference frame d-q is determined by the angle ‘ θ ’ with respect to the ‘ α - β ’ frame used in the p - q theory. In I_d - I_q control strategy [43], only the currents magnitudes are transformed and the p - q formulation is only performed on the instantaneous active I_d and reactive I_q components [49].

1.9 MOTIVATION

Issue of harmonics are of a greater concern to engineers and building designers because harmonics can do more than distort voltage waveforms, they can overheat the building wiring, causes nuisance tripping, overheat transformer units, and cause random end-user

equipment failures. Thus power quality (PQ) has become more and more serious with each passing day. As a result active power filter (APF) gains much more attention due to excellent harmonic and reactive power compensation in single phase, three-phase with and without neutral ac power networks with nonlinear loads. The APF technology has been under research and development for providing compensation for harmonics, reactive power, and/or neutral current in ac networks. Current harmonics are one of the most common power quality problems and are usually resolved by the use of shunt active filters. The performances of active filters depend on the inverter parameters, control strategies, controllers and the method for current reference determination.

To overcome the complications encountered in power systems, APF emerged as a significant solution. The performance of APF principally depends upon the selection of reference compensation current extraction method. Amongst the various APF control strategies, the instantaneous active and reactive power ($p-q$) method is most widely used. The $p-q$ control strategy yields inadequate results under un-balanced and/or non-sinusoidal source voltage conditions. The main reason behind the notches is that the controller failed to track the current correctly and thereby APF fails to compensate completely. So to avoid the difficulties occur with $p-q$ control strategy, we have considered I_d-I_q control strategy. By employing I_d-I_q method the THD in source current after compensation can be reduced below 5% under both ideal and non-ideal(un-balanced and/or non-sinusoidal) supply conditions thereby satisfying IEEE-519 standards.

Even though the APF is efficient enough for load compensation, optimal performance by the APF is always desirable. The optimal harmonic compensation is possible by minimizing the undesirable losses occurring inside the APF itself. The detrimental consequences due to current harmonics, excessive neutral current, unbalanced source current in the power system

can be avoided by the use of Type-1 and Type-2 FLC based SHAF control strategies ($p-q$ and I_d-I_q). Even though several controllers have been proposed, most of them yield inadequate result under non-ideal supply conditions. The performance of APF with conventional PI controller is not quite satisfactory under a range of operating conditions.

Recently, Fuzzy logic controllers (FLCs) have received a great deal of attention for their applications in APFs. The advantages of Fuzzy logic controllers over conventional PI controllers are that they do not require an accurate mathematical model, can work with imprecise inputs, can handle non-linearity, and are more robust than conventional controllers. With the development of Type-2 FLC and their ability to handle uncertainty, utilizing Type-2 FLC has attracted a lot of significance in recent years. The membership functions of Type-2 Fuzzy sets are three dimensional and include a Foot point of Uncertainty, which is the new third dimension of Type-2 Fuzzy sets. Hence load compensation capability of the APF can still be enhanced by using Type-2 Fuzzy logic controller.

Thus from the previous discussion it is evident that Shunt APF is one of the solution for improving the power quality by mitigating current harmonics. However there are scope for improving the performance of Shunt APF by implementing suitable current extraction techniques and controllers for maintaining DC link voltage constant, which is an indicator of the performance of the Shunt APF. These are the primary source of motivation for the present work.

The work presented here is mainly concentrated on the use of $p-q$ and I_d-I_q control strategies. Three types of controller's viz. PI controller, Type-1 and Type-2 Fuzzy logic controllers with different Fuzzy MFs (Trapezoidal, Triangular and Gaussian) have been implemented and the results obtained under balanced, un-balanced and non-sinusoidal source are compared to evaluate the degree of compensation by the APF with different control

strategies. Extensive MATLAB simulation was carried out and the results validate superior functionality of Type-2 FLC based APF employing I_d-I_q control strategy. The detailed real-time results using Real-time digital simulator are presented to support the feasibility of proposed control strategies and controllers.

1.10 DISSERTATION OBJECTIVES

From the preceding discussion, the dissertation objectives may outline as follows:

- To develop Shunt active filter *control strategies* ($p-q$ and I_d-I_q) for extracting the three-phase reference currents and to improve the power quality of power system by mitigating the current harmonics and maintaining dc link voltage constant.
- To develop PI controller, proposed Type-1 FLC and Type-2 FLC based Shunt active filter control strategies with different Fuzzy MFs for extracting the three-phase reference currents and to maintain Dc link voltage constant and to evaluate their performance under various source voltage conditions in *MATLAB/SIMULINK* environment.
- To develop *Hysteresis current control scheme* for *generation of gating signals* to the devices of the APF.
- To verify the PI controller, proposed Type-1 FLC and Type-2 FLC based shunt active filter control strategies with different Fuzzy MFs with *Real-time digital simulator* (*OPAL-RT*) to validate the proposed research.

1.11 DISSERTATION STRUCTURE

From the *introduction*, it can be observed that, several fundamental factors have been considered for the power quality improvement of power system. The importance of active

power filters and solid state devices are explained in detail and active power filter configurations, selection considerations of APFs are also presented in detail.

In *chapter – 2*, we have considered *PI controller* based Shunt active filter control strategies (*p-q and I_d-I_q*). The Shunt active filter control strategies for extracting the three-phase reference currents are compared, evaluating their performance under different source voltage conditions using PI controller. The performance of the control strategies have been evaluated in terms of harmonic mitigation and DC link voltage regulation. The detailed simulation results using *MATLAB/SIMULINK* software are presented to support the feasibility of proposed control strategies. To validate the proposed approach, the system is also implemented on *real-time digital simulator* hardware and adequate results are reported for its verifications.

In *chapter – 3*, Type-1 Fuzzy logic controller (*Type-1 FLC*) based Shunt active filter control strategies with *different Fuzzy MFs (Trapezoidal, Triangular and Gaussian)* are developed for extracting the three-phase reference currents and their performances under different source voltage conditions are compared. The performance of the control strategies has been evaluated in terms of harmonic mitigation and DC link voltage regulation. The detailed *simulation and real-time results* are presented to validate the proposed research.

Even though, TYPE-1 FLC based shunt active filter control strategies with different Fuzzy MFs are able to mitigate the harmonics but *notches are presented* in the source current. So to mitigate the harmonics perfectly one has to choose perfect controller. So in *chapter-4*, the proposed *Type-2 FLC* based shunt active filter control strategies *with different Fuzzy MFs (Trapezoidal, Triangular and Gaussian)* are introduced. With this approach the compensation capabilities of SHAF *are extremely good*. The detailed simulation results using *MATLAB/SIMULINK* are presented to support the feasibility of proposed control strategies.

In Chapter-5, a specific class of digital simulator known as a real-time simulator has been introduced by answering the questions “what is real-time simulation,” “why is it needed” and “How it works”. The latest trend in real-time simulation consists of exporting simulation models to FPGA. The proposed *TYPE-2 FLC* based shunt active filter control strategies with *different Fuzzy MFs* are verified with *Real-time digital simulator* (OPAL-RT) to validate the proposed research.

Last *Chapter –6* is dedicated to *summary of overall thesis and future work*. The comparative study of PI controller, proposed Type-1 FLC and Type-2 FLC based shunt active filter control strategies with different Fuzzy MFs using MATLAB and Real-time digital simulator is also presented.

Chapter - 2

Shunt active filter control strategies and its Performance analysis using PI controller

Shunt active filter basic compensation principle

Classifications of Shunt active filter control strategies

DC Link Voltage Regulation using PI controller

Simulation and Real-time Results

Summary

CHAPTER – 2

In the previous chapter-1, the main causes of harmonics are explained in detail. The prevalent difficulty with harmonics is voltage and current waveform distortion. The electronic equipment like; computers, battery chargers, electronic ballasts, variable frequency drives, and switching mode power supplies generate perilous harmonics. Issue of harmonics are of a greater concern to engineers and building designers because they do more than distort voltage waveforms, they can overheat the building wiring, causes nuisance tripping, overheat transformer units, and cause random end-user equipment failures. Thus power quality has become more and more serious with each passing day. As a result active power filter gains much more attention due to excellent harmonic compensation. The importance of active power filters and solid state devices are explained in details and active power filter (APF) configurations, selection considerations of APFs are also presented in details. The list of harmonics mitigation techniques is also provided in chapter-1.

*In this **chapter-2**, shunt active filter **control strategies (p-q and I_d-I_q)** for extracting the three-phase reference currents are compared, evaluating their performance under **different source voltage conditions (balanced, un-balanced and non-sinusoidal)** using **PI controller**. The performance of the control strategies has been evaluated in terms of **harmonic mitigation** and **DC link voltage regulation**. The detailed simulation results using **MATLAB/SIMULINK** software are presented to support the feasibility of proposed control strategies. To validate the proposed approach, the system is also implemented on **real-time digital simulator hardware** and adequate results are reported for its verifications.*

This chapter-2 is organized as follows: Section 2.1 provides the details of shunt active filter basic compensation principle, Section 2.2 provides the classifications of Shunt active filter control strategies, Section 2.3 provides introduction to DC link voltage regulation using PI controller. Simulation results of p-q and I_d-I_q control strategies with PI controller using MATLAB/SIMULINK are presented in section 2.4. Real-time results of p-q and I_d-I_q control strategies with PI controller using real-time digital simulator are presented in Section 2.5 and finally Section 2.6 states all concluding remarks.

2.1 Shunt active filter basic compensation principle

Shunt active filter (SHAF) [7, 9-15, 22, 24, 26, 36, 48, 50, 61] design is an important criterion to compensate current harmonics effectively [6-9, 12-16, 26, 47, 50, 60, 65].

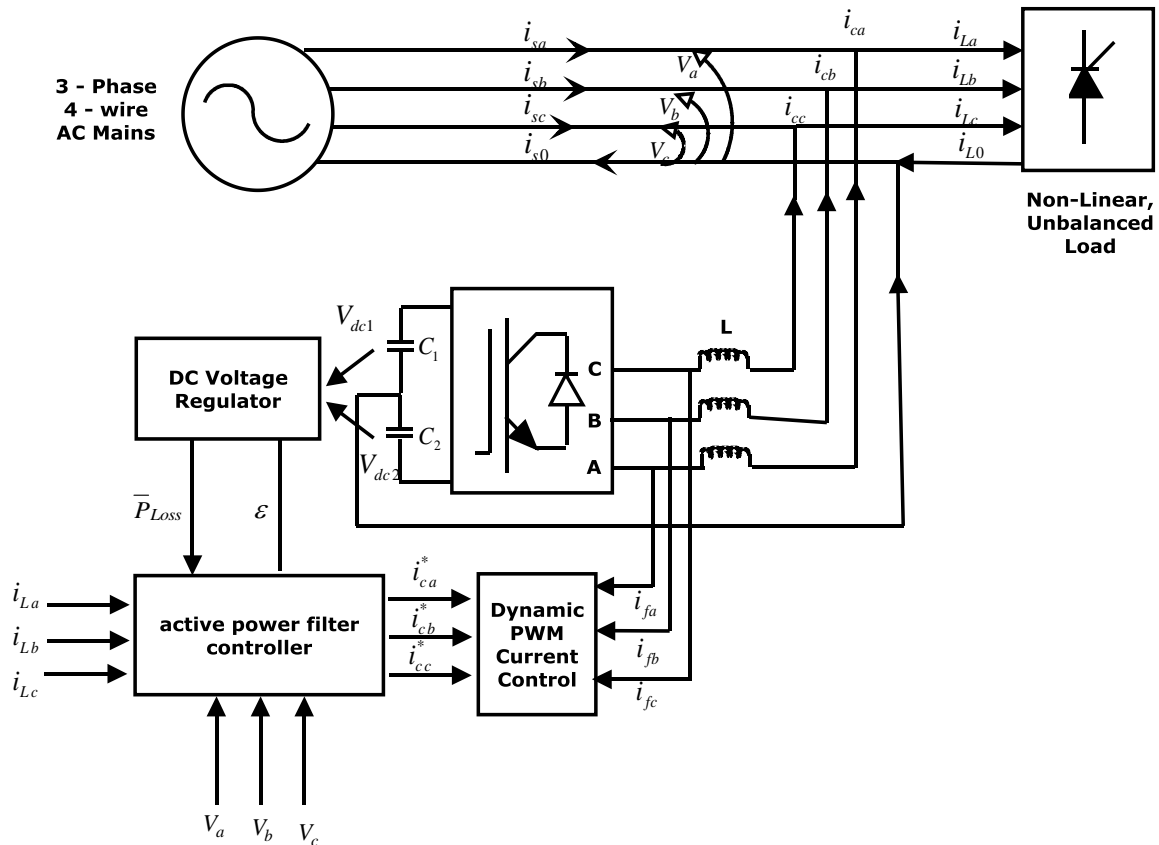


Fig.2.1 Basic architecture of three-phase four-wire shunt active filter

In brief for perfect compensation, controller must be capable to achieve the following requirements:

- i) Extract and inject load harmonic currents,
- ii) Maintain a constant dc link voltage,
- iii) Avoid absorbing or generating the reactive power with fundamental frequency components.

Fig.2.1 shows a basic architecture of three-phase four-wire shunt active filter. The active power filter [1-65] is controlled to supply the compensating current [30] to the load to cancel

out the current harmonics on AC side and reactive power flow to the source thereby making the source current in phase with source voltage.

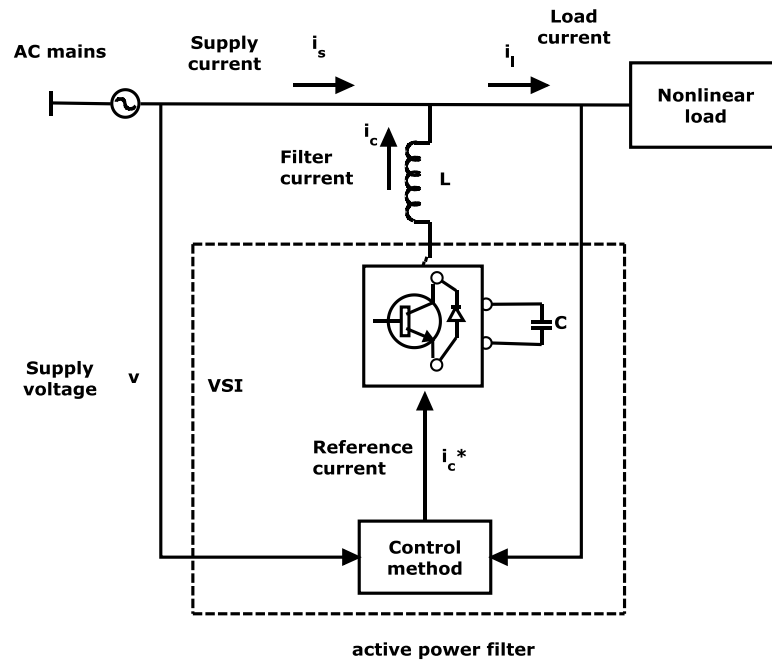


Fig. 2.2 Basic Compensation Principle

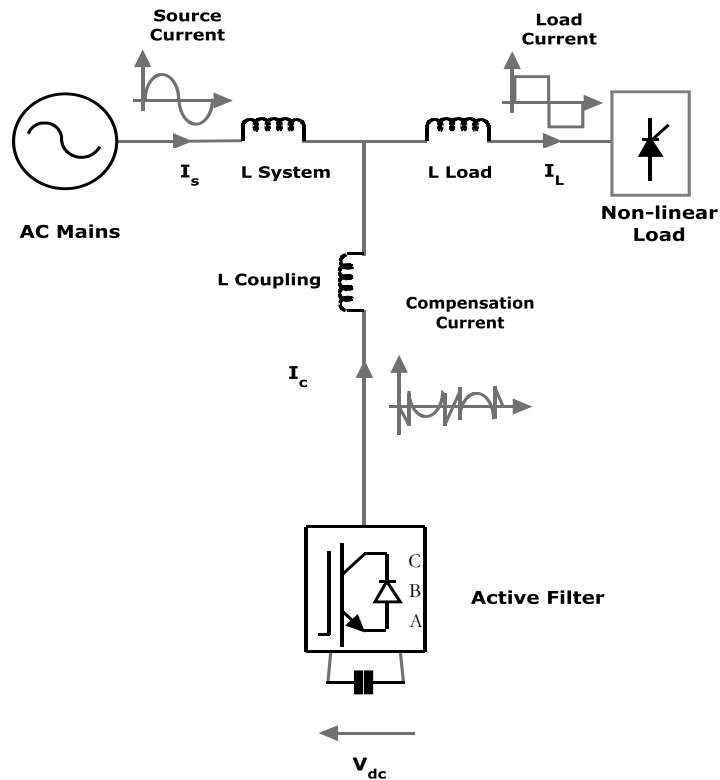


Fig. 2.3 Compensation Principle of a Shunt Active power filter

Fig. 2.2 and **Fig. 2.3** show the basic compensation principle of the active power filter and it serves as an energy storage element to supply the real power difference between load and source during the transient period. When the load condition changes the real power balance between the mains and the load will be disturbed. This real power difference is to be compensated by the DC capacitor. This changes the DC capacitor voltage away from the reference voltage.

In order to keep satisfactory operation of the active filter [31], the peak value of the reference source current must be adjusted to proportionally change the real power drawn from the source. This real power absorbed/released by the capacitor compensates the real power difference between the power consumed by the load and the power supplied from the source [32]. If the DC capacitor voltage is recovered and attains the reference voltage, the real power supplied by the source is supposed to be equal to that consumed by the load again.

2.2 Active Power filter control strategies

Control strategy [7] is the heart of the APF and is implemented in **three stages**.

- i)** In the first stage, the essential **voltage and current signals are sensed** using potential transformers (P.Ts) and current transformers (C.Ts).
- ii)** In the second stage, **compensating** commands in terms of **current** or **voltage levels are derived** based on control techniques [7, 33-50] and APF configurations.
- iii)** In the third stage of control, **the gating signals** for the solid state devices of the APF **are generated** using PWM, hysteresis, sliding-mode, PI controller and/or Fuzzy-logic-based controllers.

The control of the APF is realized using discrete analog and digital devices or advanced micro-electronic devices, such as single-chip microcomputers, DSP, etc. There are numerous published methods that describe different topologies and different algorithms used for active

filtering. In many of them, it usually prevails the description of a single method but there are publications which explain and compare couples of such methods describing their advantages and disadvantages by giving final indices as the dynamics, the THD reduction, the inverter efficiency or the cost of the entire active filter.

2.2.1 Signal Conditioning

For the purpose of implementation of the control algorithm, several instantaneous voltage and current signals are required. These signals are also useful to monitor, measure, and record various performance indices, such as; total harmonic distortion (THD) [50], power factor, active and reactive power etc.

The typical voltage signals are ac terminal voltages, dc bus voltage of the APF, and voltages across series elements. The current signals to be sensed are load currents, supply currents, and compensating currents of the APF. Current signals are sensed using C.Ts. and/or Hall-effect current sensors. Voltage signals are sensed using either P.Ts. or Hall-effect voltage sensors or isolation amplifiers. The voltage and current signals are sometimes filtered to avoid noise problems. The filters are either hardware based (analog) or software based (digital) with low-pass, high-pass, or band pass characteristics.

2.2.2. Derivation of Compensating Signals

In an attempt to minimize the harmonic disturbances created by the non-linear loads the choice of the active power filters comes out to improve the filtering efficiency and to solve many issues existing with classical passive filters. One of the key points for a proper implementation of an active filter is to use optimized techniques for current/voltage reference generation. There exist many implementations supported by different strategies based on

- (a) Frequency-domain harmonic detection methods
- (b) Time-domain harmonic detection methods

The classification of harmonics methods can be done relative to the domain where the mathematical model is developed. Thus, two major directions are described here, the time domain and the frequency-domain methods [33-34]. Such classification is given in Table 2.1. The description of the methods will be provided in the subsequent sections.

Table.2.1 Classification of Harmonic Detection methods

Classification of harmonic detection methods

Domain	Harmonic Detection Method
Frequency-domain	<p>Discrete Fourier Transform (DFT) Fast Fourier Transform (FFT) Recursive Discrete Fourier Transform (RDFT)</p>
Time-domain	<p>Instantaneous power p-q theory Instantaneous current (I_d-I_q) theory</p>

Development of compensating signals either in terms of voltages or currents is the important part of APF control [35] and affects their ratings and transient, as well as steady-state performance. One of the most discussed software part (in the case of a DSP implementation) of an active filter is the harmonic detection method. In brief, it represents the part that has the capability of determining specific signal attributes (for instance the frequency, the amplitude, the phase, the time of occurrence, the duration, energy, etc.) from an input signal (that can be voltage, current or both) by using a special mathematical algorithm. Then, with the achieved information, the controller is imposed to compensate for the existing distortion. It can be easily seen that, if there are some errors when estimating one of the above attributes, the overall performance of the active filter could be seriously degraded in such a way that even sophisticated control algorithms cannot recover the original

information. Therefore, different algorithms [7, 36] emerged for the harmonic detection, which led to a large scientific debate on which part the focus should be put on, the detection accuracy, the speed, the filter stability, easy and inexpensive implementation, etc.

2.2.2.1 Compensation in Frequency Domain

Control strategy in the frequency domain is based on the Fourier analysis of the distorted voltage or current signals to extract compensating commands [33, 34]. Using the Fourier transformation, the compensating harmonic components are separated from the harmonic-polluted signals and combined to generate compensating commands. The device switching frequency of the APF is kept generally more than twice the highest compensating harmonic frequency for effective compensation. The on-line application of Fourier transform (solution of a set of non-linear equations) is a cumbersome computation and results in a large response time.

2.2.2.2 Compensation in Time Domain

Control methods of the APFs in the time domain are based on instantaneous derivation of compensating commands in the form of either voltage or current signals from distorted and harmonic-polluted voltage or current signals [33-50]. There are a large number of control strategies in the time domain, which are known as

- (a) Instantaneous active and reactive power “ $p-q$ ” control strategy,
- (b) Instantaneous active and reactive current “ I_d-I_q ” control strategy.

2.2.2.2.1 Instantaneous Active and Reactive Power (P-Q) Control Strategy

Instantaneous active and reactive power control strategy (or $p-q$ control strategy) was first proposed by H. Akagi and co-authors in 1984 [37], and has since been the subject of various interpretations and improvements. The instantaneous active and reactive power ($p-q$) control strategy [38, 78, 79] has been widely used and is based on Clarke’s (“ $\alpha-\beta$ ”)

transformation of voltage and current signals to derive compensating signals [39-40]. In Fig. 2.4 and Fig. 2.5 the entire reference current generation with conventional $p-q$ control strategy using PI controller and Fuzzy logic controller (FLC) has been illustrated. In order to maintain DC link voltage [41] constant, a PI controller (or FLC) is added to control the active power component.

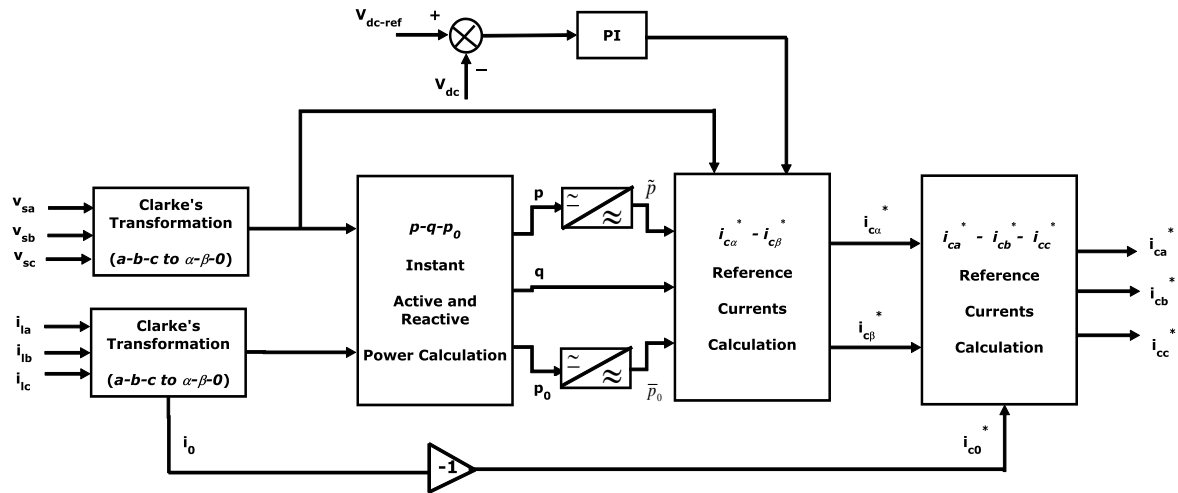


Fig. 2.4 Reference current extraction with $p-q$ control strategy using PI controller

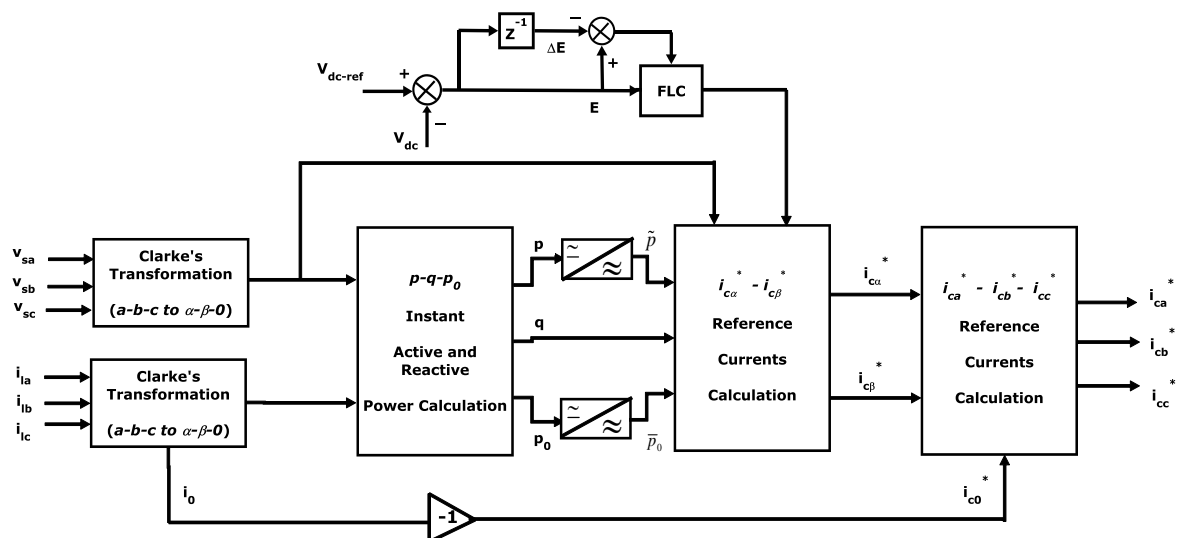


Fig. 2.5 Reference current extraction with $p-q$ control strategy using Fuzzy logic controller

The PI controller (or FLC) controls this small amount of active current and then the current controller regulates this current to maintain the DC link capacitor voltage [42]

constant. To achieve this, the DC link voltage is detected and compared with the reference voltage setting by control circuit and then the difference is fed to the PI or FLC. According to the voltage difference, the PI controller (or FLC) decides how much active current is needed to maintain the DC link voltage. The output of the PI controller (or FLC) is an active current that is the corresponding power flow needed to maintain the DC link voltage. It is used as a part of the reference current for the current controller, which controls the inverter to provide the required compensation current.

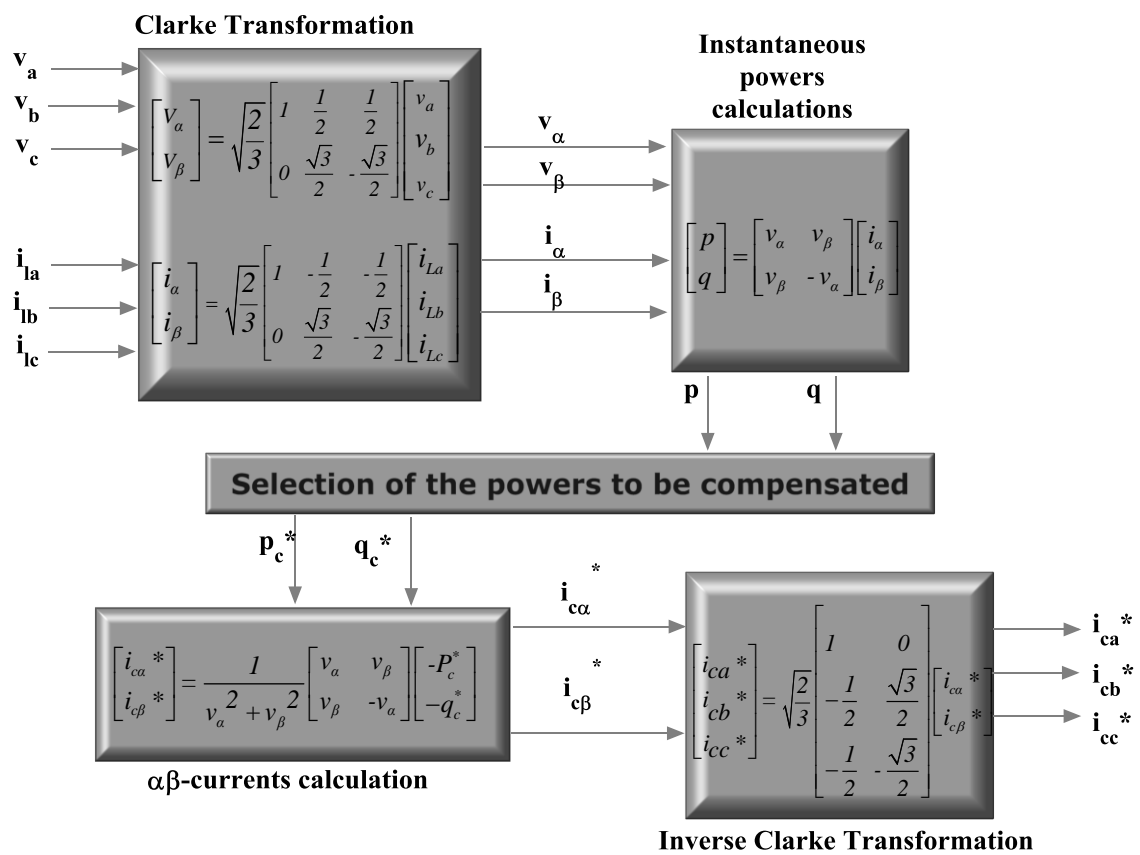


Fig. 2.6 Control method for Shunt current compensation based on p - q control strategy

The instantaneous active and reactive power can be computed in terms of transformed voltage and current signals. From instantaneous active and reactive powers, harmonic active and reactive powers are extracted using low-pass and high-pass filters. From harmonic active and reactive powers, using inverse " α - β " transformation [39], compensating commands in terms of either currents or voltages are derived. The active filter currents are achieved from

the instantaneous active and reactive powers p and q of the non-linear load. Transformation of the phase voltages V_a , V_b , and V_c and the load currents i_{la} , i_{lb} , and i_{lc} into the $\alpha - \beta$ orthogonal coordinates using Clarke's transformation [40] are given in equation (2.1-2.2) which is shown in **Fig. 2.6**. The compensation objectives of active power filters are the harmonics present in the input currents. Present architecture represents three-phase four-wire and it is realized with constant power controls strategy [5].

$$\begin{bmatrix} V_0 \\ V_\alpha \\ V_\beta \end{bmatrix} = C \begin{bmatrix} v_a \\ v_b \\ v_c \end{bmatrix}; \quad \begin{bmatrix} i_0 \\ i_\alpha \\ i_\beta \end{bmatrix} = C \begin{bmatrix} i_{la} \\ i_{lb} \\ i_{lc} \end{bmatrix} \quad (2.1)$$

$$C = \sqrt{\frac{2}{3}} \begin{bmatrix} \frac{1}{\sqrt{2}} & \frac{1}{\sqrt{2}} & \frac{1}{\sqrt{2}} \\ 1 & -\frac{1}{2} & -\frac{1}{2} \\ 0 & \frac{\sqrt{3}}{2} & -\frac{\sqrt{3}}{2} \end{bmatrix} \quad (2.2)$$

Where C is the so called transformation matrix $\|C\| = 1$ and $C^{-1} = C^T$

Generalized instantaneous power, $p(t)$

$$P = \begin{bmatrix} v_a \\ v_b \\ v_c \end{bmatrix} \bullet \begin{bmatrix} i_{la} & i_{lb} & i_{lc} \end{bmatrix} = v_a i_{la} + v_b i_{lb} + v_c i_{lc} \quad (2.3)$$

The p - q formulation defines the generalized instantaneous power $p(t)$, and instantaneous reactive power vector $q(t)$ in terms of the α - β -0 components as

$$P = v_{\alpha\beta 0} \bullet i_{\alpha\beta 0} = v_\alpha i_\alpha + v_\beta i_\beta + v_0 i_0 \quad (2.4)$$

$$q = v_{\alpha\beta 0} \times i_{\alpha\beta 0} = \begin{bmatrix} q_\alpha \\ q_\beta \\ q_0 \end{bmatrix} = \begin{bmatrix} \begin{vmatrix} v_0 & v_\alpha \\ i_0 & i_\alpha \end{vmatrix} \\ \begin{vmatrix} v_\alpha & v_\beta \\ i_\alpha & i_\beta \end{vmatrix} \\ \begin{vmatrix} v_\beta & v_0 \\ i_\beta & i_0 \end{vmatrix} \end{bmatrix} \quad (2.5)$$

$$q = \|\vec{q}\| = \sqrt{q_\alpha^2 + q_\beta^2 + q_0^2} \quad (2.6)$$

$$\begin{bmatrix} p \\ q_\alpha \\ q_\beta \\ q_0 \end{bmatrix} = \begin{bmatrix} v_\alpha & v_\beta & v_0 \\ 0 & -v_0 & v_\beta \\ v_0 & 0 & -v_\alpha \\ -v_\beta & v_\alpha & 0 \end{bmatrix} \begin{bmatrix} i_\alpha \\ i_\beta \\ i_0 \end{bmatrix} \quad (2.7)$$

$$\begin{bmatrix} i_\alpha \\ i_\beta \\ i_0 \end{bmatrix} = \frac{1}{v_{\alpha\beta 0}} \begin{bmatrix} v_\alpha & 0 & v_0 & -v_\beta \\ v_\beta & -v_0 & 0 & v_\alpha \\ v_0 & v_\beta & -v_\alpha & 0 \end{bmatrix} \begin{bmatrix} p \\ q_\alpha \\ q_\beta \\ q_0 \end{bmatrix} \quad (2.8)$$

Where $v_{\alpha\beta 0} = \begin{bmatrix} v_\alpha \\ v_\beta \\ v_0 \end{bmatrix}$; $i_{\alpha\beta 0} = \begin{bmatrix} i_\alpha \\ i_\beta \\ i_0 \end{bmatrix}$; $v_{\alpha\beta 0}^2 = v_\alpha^2 + v_\beta^2 + v_0^2$

Instantaneous zero-sequence active current ' i_{0p} ' is $i_{0p} = \frac{v_0}{2} \frac{P}{v_{\alpha\beta 0}}$ (2.9)

Instantaneous zero-sequence reactive current ' i_{0q} ' is $i_{0q} = \frac{v_\beta}{2} \frac{q_\alpha}{v_{\alpha\beta 0}} - \frac{v_\alpha}{2} \frac{q_\beta}{v_{\alpha\beta 0}}$ (2.10)

Instantaneous active current on α -axis ' $i_{\alpha p}$ ' is $i_{\alpha p} = \frac{v_\alpha}{2} \frac{P}{v_{\alpha\beta 0}}$ (2.11)

Instantaneous reactive current on α -axis ' $i_{\alpha q}$ ' is $i_{\alpha q} = \frac{v_0}{2} \frac{q_\beta}{v_{\alpha\beta 0}} - \frac{v_\beta}{2} \frac{q_0}{v_{\alpha\beta 0}}$ (2.12)

Instantaneous active current on β -axis ' $i_{\beta p}$ ' is $i_{\beta p} = \frac{v_\beta}{2} \frac{P}{v_{\alpha\beta 0}}$ (2.13)

Instantaneous reactive current on β -axis ' $i_{\beta q}$ ' is $i_{\beta q} = \frac{v_{\alpha}}{v_{\alpha\beta 0}^2} q_0 - \frac{v_0}{v_{\alpha\beta 0}^2} q_{\alpha}$ (2.14)

In the new coordinates system, the instantaneous power has two components: the zero-sequence instantaneous real power ' P_0 ' and the instantaneous real power due to positive and negative sequence components ' $P_{\alpha\beta}$ '.

$$P(t) = P_0(t) + P_{\alpha\beta}(t) \quad (2.15)$$

$$P_0(t) = v_0 i_0 \quad (2.16)$$

$$P_{\alpha\beta}(t) = \begin{bmatrix} v_{\alpha} \\ v_{\beta} \end{bmatrix} \begin{bmatrix} i_{\alpha} & i_{\beta} \end{bmatrix} = v_{\alpha} i_{\alpha} + v_{\beta} i_{\beta} \quad (2.17)$$

Using the above equations and considering the orthogonal nature of vectors \bar{v} and \bar{q} ($\bar{v} \cdot \bar{q} = 0$) the reference source current in the $\alpha\beta 0$ frame is

$$\begin{bmatrix} i_{s\alpha} \\ i_{s\beta} \\ i_{s0} \end{bmatrix} = \frac{1}{2} \begin{bmatrix} v_{\alpha} & 0 & v_0 & -v_{\beta} \\ v_{\beta} & -v_0 & 0 & v_{\alpha} \\ v_0 & v_{\beta} & -v_{\alpha} & 0 \end{bmatrix} \begin{bmatrix} p \\ q_{\alpha} \\ q_{\beta} \\ q_0 \end{bmatrix} \quad (2.18)$$

$$\begin{bmatrix} i_{s\alpha ref} \\ i_{s\beta ref} \\ i_{s0 ref} \end{bmatrix} = \frac{1}{2} \begin{bmatrix} v_{\alpha} & 0 & v_0 & -v_{\beta} \\ v_{\beta} & -v_0 & 0 & v_{\alpha} \\ 0 & v_{\beta} & -v_{\alpha} & 0 \end{bmatrix} \begin{bmatrix} \overline{P_{L\alpha\beta} + P_{L0}} \\ 0 \\ 0 \\ 0 \end{bmatrix} \quad (2.19)$$

$$\begin{bmatrix} i_{s\alpha ref} \\ i_{s\beta ref} \\ i_{s0 ref} \end{bmatrix} = \frac{\overline{P_{L\alpha\beta} + P_{L0}}}{2} \begin{bmatrix} v_{\alpha} \\ v_{\beta} \\ 0 \end{bmatrix} \quad (2.20)$$

2.2.2.2 Instantaneous Active and Reactive Current (I_d - I_q) Control Strategy

In Fig. 2.7, the entire reference current generation scheme has been illustrated. This control strategy is also known as synchronous reference frame (SRF) [7, 26, 43-50]. Here, the reference frame d-q is determined by the angle ' θ ' with respect to the ' α - β ' frame used in the p - q theory. In I_d - I_q control strategy [43], only the currents magnitudes are transformed and the p - q formulation is only performed on the instantaneous active I_d and reactive I_q components.

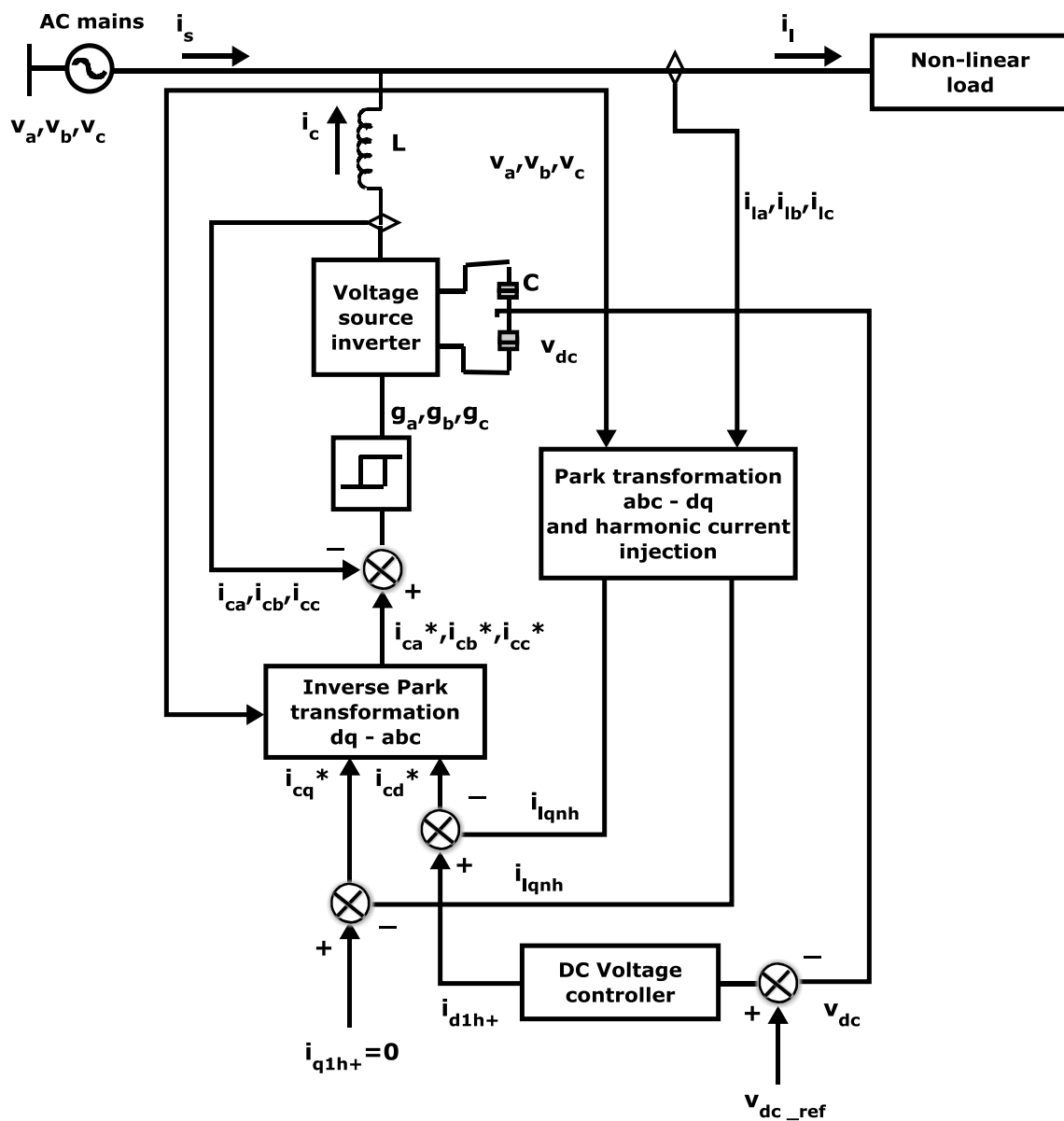


Fig. 2.7 Control method for Shunt current compensation based on I_d - I_q control strategy

In the synchronous d-q reference frame [44], voltage and current signals are transformed to a synchronously rotating frame, in which fundamental quantities become dc quantities, and then the harmonic compensating commands are extracted. The dc-bus voltage feedback is generally used to achieve a self-supporting dc bus in voltage-fed APFs [45]. If the d axis has the same direction as the voltage space vector \bar{v} , then the zero-sequence component of the current remains invariant. Therefore, the I_d - I_q method can be expressed as follows:

$$\begin{bmatrix} i_0 \\ i_{ld} \\ i_{lq} \end{bmatrix} = \frac{1}{v_{\alpha\beta}} \begin{bmatrix} 1 & 0 & 0 \\ 0 & \cos\theta & \sin\theta \\ 0 & -\sin\theta & \cos\theta \end{bmatrix} \begin{bmatrix} i_0 \\ i_{l\alpha} \\ i_{l\beta} \end{bmatrix} \quad (2.21)$$

$$\begin{bmatrix} i_{ld} \\ i_{lq} \end{bmatrix} = S \begin{bmatrix} i_{l\alpha} \\ i_{l\beta} \end{bmatrix} \quad (2.22)$$

$$S = \frac{1}{v_{\alpha\beta}} \begin{bmatrix} v_{\alpha} & v_{\beta} \\ -v_{\beta} & v_{\alpha} \end{bmatrix} \quad (2.23)$$

$$S = \frac{1}{\sqrt{\frac{v_{\alpha}^2}{2} + \frac{v_{\beta}^2}{2}}} \begin{bmatrix} v_{\alpha} & v_{\beta} \\ -v_{\beta} & v_{\alpha} \end{bmatrix} \quad (2.24)$$

Where the transformation matrix S, satisfies $\|S\| = 1$ and $S^{-1} = S^T$

Each current component (I_d , I_q) has an average value or dc component and an oscillating value or ac component

$$i_{ld} = \overline{i_{ld}} + i_{ld} \quad \text{and} \quad i_{lq} = \overline{i_{lq}} + i_{lq} \quad (2.25)$$

The compensating strategy [26] (for harmonic reduction and reactive power compensation) assumes that the source must only deliver the mean value of the direct-axis component [46] of the load current. The reference source current will therefore be

$$i_{sdref} = \overline{i_{Ld}} \quad ; \quad i_{sqref} = i_{s0ref} = 0 \quad (2.26)$$

$$\begin{bmatrix} i_{ld} \\ i_{lq} \\ i_{l0} \end{bmatrix} = \frac{1}{v_{\alpha\beta}} \begin{bmatrix} v_{\alpha} & v_{\beta} & 0 \\ -v_{\beta} & v_{\alpha} & 0 \\ 0 & 0 & v_{\alpha\beta} \end{bmatrix} \begin{bmatrix} i_{L\alpha} \\ i_{L\beta} \\ i_{L0} \end{bmatrix} \quad (2.27)$$

$$i_{Ld} = \frac{v_{\alpha} i_{L\alpha} + v_{\beta} i_{L\beta}}{v_{\alpha\beta}} = \frac{P_{L\alpha\beta}}{\sqrt{\frac{2}{v_{\alpha} + v_{\beta}}}} \quad (2.28)$$

The dc component of the above equation will be

$$\overline{i_{Ld}} = \left(\frac{P_{L\alpha\beta}}{v_{\alpha\beta}} \right)_{dc} = \left(\frac{P_{L\alpha\beta}}{\sqrt{\frac{2}{v_{\alpha} + v_{\beta}}}} \right)_{dc} \quad (2.29)$$

Where, the subscript “dc” means the average value of the expression within the parentheses.

Since the reference source current must be in phase with the voltage at the PCC [47] (and have no zero-sequence component), it will be calculated (in α - β -0 coordinate) by multiplying the above equation by a unit vector in the direction of the PCC voltage space vector (excluding the zero-sequence component):

$$i_{sref} = \overline{i_{Ld}} \frac{1}{v_{\alpha\beta}} \begin{bmatrix} v_{\alpha} \\ v_{\beta} \\ 0 \end{bmatrix} \quad (2.30)$$

$$\begin{bmatrix} i_{saref} \\ i_{s\beta ref} \\ i_{s0ref} \end{bmatrix} = \left(\frac{P_{L\alpha\beta}}{v_{\alpha\beta}} \right)_{dc} \frac{1}{v_{\alpha\beta}} \begin{bmatrix} v_{\alpha} \\ v_{\beta} \\ 0 \end{bmatrix} \quad (2.31)$$

$$\begin{bmatrix} i_{saref} \\ i_{s\beta ref} \\ i_{s0ref} \end{bmatrix} = \left(\frac{P_{L\alpha\beta}}{\sqrt{\frac{2}{v_{\alpha} + v_{\beta}}}} \right)_{dc} \frac{1}{\sqrt{\frac{2}{v_{\alpha} + v_{\beta}}}} \begin{bmatrix} v_{\alpha} \\ v_{\beta} \\ 0 \end{bmatrix} \quad (2.32)$$

The reference signals thus obtained are compared with the actual compensating filter currents in a hysteresis comparator, where the actual current is forced to follow the reference and provides instantaneous compensation by the APF [48] on account of its easy implementation and quick prevail over fast current transitions. This consequently provides switching signals to trigger the IGBTs inside the inverter. Ultimately, the filter provides necessary compensation for harmonics in the source current and reactive power unbalance in the system. **Fig. 2.8** shows, voltage and current vectors in stationary and rotating reference frames. The transformation angle ' θ ' is sensible to all voltage harmonics and unbalanced voltages; as a result $d\theta/dt$ may not be constant.

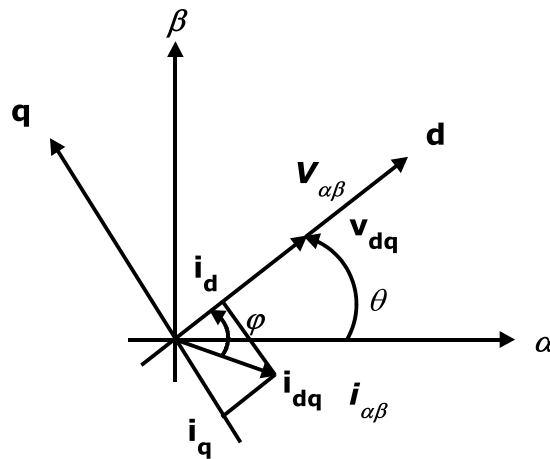


Fig. 2.8 Instantaneous voltage and current vectors

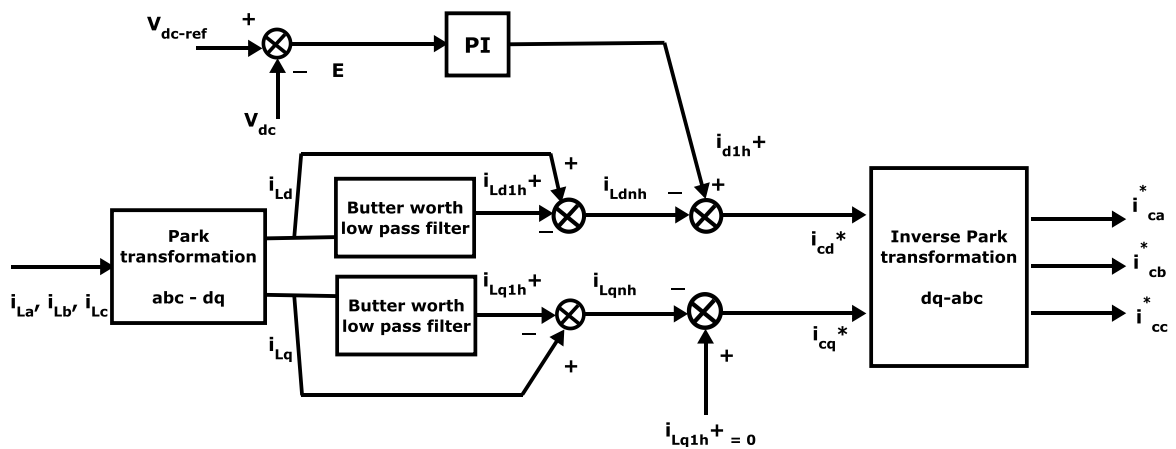


Fig. 2.9 Reference current extraction with I_d - I_q control strategy with PI controller

Therefore, current control of PWM converters is one of the most important subjects of modern power electronics. In comparison to conventional open-loop voltage PWM converters, the current controlled PWM (CC-PWM) [51] converters have the following advantages:

- ↪ Control of instantaneous current waveform and high accuracy;
- ↪ Peak current protection;
- ↪ Overload rejection;
- ↪ Extremely good dynamics;
- ↪ Compensation of the semiconductor voltage drop and dead times of the converter;
- ↪ Compensation of the dc-link and ac-side voltage changes.

2.2.3.1 Generation of Gating Signals to the Devices of the APF

The third stage of control of the APF is to generate gating signals for the solid-state devices of the APF based on the derived compensating commands, in terms of voltages or currents. A variety of approaches, such as; hysteresis-based current control, PWM current or voltage control, deadbeat control, sliding mode of current control, PI controller, Fuzzy-based current control, Neural network-based current control, etc., can be implemented, either through hardware or software to obtain the control signals for the switching devices of the APF. Out of all these approaches we have considered, hysteresis-based current control [50-54], Proportional – Integral (PI) controller [7] and Fuzzy logic controller [7-11, 26, 50]. In Chapter – 3, Fuzzy logic controller is explained in detail.

2.2.3.1.1 Hysteresis Current Control Scheme

The hysteresis band current control technique [50] is the most suitable for the applications of current controlled voltage source inverters in active power filters, grid

connected systems and IPM (interior permanent magnet) machines. Basic requirements of a CC-PWM are the followings:

- ↳ No phase and amplitude errors (ideal tracking) over a wide output frequency range
- ↳ To provide better dynamic response of the system
- ↳ Low harmonic content
- ↳ Limited or constant switching frequency to guarantees APF operation of converter semiconductor power devices.

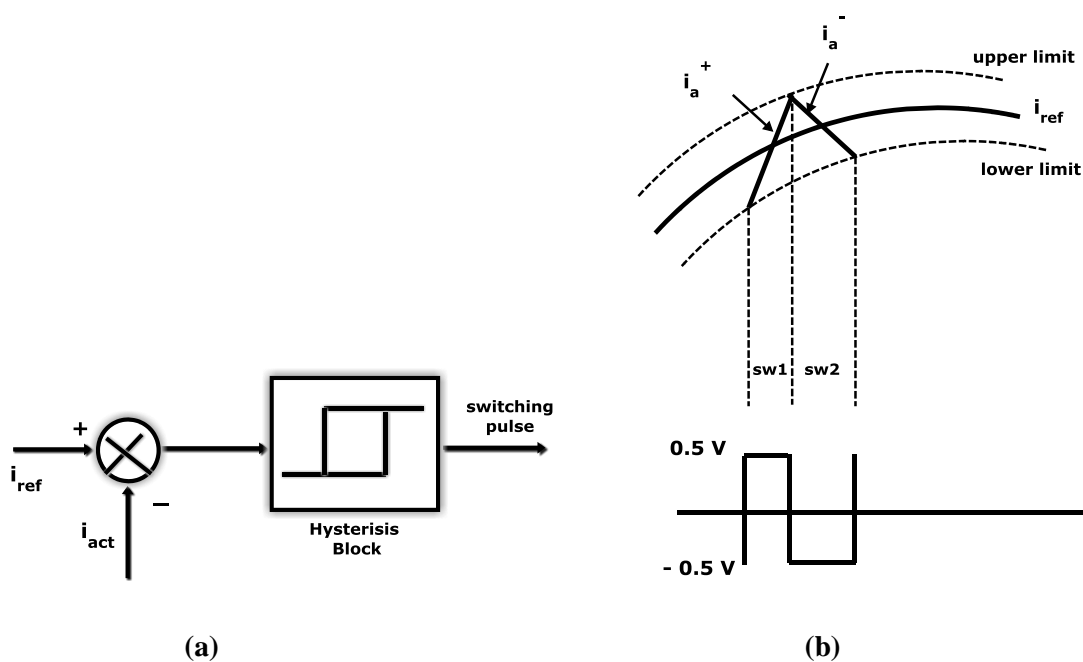


Fig. 2.11 (a) Details of voltage and current wave with hysteresis band current controller.

(b) Details of hysteresis band current controller

The hysteresis band current control is characterized by unconditioned stability, very fast response, and good accuracy [50]. However, this control scheme exhibits several demerits, such as variable switching frequency, possible to generate resonances and difficult to design the passive filter system. This unpredictable switching function affects the active filter efficiency and reliability. It may well be that Fuzzy logic systems [7, 11-13, 26, 50, 54, 62, 65], resolve some of the challenges which existing methods face. The hysteresis band current

control idea used for the control of active power filter line current is demonstrated in **Fig. 2.11 (a) and (b)**.

The actual source currents are monitored instantaneously, and then compared to the reference currents generated by the proposed algorithm. In order to get accurate control, switching of IGBT [29] device should be such that the error signal should approaches to zero, thus provides quick response. For this reason, hysteresis current controller with fixed band [51] which derives the switching signals of three phase IGBT based VSI bridge is used.

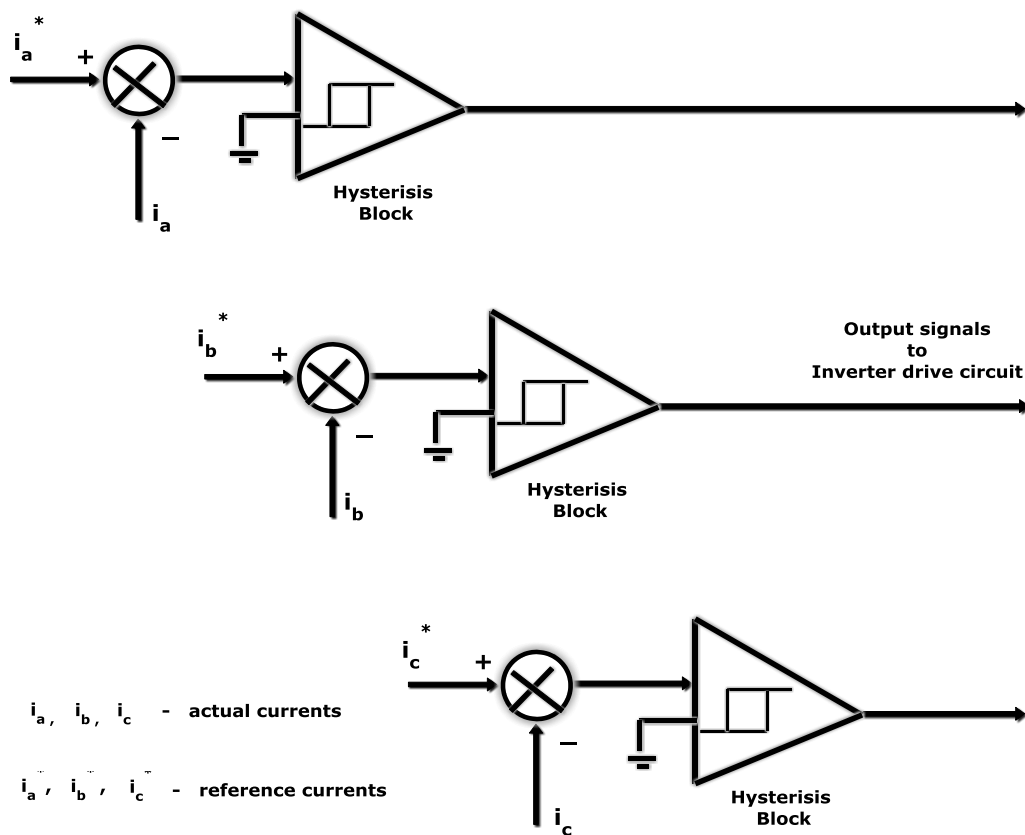


Fig 2.11 (c) Typical Hysteresis Current Controller

Hysteresis control schemes are based on a non-linear feedback loop with two level hysteresis comparators (**Fig. 2.11(a)**). The switching signals are produced directly when the error exceeds an assigned tolerance band (**Fig. 2.11 (b)**). The controller generates the sinusoidal reference current of desired magnitude and frequency that is compared with the actual motor line current. If the current exceeds the upper limit of the hysteresis band [52],

the upper switch of the inverter arm is turned off and the lower switch is turned on. As a result, the current starts to decay. If the current crosses the lower limit of the hysteresis band, the lower switch of the inverter arm is turned off and the upper switch is turned on. As a result, the current gets back into the hysteresis band. Hence, the actual current is forced to track the reference current within the hysteresis band [53].

The upper device and the lower device in one phase leg of VSI are switched in complementary manner else a dead short circuit will take place. The APF reference currents I_{sa}^* , I_{sb}^* , I_{sc}^* compared with the sensed source currents I_{sa} , I_{sb} , I_{sc} and the error signals are operated by the hysteresis current controller to generate the firing pulses, which activate the inverter power switches in a manner that reduces the current error. The hysteresis band current controller [54] decides the switching pattern of active power filter. **Fig. 2.11 (c)** shows, the hysteresis current control modulation scheme, consisting of three hysteresis comparators, one for each phase.

2.3 Introduction to DC Link Voltage Regulation

For regulating and maintaining the DC link capacitor voltage constant, the active power flowing into the active filter needs to be controlled. If the active power flowing into the filter can be controlled equal to the losses inside the filter, the DC link voltage [59] can be maintained at the desired value. The quality [60] and performance of the SHAF depend mainly on the method implemented to generate the compensating reference currents [61]. This dissertation presented two methods to get the reference current, which is the key issue in the control of the SHAF [62]. In order to maintain DC link voltage constant and to generate the compensating reference currents, we have developed the following controllers:

1. PI Controller
2. Fuzzy logic controller

(a) Type – 1 Fuzzy logic controller with different Fuzzy MFs

(b) Type – 2 Fuzzy logic controller with different Fuzzy MFs

2.3.1. Dc Link Voltage Regulation with PI Controller

Fig 2.12 shows, the internal structure of the control circuit. The control scheme consists of PI controller, limiter, and three phase sine wave generator for reference current generation and generation of switching signals. The peak value of reference currents [63] is estimated by regulating the DC link voltage. The actual capacitor voltage is compared with a set reference value. The error signal is then processed through a PI controller, which contributes to zero steady error in tracking the reference current signal.

The output of the PI controller [64] is considered as peak value of the supply current (I_{max}), which is composed of two components:

(a) Fundamental active power component of load current, and

(b) Loss component of APF, to maintain the average capacitor voltage to a constant value.

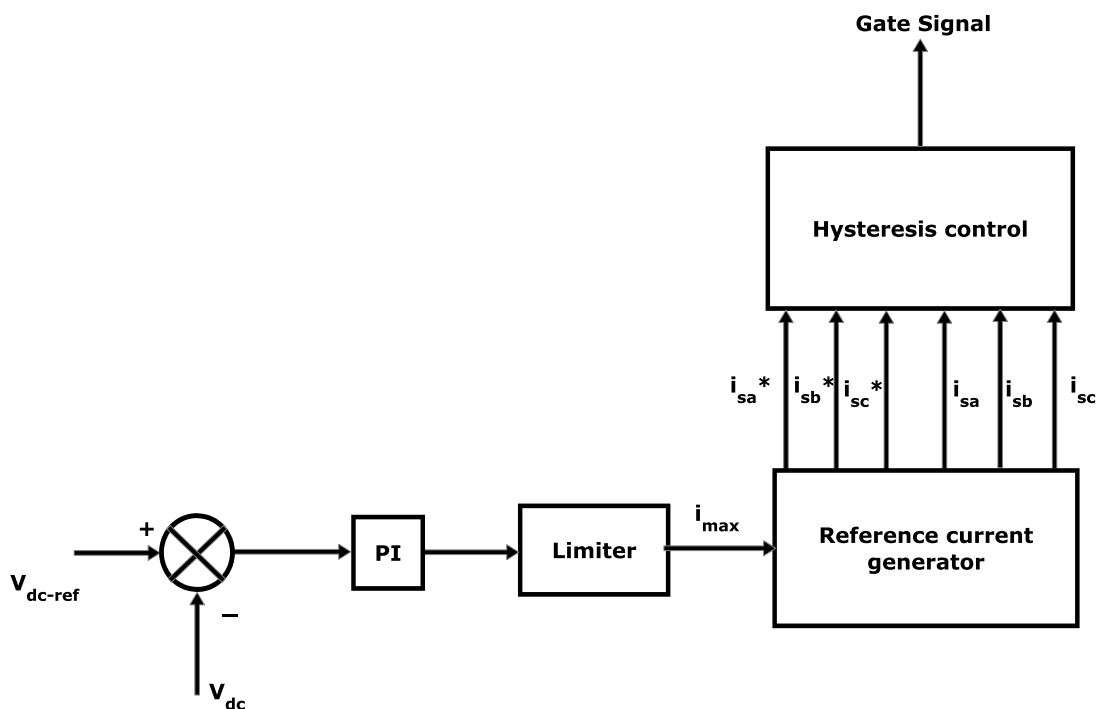


Fig 2.12 Conventional PI Controller

The peak value of the current (I_{\max}) so obtained, is multiplied by the unit sine vectors in phase with the respective source voltages to obtain the reference compensating currents. These estimated reference currents (I_{sa}^* , I_{sb}^* , I_{sc}^*) and sensed actual currents (I_{sa} , I_{sb} , I_{sc}) are compared in a hysteresis band, which gives the error signal for the modulation technique. This error signal decides the operation of the converter switches. In this current control circuit configuration, the source/supply currents I_{sabc} are made to follow the sinusoidal reference current I_{abc} , within a fixed hysteretic band [65, 81]. The width of hysteresis window determines the source current pattern, its harmonic spectrum and the switching frequency of the devices.

The DC-link capacitor voltage is kept constant throughout the operating range of the converter. In this scheme, each phase of the converter is controlled independently. To increase the current of a particular phase, the lower switch of the converter associated with that particular phase is turned on while to decrease the current the upper switch of the respective converter phase is turned on. With this one can realize the potential and feasibility of PI controller.

2.4. System performance of $p-q$ and I_d-I_q control strategies with PI controller using MATLAB/SIMULINK.

Fig. 2.13 and Fig. 2.14, highlights the performance of SHAF using $p-q$ and I_d-I_q control strategies with PI controller under balanced, un-balanced and non- sinusoidal conditions, using MATLAB/SIMULINK. As load is highly inductive, current draw by load is integrated with rich harmonics. **Fig. 2.13 and Fig. 2.14**, gives the details of Source Voltage, Load Current, Compensation current, Source Current with filter, DC Link Voltage, THD (Total harmonic distortion) of $p-q$ and I_d-I_q control strategies with PI controller using MATLAB under balanced, un-balanced and non-sinusoidal supply voltage conditions.

When the supply voltages are balanced and sinusoidal, the two control strategies; Instantaneous Active and Reactive power ($p-q$) control strategy and Instantaneous Active and Reactive current (I_d-I_q) control strategy are converging to the same compensation characteristics. But, when the supply voltages are distorted and/or un-balanced sinusoidal, these control strategies result in different degrees of compensation of harmonics. The $p-q$ control strategy is unable to yield an adequate solution, when source voltages are not ideal.

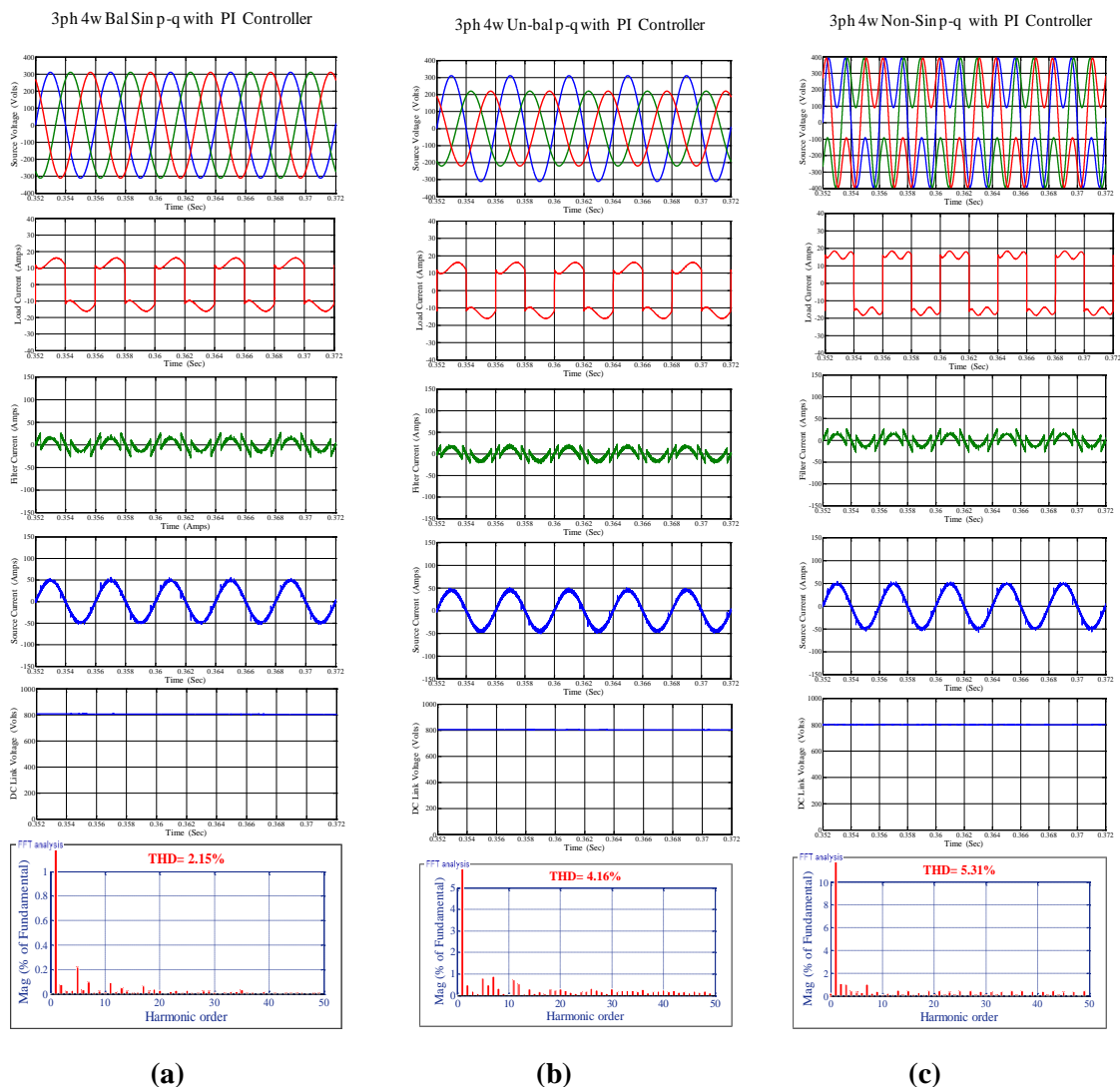


Fig. 2.13 SHAF response using $p-q$ control strategy with PI controller using MATLAB under

(a) *Balanced Sinusoidal* (b) *Un-balanced Sinusoidal* and (c) *Balanced Non-Sinusoidal*.

(i) Source Voltage (ii) Load Current (iii) Compensation current (iv) Source Current with filter

(v) DC Link Voltage (vi) THD of Source current

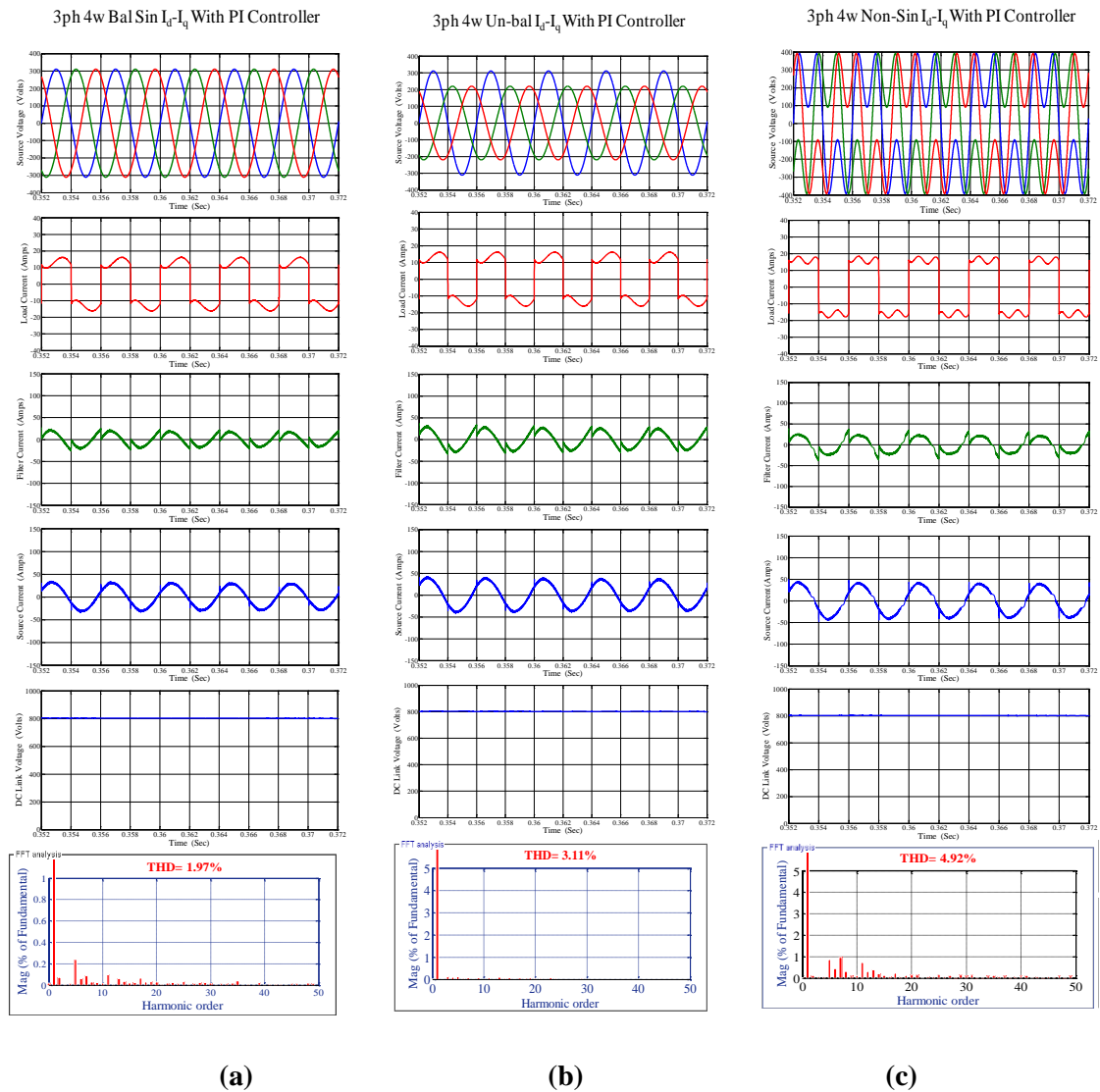


Fig. 2.14 SHAF response using I_d-I_q control strategy with PI controller using MATLAB under

(a) *Balanced Sinusoidal* (b) *Un-balanced Sinusoidal* and (c) *Balanced Non-Sinusoidal*.

(i) Source Voltage (ii) Load Current (iii) Compensation current (iv) Source Current with filter

(v) DC Link Voltage (vi) THD of Source current

The THD of $p-q$ control strategy with PI controller under balanced, un-balanced and non-sinusoidal conditions using MATLAB is 2.15%, 4.16% and 5.31% respectively and the THD of I_d-I_q control strategy with PI controller is 1.97%, 3.11% and 4.93% respectively.

2.5 system performance of $p-q$ and I_d-I_q control strategies with PI controller using Real-time digital simulator

In Chapter-5, a specific class of digital simulator known as a real-time simulator has been introduced by answering the questions “what is real-time simulation”, “why is it needed” and “How it works”. Real-time implementation of Shunt active filter model is shown in Fig.

2.15. It consists of

- a) **Host computer**
- b) **Target (Real-time Simulator)** and
- c) **Oscilloscope**

In host computer, Edition of Simulink model; Model compilation with RT-LAB and user interface is done. In target system, I/O and model execution process is done and results are displayed in oscilloscope. In Fig. 2.15, oscilloscope displays four waveforms, first waveform is **Load Current (or Source current before filtering)**; second waveform is **Filter Current (Compensation Current)**; third waveform is **Source current after filtering** and finally fourth waveform is **DC-Link voltage**.



Fig. 2.15 Real-time implementation of Shunt active filter control strategies using OPAL – RT

Application fields of OPAL-RT Simulator are

- Electrical & Power Systems
- Aerospace & Defence
- Automotive
- Academic & Research

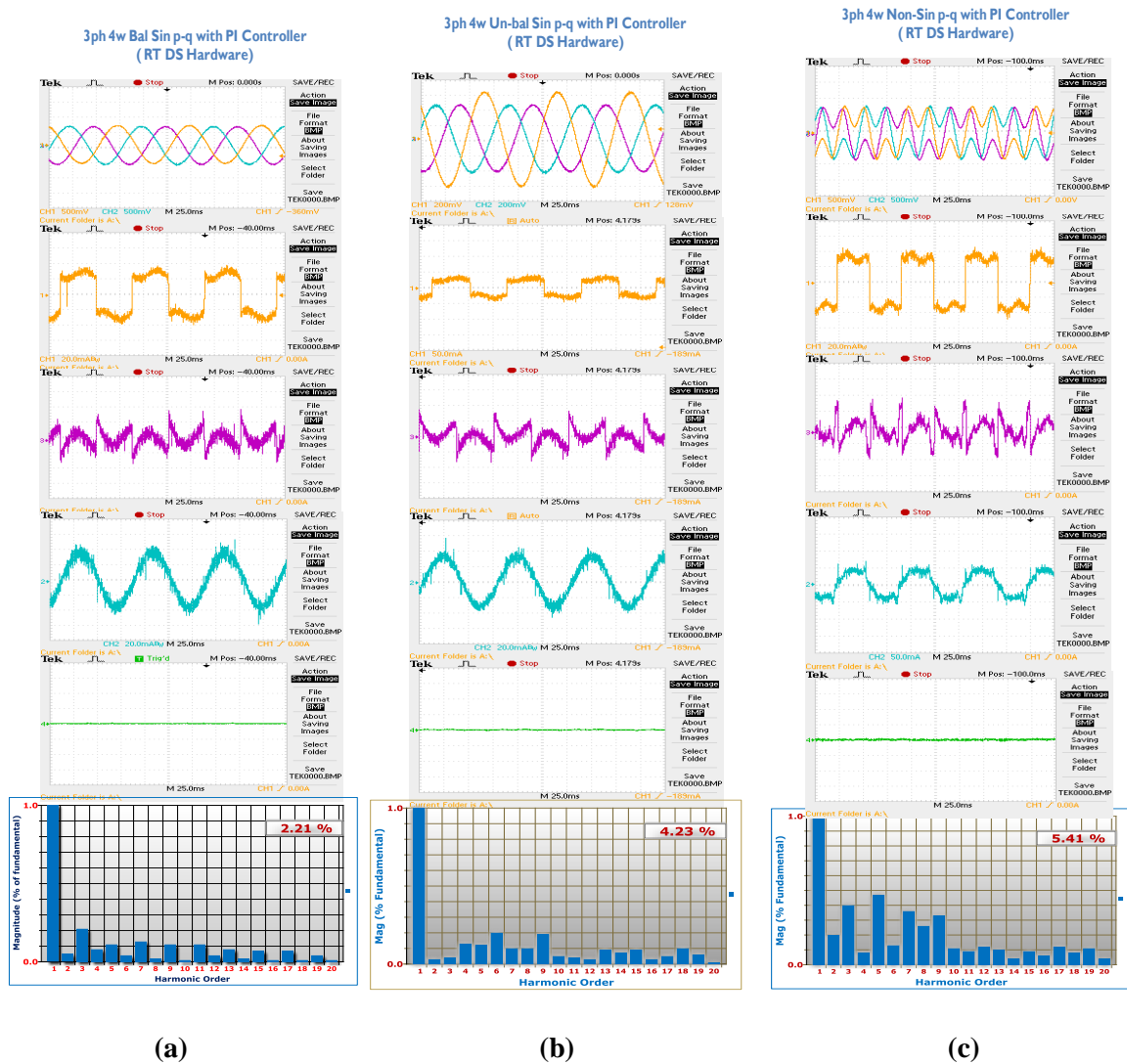


Fig. 2.16 SHAF response using p - q control strategy with PI controller using Real-time digital simulator under

(a) *Balanced Sinusoidal* (b) *Un-balanced Sinusoidal* and (c) *Balanced Non-Sinusoidal*.

(i) Source Voltage (ii) Load Current (Scale 20A/div) (iii) Compensation current (Scale 20A/div) (iv) Source Current (Scale 30A/div) with filter (v) DC Link Voltage (vi) THD of Source current

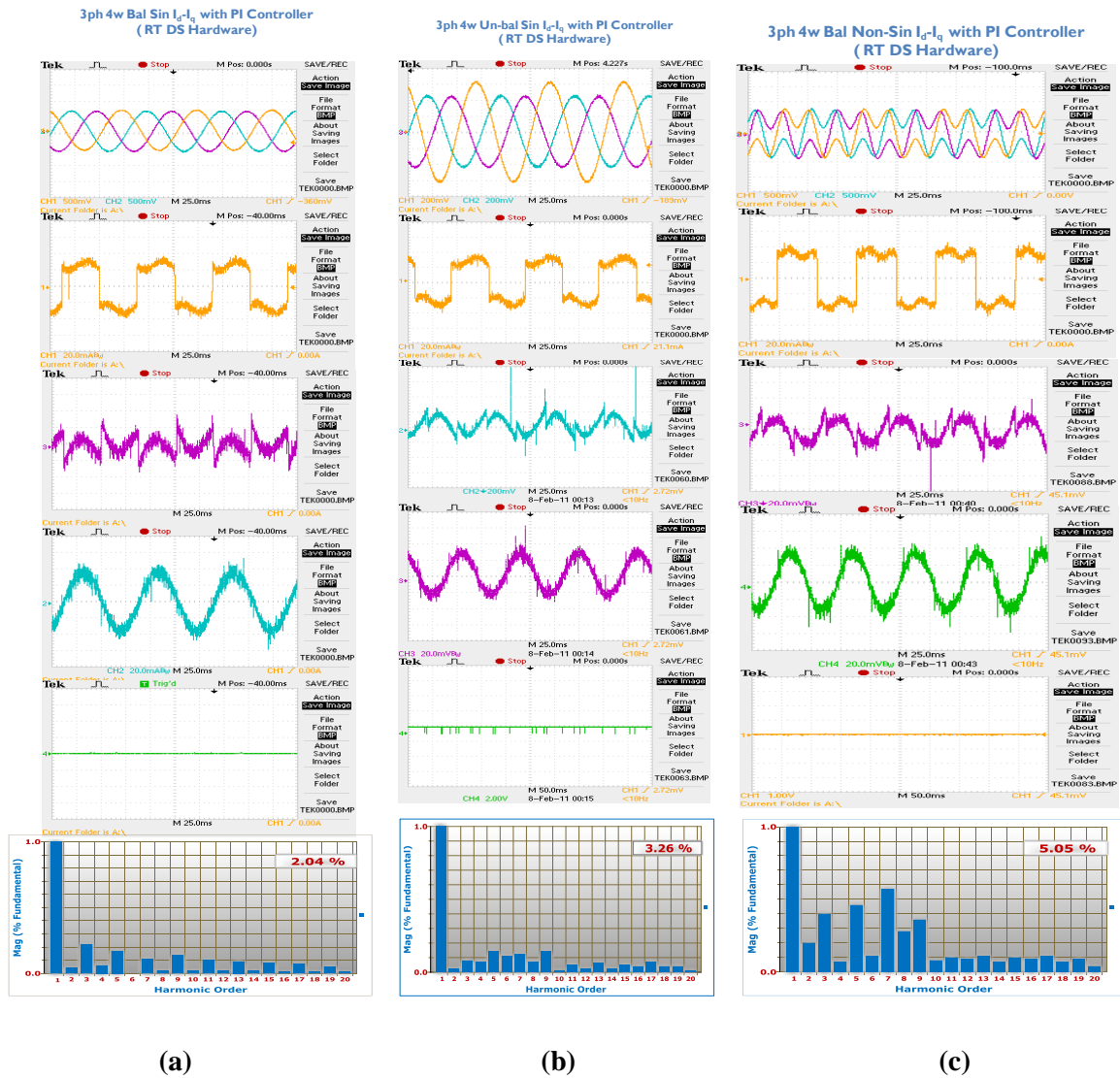


Fig. 2.17 SHAF response using I_d - I_q control strategy with PI controller using Real-time digital simulator under

(a) Balanced Sinusoidal (b) Un-balanced Sinusoidal and (c) Balanced Non-Sinusoidal.

(i) Source Voltage (ii) Load Current (**Scale 20A/div**) (iii) Compensation current (**Scale 20A/div**) (iv) Source Current (**Scale 30A/div**) with filter (v) DC Link Voltage (vi) THD of Source current

Fig. 2.16 and **Fig. 2.17**, presents the details of Source Voltage, Load Current, Compensation current, Source Current with filter, DC Link Voltage, THD of p - q and I_d - I_q control strategies with PI controller using Real-time digital simulator under balanced, un-balanced and non-sinusoidal supply voltage conditions.

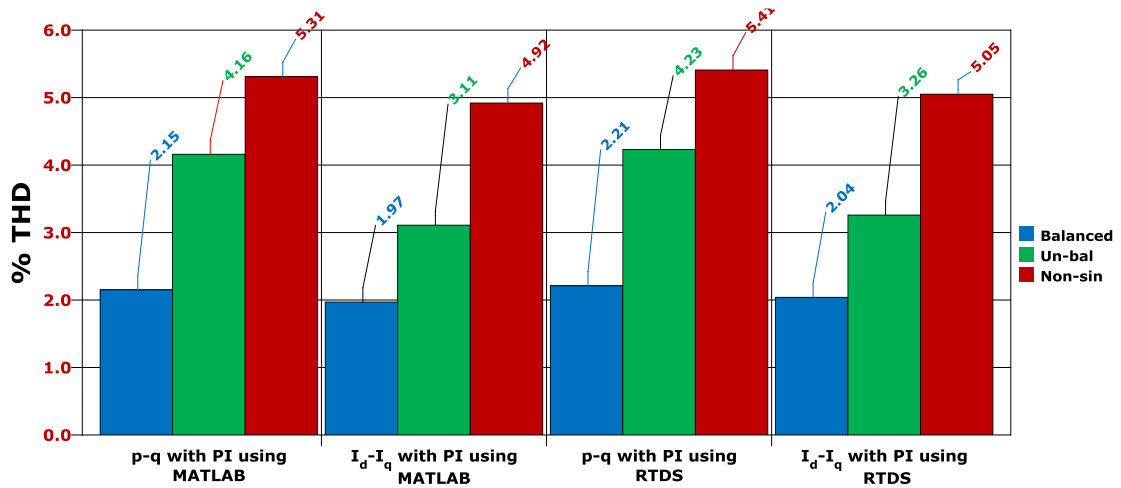


Fig. 2.18 THD of Source Current for $p-q$ and I_d-I_q control strategies with PI Controller Using MATLAB and Real-time digital simulator

Table 2.2 System parameters

Parameter	Value
Supply Voltage	$V_s = 311.12 \text{ V}$
Source Resistance	$R_s = 0.1 \Omega$
Source Inductance	$L_s = 1 \text{ mH}$
Filter Phase-branch Resistance	$R_f = 0.01 \Omega$
Filter Phase-branch Inductance	$L_f = 0.1 \text{ mH}$
DC Link Capacitance	$C_{dc} = 3000 \mu\text{f}$
DC Link Voltage	$V_{dc} = 800 \text{ V}$
Hysterisis band	$\pm 0.2 \text{ A}$
Load	Diode rectifier Snubber Resistance $R_{sn} = 500 \Omega$ Snubber Capacitance $L_{sn} = 250 \text{ e-9 f}$
Load Resistance	$R_L = 15 \Omega$
Load Inductance	$L_L = 60 \text{ mH}$

The THDs of $p-q$ control strategy with PI controller under balanced, un-balanced and non-sinusoidal conditions using Real-Time Digital Simulator are 2.21%, 4.23% and 5.41% respectively and the THDs of I_d-I_q control strategy with PI controller are 2.04%, 3.26% and

5.05% respectively. **Fig. 2.18, bar graph** clearly illustrates the THD of source current for shunt active filter control strategies ($p-q$ and I_d-I_q) with PI controller using MATLAB and Real-time digital simulator under various source voltage conditions.

While considering $p-q$ control strategy with PI controller, SHAF is not succeeded in compensating harmonic currents, notches are observed in the source current. The main reason behind the notches is that the controller failed to track the current correctly and thereby APF fails to compensate completely. The PI controller is unable to mitigate the harmonics effectively, notches are observed in the source current. So to mitigate the harmonics perfectly, one has to choose perfect controller. So to avoid the difficulties occur with PI controller, we have considered Type-1 Fuzzy logic controller (**Type-1 FLC**) based $p-q$ and I_d-I_q control strategies with different Fuzzy MFs (Trapezoidal, Triangular and Gaussian MF). The System Parameters are given in **Table. 2.2**

2.6 Summary

In this chapter, PI controller based shunt active filter control strategies ($p-q$ and I_d-I_q) are considered for extracting the three-phase reference currents for power quality improvement. Three-phase reference current waveforms generated by proposed scheme are tracked by the three-phase voltage source converter in a hysteresis band control scheme. The performance of the control strategies has been evaluated in terms of harmonic mitigation and DC link voltage regulation using MATLAB/SIMULINK and real-time digital simulator.

The mitigation of harmonics is poor, when the THD of source current is more. Under unbalanced and non-sinusoidal conditions PI controller based shunt active filter ($p-q$ and I_d-I_q) control strategies are unable to mitigate harmonics completely and THD is close to 5%. But, according to IEEE 519-1992 standard THD must be less than 5%. So to mitigate harmonics effectively, we have considered Type-1 FLC based $p-q$ and I_d-I_q control strategies with different Fuzzy MFs (Trapezoidal, Triangular and Gaussian MF).

Chapter - 3

Performance analysis of Shunt active filter control strategies using Type-1 FLC with different Fuzzy MFs

Type-1 Fuzzy logic Controller

- ↳ *Fuzzy Inference Systems*
- ↳ *De-fuzzification methods*
- ↳ *Design of control rules*

Simulation and Real-time results

Comparative study

Summary

CHAPTER – 3

In the previous chapter-2, shunt active filter control strategies are discussed. It is concluded that under un-balanced and non-sinusoidal conditions PI controller is unable to mitigate the harmonics completely and THD is close to 5%. But, according to IEEE 519-1992 standard THD must be less than 5%. So to mitigate the harmonics perfectly, one has to choose perfect controller.

*In this **chapter**, we have developed Type-1 Fuzzy logic controller (**Type-1 FLC**) with **different Fuzzy MFs (trapezoidal, triangular and Gaussian)**. The Shunt active filter control strategies (**p-q** and **I_d-I_q**) for extracting the three-phase reference currents are compared, evaluating their performance under different source voltage conditions using Type-1 FLC. The performance of the control strategies have been evaluated in terms of harmonic mitigation and DC link voltage regulation. The detailed simulation results using **MATLAB/SIMULINK** software are presented to support the feasibility of proposed control strategies. To validate the proposed approach, the system is also implemented on a **Real-Time Digital Simulator** and adequate results are reported for its verifications.*

This chapter is organized as follows: Section 3.1 provides the details of Type-1 Fuzzy Logic Controller which includes types of Fuzzy Inference Systems, Defuzzification methods and design of control rules, Simulation results of Type-1 FLC based p-q and I_d-I_q control strategies with different Fuzzy MFs using MATLAB are presented in Sections 3.2 and 3.3 respectively, real-time results of Type-1 FLC based p-q and I_d-I_q control strategies with different Fuzzy MFs using real-time digital simulator (OPAL-RT) are presented in Sections 3.4 and 3.5 respectively, Section 3.6 provides the comparative study and finally Section 3.7 states all concluding remarks.

3.1. Type-1 Fuzzy Logic Controller

The concept of Fuzzy Logic (FL) [82] was proposed by Professor Lofti Zadeh in 1965, at first as a way of processing data by allowing partial set membership rather than crisp

membership. Soon after [83-107], it was proven to be an excellent choice for many control system applications [84] since it mimics human control logic.

Fig 3.1 shows, the internal structure of the control circuit. The control scheme consists of Fuzzy logic controller (FLC) [85], limiter, and three phase sine wave generator for reference current generation and generation of signals for the switching devices of APF. The peak value of reference currents is estimated by regulating the DC link voltage [26]. The actual capacitor voltage is compared with a set reference value. The error signal is then processed through FLC, which contributes to zero steady error in tracking the reference current signal.

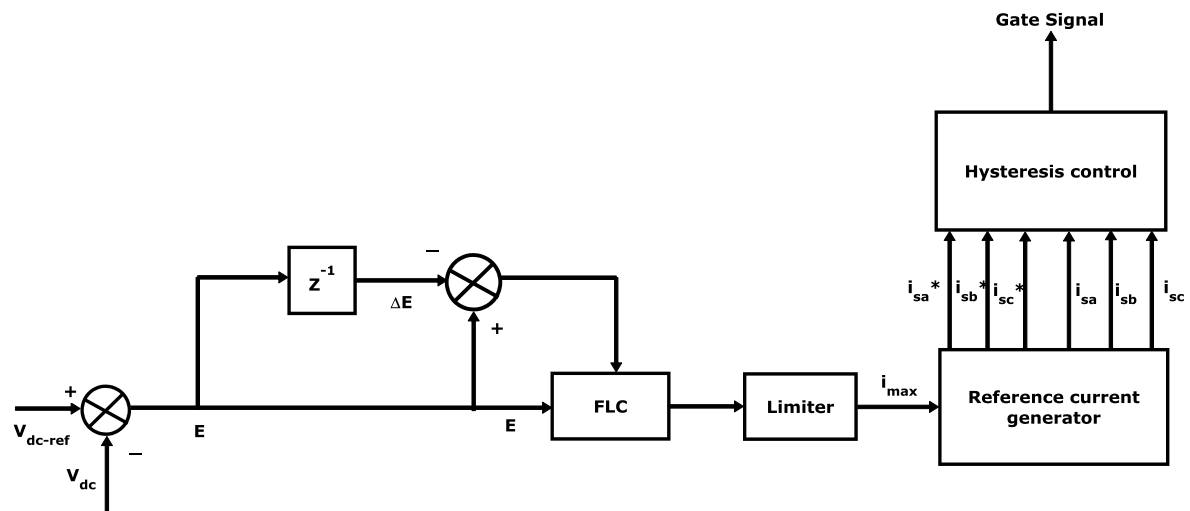


Fig. 3.1 Proposed Fuzzy logic Controller

The block diagram [50] of Fuzzy logic controller is shown in **Fig 3.2**. It consists of blocks

- ↳ Fuzzification
- ↳ Fuzzy Inference system
- ↳ Knowledge base
- ↳ Defuzzification

3.1.1. Fuzzification

The process of converting a numerical variable (real number) to a linguistic variable (Fuzzy number) is called fuzzification [86].

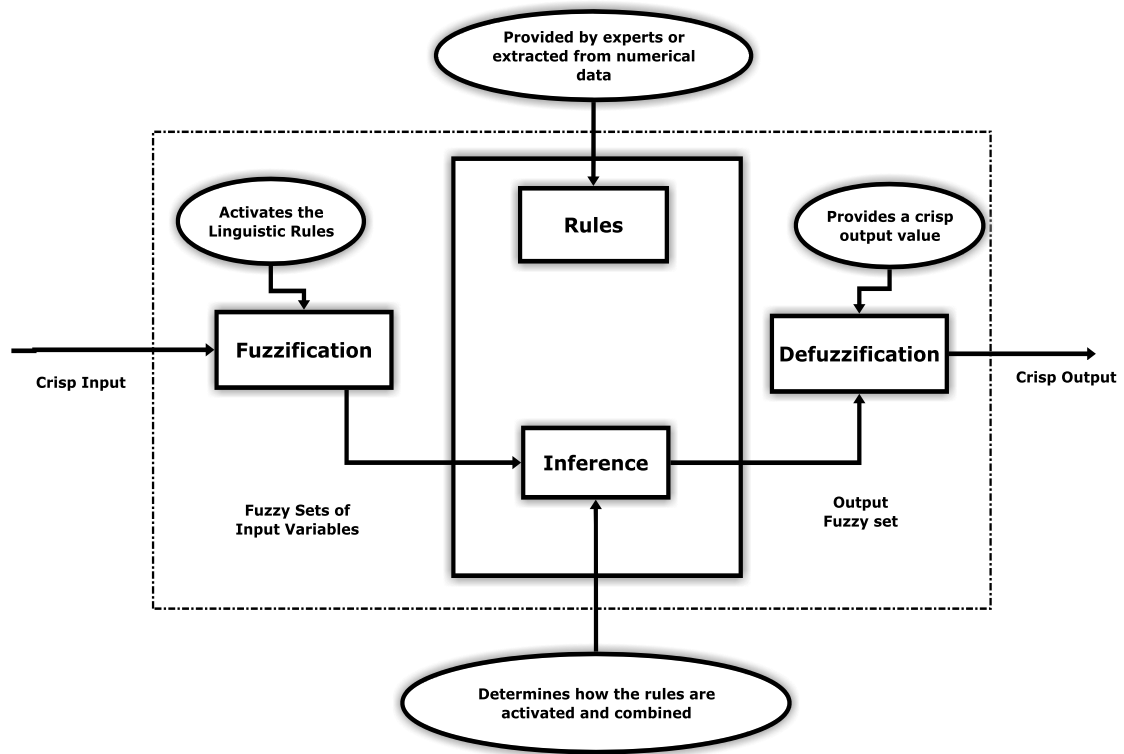


Fig.3.2 Block Diagram of Fuzzy Logic Controller (FLC)

3.1.2. Fuzzy Inference Systems

The Fuzzy inference system (FIS) [87] is a popular computing framework based on the concepts of Fuzzy set theory [88], Fuzzy if-then rules and Fuzzy reasoning. It has found successful applications in a wide variety of fields, such as expert systems, data classification, decision analysis, time-series prediction, automatic control, pattern recognition and robotics. Because of its multi-disciplinary nature, the FIS is known by various other names, such as; Fuzzy rule-based system, Fuzzy expert system [89], Fuzzy model [90], Fuzzy logic controller [91], Fuzzy associative memory [92] and simply Fuzzy system.

The basic structure of a FIS consists of three components: a **rule base**, which contains a selection of rules, a **data base**, which defines the membership functions used in the Fuzzy rules and a **reasoning mechanism**, which performs the inference procedure upon the rules and given facts to derive a reasonable output. The basic FIS [93] can take either crisp inputs or Fuzzy singletons, but the outputs it produces are almost always fuzzy sets. Sometimes it is

necessary to have a crisp output, especially in a situation where a FIS is used as a controller. Therefore, we need a method of defuzzification to extract a crisp value that best represents a Fuzzy set. A FIS with a crisp output is shown in **Fig. 3.3**. Where the dashed line indicates a basic Fuzzy inference system with Fuzzy output and defuzzification [94] block serves the purpose of transforming an output Fuzzy set into a crisp value. Defuzzification strategies [95] are explained in section 3.1.3.

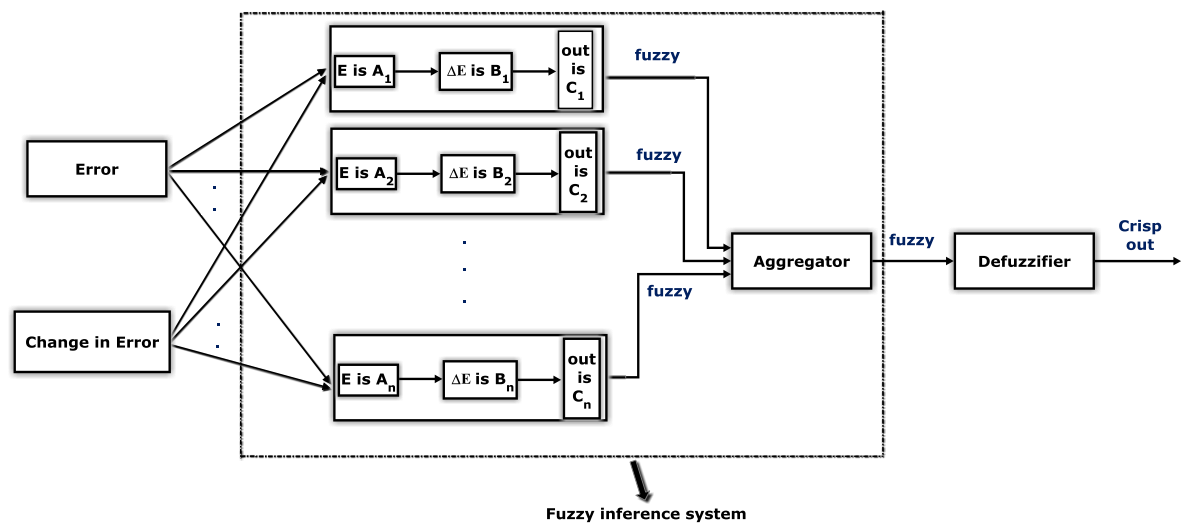


Fig. 3.3 Block diagram of Fuzzy Inference system

The **Mamdani** Fuzzy implication models [97] are used for evaluation of individual rules. There are mainly two types implication methods are used. The differences between these two Fuzzy inference systems lie in the consequents of their Fuzzy rules, and thus their aggregation and differ accordingly.

1. Mamdani **Max-min** composition scheme
2. Mamdani **Max-prod** composition scheme

3.1.2.1 Mamdani Max-min composition scheme

The Mamdani Fuzzy inference system using **Max-Min** composition [50] scheme is shown in **Fig. 3.4**. In this Fig. 3.4 aggregation used is Maximum operation and implication is Minimum operation.

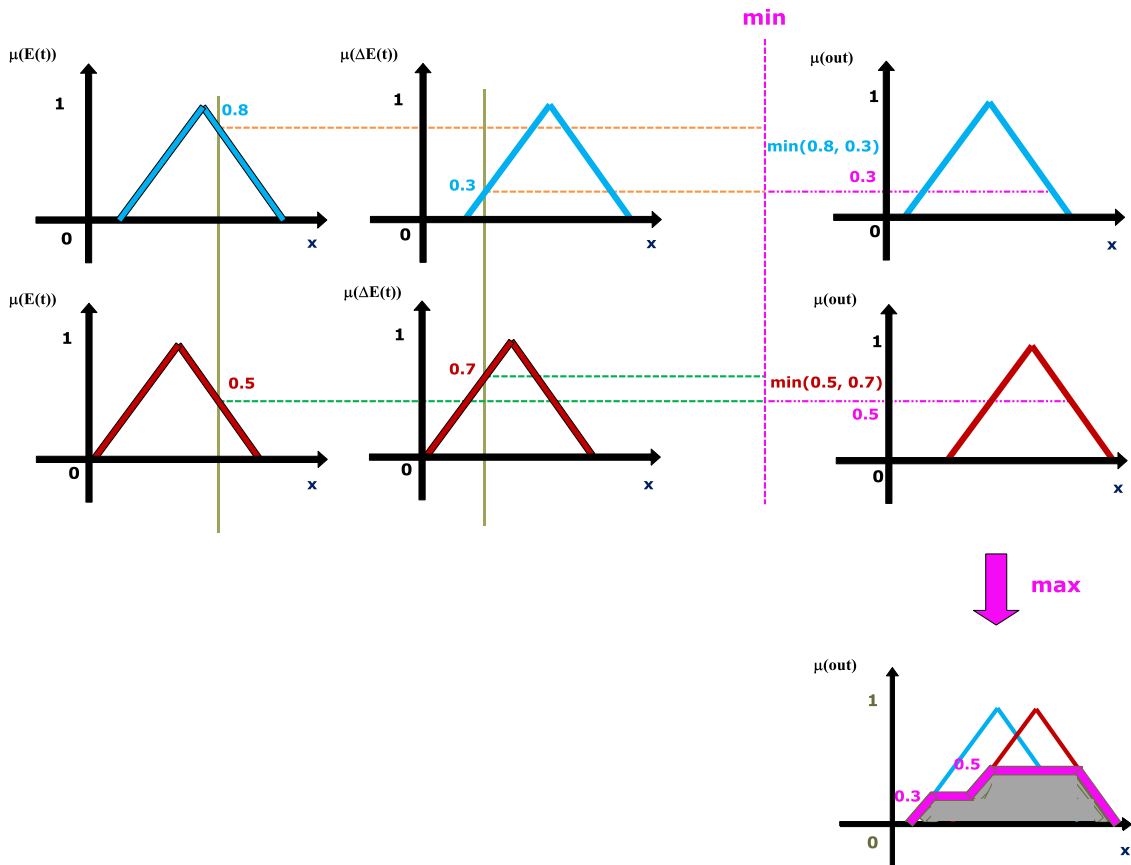


Fig. 3.4 The Mamdani Fuzzy inference system using Max-Min composition

3.1.2.2. Mamdani Max-prod composition scheme

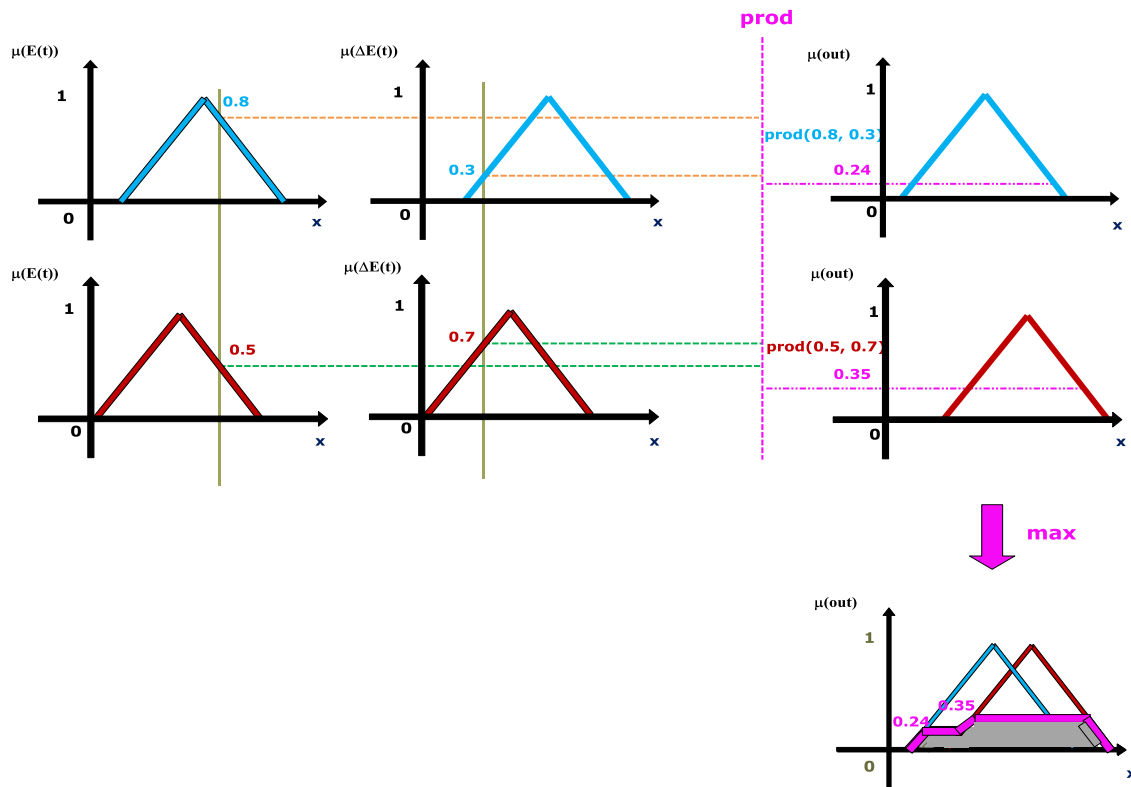


Fig. 3.5 The Mamdani Fuzzy inference system using Max-Prod composition

The Mamdani Fuzzy inference system using **Max-Prod** composition [96] scheme is shown in **Fig. 3.5**. In this Fig. 3.5 aggregation used is Maximum operation and implication is product operation.

3.1.3. De-fuzzification:

The rules of FLC generate required output in a linguistic variable [97] (Fuzzy Number), according to real world requirements, linguistic variables have to be transformed to crisp output (Real number).

$$\mu_A(x) = \text{defuzz}(x, \text{mf}, \text{Type}) \quad (3.1)$$

Where $\text{defuzz}(x, \text{mf}, \text{Type})$ gives a defuzzified value of a membership function (MF) positioned at associated variable value x using one of several defuzzification methods [98] according to the argument type. The variable type can be one of the followings:

- ↪ COA : centroid of area,
- ↪ BOA : bisector of area,
- ↪ MOM : mean value of maximum
- ↪ SOM : smallest (absolute) value of maximum
- ↪ LOM : largest (absolute) value of maximum.

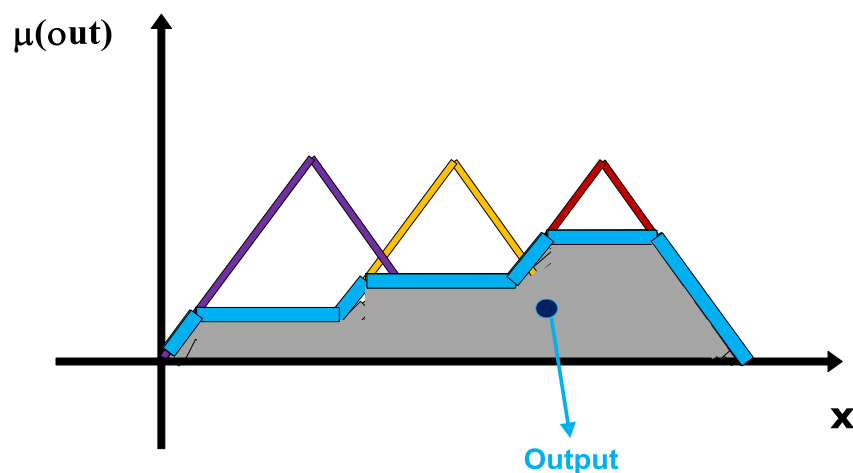


Fig.3.6 Defuzzification

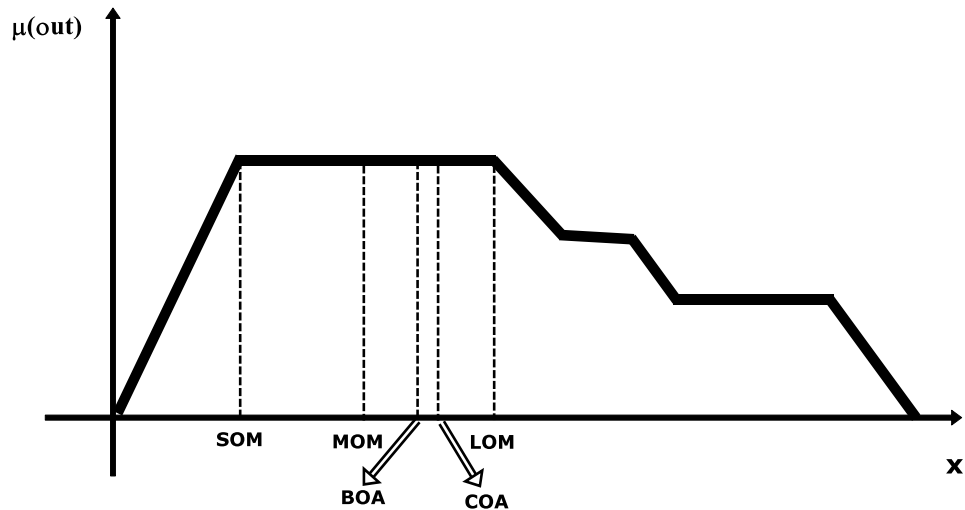


Fig.3.7 Defuzzification methods

After the inference step, the overall result is a Fuzzy value. This result should be defuzzified to obtain a final crisp output. This is the purpose of the defuzzifier component of a FLC. Defuzzification [99] is performed according to the membership function of the output variable. For instance, assume that we have the result in Fig. 3.4 at the end of the inference. In this **Fig. 3.6**, the shaded areas all belong to the Fuzzy result. The purpose is to obtain a crisp value, represented with a dot in the **Fig. 3.6**, from this Fuzzy result. Defuzzification methods are shown in **Fig. 3.7**.

3.1.3.1. Centroid of Area

Centroid defuzzification returns the centre of area under the curve [100]. Mathematically centroid of area (**COA**) can be expressed as:

$$COA = \frac{\int_a^b \mu_A(x) \cdot x \cdot dx}{\int_a^b \mu_A(x) \cdot dx} \quad (3.2)$$

With a discretized universe of discourse, the expression is

$$COA = \frac{\sum_{i=1}^n \mu_A(x_i) \cdot x_i}{\sum_{i=1}^n \mu_A(x_i)} \quad (3.3)$$

3.1.3.2. Bisector of Area

The bisector is the vertical line that will divide the region into two sub-regions of equal area. It is sometimes, but not always coincident with the centroid line. Mathematically bisector of area (**BOA**) can be expressed as:

$$\int_{\alpha}^{X_{BOA}} \mu_A(x) dx = \int_{X_{BOA}}^{\beta} \mu_A(x) dx \quad (3.4)$$

3.1.3.3. Mean, Smallest, and Largest of Maximum

MOM, SOM, and LOM stand for Mean, Smallest, and Largest of Maximum respectively. These three methods key off the maximum value assumed by the aggregate membership function. If the aggregate membership function has a unique maximum, then **MOM**, **SOM**, and **LOM** [101] all take on the same value. Mathematically mean of maximum (MOM) can be expressed as:

$$X_{MOM} = \frac{\int_{X'} x dx}{\int_{X'} dx} \quad (3.5)$$

where $X' = \{x; \mu_A(x) = \mu^*\}$

The Fuzzy controller is characterized as follows:

- ↪ **Seven** Fuzzy sets for each input and output.
- ↪ Fuzzification using continuous universe of discourse.
- ↪ Implication using **Mamdani's 'min'** operator.
- ↪ De-fuzzification using the '**centroid**' method.

3.1.4. Design of control rules

In a FLC [102], a rule base is constructed to control the output variable. A Fuzzy rule is a simple **IF-THEN** rule with a condition and a conclusion. The Fuzzy control rule design involves defining rules that relate the input variables to the output model properties. As FLC

is independent of system model, the design is mainly based on the intuitive feeling for, and experience of the process [103]. The rules are expressed in English like language with syntax such as; **If {error E is X and change in error ΔE is Y} then {control output is Z}**.

For better control performance finer Fuzzy partitioned subspaces {**NB** (negative big), **NM** (negative medium), **NS** (negative small), **ZE** (zero), **PS** (positive small), **PM** (positive medium) and **PB** (positive big)} are used. These **seven** membership functions are same for input and output and characterized using **trapezoidal**, **triangular** and **Gaussian** membership functions [104], as can be seen in **Fig 3.8, 3.9 and 3.10**.

Fuzzy Sets [105, 106] are chosen based on the error in the dc link voltage. We have considered **7x7** membership function. Readers may raise question like; Why 7x7 MF only, Why not 3x3 or 5x5 MF? While considering 3x3 or 5x5 MF, the SHAF is unable to maintain the dc link voltage constant and error voltage is developing due to voltage difference. Because of this error voltage, the system is unable to track the currents perfectly and THD also becomes high. So to avoid these difficulties we have considered 7x7 membership functions. With the use of 7x7 MF, SHAF is able to maintain the DC link voltage constant, which is nearly equal to reference voltage and it is also tracking the currents perfectly [50].

3.1.4.1. Trapezoidal membership function

The trapezoidal curve is a function of a vector, x , and depends on four scalar parameters [50, 65, 98, 104] a , b , c , and d , as given by

$$\mu_A(x) = \begin{cases} 0 & \text{if } x \leq a \\ \frac{x-a}{b-a} & \text{if } a \leq x \leq b \\ 1 & \text{if } b \leq x \leq c \\ \frac{d-x}{d-c} & \text{if } c \leq x \leq d \\ 0 & \text{if } x \geq d \end{cases} \quad (3.6)$$

$$\text{It can also be represented as } \mu_A(x) = \max\left(\min\left(\frac{x-a}{b-a}, 1, \frac{d-x}{d-c}\right), 0\right) \quad (3.7)$$

The parameters 'a' and 'd' locate the "feet" of the trapezoid and the parameters 'b' and 'c' locate the "shoulders."

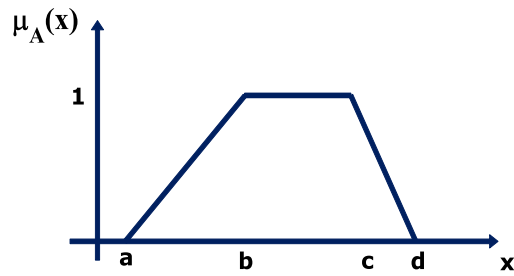


Fig. 3.8 (a) Trapezoidal MF

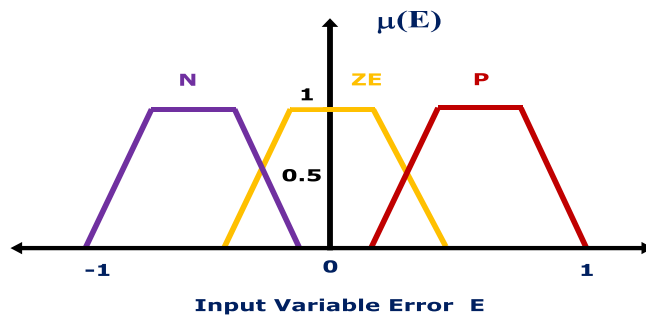


Fig. 3.8 (b) Input Variable Error 'E' Trapezoidal MF 3x3

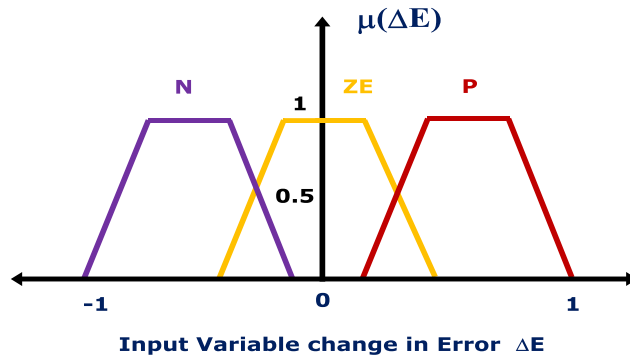


Fig. 3.8 (c) Input Change in Error Normalized Trapezoidal MF 3x3

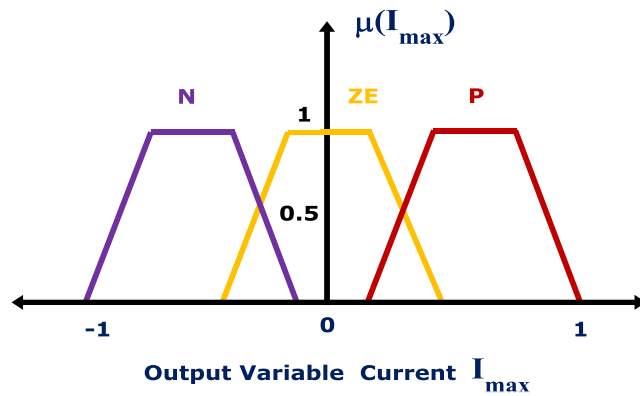


Fig. 3.8 (d) Output I_{max} Normalized Trapezoidal MF 3x3

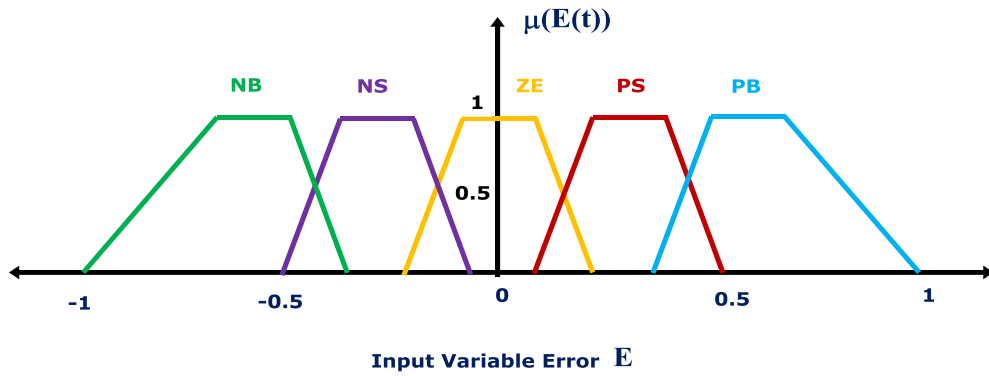


Fig. 3.8 (e) Input Variable Error 'E' Trapezoidal MF 5x5

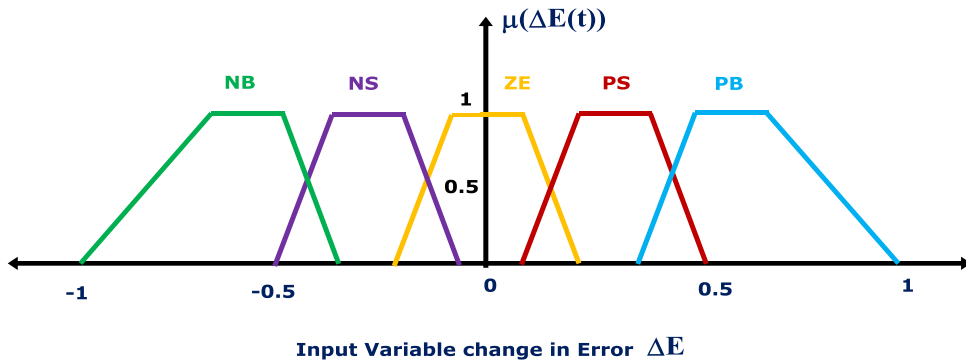


Fig. 3.8 (f) Input Change in Error Normalized Trapezoidal MF 5x5

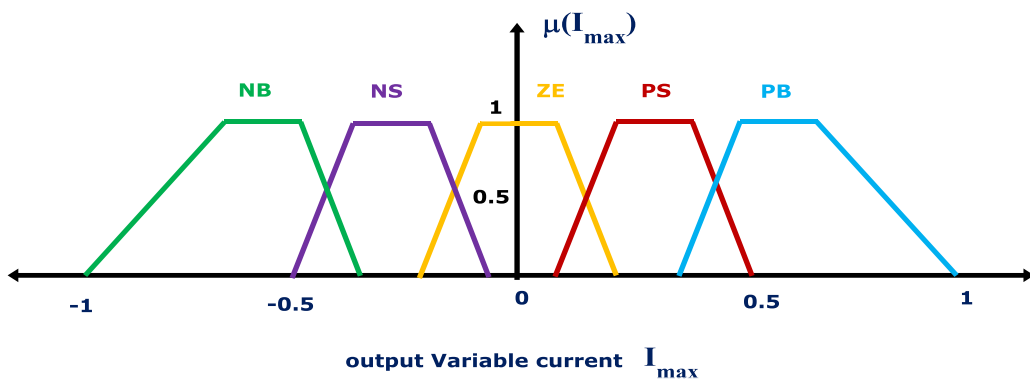


Fig. 3.8 (g) Output I_{max} Normalized Trapezoidal MF 5x5

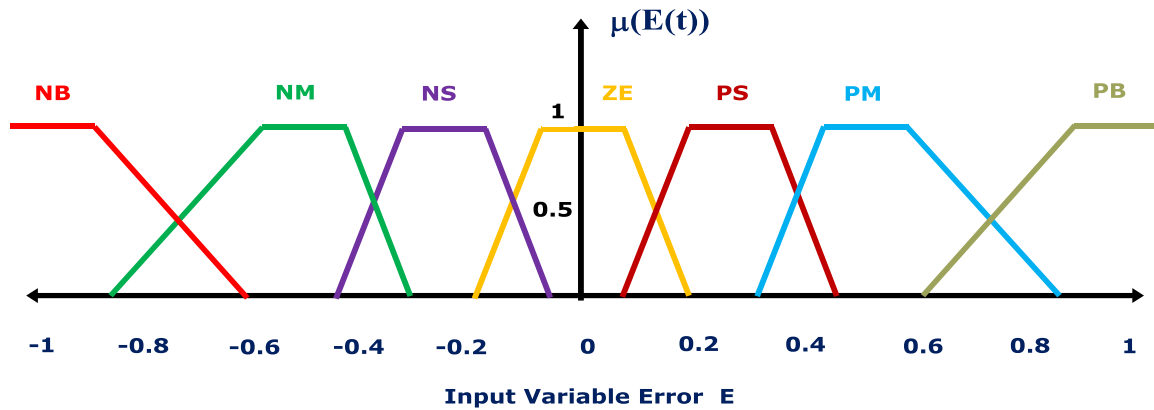


Fig. 3.8 (h) Input Variable Error 'E' Trapezoidal MF 7x7

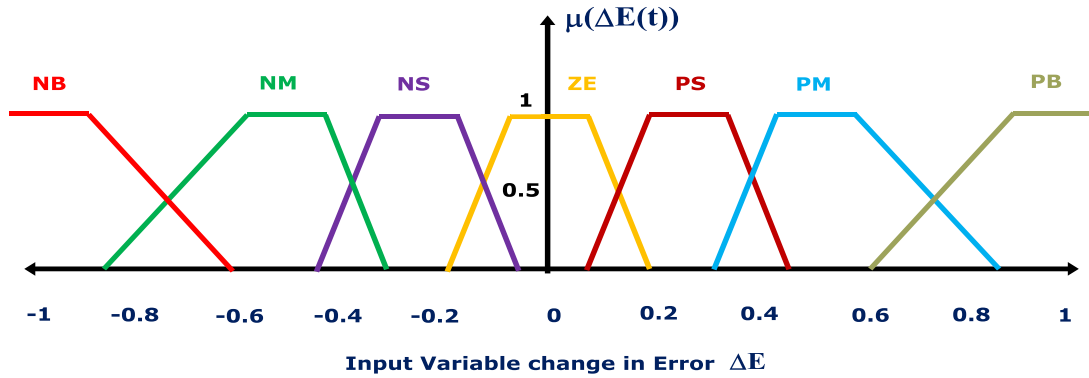


Fig. 3.8 (i) Input Change in Error Normalized Trapezoidal MF 7x7

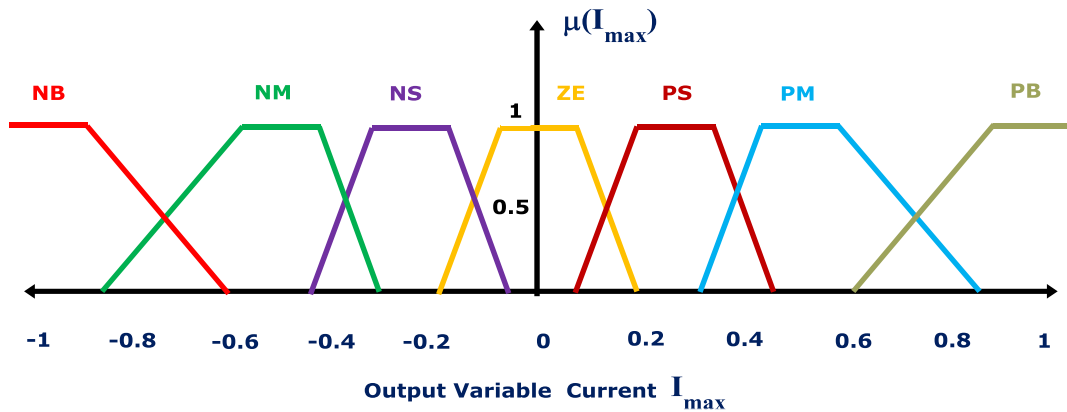


Fig. 3.8 (j) Output I_{\max} Normalized Trapezoidal MF 7x7

3.1.4.2. Triangular membership function

In Fig. 3.9 (a), the parameters a , b and c represent the x coordinates of the three vertices of $\mu_A(x)$ in a fuzzy set 'A' [50] (a : lower boundary and c : upper boundary where membership degree is zero, b : the centre where membership degree is 1). The triangular curve is a function of a vector, x , and depends on three scalar parameters a , b , and c , as given by

$$\mu_A(x) = \begin{cases} 0 & \text{if } x \leq a \\ \frac{x-a}{b-a} & \text{if } a \leq x \leq b \\ \frac{c-x}{c-b} & \text{if } b \leq x \leq c \\ 0 & \text{if } x \geq c \end{cases} \quad (3.8)$$

It can also be represented as

$$\mu_A(x) = \max\left(\min\left(\frac{x-a}{b-a}, \frac{c-x}{c-b}\right), 0\right) \quad (3.9)$$

The parameters 'a' and 'c' locate the "feet" of the triangle and the parameter 'b' locates the peak.

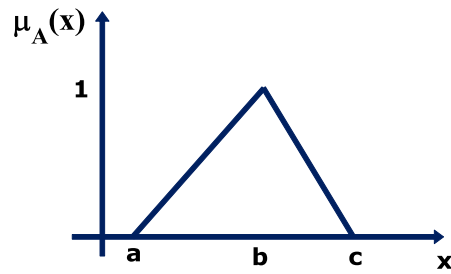


Fig. 3.9 (a) Triangular MF

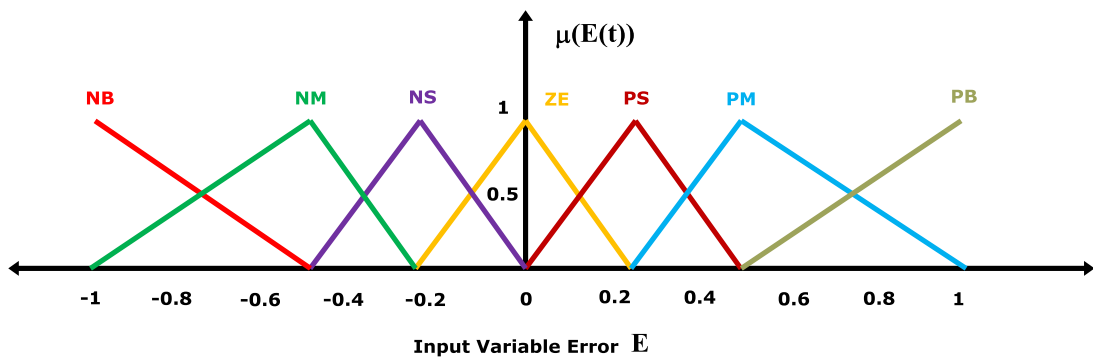


Fig. 3.9 (b) Input Variable Error 'E' Triangular MF 7x7

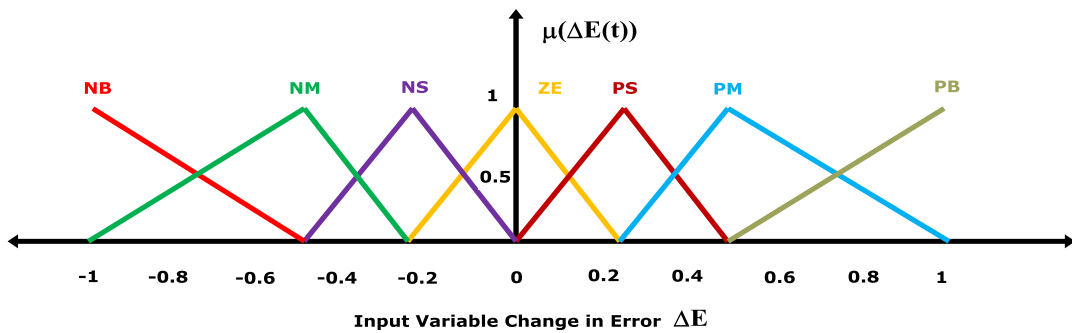


Fig. 3.9 (c) Input Change in Error Normalized Triangular MF 7x7

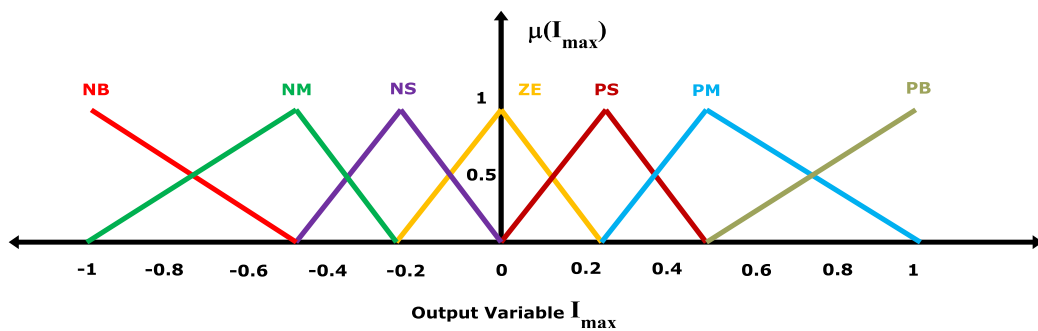


Fig. 3.9 (d) Output I_{max} Normalized Triangular MF 7x7

3.1.4.3. Gaussian membership function

The Gaussian [26, 50, 65, 98, 104] curve is a function of a vector, x , and depends on three scalar parameters c , s , and m , as given by

$$\mu_A(x, c, s, m) = \exp\left[-\frac{1}{2}\left|\frac{x-c}{\sigma}\right|^m\right] \quad (3.10)$$

Where c : centre

σ : width

m : fuzzification factor

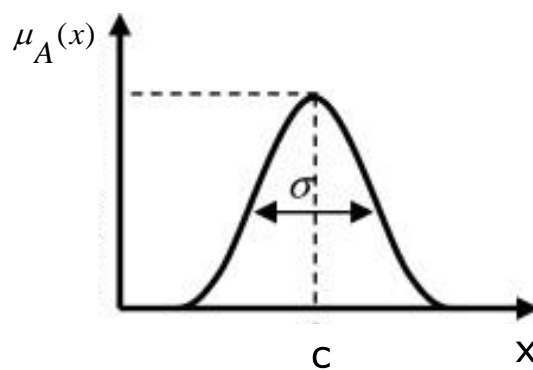


Fig. 3.10 (a) Gaussian MF

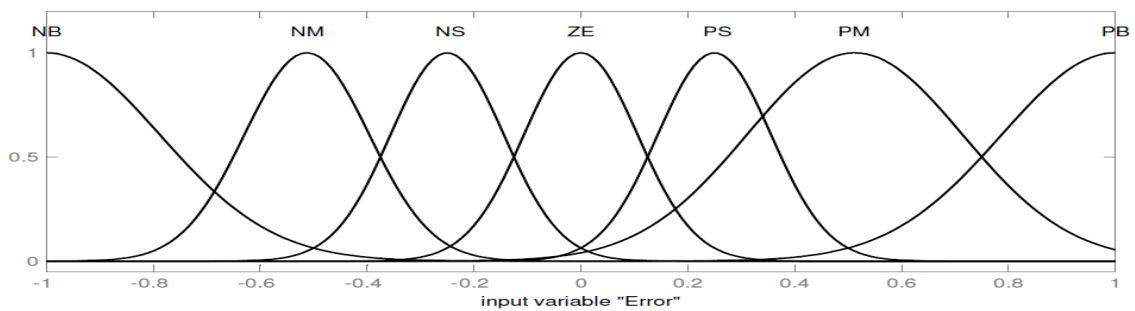


Fig. 3.10 (b) Input Variable Error 'E' Gaussian MF 7x7

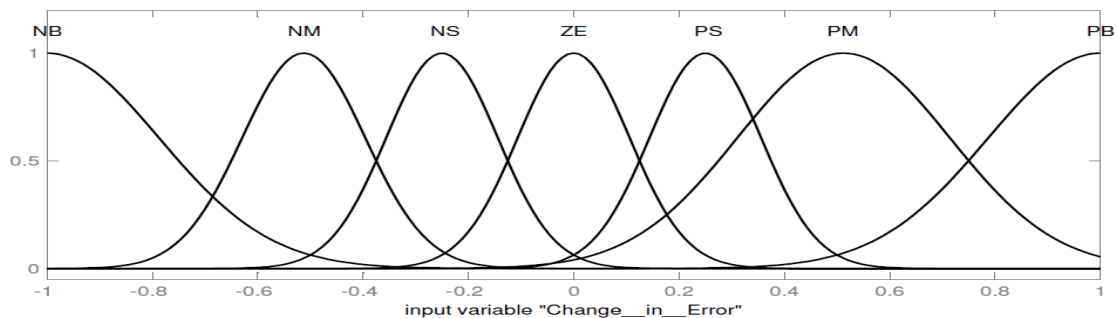


Fig. 3.10 (c) Input Change in Error Normalized Gaussian MF 7x7

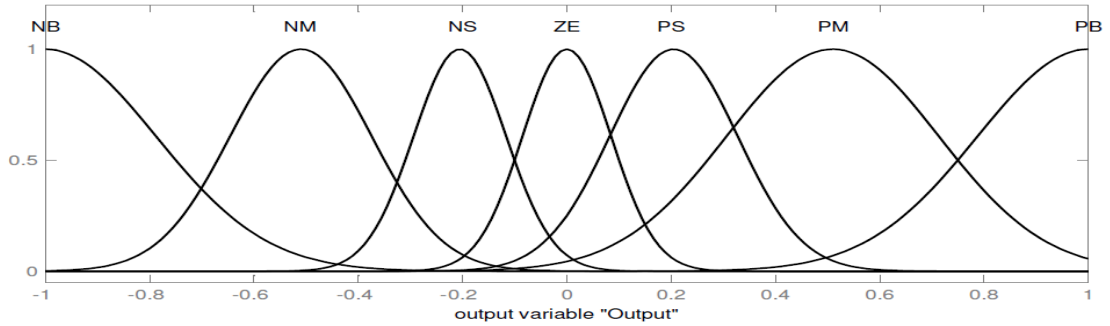


Fig. 3.10 (d) Output I_{\max} Normalized Gaussian MF 7x7

3.1.5. Rule Base

The elements of this rule base [7, 26, 50, 65, 98, 104] table are determined based on the theory that in the transient state, large errors need coarse control, which requires coarse input/output variables. In the steady state, small errors need fine control, which requires fine input/output variables [104]. Based on this the elements of the rule table are obtained as shown in **Table 3.1, 3.2 and 3.3** with ‘E’ and ‘ ΔE ’ as inputs.

Table 3.1 Rule base 3x3

ΔE E	N	Z	P
N	N	N	Z
Z	N	Z	P
P	Z	P	P

Table 3.2 Rule base 5x5

ΔE E	NB	NS	Z	PS	PB
NB	NB	NB	NB	NS	Z
NS	NB	NB	NS	Z	PS
Z	NB	NS	Z	PS	PB
PS	NS	Z	PS	PB	PB
PB	Z	PS	PB	PB	PB

Table 3.3 Rule base 7x7

ΔE E	NB	NM	NS	Z	PS	PM	PB
NB	NB	NB	NB	NB	NM	NS	Z
NM	NB	NB	NB	NM	NS	Z	PS
NS	NB	NB	NM	NS	Z	PS	PM
Z	NB	NM	NS	Z	PS	PM	PB
PS	NM	NS	Z	PS	PM	PB	PB
PM	NS	Z	PS	PM	PB	PB	PB
PB	Z	PS	PM	PB	PB	PB	PB

Fig. 3.11 shows the Fuzzy inference system. It consists of

- ↳ Fuzzy Inference System (FIS) Editor
- ↳ Membership Function Editor
- ↳ Rule Editor
- ↳ Rule Viewer and
- ↳ Surface Viewer

The FIS Editor [104] handles the high-level issues for the system: How much input and output variables? What are their names? The Present model consists of two inputs and one output, named as Error, change in Error and output respectively. The Membership Function Editor is used to define the shapes of all the membership functions associated with each variable. The Rule Editor is used for editing the list of rules that defines the behaviour of the system. In the Present model 49 rules are developed.

The Rule Viewer and the Surface Viewer are used for looking at, as opposed to editing, the FIS. They are strictly read-only tools. Used as a diagnostic, it can show which rules are active, or how individual membership function [26] shapes are influencing the results. The

Surface Viewer is used to display the dependency of one of the outputs on any one or two of the inputs i.e., it generates and plots an output surface map for the system.



Fig. 3.11 (a) Type-1 Fuzzy Inference System with Trapezoidal MF 7x7

The FIS editor [7, 26, 50, 65, 98, 104], the membership function editor, and the rule editor can all read and modify the FIS data, but the rule viewer and the surface viewer do not modify anything in the FIS data.

- ↪ One of the key issues in all Fuzzy sets is how to determine Fuzzy MFs.
- ↪ The membership function fully defines the Fuzzy set.
- ↪ A membership function provides a measure of the degree of similarity of an element to a Fuzzy set.

- Membership functions can take any form, but there are some common examples that appear in real applications.
- Membership functions can either be chosen by the user arbitrarily, based on the user's experience (membership function chosen by two users could be different depending upon their experiences, perspectives, etc.) or be designed using machine learning methods (e.g., artificial neural networks, genetic algorithms, etc.)
- There are different shapes of membership functions [7, 26, 50, 65, 98, 104]; trapezoidal, triangular, sigmoidal, Gaussian, bell-shaped, etc. Out of all these approaches, we have considered trapezoidal, triangular, and Gaussian MFs.

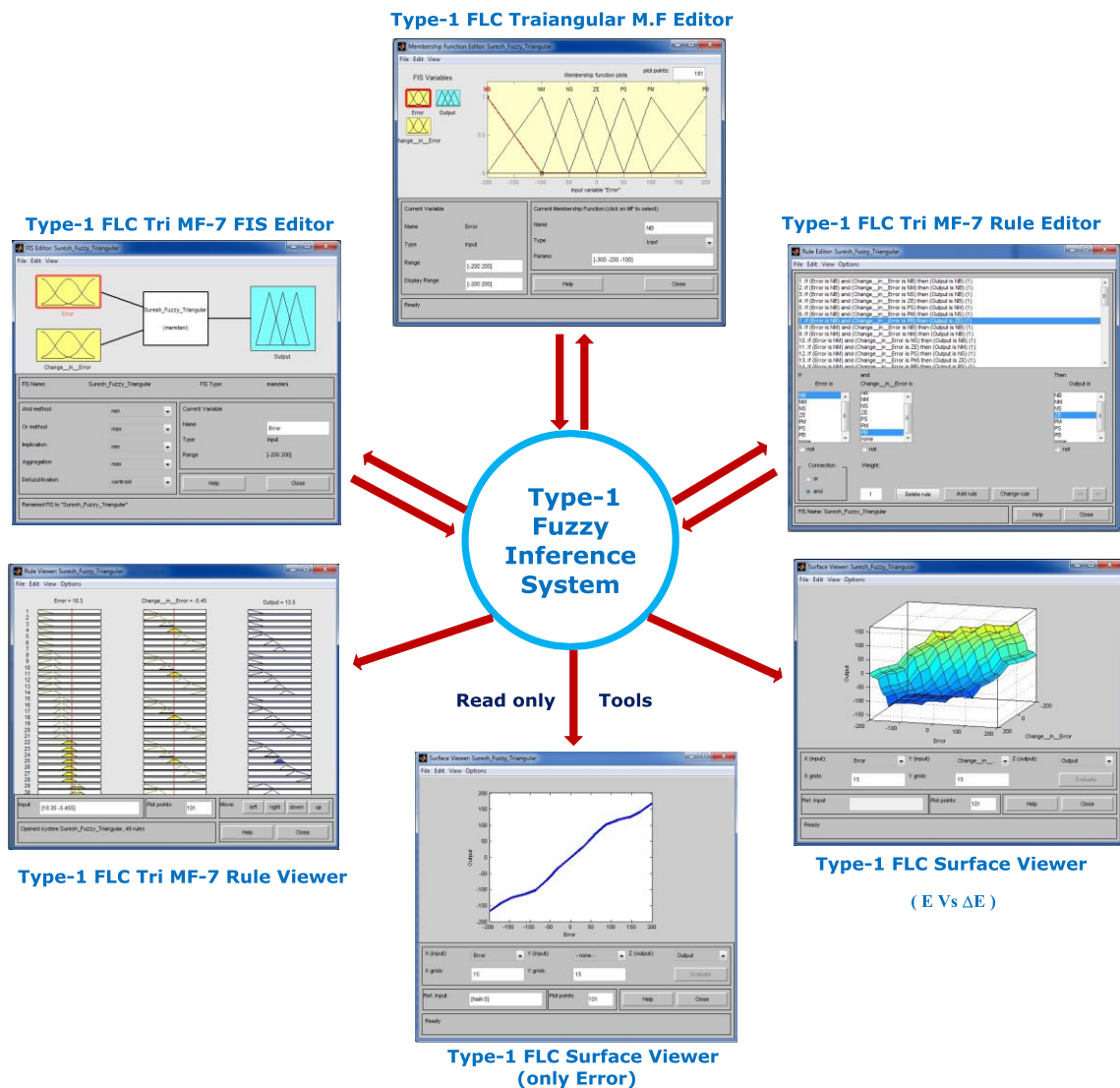


Fig. 3.11 (b) Type-1 Fuzzy Inference System with **Triangular MF 7x7**

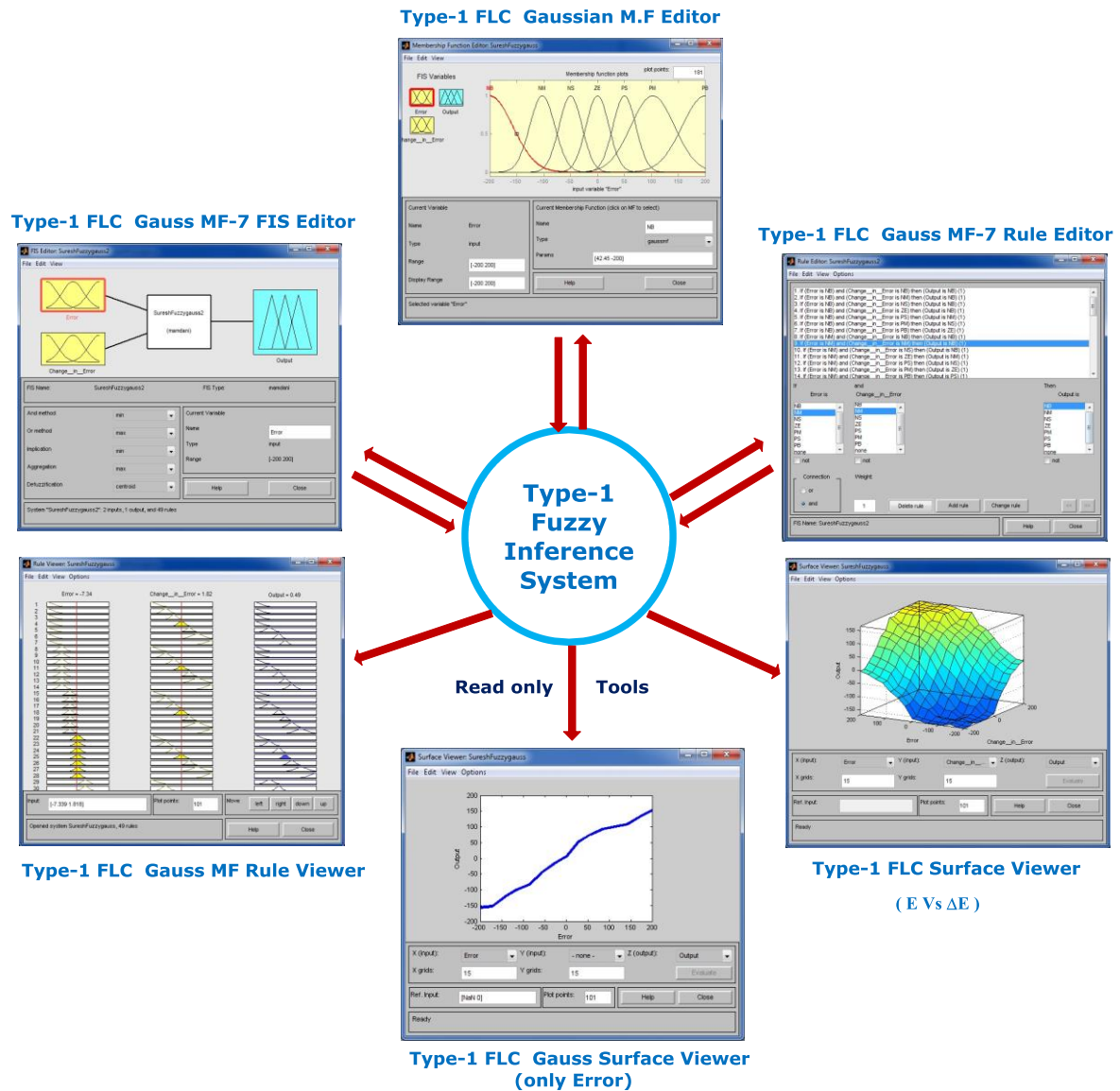


Fig. 3.11 (c) Type-1 Fuzzy Inference System with Gaussian MF 7x7

3.2. System Performance of Type-1 FLC based P - Q Control Strategy with different Fuzzy MFs Using MATLAB.

Fig.3.12, Fig.3.13 and Fig.3.14, presents the details of Source Voltage, Load Current, Compensation current, Source Current with filter, DC Link Voltage, THD of Type-1 FLC based p - q control strategy with different Fuzzy MFs (trapezoidal, triangular and Gaussian) using MATLAB/SIMULINK under balanced, un-balanced and non-sinusoidal supply voltage conditions.

Initially the system performance is analysed under balanced sinusoidal conditions, during which the Type-1 FLC with all MFs are good enough at suppressing the harmonics and THD is 1.87%, 1.27% and 0.76% respectively using MATLAB. However, under un-balanced and non-sinusoidal conditions, the Type-1 FLC with Gaussian MF shows superior performance over the Type-1 FLC with other two MFs.

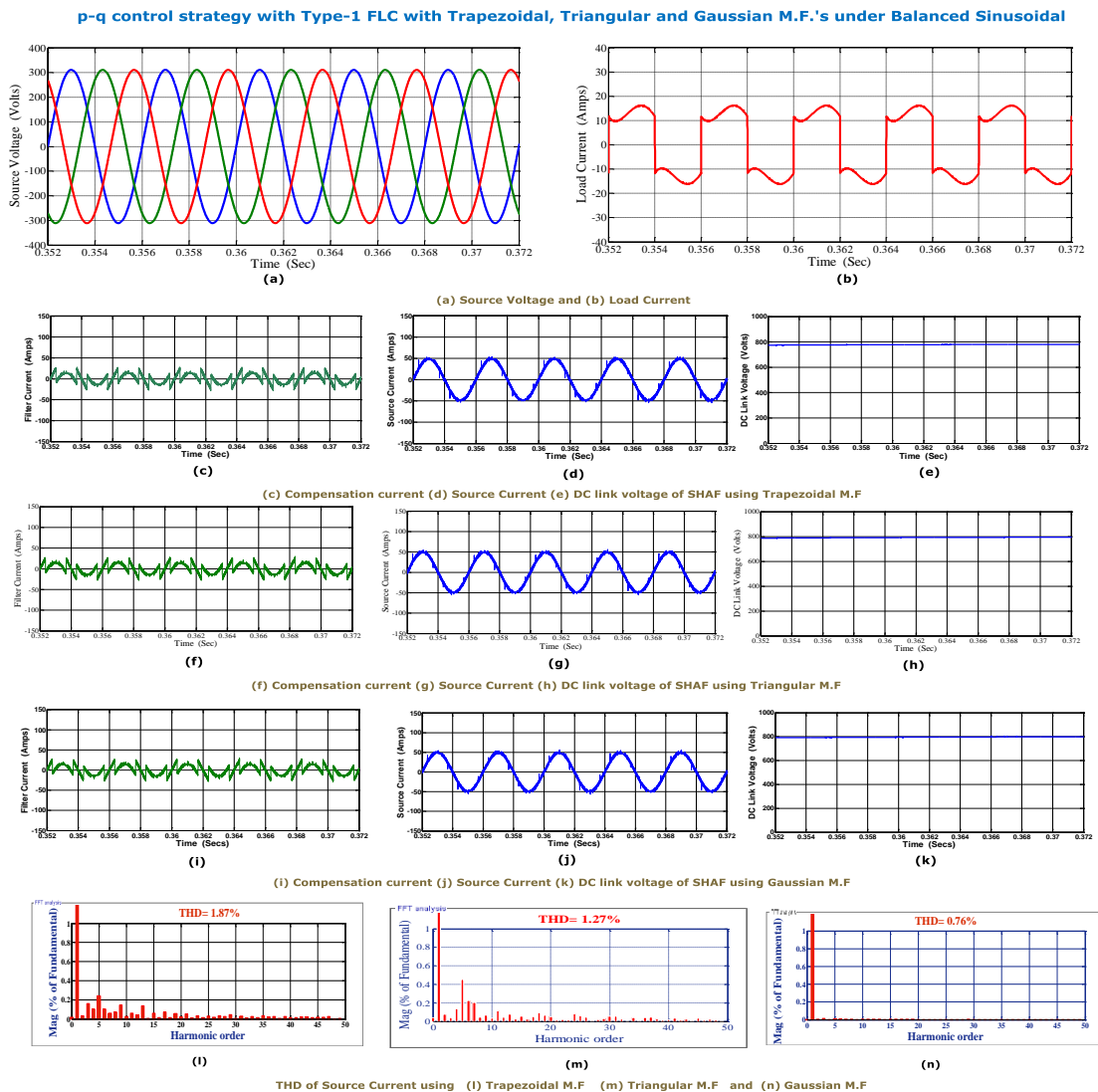


Fig. 3.12 SHAF response using p - q control strategy with Type-1 FLC (Trapezoidal, Triangular and Gaussian MF) under balanced Sinusoidal condition using MATLAB

(a) Source Voltage (b) Load Current (c) Compensation current using **Trapezoidal MF** (d) Source Current with filter using Trapezoidal MF (e) DC Link Voltage using Trapezoidal MF (f) Compensation current using **Triangular MF** (g) Source Current with filter using Triangular MF (h) DC Link Voltage using Triangular MF (i) Compensation current using **Gaussian MF** (j) Source Current with filter using Gaussian MF (k) DC Link Voltage using Gaussian MF (l) THD of Source current with Trapezoidal MF (m) THD of Source current with Triangular MF (n) THD of Source current with Gaussian MF

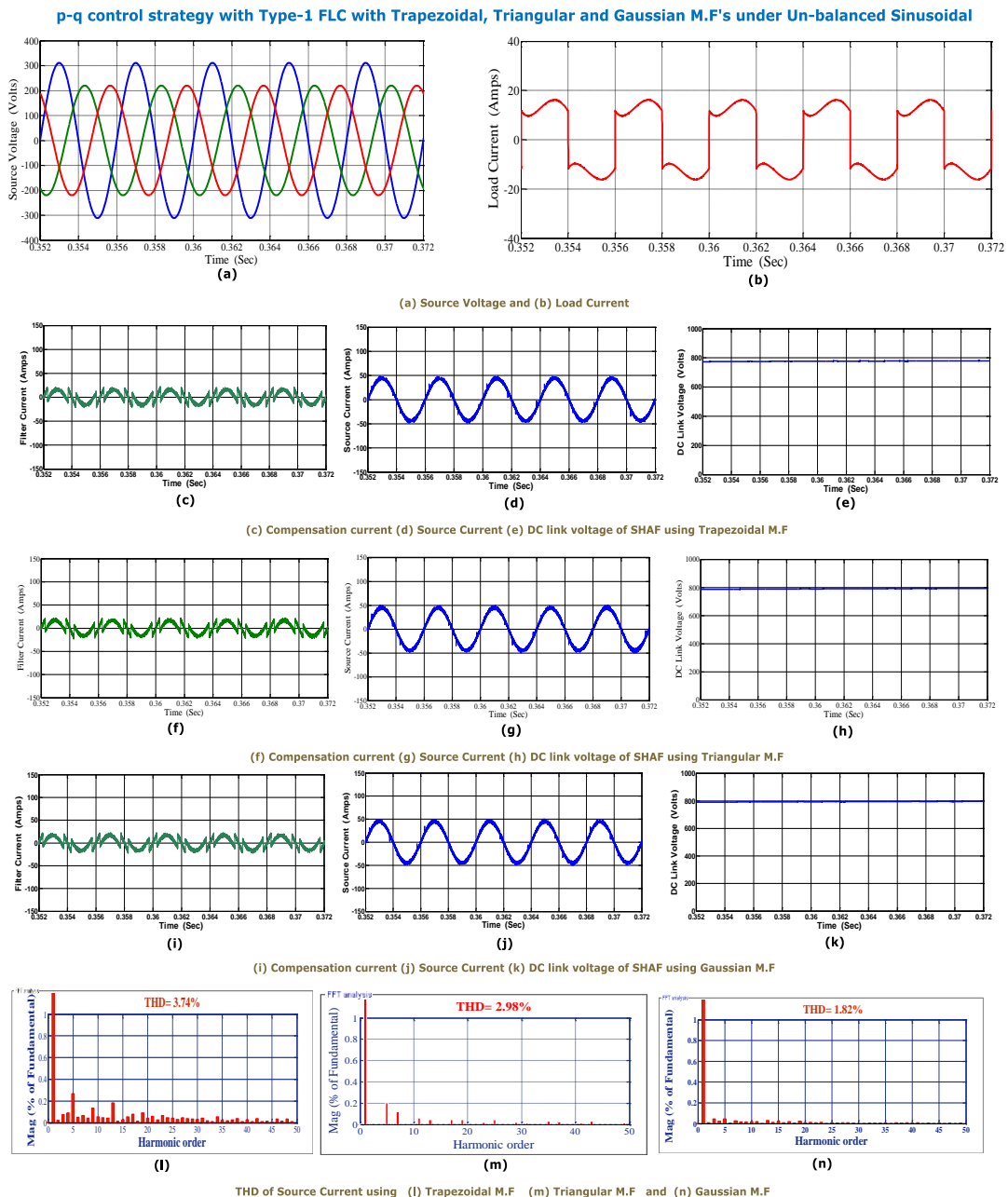


Fig. 3.13 SHAF response using *p-q* control strategy with **Type-1 FLC (Trapezoidal, Triangular and Gaussian MF)** under **un-balanced Sinusoidal** condition using **MATLAB**

(a) Source Voltage (b) Load Current (c) Compensation current using **Trapezoidal MF** (d) Source Current with filter using Trapezoidal MF (e) DC Link Voltage using Trapezoidal MF (f) Compensation current using **Triangular MF** (g) Source Current with filter using Triangular MF (h) DC Link Voltage using Triangular MF (i) Compensation current using **Gaussian MF** (j) Source Current with filter using Gaussian MF (k) DC Link Voltage using Gaussian MF (l) THD of Source current with Trapezoidal MF (m) THD of Source current with Triangular MF (n) THD of Source current with Gaussian MF

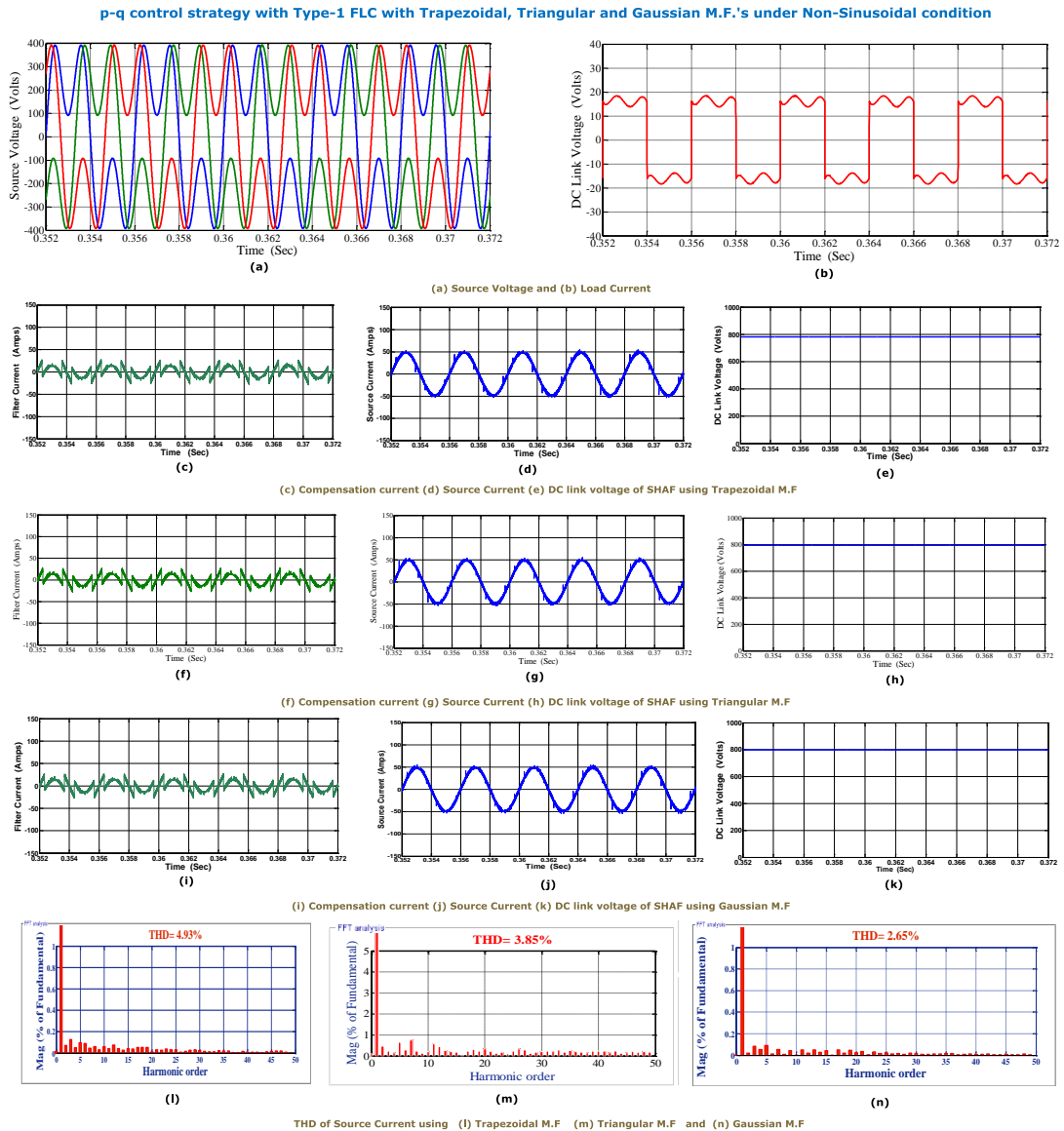


Fig. 3.14 SHAF response using p - q control strategy with Type-1 FLC (Trapezoidal, Triangular and Gaussian MF) under Non-Sinusoidal condition using MATLAB

(a) Source Voltage (b) Load Current (c) Compensation current using **Trapezoidal MF** (d) Source Current with filter using Trapezoidal MF (e) DC Link Voltage using Trapezoidal MF (f) Compensation current using **Triangular MF** (g) Source Current with filter using Triangular MF (h) DC Link Voltage using Triangular MF (i) Compensation current using **Gaussian MF** (j) Source Current with filter using Gaussian MF (k) DC Link Voltage using Gaussian MF (l) THD of Source current with Trapezoidal MF (m) THD of Source current with Triangular MF (n) THD of Source current with Gaussian MF

The THD of p - q control strategy using Type-1 FLC with Trapezoidal MF under unbalanced condition is 3.74% and under non-sinusoidal condition it is 4.93%. The THD of p - q

control strategy using Type-1 FLC with Triangular MF under un-balanced condition is about 2.98% and under non-sinusoidal condition it is about 3.85%. The THD of p - q control strategy using Type-1 FLC with Gaussian MF under un-balanced condition is 1.82% and under non-sinusoidal condition it is 2.65%.

When the supply voltages are balanced and sinusoidal, p - q control strategy using Type-1 FLC with all membership functions (Trapezoidal, Triangular and Gaussian) are converging to the similar compensation characteristics. However, under unbalanced and non-sinusoidal conditions, the p - q control strategy using Type-1 FLC with Gaussian MF shows superior performance over the Type-1 FLC with other two MFs.

The p - q control strategy using Type-1 FLC with different MFs is unable to mitigate the harmonics perfectly, notches are observed in the source current. The main reason behind the notches is that, the controller failed to track the current correctly, and thereby APF fails to compensate completely. So to mitigate the harmonics perfectly, one has to choose perfect control strategy. So to avoid the difficulties occur with p - q control strategy, we have considered I_d - I_q control strategy.

3.3. System Performance of Type-1 FLC based I_d - I_q Control Strategy with different Fuzzy MFs using MATLAB.

Fig. 3.15, 3.16 and 3.17, presents the details of Source Voltage, Load Current, Compensation current, Source Current with filter, DC Link Voltage, THD (Total harmonic distortion) of Type-1 FLC based I_d - I_q control strategy with different Fuzzy MFs (trapezoidal, triangular and Gaussian) under balanced, un-balanced and non-sinusoidal supply voltage conditions.

Initially, the system performance is analysed under balanced sinusoidal conditions, during which the Type-1 FLC with all MFs are good enough at suppressing the harmonics. The corresponding THDs are 1.15%, 0.97% and 0.64% respectively using MATLAB.

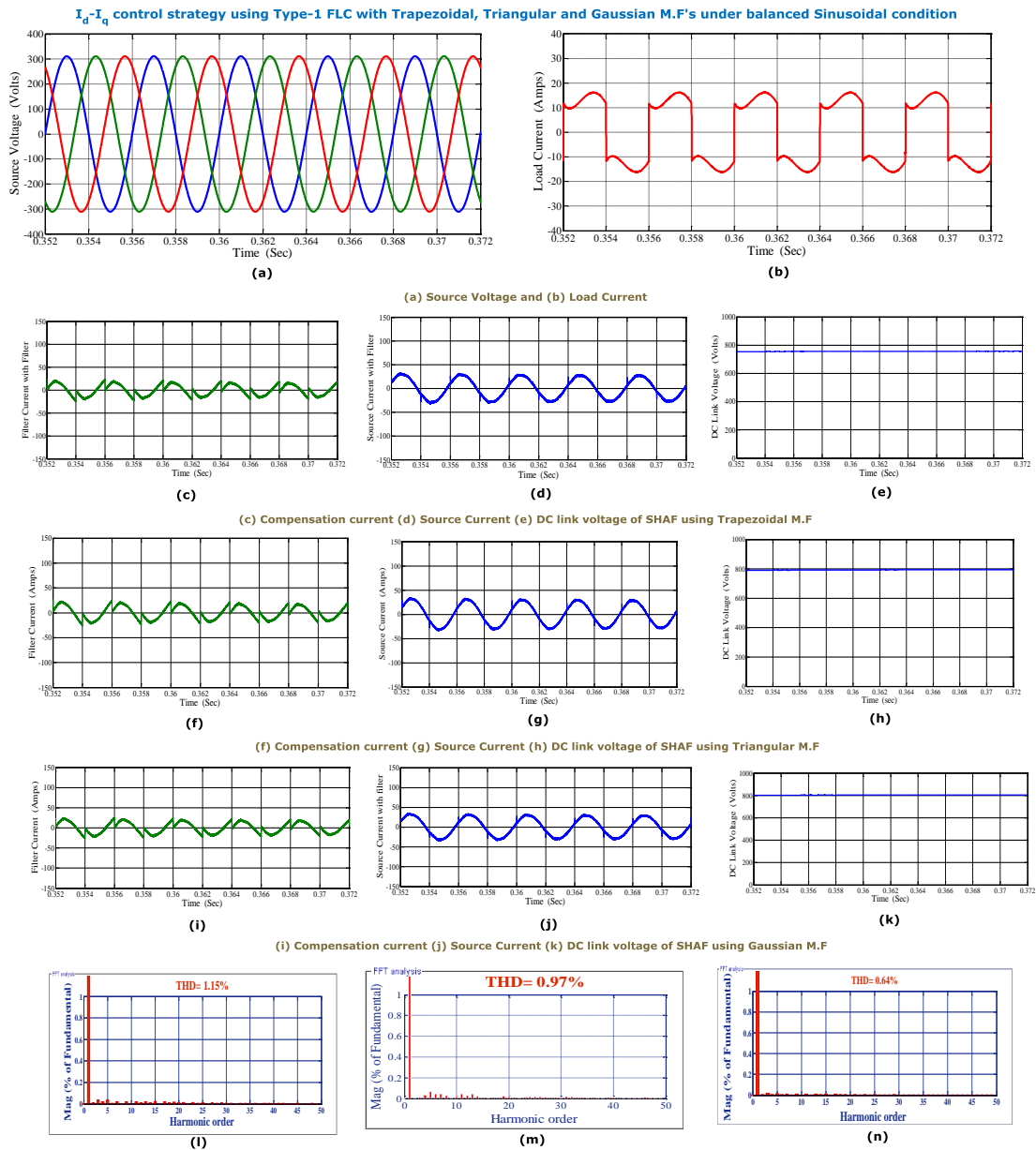


Fig. 3.15 SHAF response using I_d-I_q control strategy with **Type-1 FLC (Trapezoidal, Triangular and Gaussian MF)** under **balanced Sinusoidal** condition using **MATLAB**

(a) Source Voltage (b) Load Current (c) Compensation current using **Trapezoidal MF** (d) Source Current with filter using Trapezoidal MF (e) DC Link Voltage using Trapezoidal MF (f) Compensation current using **Triangular MF** (g) Source Current with filter using Triangular MF (h) DC Link Voltage using Triangular MF (i) Compensation current using **Gaussian MF** (j) Source Current with filter using Gaussian MF (k) DC Link Voltage using Gaussian MF (l) THD of Source current with Trapezoidal MF (m) THD of Source current with Triangular MF (n) THD of Source current with Gaussian MF

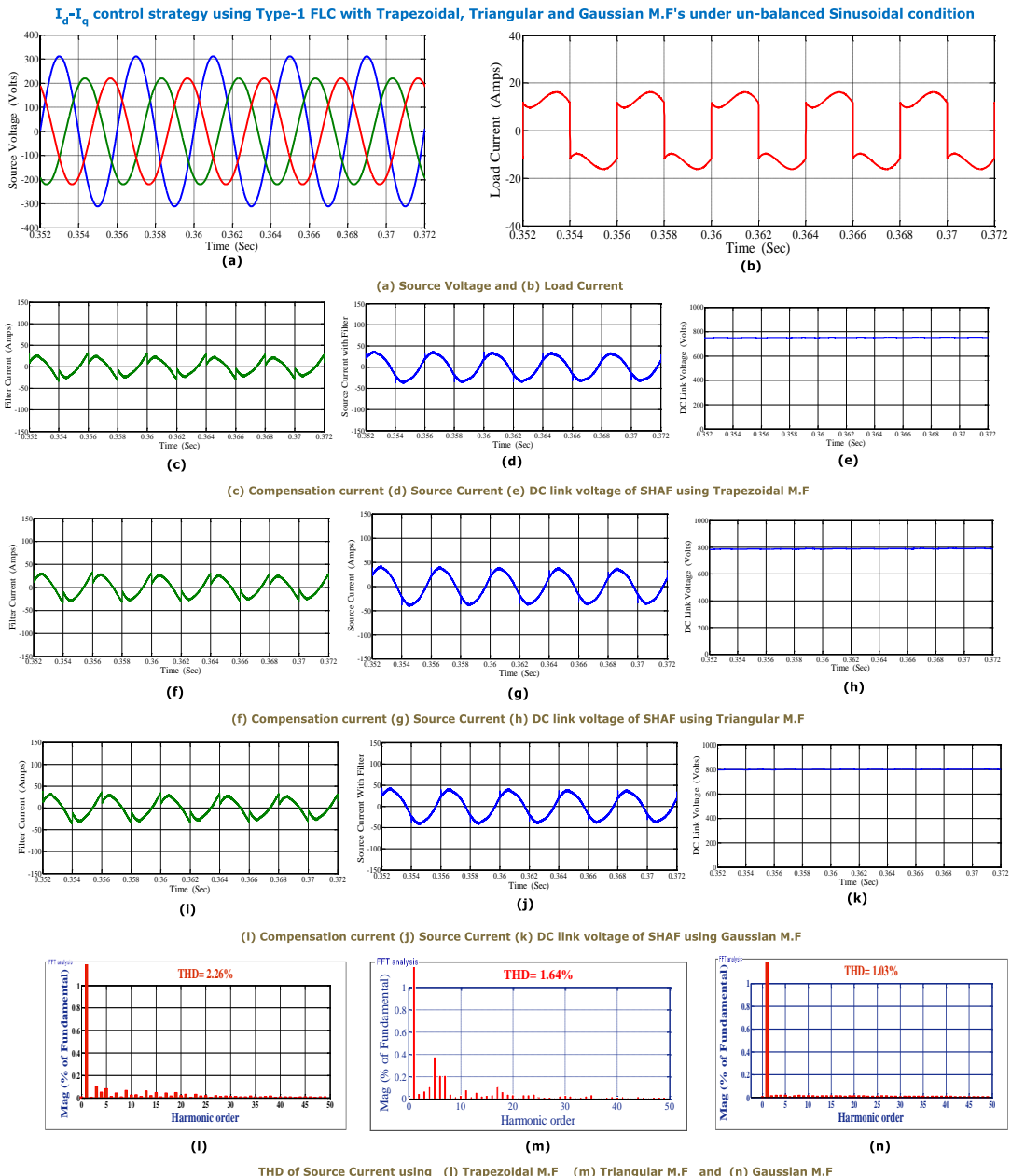


Fig 3.16 SHAF response using I_d-I_q control strategy with **Type-1 FLC (Trapezoidal, Triangular and Gaussian MF)** under **un-balanced Sinusoidal** condition using MATLAB

(a) Source Voltage (b) Load Current (c) Compensation current using **Trapezoidal MF** (d) Source Current with filter using **Trapezoidal MF** (e) DC Link Voltage using **Trapezoidal MF** (f) Compensation current using **Triangular MF** (g) Source Current with filter using **Triangular MF** (h) DC Link Voltage using **Triangular MF** (i) Compensation current using **Gaussian MF** (j) Source Current with filter using **Gaussian MF** (k) DC Link Voltage using **Gaussian MF** (l) THD of Source current with **Trapezoidal MF** (m) THD of Source current with **Triangular MF** (n) THD of Source current with **Gaussian MF**

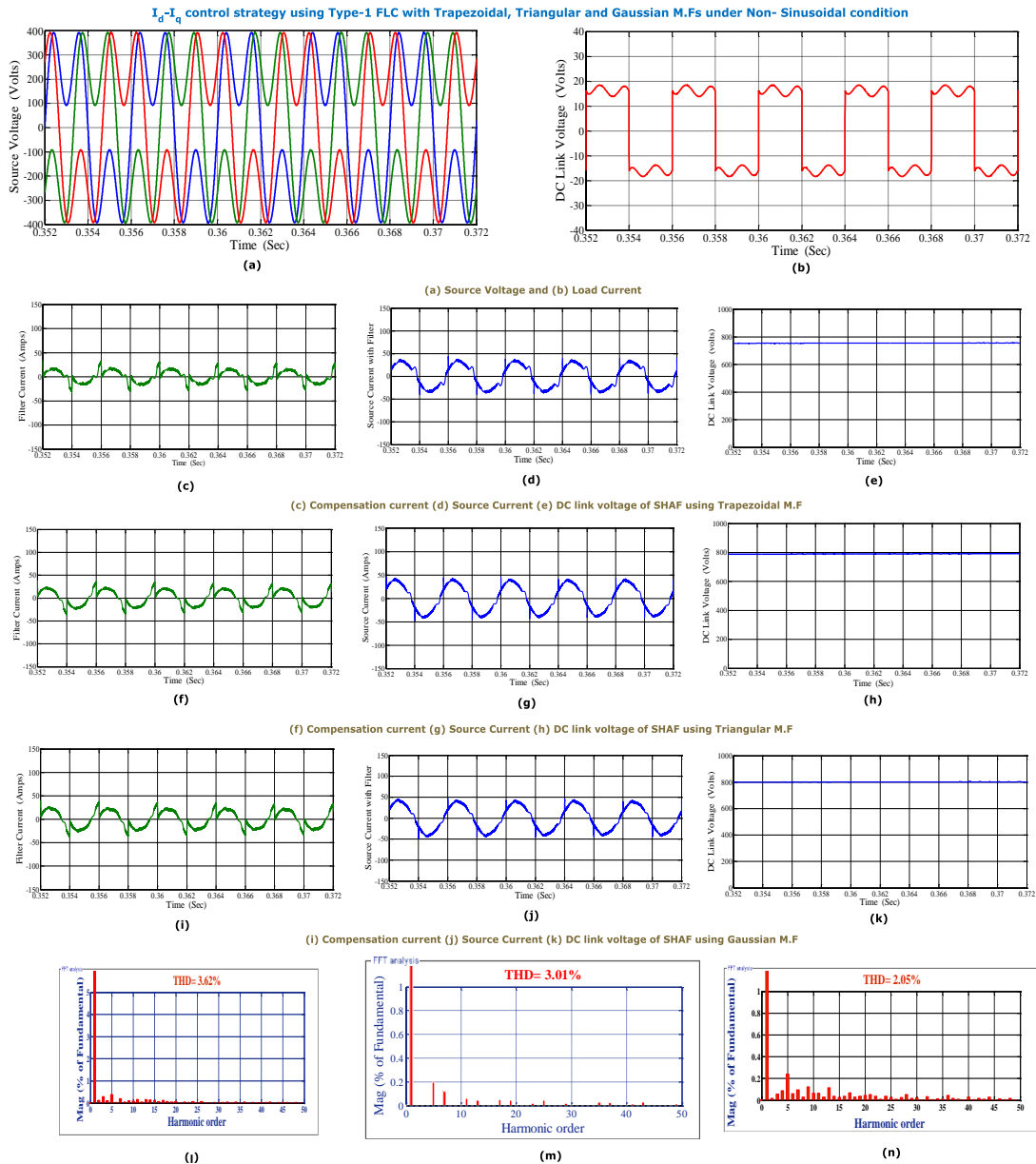


Fig. 3.17 SHAF response using I_d-I_q control strategy with Type-1 FLC (Trapezoidal, Triangular and Gaussian MF) under Non-Sinusoidal condition using MATLAB

(a) Source Voltage (b) Load Current (c) Compensation current using **Trapezoidal MF** (d) Source Current with filter using Trapezoidal MF (e) DC Link Voltage using Trapezoidal MF (f) Compensation current using **Triangular MF** (g) Source Current with filter using Triangular MF (h) DC Link Voltage using Triangular MF (i) Compensation current using **Gaussian MF** (j) Source Current with filter using Gaussian MF (k) DC Link Voltage using Gaussian MF (l) THD of Source current with Trapezoidal MF (m) THD of Source current with Triangular MF (n) THD of Source current with Gaussian MF

The THD of I_d - I_q control strategy using Type-1 FLC with Trapezoidal MF under un-balanced condition is 2.26% and under non-sinusoidal condition it is 3.62%. The THD of I_d - I_q control strategy using Type-1 FLC with Triangular MF under un-balanced condition is 1.64% and under non-sinusoidal condition it is 3.01%. The THD of I_d - I_q control strategy using Type-1 FLC with Gaussian MF under un-balanced condition is 1.03% and under non-sinusoidal condition it is 2.05% using MATLAB.

3.4. System Performance of Type-1 FLC based P - Q Control Strategy with different Fuzzy MFs using Real-Time Digital Simulator

Fig. 3.18, 3.19 and 3.20, highlights the performance of Type-1 FLC based p - q control strategy with different Fuzzy MFs under balanced, un-balanced and Non- Sinusoidal conditions using Real-Time Digital Simulator.

Initially, the system performance is analysed under balanced sinusoidal conditions, during which the Type-1 FLC with all MFs are good enough at suppressing the harmonics and the THD of p - q control strategy using real-time digital simulator is 2.12%, 1.45% and 1.23%. However, under unbalanced and non-sinusoidal conditions, the Type-1 FLC with Gaussian MF shows superior performance over the Type-1 FLC with other two MFs.

The THD of the Type-1 FLC with Trapezoidal MF under un-balanced condition is 3.98% and under non-sinusoidal condition it is 5.23%. The THD of the Type-1 FLC with Triangular MF under un-balanced condition is about 3.27% and under non-sinusoidal condition it is 4.15%. The THD of the Type-1 FLC with Gaussian MF under un-balanced condition is 2.26% and under non-sinusoidal condition it is 2.89% using p - q strategy with real-time digital simulator.

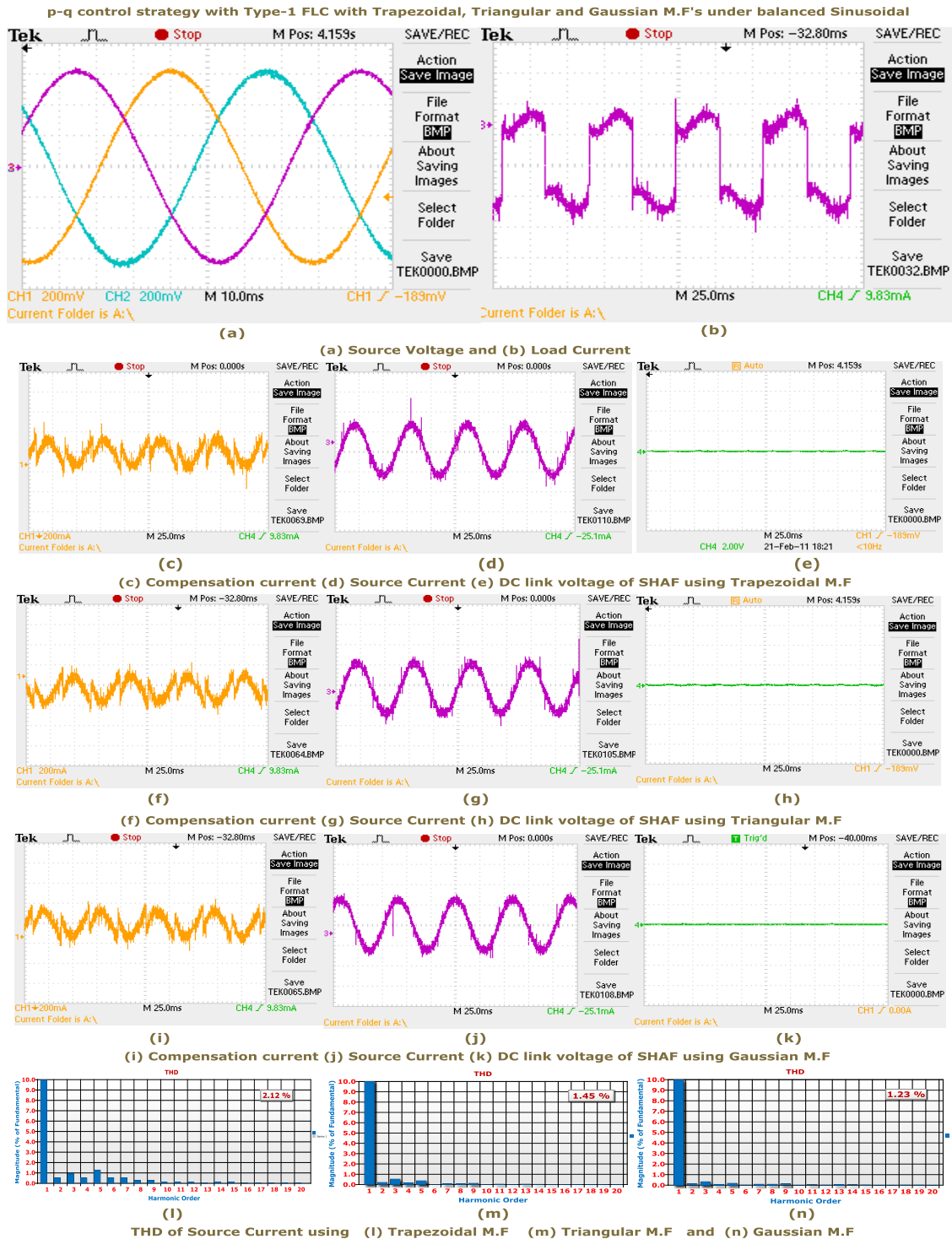
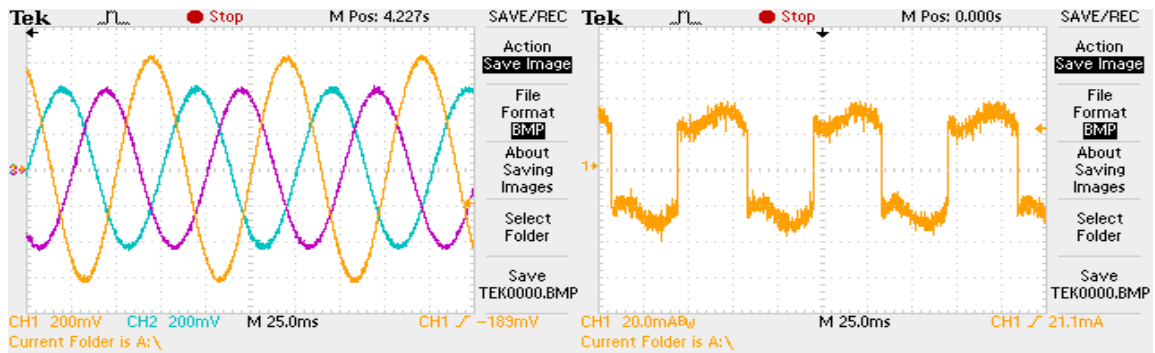


Fig. 3.18 SHAF response using $p-q$ control strategy with Type-1 FLC (Trapezoidal, Triangular and Gaussian MF) under balanced Sinusoidal condition using real-time digital simulator

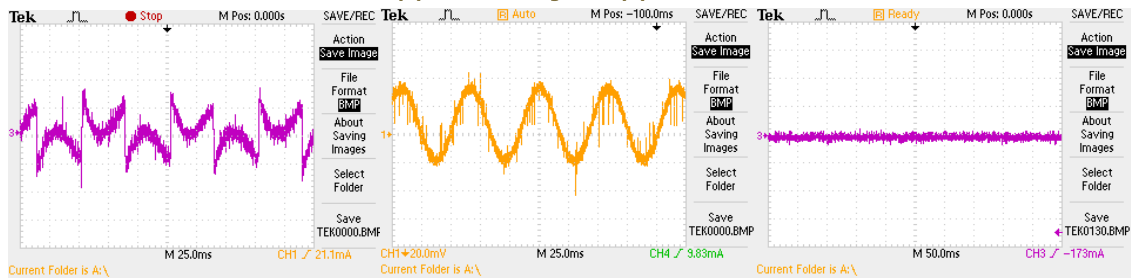
(a)Source Voltage (b)Load Current (Scale 20A/div) (c)Compensation current (Scale 20A/div) using Trapezoidal MF (d)Source Current (Scale 30A/div) with filter using Trapezoidal MF (e)DC Link Voltage using Trapezoidal MF (f)Compensation current using Triangular MF (g)Source Current with filter using Triangular MF (h)DC Link Voltage using Triangular MF(i)Compensation current using Gaussian MF (j)Source Current with filter using Gaussian MF (k)DC Link Voltage using Gaussian MF (l)THD of Source current with Trapezoidal MF (m)THD of Source current with Triangular MF (n)THD of Source current with Gaussian MF

p-q control strategy with Type-1 FLC with Trapezoidal, Triangular and Gaussian M.F.'s under Un-balanced Sinusoidal



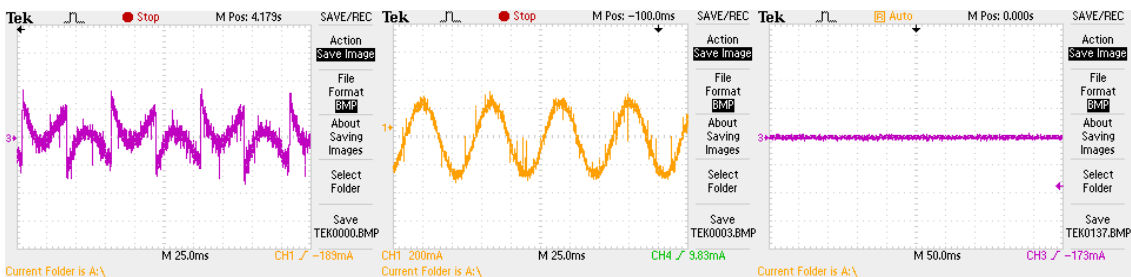
(a) (b)

(a) Source Voltage and (b) Load Current



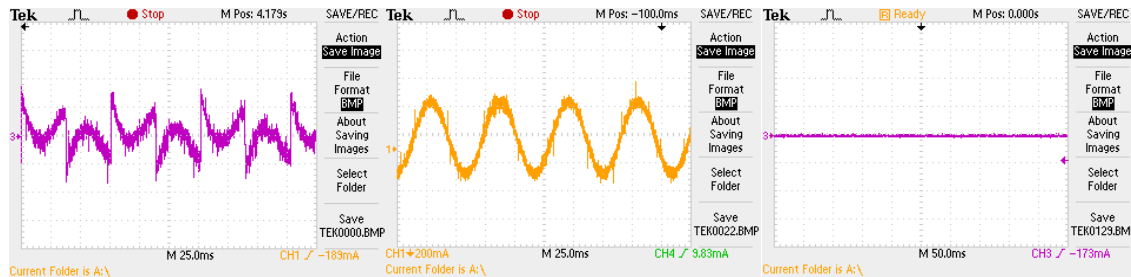
(c) (d) (e)

(c) Compensation current (d) Source Current (e) DC link voltage of SHAF using Trapezoidal M.F



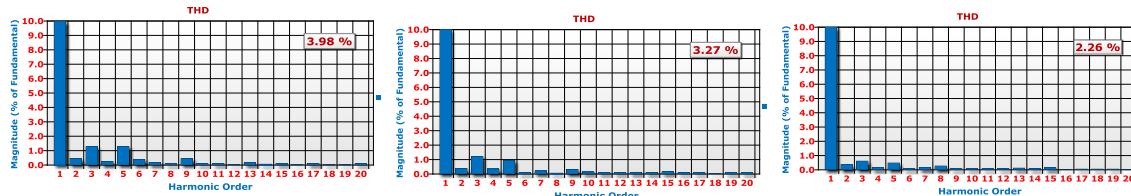
(f) (g) (h)

(f) Compensation current (g) Source Current (h) DC link voltage of SHAF using Triangular M.F



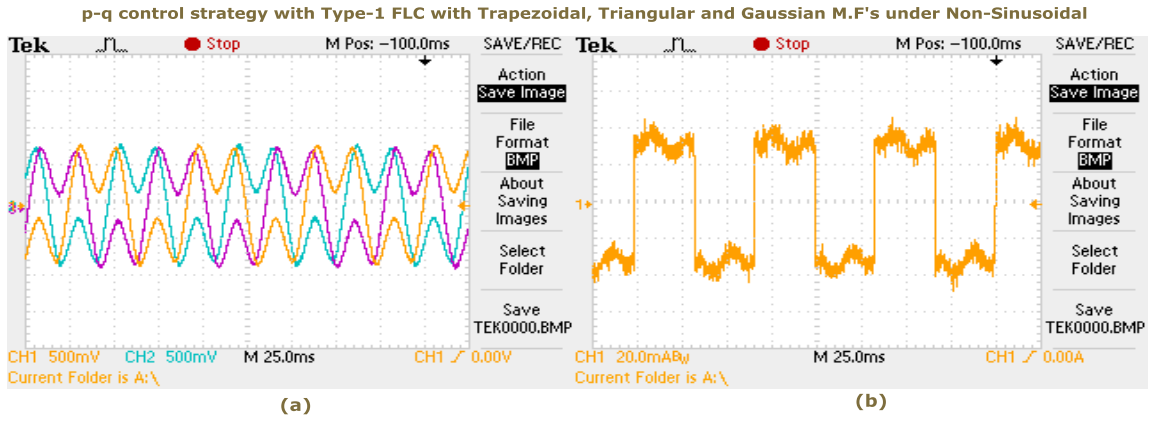
(i) (j) (k)

(i) Compensation current (j) Source Current (k) DC link voltage of SHAF using Gaussian M.F

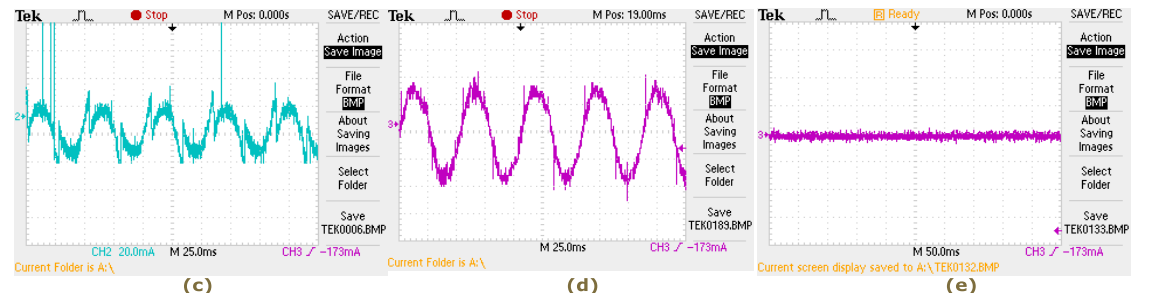


THD of Source Current using (l) Trapezoidal M.F (m) Triangular M.F and (n) Gaussian M.F

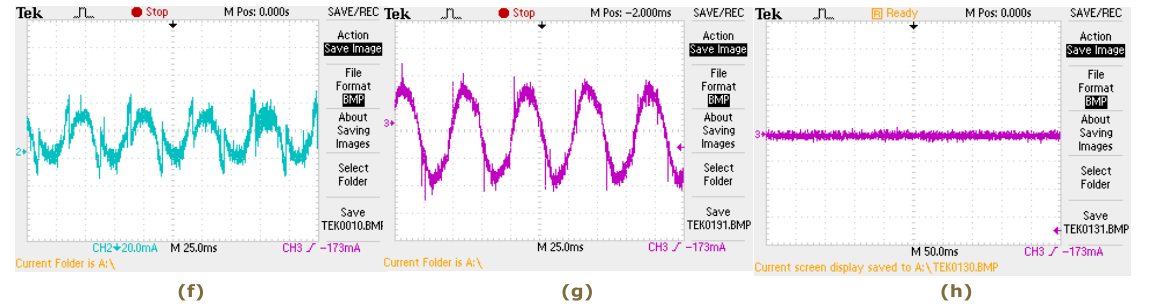
Fig. 3.19 SHAF response using $p-q$ control strategy with Type-1 FLC under un-balanced Sinusoidal condition using real-time digital simulator



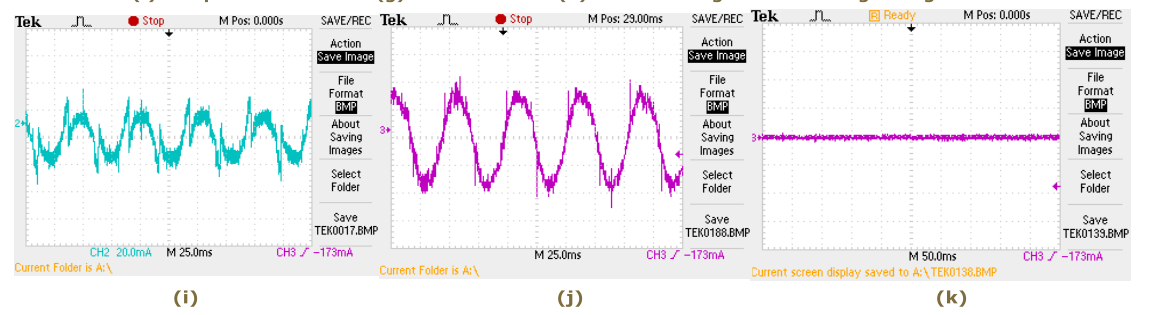
(a) Source Voltage and (b) Load Current



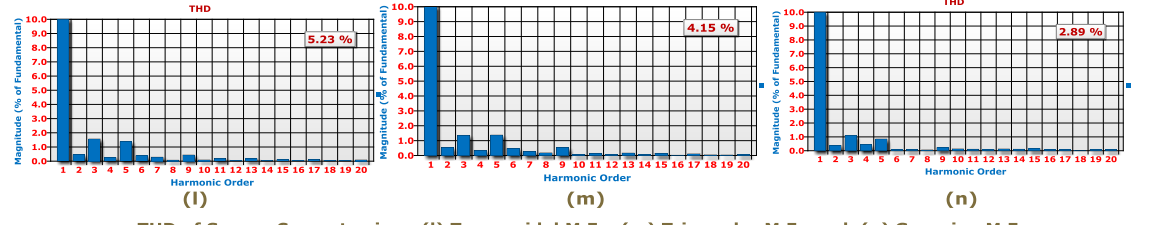
(c) Compensation current (d) Source Current (e) DC link voltage of SHAF using Trapezoidal M.F



(f) Compensation current (g) Source Current (h) DC link voltage of SHAF using Triangular M.F



(i) Compensation current (j) Source Current (k) DC link voltage of SHAF using Gaussian M.F



THD of Source Current using (l) Trapezoidal M.F (m) Triangular M.F and (n) Gaussian M.F

Fig. 3.20 SHAF response using $p-q$ control strategy with Type-1 FLC (Trapezoidal, Triangular and Gaussian MF) under Non-Sinusoidal condition using real-time digital simulator

3.5. System Performance of Type-1 FLC based I_dI_q Control Strategy with different Fuzzy MFs using Real-Time Digital Simulator

I_dI_q control strategy with Type-1 FLC with Trapezoidal, Triangular and Gaussian M.F's under balanced Sinusoidal condition

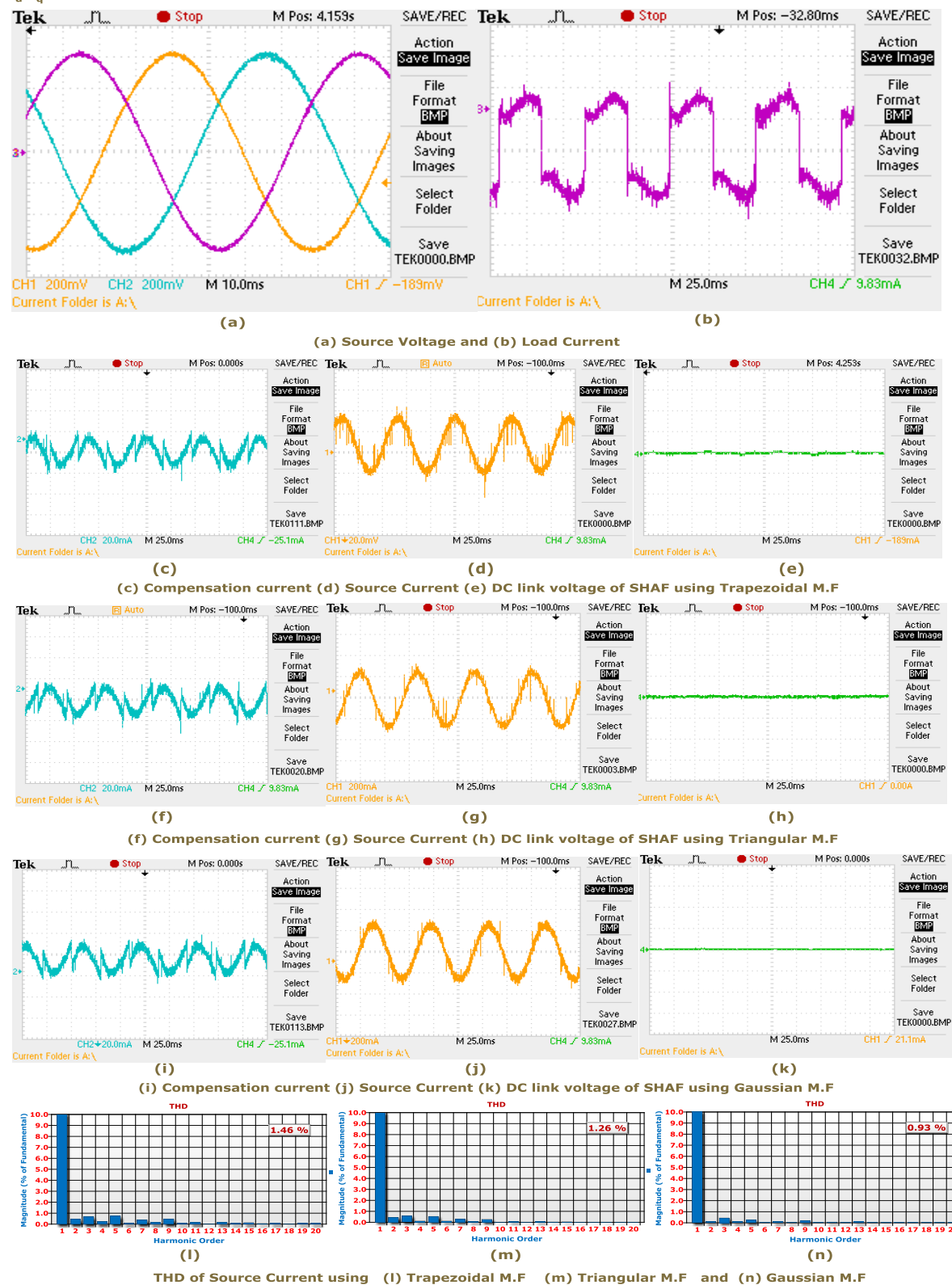
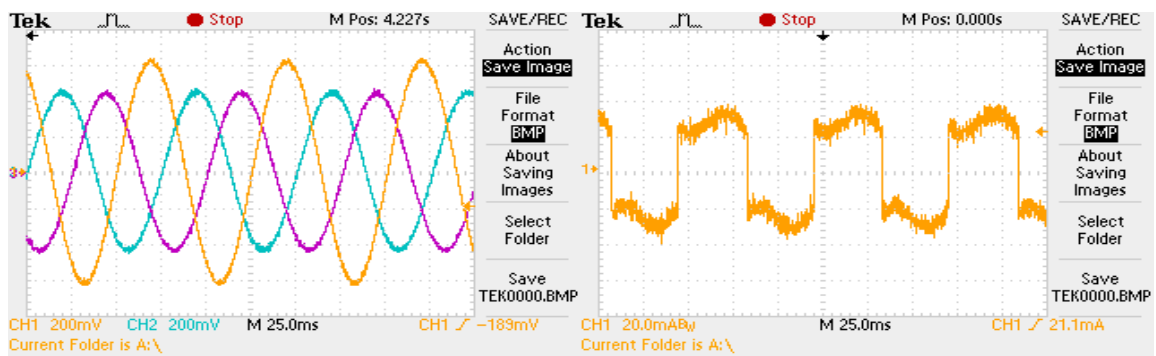
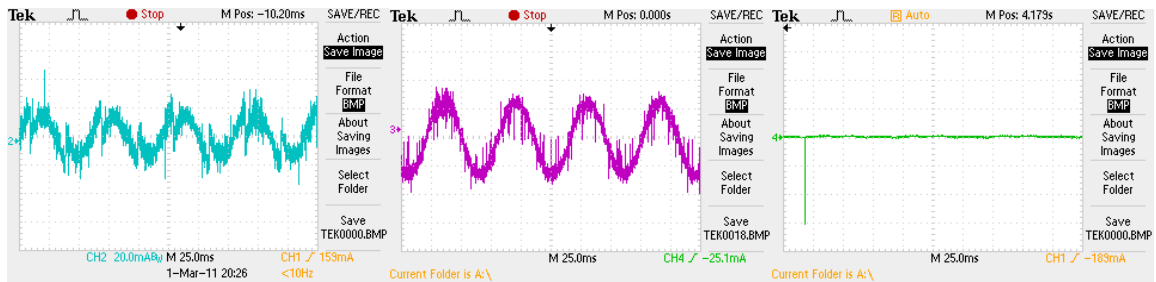


Fig. 3.21 SHAF response using I_dI_q control strategy with Type-1 FLC (Trapezoidal, Triangular and Gaussian MF) under balanced Sinusoidal condition using real-time digital simulator

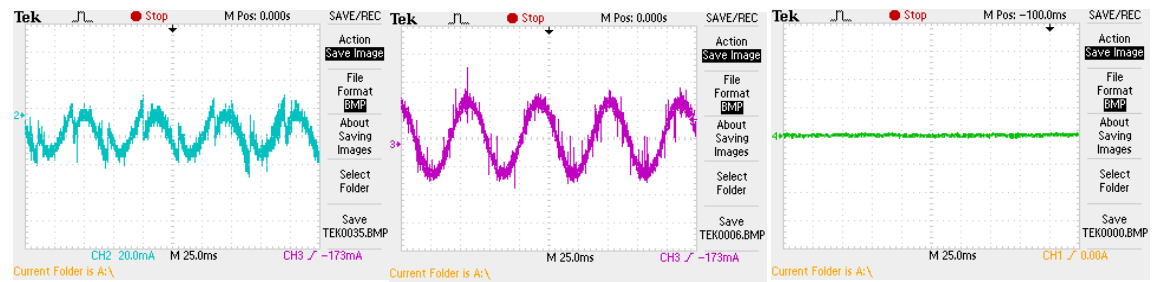
I_d - I_q control strategy with Type-1 FLC with Trapezoidal, Triangular and Gaussian M.F's under Un-balanced Sinusoidal



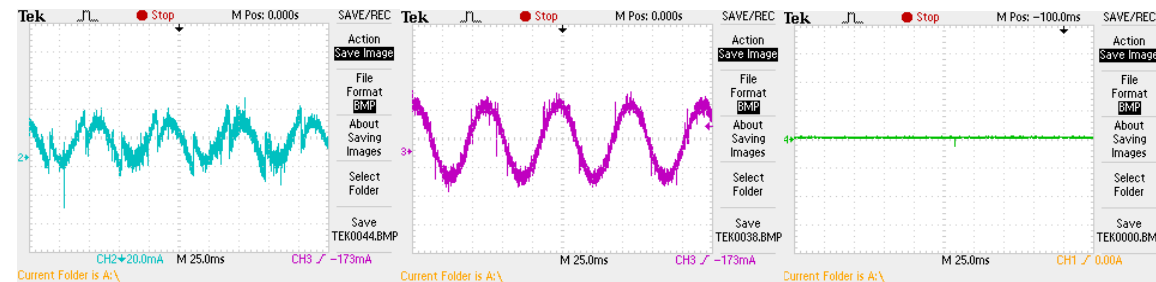
(a) Source Voltage and (b) Load Current



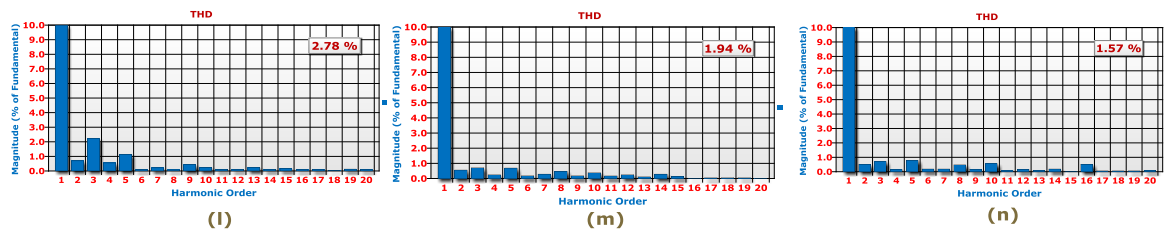
(c) Compensation current (d) Source Current (e) DC link voltage of SHAF using Trapezoidal M.F



(f) Compensation current (g) Source Current (h) DC link voltage of SHAF using Triangular M.F



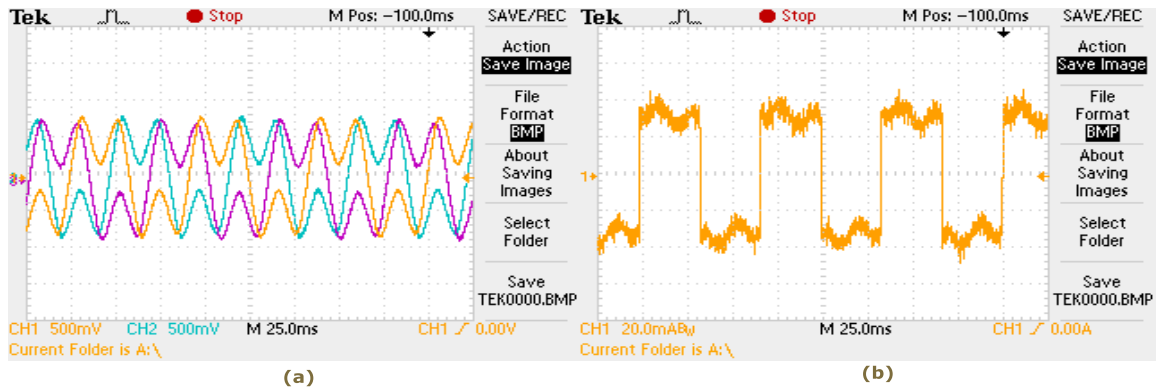
(i) Compensation current (j) Source Current (k) DC link voltage of SHAF using Gaussian M.F



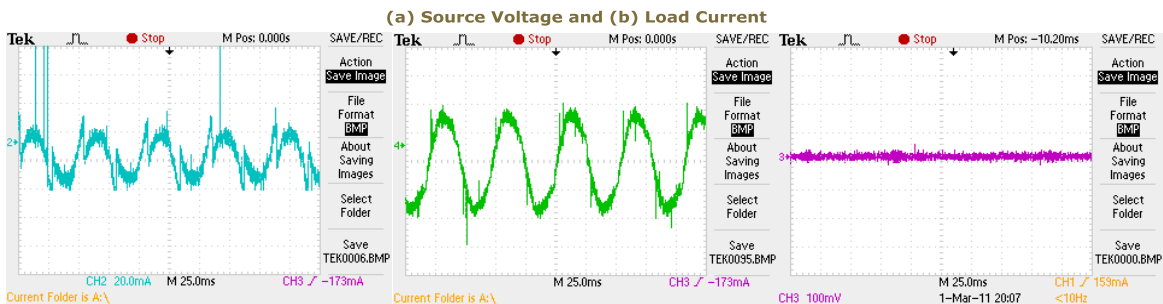
THD of Source Current using (l) Trapezoidal M.F (m) Triangular M.F and (n) Gaussian M.F

Fig. 3.22 SHAF response using I_d - I_q control strategy with Type-1 FLC (Trapezoidal, Triangular and Gaussian MF) under un-balanced Sinusoidal condition using real-time digital simulator

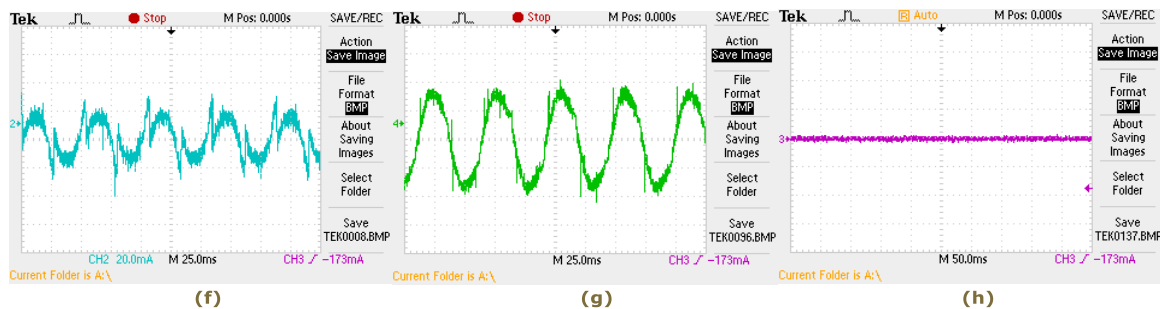
I_d - I_q control strategy with Type-1 FLC with Trapezoidal, Triangular and Gaussian M.F.s under Non-Sinusoidal condition



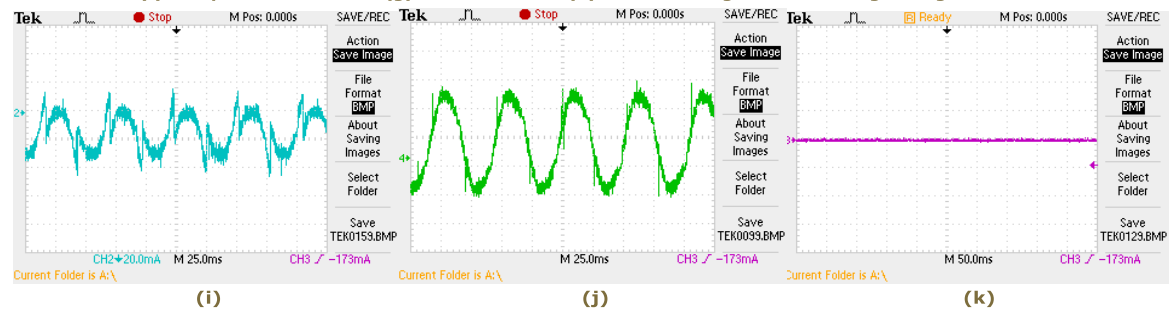
(a) Source Voltage and (b) Load Current



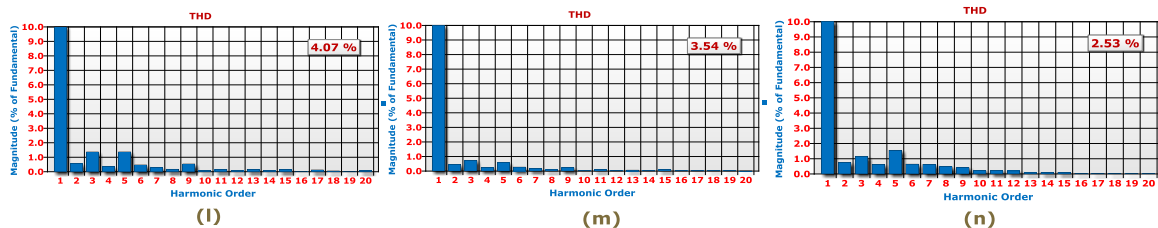
(c) Compensation current (d) Source Current (e) DC link voltage of SHAF using Trapezoidal M.F



(f) Compensation current (g) Source Current (h) DC link voltage of SHAF using Triangular M.F



(i) Compensation current (j) Source Current (k) DC link voltage of SHAF using Gaussian M.F



THD of Source Current using (l) Trapezoidal M.F (m) Triangular M.F and (n) Gaussian M.F

Fig. 3.23 SHAF response using I_d - I_q control strategy with Type-1 FLC (Trapezoidal, Triangular and Gaussian MF) under Non-Sinusoidal condition using real-time digital simulator

Fig. 3.21, 3.22 and 3.23; highlights the performance of Type-1 FLC based I_d-I_q control strategy with different Fuzzy MFs under balanced, un-balanced and Non- Sinusoidal conditions using real-time digital simulator.

Initially, the system performance is analysed under balanced sinusoidal conditions, during which the Type-1 FLC with all MFs (Trapezoidal, Triangular and Gaussian) are good enough at suppressing the harmonics. The respective THDs of Type-1 FLC based I_d-I_q control strategy in real-time digital simulator are 1.46%, 1.26% and 0.93%.

The THD of the Type-1 FLC with Trapezoidal MF under un-balanced condition is 2.78% and under non-sinusoidal condition it is 4.07%. The THD of the Type-1 FLC with Triangular MF under un-balanced condition is 1.94% and under non-sinusoidal condition it is 3.54%. The THD of the Type-1 FLC with Gaussian MF under unbalanced condition is 1.57% and under non-sinusoidal condition it is 2.53% with I_d-I_q control strategy using real-time digital simulator.

I_d-I_q control strategy using Type-1 FLC with different Fuzzy MFs, the SHAF is able to mitigate harmonics in a better way than that of $p-q$ control strategy using Type-1 FLC with different Fuzzy MFs. Even though, the I_d-I_q control strategy using Type-1 FLC is able to mitigate the harmonics, notches (small amount of harmonics) are present in the source current. So to mitigate the harmonics perfectly, one has to choose perfect controller. So to avoid the difficulties occur with $p-q$ and I_d-I_q control strategies using Type-1 FLC with different Fuzzy MFs, we have considered Type-2 FLC with different Fuzzy MFs. In chapter-4, Type-2 FLC with different Fuzzy MFs. is explained in detail.

3.6. Comparative Study

Fig. 3.24, Fig. 3.25, Fig. 3.26 and Fig. 3.27; bar graphs, clearly illustrates the THD of source current for shunt active filter control strategies ($p-q$ and I_d-I_q) using PI controller and Type-1 FLC with different Fuzzy MFs using MATLAB and real-time digital simulator.

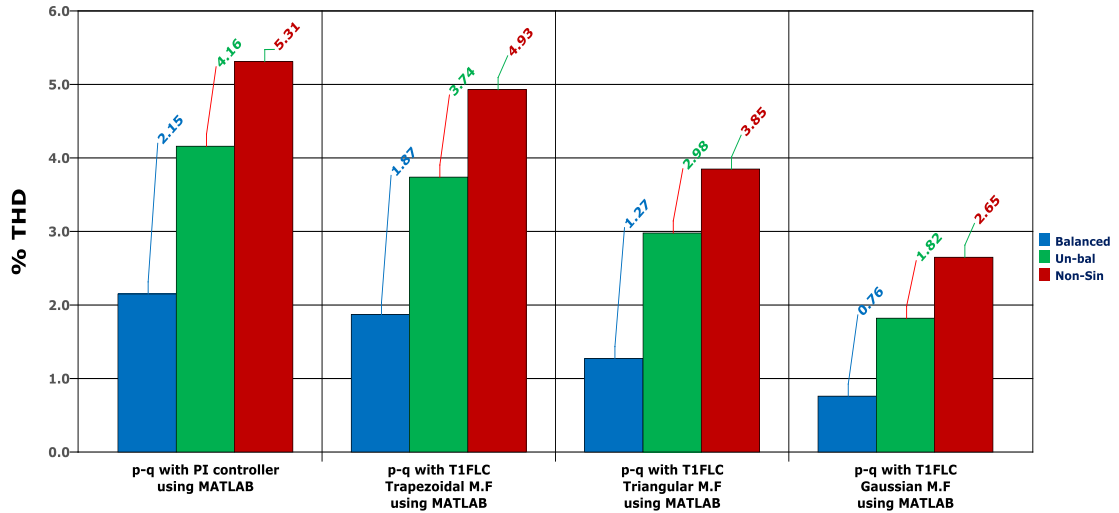


Fig. 3.24. THD of Source Current for $p-q$ method using PI controller and Type-1 FLC with different Fuzzy MFs using MATLAB

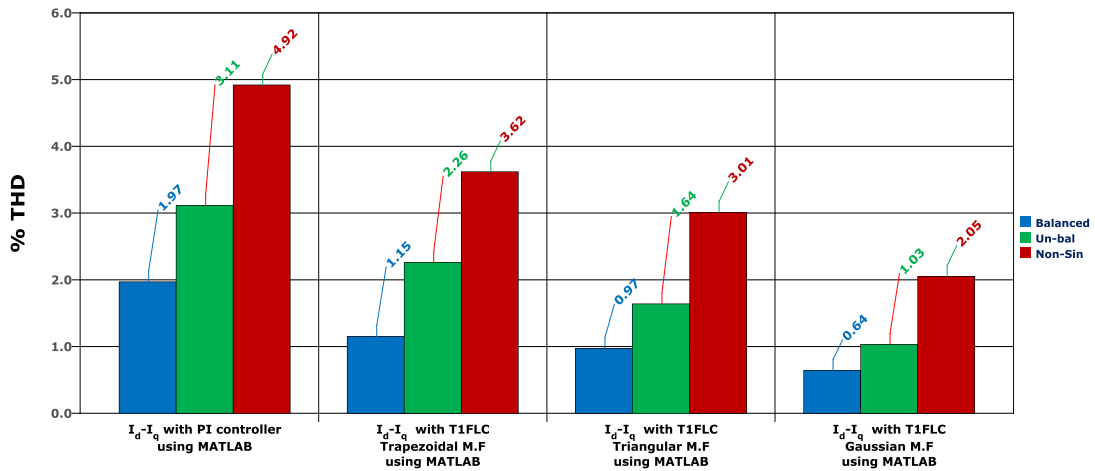


Fig. 3.25. THD of Source Current for I_d-I_q method using PI controller and Type-1 FLC with different Fuzzy MFs using MATLAB

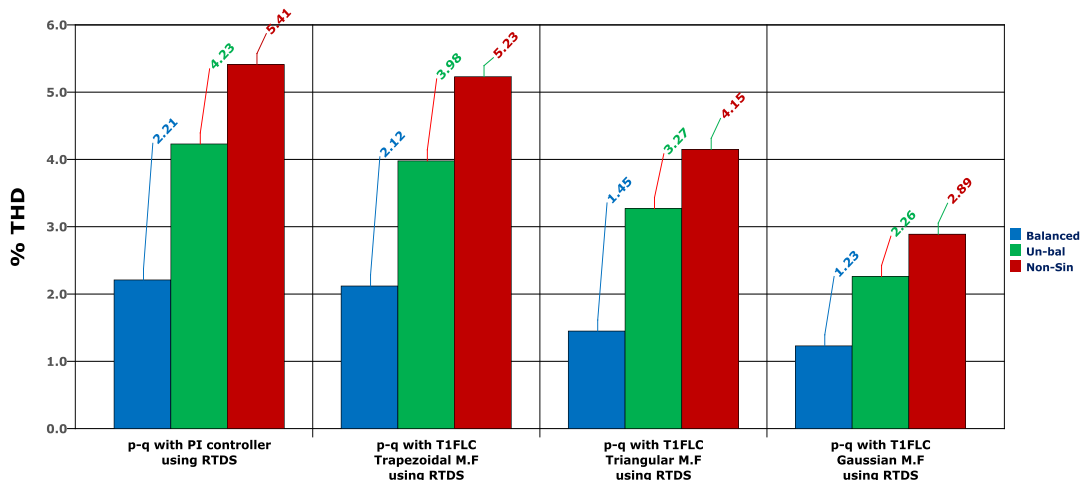


Fig. 3.26. THD of Source Current for $p-q$ method using PI controller and Type-1 FLC with different Fuzzy MFs using real-time digital simulator

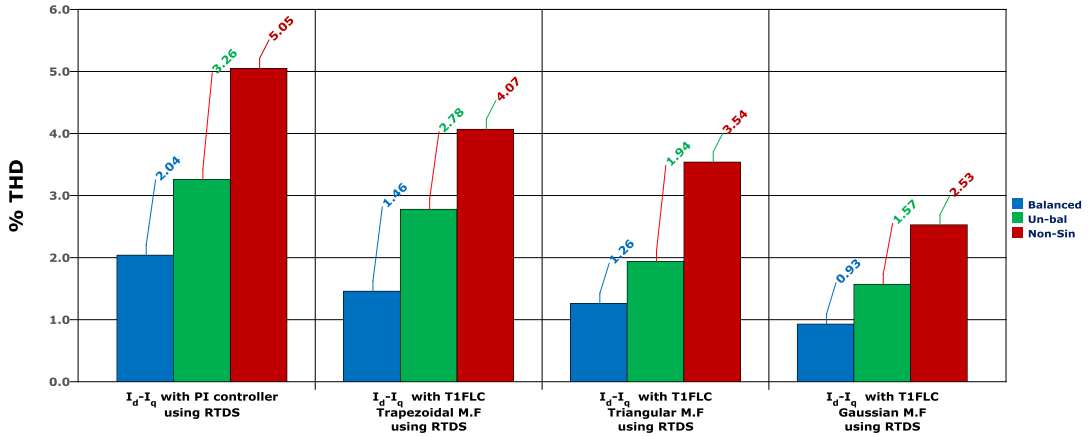


Fig. 3.27. THD of Source Current for I_d-I_q method using PI controller and Type-1 FLC with different Fuzzy MFs using real-time digital simulator

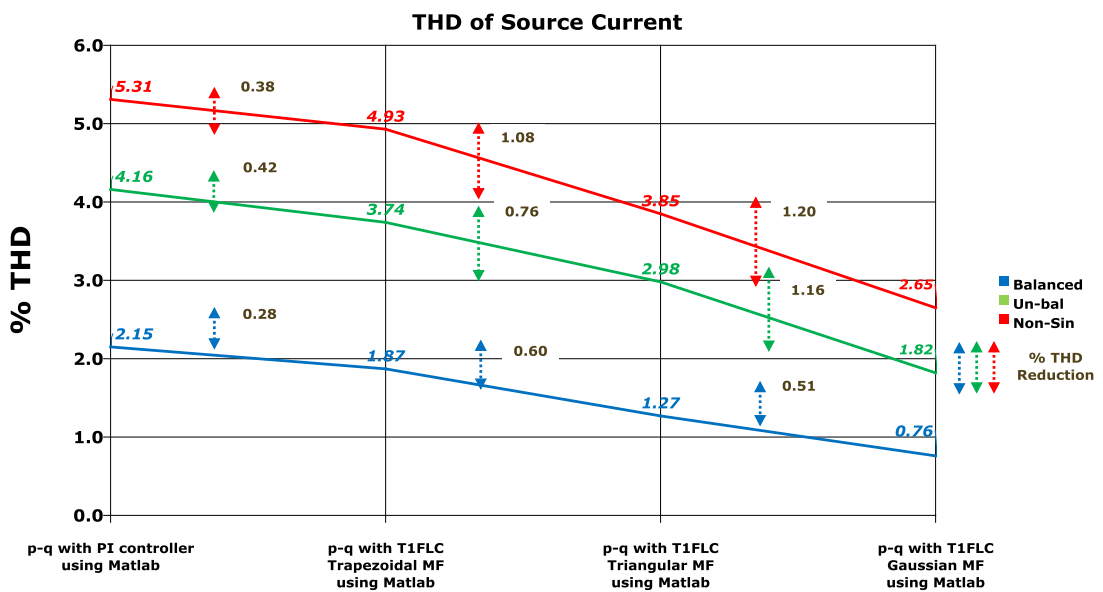


Fig. 3.28. The amount of THD reduced for PI controller and Type-1 FLC with different Fuzzy MFs using $p-q$ control strategy with MATLAB

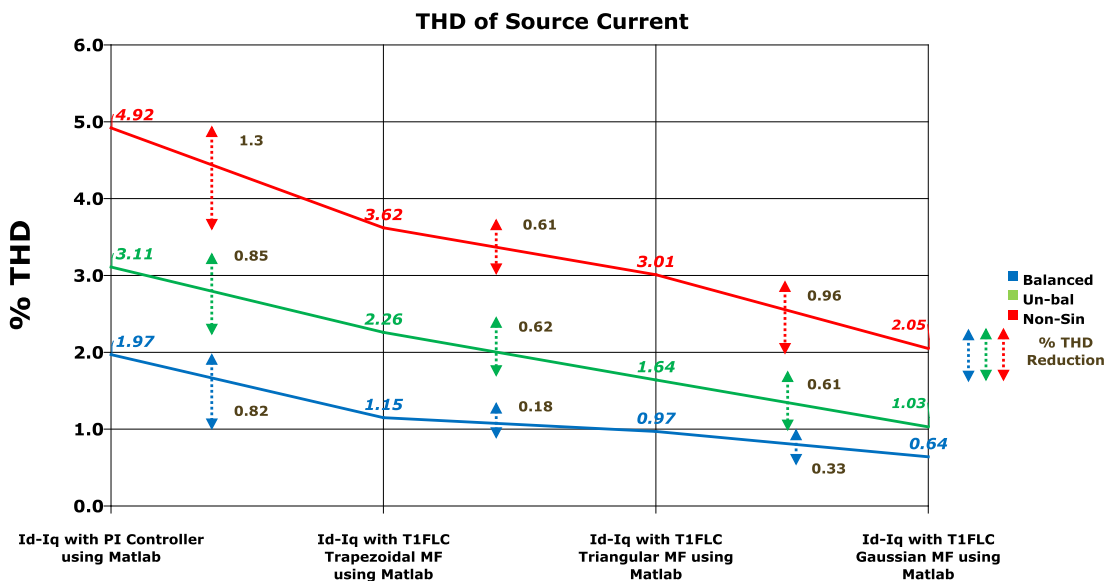


Fig. 3.29. The amount of THD reduced for PI controller and Type-1 FLC with different Fuzzy MFs using I_d-I_q control strategy with MATLAB

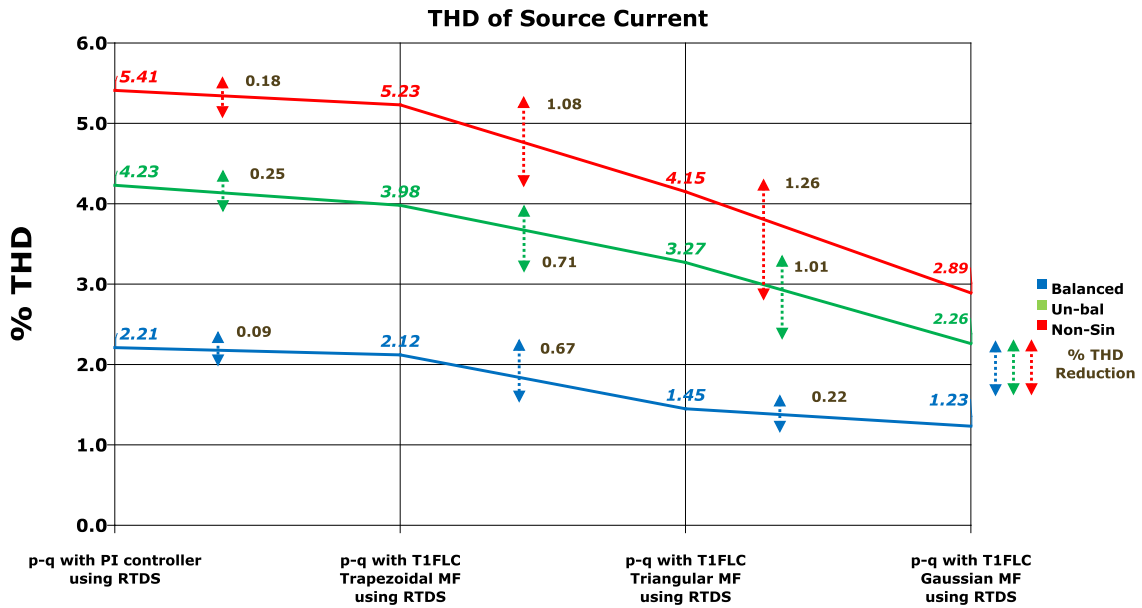


Fig. 3.30. The amount of THD reduced for PI controller and Type-1 FLC with different Fuzzy MFs using $p-q$ control strategy with real-time digital simulator

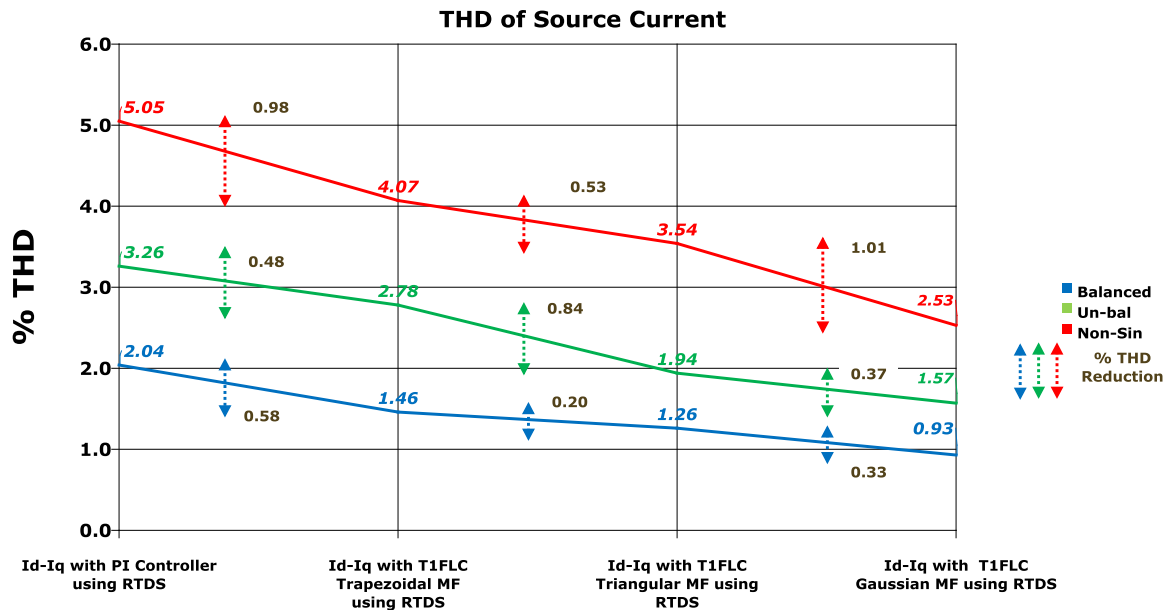


Fig. 3.31. The amount of THD reduced for PI controller and Type-1 FLC with different Fuzzy MFs using I_d-I_q control strategy with real-time digital simulator

Fig. 3.28, Fig. 3.29, Fig. 3.30 and Fig. 3.31; line graphs, clearly illustrates the amount of THD of source current reduced from one controller to other controller for shunt active filter control strategies ($p-q$ and I_d-I_q) under various source conditions (balanced, unbalanced and non-sinusoidal) using MATLAB and real-time digital simulator.

3.7. Summary

In the present chapter, Type-1 FLC with different Fuzzy MFs (Trapezoidal, Triangular and Gaussian) are developed to improve the power quality of shunt active filter control strategies ($p-q$ and I_d-I_q) by mitigating the current harmonics. The control scheme using three independent hysteresis current controllers have been implemented. The simulation results are validated with real-time implementation on real-time digital simulator.

The Real-time implementation and simulation results demonstrate that, even if the supply voltage is non-sinusoidal, the performance of Type-1 FLC based I_d-I_q theory with Gaussian MF showing better compensation capabilities in terms of THD compared to I_d-I_q control strategy with PI, and Type-1 FLC with Trapezoidal and Triangular MF and also $p-q$ theory with PI, and Type-1 FLC with all MFs.

The control approach has compensated the neutral harmonic currents and the dc bus voltage of SHAF is almost maintained at the reference value under all disturbances, which confirm the effectiveness of the controller. While considering the I_d-I_q control strategy using FLC with Gaussian MF, the SHAF has been found to meet the IEEE 519-1992 standard recommendations on harmonic levels, making it easily adaptable to more severe constraints, such as highly distorted and/or un-balanced supply voltage.

I_d-I_q control strategy using Type-1 FLC with different Fuzzy MFs, the SHAF is able to mitigate current harmonics in a better way than that of $p-q$ control strategy using Type-1 FLC with different Fuzzy MFs. Even though, Type-1 FLC based I_d-I_q control strategy with different Fuzzy MFs is able to mitigate the current harmonics, but notches (small amount of harmonics) are present in the source current. So to mitigate the current harmonics perfectly, one has to choose appropriate controller. Hence to avoid the difficulties occur with Type-1 FLC based $p-q$ and I_d-I_q control strategies using different Fuzzy MFs, we have considered Type-2 FLC based $p-q$ and I_d-I_q control strategies with different Fuzzy MFs.

Chapter - 4

Performance analysis of Shunt active filter control strategies using Type-2 FLC with different Fuzzy MFs

Introduction to TYPE-2 FLC

The structure and MF of Type-2 Fuzzy Sets

Type-2 Fuzzy inference system with different Fuzzy MFs

Simulation results (Type-2 FLC)

Summary

CHAPTER - 4

*In the previous chapter-3, Type-1 FLC based shunt active filter control strategies with different Fuzzy MFs are discussed. Simulation and real-time results are also presented. Even though, Type-1 FLC based shunt active filter control strategies with different Fuzzy MFs are able to mitigate the harmonics, notches are present in the source current. So to mitigate the harmonics perfectly, one has to choose perfect controller. In this **chapter-4**, the proposed **Type-2 FLC based shunt active filter control strategies with different Fuzzy MFs are introduced. The detailed simulation results using MATLAB/SIMULINK software are presented to support the feasibility of the proposed control strategies. With this approach, the compensation capabilities of SHAF are extremely good.***

This chapter is organized as follows: Section 4.1 introduces the advantages of using Type-2 FLC, Section 4.2 presents the detailed structure of Type-2 FLC, Section 4.3 presents the details of Type-2 Fuzzy inference system with different Fuzzy MFs, Simulation results of Type-2 FLC based p - q control strategy with different Fuzzy MFs using MATLAB are presented in Section 4.4, Simulation results of Type-2 FLC based I_d - I_q control strategy with different Fuzzy MFs using MATLAB is presented in Section 4.5, Section 4.6 provides the comparative study and finally Section 4.7 states all concluding remarks.

4.1 Introduction to Type-2 FLC

The concept of Fuzzy systems was introduced by Lotfi Zadeh in 1965 to process data and information affected by non-probabilistic uncertainty/imprecision [82]. Soon after, it was proven to be an excellent choice for many applications, since it mimics human control logic. These were designed to represent mathematically the vagueness and uncertainty of linguistic problems [84], thereby obtaining formal tools to work with intrinsic imprecision in different type of problems. It is considered as a generalization of the classic set theory [85]. Intelligent

systems based on Fuzzy logic controller are fundamental tools for nonlinear complex system modelling [108].

The advantages of Fuzzy logic controllers [7, 26, 50, 65, 98, 104] over conventional (PI) controllers are that they do not require an accurate mathematical model, can work with imprecise inputs, can handle non-linearity and are more robust than conventional PI controllers.

With the development of Type 2 FLCs [105] and their ability to handle uncertainty [109], utilizing Type-2 FLC has attracted a lot of significance in recent years. It is an extension [110] of the concept of well-known Type-1 Fuzzy sets. A Type-2 Fuzzy set is characterized by a Fuzzy membership function i.e. the membership grade for each element is also a Fuzzy set in $[0, 1]$, unlike a Type-1 Fuzzy set, where the membership grade is a crisp number in $[0, 1]$. The membership functions of Type-2 Fuzzy sets are three dimensional and include a foot point of Uncertainty (FOU) [107-113], which is the new third dimension of Type-2 Fuzzy sets. The foot point of uncertainty provides an additional degree of freedom to handle uncertainties.

Type-2 Fuzzy sets [114] are used for modelling uncertainty and imprecision in a better way. The concept of Type-2 Fuzzy sets was first proposed by Lofti Zadeh in 1975 and is essentially “Fuzzy- Fuzzy” [115] sets where the Fuzzy degree of membership is a Type-1 Fuzzy set. The new concepts were introduced by Mendel [117-122] and Liang [118, 122] allowing the characterization of a Type-2 Fuzzy set with a superior membership function and an inferior membership function, these two functions can be represented each one by a Type-1 Fuzzy set membership function.

There are different sources of uncertainty [123] in the evaluation process. The five types of uncertainty that emerge from the imprecise knowledge natural state are:

↳ *Measurement uncertainty* - It is the error on observed quantities.

- ↳ *Process uncertainty* - It is the dynamic randomness.
- ↳ *Model uncertainty* - It is the wrong specification of the model structure.
- ↳ *Estimate uncertainty* - It is the one that can appear from any of the previous uncertainties or a combination of them, and it is called inexactness and imprecision.
- ↳ *Implementation uncertainty* - It is the consequence of the variability that results from sorting politics, i.e. incapacity to reach the exact strategic objective.

4.1.1 Why Type-2 FLCs?

Using Type-2 Fuzzy sets to represent the inputs/outputs of a FLC has many advantages when compared to the Type-1 Fuzzy sets. As the Type-2 Fuzzy sets membership functions are Fuzzy and contain a FOU, they can model and handle the linguistic [125] and numerical uncertainties associated with the inputs and outputs of the FLC [125]. Using Type-2 Fuzzy sets to represent the FLC inputs and outputs will result in the reduction of the FLC rule base when compared to using Type-1 Fuzzy sets [126]. This is because the uncertainty represented in the FOU in Type-2 Fuzzy sets allows us to cover the same range as Type-1 Fuzzy sets with a smaller number of labels.

It has been recently shown that the extra degrees of freedom provided by the FOU enables a Type-2 FLC to produce outputs that cannot be achieved by Type-1 FLCs [127] with the same number of membership functions [128]. Where a Type-2 Fuzzy set may give rise to an equivalent Type-1 membership grade [129] that is negative or larger than unity. Each input and output will be represented by a large number of Type-1 Fuzzy sets, which are embedded in the Type-2 Fuzzy sets [130]. The use of such a large number of Type-1 Fuzzy sets to describe the input and output variables allows for a detailed description of the analytical control surface as the addition of the extra levels of classification give a much smoother control surface and response. In addition, the Type-2 FLC can be thought of as a collection of many different embedded Type-1 FLCs.

4.2 The Structure of Type-2 FLC

From **Fig. 4.2**, it can be seen that the structure of a Type-2 FLC [131, 132] is very similar to the structure of a Type-1 FLC (**Fig.4.1**) and the only difference exists in the output processing block. For a Type-1 FLC [104, 132], the output processing block only contains a defuzzifier, but for a Type-2 FLC, the output processing block includes Type-reducer [104].

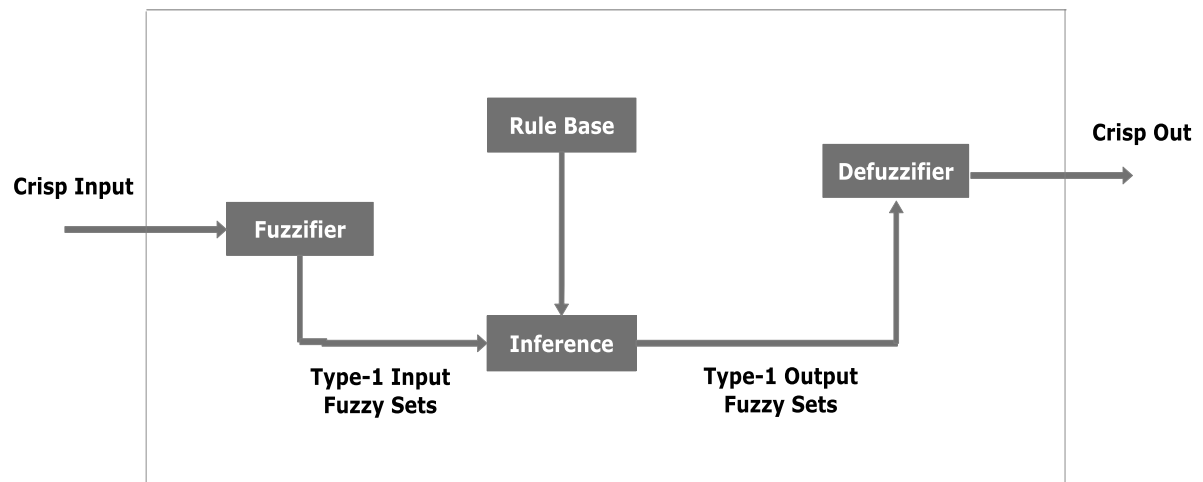


Fig. 4.1 The architecture of Type-1 FLC

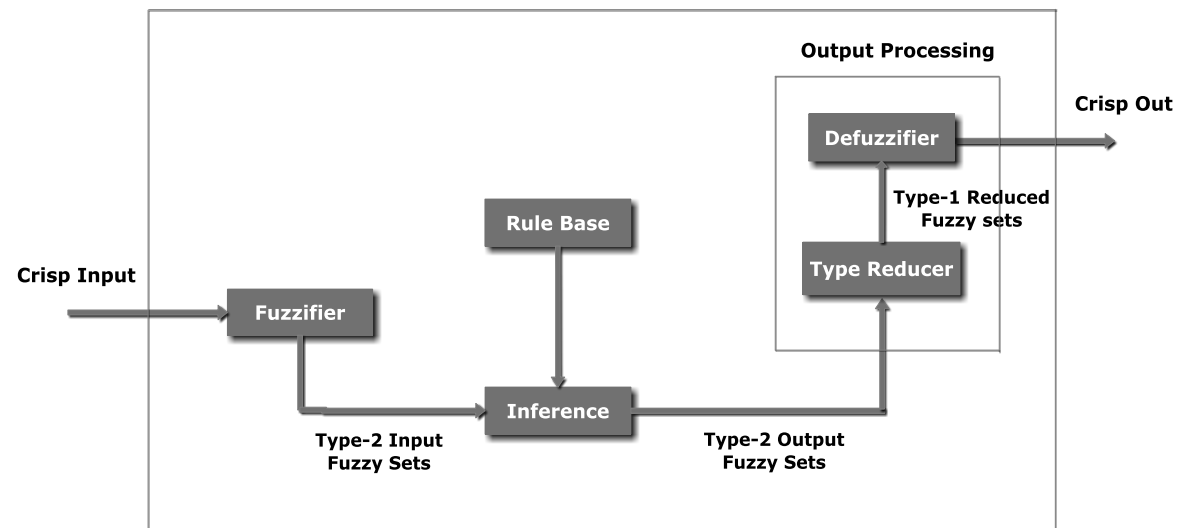


Fig. 4.2 The architecture of Type-2 FLC

Fuzzy logic theory [133] is based on the computation with Fuzzy sets. While Type-1 Fuzzy sets allow for a Fuzzy representation of a term to be made, the fact that the membership function of a Type-1 set is crisp means that the degrees of membership set are completely

crisp – not Fuzzy. In a Type-1 Fuzzy set (**Fig. 4.3(a)**) the membership grade [134] for each element is a crisp number in $[0, 1]$. A Type-2 Fuzzy (**Fig. 4.3(b)**) set is characterised by a three dimensional membership function and a Foot point of uncertainty (FOU).

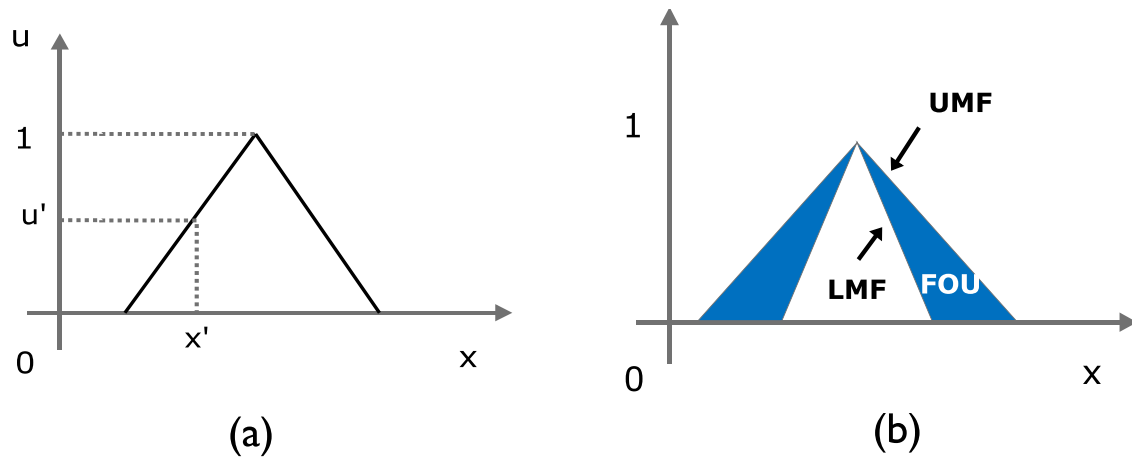


Fig. 4.3 Membership Function (a) Type-1 FLC and (b) Type-2 FLC

In the design of Type-2 FLC [135], the same configuration as that of Type-1 FLC is chosen. There are two-input, single-output and each input/output variable has same seven linguistic variables which are defined in **Fig. 4.3(b)**. In this thesis Mamdani Fuzzy Inference system is used. Operation on Type-2 Fuzzy set is identical with an operation on Type-1 Fuzzy set. However, on Type-2 Fuzzy system, Fuzzy operation [136] is done at two Type-1 membership function [137] which limits the FOU, LMF (lower membership function) and UMF (upper membership function) to produce firing strengths. Hence, the membership value (or membership grade); for each element of this set is a Fuzzy set in $[0, 1]$.

A Type-2 Fuzzy set [138] is bounded from below by a Lower Membership Function. The Type-2 Fuzzy set is bounded from above by an Upper Membership Function. The area between the lower membership function and the upper membership is entitled the Footprint of Uncertainty (FOU) [139]. The new third-dimension of Type-2 Fuzzy sets and the footprint of uncertainty provide additional degrees of freedom that make it possible to directly model

and handle uncertainties. Hence, Type-2 FLCs that use Type-2 Fuzzy sets in either their inputs or outputs have the potential to provide a suitable framework to handle the uncertainties in real world environments. It is worth noting that a Type-2 Fuzzy set embeds a huge number of Type-1 Fuzzy sets [140]. A is a Type-1 Fuzzy set [141] and the membership grade [142] of $x \in X$ in A is $\mu_A(x)$, which is a crisp number in $[0, 1]$; a Type-2 Fuzzy set in X is \tilde{A} and the membership grade of $x \in X$ in \tilde{A} is $\mu_{\tilde{A}}(x)$, which is a Type-1 Fuzzy set in $[0, 1]$.

A Type-2 Fuzzy set, denoted \tilde{A} , is characterized by a Type-2 MF $\mu_{\tilde{A}}(x, u)$, where $x \in X$ and $u \in J_x \subseteq [0, 1]$, i.e.,

$$\tilde{A} = \left\{ \left((x, u), \mu_{\tilde{A}}(x, u) \right) \mid \forall x \in X, \forall u \in J_x \subseteq [0, 1] \right\} \quad (4.1)$$

In which $0 \leq \mu_{\tilde{A}}(x, u) \leq 1$

$$\tilde{A} \text{ can also be expressed as } \tilde{A} = \int_{x \in X} \int_{u \in J_x} \mu_{\tilde{A}}(x, u) / (x, u) \quad J_x \subseteq [0, 1] \quad (4.2)$$

Where $\int \int$ denotes union over all admissible x and u . For discrete universe of discourse

\int is replaced by \sum .

$$\tilde{A} \text{ can be re-expressed as } \tilde{A} = \left\{ \left(x, \mu_{\tilde{A}}(x) \right) \mid \forall x \in X \right\} \quad (4.3)$$

$$\tilde{A} = \int_{x \in X} \mu_{\tilde{A}}(x) / x = \int_{x \in X} \left[\int_{u \in J_x} f_x(u) / u \right] / x \quad J_x \subseteq [0, 1] \quad (4.4)$$

$$\text{If } X \text{ and } J_x \text{ are both discrete then } \tilde{A} = \sum_{x \in X} \left[\sum_{u \in J_x} f_x(u) / u \right] / x$$

$$\tilde{A} = \sum_{i=1}^N \left[\sum_{u \in J_{x_i}} f_{x_i}(u) / u \right] /_{x_i} \quad (4.5)$$

$$\begin{aligned} \tilde{A} = & \sum_{K=1}^{M_1} \left[\sum_{u \in J_{x_1}} f_{x_1}(u_{1k}) / u_{1k} \right] /_{x_1} + \sum_{K=2}^{M_2} \left[\sum_{u \in J_{x_2}} f_{x_2}(u_{2k}) / u_{2k} \right] /_{x_2} + \dots \\ & + \sum_{K=1}^{M_N} \left[\sum_{u \in J_{x_N}} f_{x_N}(u_{Nk}) / u_{Nk} \right] /_{x_N} \end{aligned} \quad (4.6)$$

The discretization [29] along each u_{ik} does not have to be the same, which is why we have shown a different upper sum for each of the bracketed terms. If, however, the discretization along each u_{ik} is the same, then $M_1 = M_2 = \dots = M_N = M$. Uncertainty in the primary memberships of a Type-2 Fuzzy set \tilde{A} consists of a bounded region that we call the footprint of uncertainty [143] (FOU). It is the union of all primary memberships, i.e.,

$$FOU(\tilde{A}) = \bigcup_{x \in X} J_x \quad (4.7)$$

4.3 Type-2 Fuzzy inference system with different Fuzzy MFs

Fig. 4.4 shows the Type-2 FLS [104, 132] with different MFs. It consists of

- ↗ Type 2 Fuzzy Inference System (Type-2 FIS) Editor
- ↗ Type 2 Fuzzy Membership Function Editor
- ↗ Type 2 Fuzzy Rule Editor
- ↗ Type 2 Fuzzy Rule Viewer
- ↗ Type 2 Fuzzy Surface Viewer and
- ↗ Type 2 Fuzzy reduced surface viewer

Fig.4.4 (a), Fig.4.4 (b) and Fig.4.4 (c) show the Type-2 FIS implementation with different Fuzzy MFs using MATLAB. In this FIS we have designed [104, 132]

- ↪ No. of inputs and outputs - **(Dual input and single output)**,
- ↪ No. of rules - **(49 rules)**,
- ↪ Type of membership function - **(Trapezoidal, Triangular and Gaussian)**,
- ↪ No. of membership functions - **(seven)**
- ↪ Type of implication - **(Mamdani Max-Min Operation)**
- ↪ Type of defuzzification method - **(centroid of area method)**

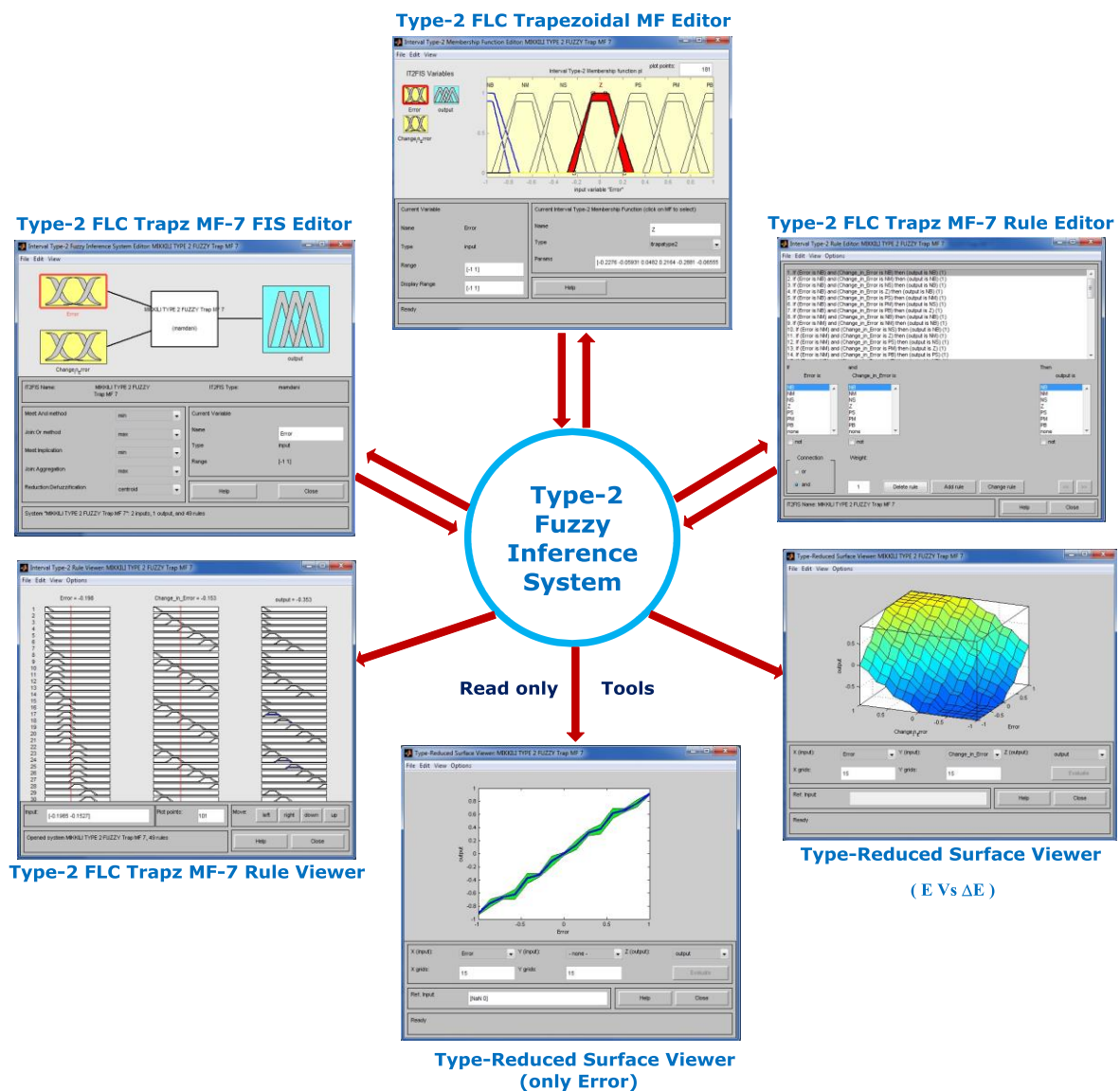


Fig. 4.4(a) Type-2 Fuzzy Inference System with Trapezoidal MF 7x7

The Type-2 FIS [104] Editor handles the high-level issues for the system. How many input and output variables? What are their names? The Type-2 FIS doesn't limit the number of inputs. However, the number of inputs may be limited by the available memory of the PC (personal computer). If the number of inputs is too large, or the number of Type-2 membership functions [38] is too big, then it may also be difficult to analyse the Type-2 FIS using the other GUI tools. The Type-2 Membership Function Editor is used to define the shapes of all the Type-2 Membership functions associated with each variable. The Type-2 Rule Editor is for editing the list of rules that defines the behaviour of the systems.

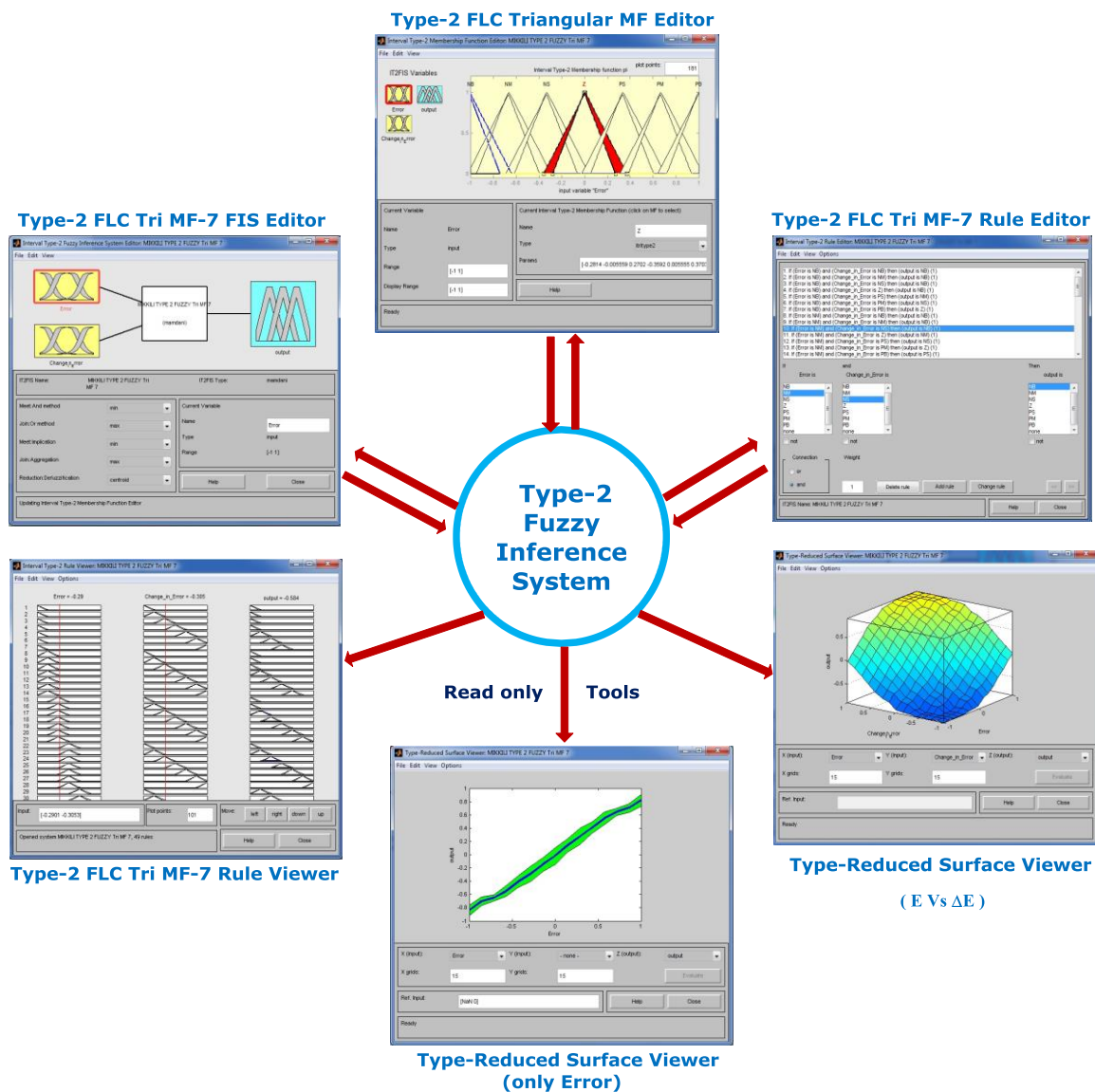


Fig. 4.4(b) Type-2 Fuzzy Inference System with Triangular MF 7x7

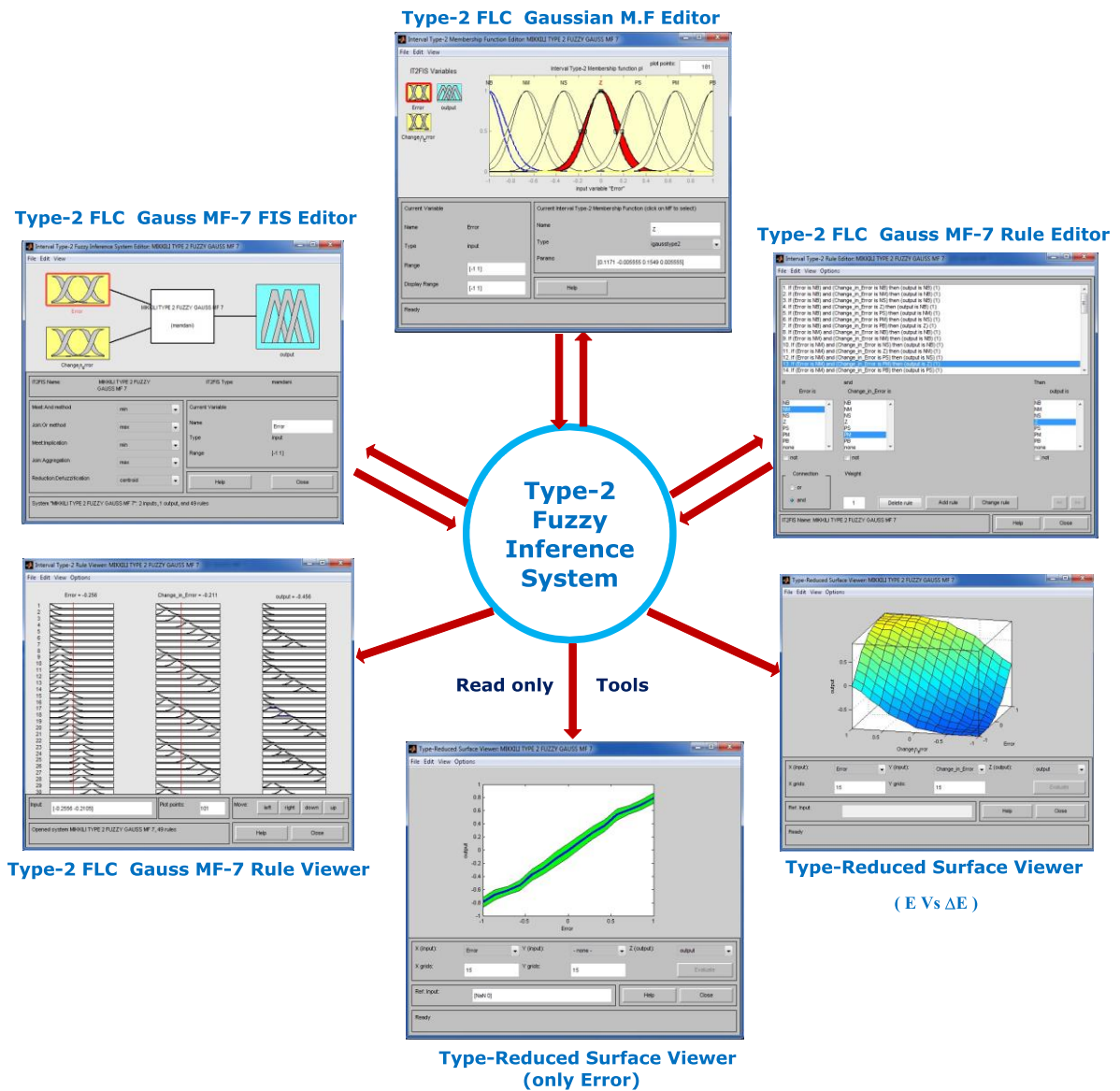


Fig. 4.4(c) Type-2 Fuzzy Inference System with Gaussian MF 7x7

The Type-2 Rule Viewer and the Surface Viewer or Type-reduced Surface Viewer used for looking at, as opposed to editing the Type-2 FIS [132]. They are strictly read-only tools. The Type-2 Rule Viewer is a MATLAB based display of the Type-2 Fuzzy inference diagram shown in Fig. 4.4. Used as a diagnostic, it can show which rules are active, or how individual Type-2 Membership Function shapes are influencing the results. The Surface viewer is used to display the dependency of one of the outputs on any one or two of the inputs i.e., it generates and plots an output surface map for the system.

4.4 System Performance of Type-2 FLC based P - Q Control Strategy with different Fuzzy MFs using MATLAB

Fig. 4.5, Fig. 4.6 and Fig. 4.7 gives the details of Source Voltage, Load Current, Compensation current, Source Current with filter, DC Link Voltage, THD (Total harmonic distortion) of Type-2 FLC based p - q control strategy with different Fuzzy MFs using MATLAB under balanced, un-balanced and non-sinusoidal supply voltage conditions.

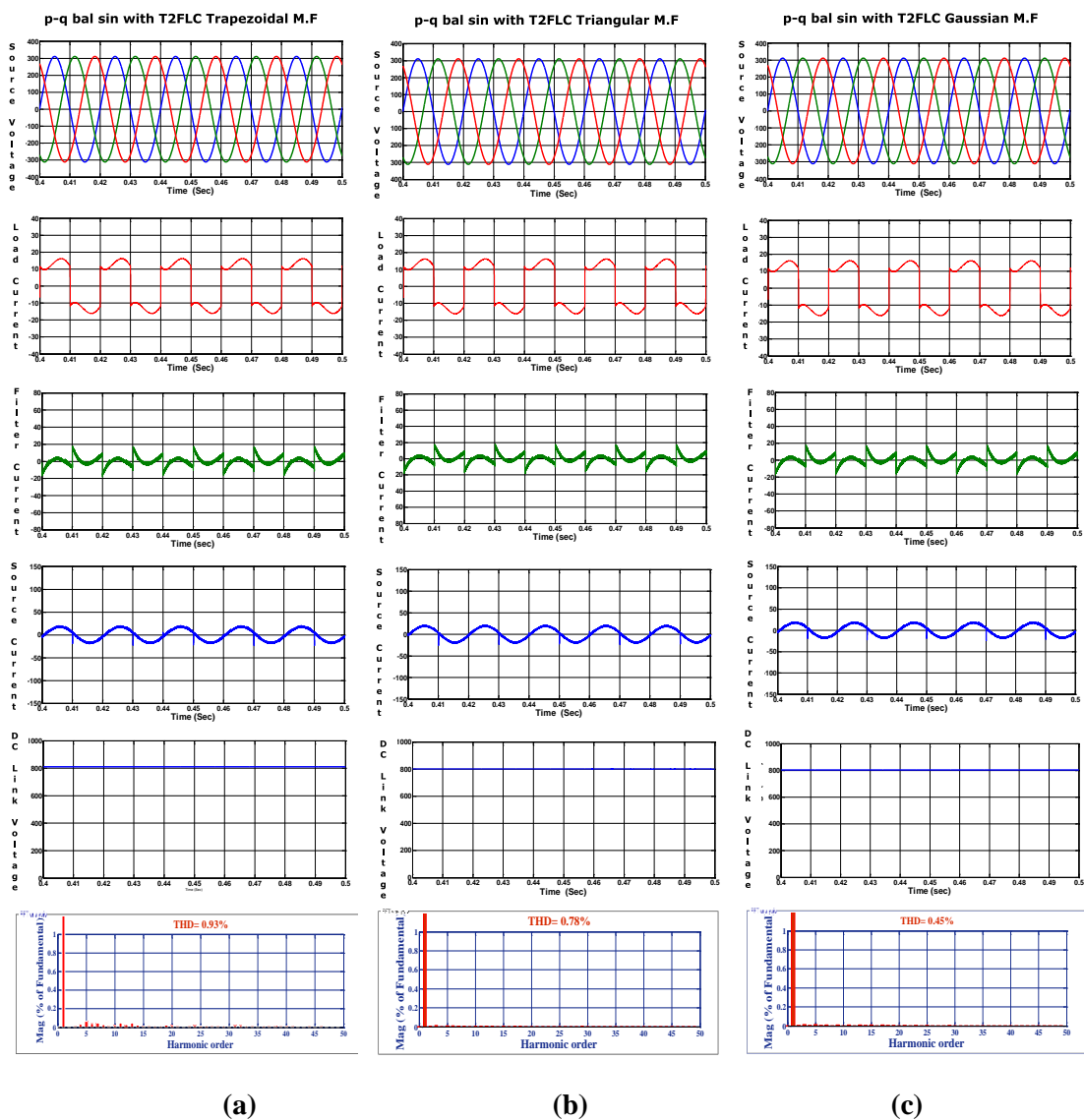


Fig. 4.5 SHAF response using p - q control strategy with Type-2 FLC under balanced Sinusoidal condition using MATLAB

(a) Trapezoidal MF (b) Triangular MF and (c) Gaussian MF

(i) Source Voltage (ii) Load Current (iii) Compensation current (iv) Source Current with filter (v) DC Link Voltage (vi) THD of Source current

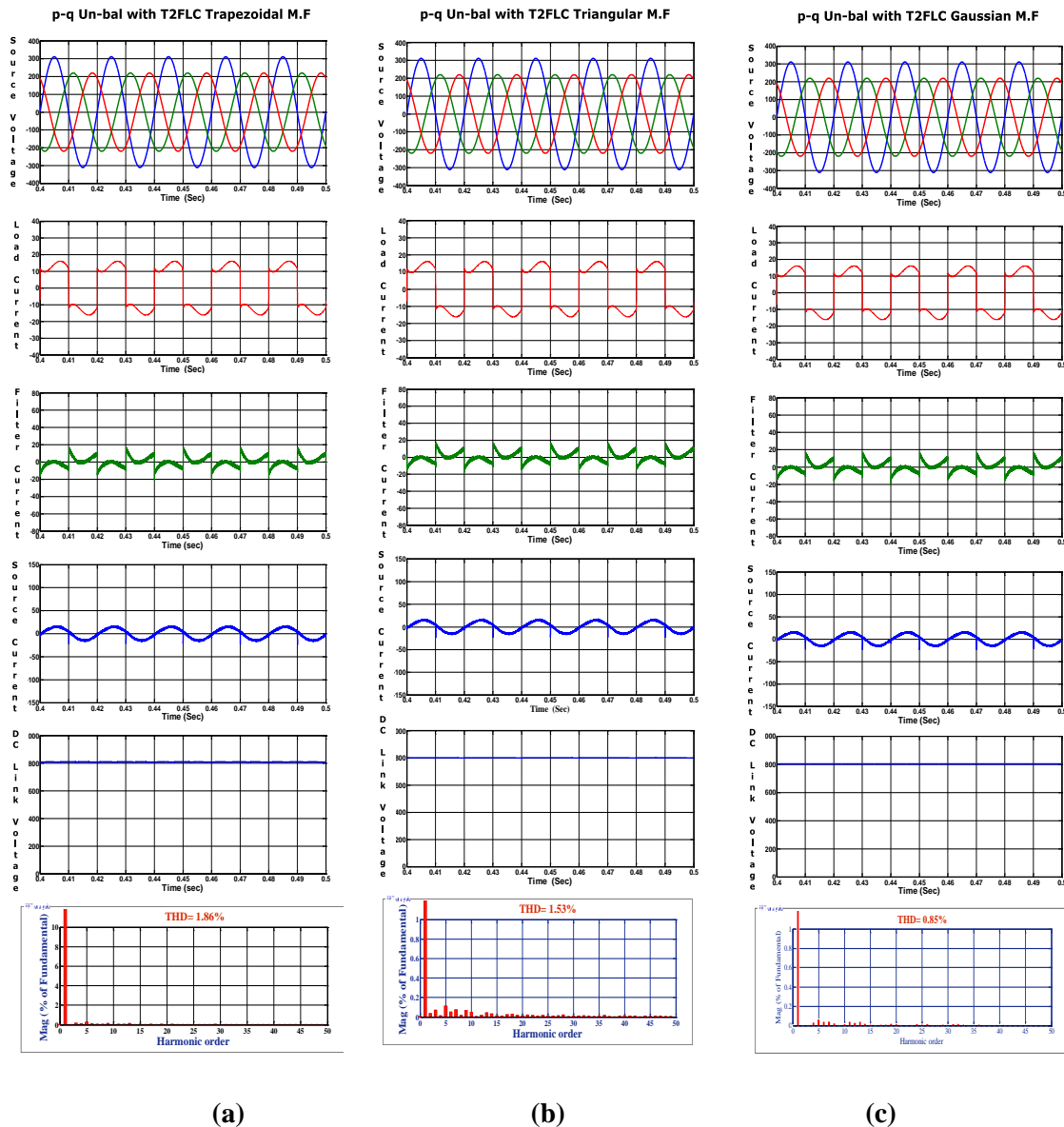


Fig. 4.6 SHAF response using *p-q* control strategy with **Type-2 FLC** under **un-balanced Sinusoidal** condition using **MATLAB**

Initially, the system performance is analysed under balanced sinusoidal conditions, during which it is observed that, the Type-2 FLC with all MFs are good enough at suppressing the harmonics. The respective THDs of SHAF using *p-q* control strategy in MATLAB is 0.93%, 0.78% and 0.45%. The THD of the *p-q* control strategy using Type-2 FLC with Trapezoidal MF under un-balanced condition is 1.86% and under non-sinusoidal condition it is 2.95%. The THD of the *p-q* control strategy using Type-2 FLC with

Triangular MF under unbalanced condition is 1.53% and under non-sinusoidal condition it is 2.66%. The THD of the $p-q$ control strategy using Type-2 FLC with Gaussian MF under unbalanced condition is 0.85% and under non-sinusoidal condition it is 1.29%. These simulations results are obtained using MATLAB.

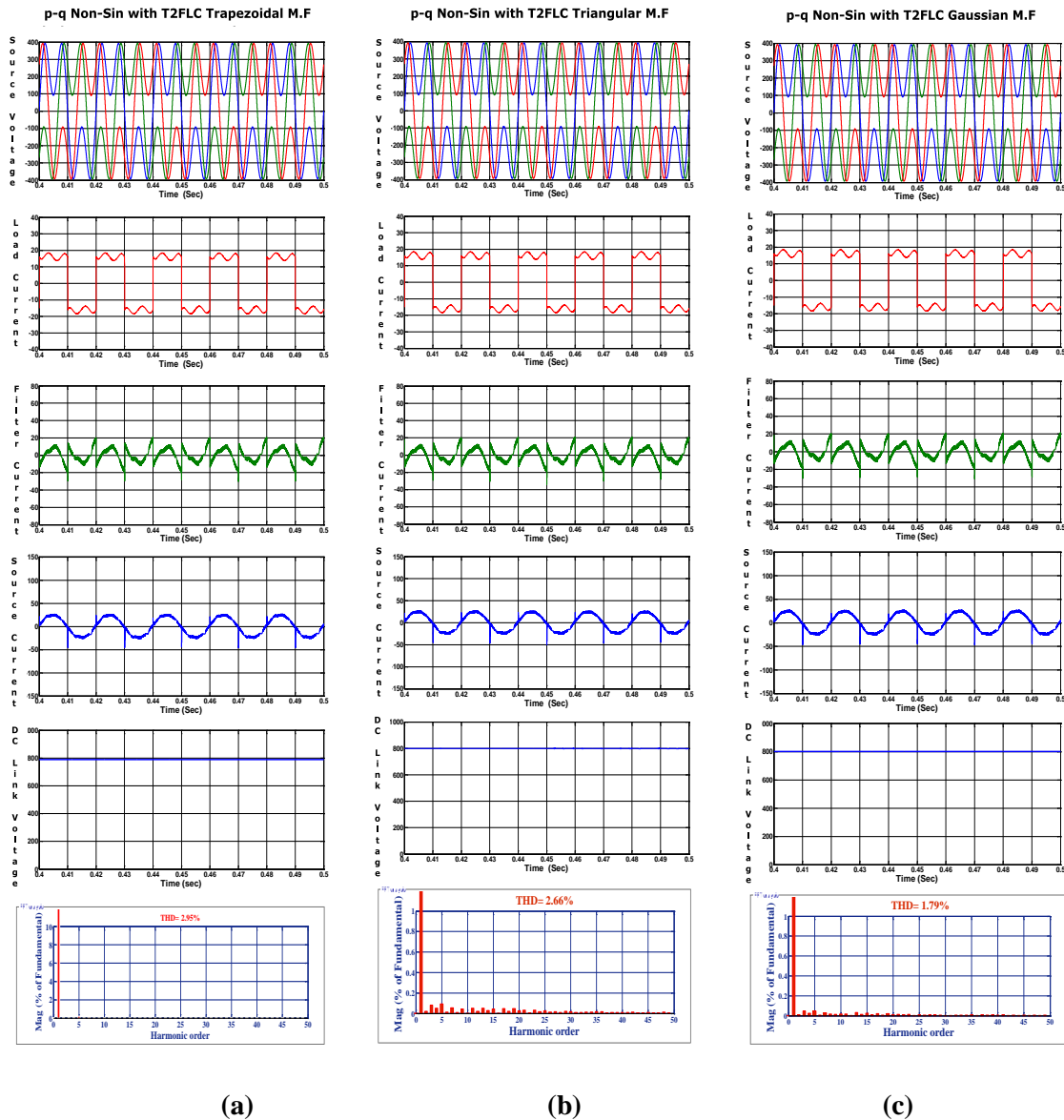


Fig. 4.7 SHAF response using $p-q$ control strategy with **Type-2 FLC** under **Non-Sinusoidal** condition using **MATLAB**

(a) Trapezoidal MF (b) Triangular MF and (c) Gaussian MF.

(i) Source Voltage (ii) Load Current (iii) Compensation current (iv) Source Current with filter (v) DC Link Voltage (vi) THD of Source current

While considering p - q control strategy using Type-2 FLC with trapezoidal MF, SHAF is succeeded in compensating harmonic currents, but notches are observed in the source current. The main reason behind the notches is that the controller failed to track the current correctly and thereby SHAF fails to compensate completely. It is observed that, source current waveform is somewhat better; notches in the waveform are eliminated by using p - q control strategy with Type-2 FLC triangular MF. By using p - q control strategy with Type-2 FLC Gaussian MF, the source current waveform is improved in quality and notches in the waveform are minimized.

Even though, the p - q control strategy using Type-2 FLC with different Fuzzy MFs is able to mitigate the harmonics, notches are observed in the source current. So to mitigate the harmonics perfectly, one has to choose perfect method. To avoid the difficulties occur with p - q control strategy, we have considered Type-2 FLC based I_d - I_q control strategy.

4.5 System Performance of Type-2 FLC based I_d - I_q Control Strategy with different Fuzzy MFs using MATLAB

Fig. 4.8, Fig. 4.9 and Fig. 4.10 give the details of Source Voltage, Load Current, compensation current, Source Current with filter, DC Link Voltage, THD (Total harmonic distortion) of Type-2 FLC based I_d - I_q control strategy with different Fuzzy MFs using MATLAB under balanced, un-balanced and non-sinusoidal supply voltage conditions.

Initially the system performance is analysed under balanced sinusoidal conditions, during which the Type-2 FLC with all MFs are good enough at suppressing the harmonics. The respective THDs of SHAF in MATLAB are 0.48%, 0.35% and 0.27%. The THD of the I_d - I_q control strategy using Type-2 FLC with Trapezoidal MF under un-balanced condition is 1.23% and under non-sinusoidal condition it is 2.46%. The THD of the I_d - I_q control strategy using Type-2 FLC with Triangular MF under unbalanced condition is 0.96%

and under non-sinusoidal condition it is 1.83%. The THD of the I_d-I_q control strategy using Type-2 FLC with Gaussian MF under unbalanced condition is 0.66% and under non-sinusoidal condition it is 1.44%. The simulations are performed using MATLAB.

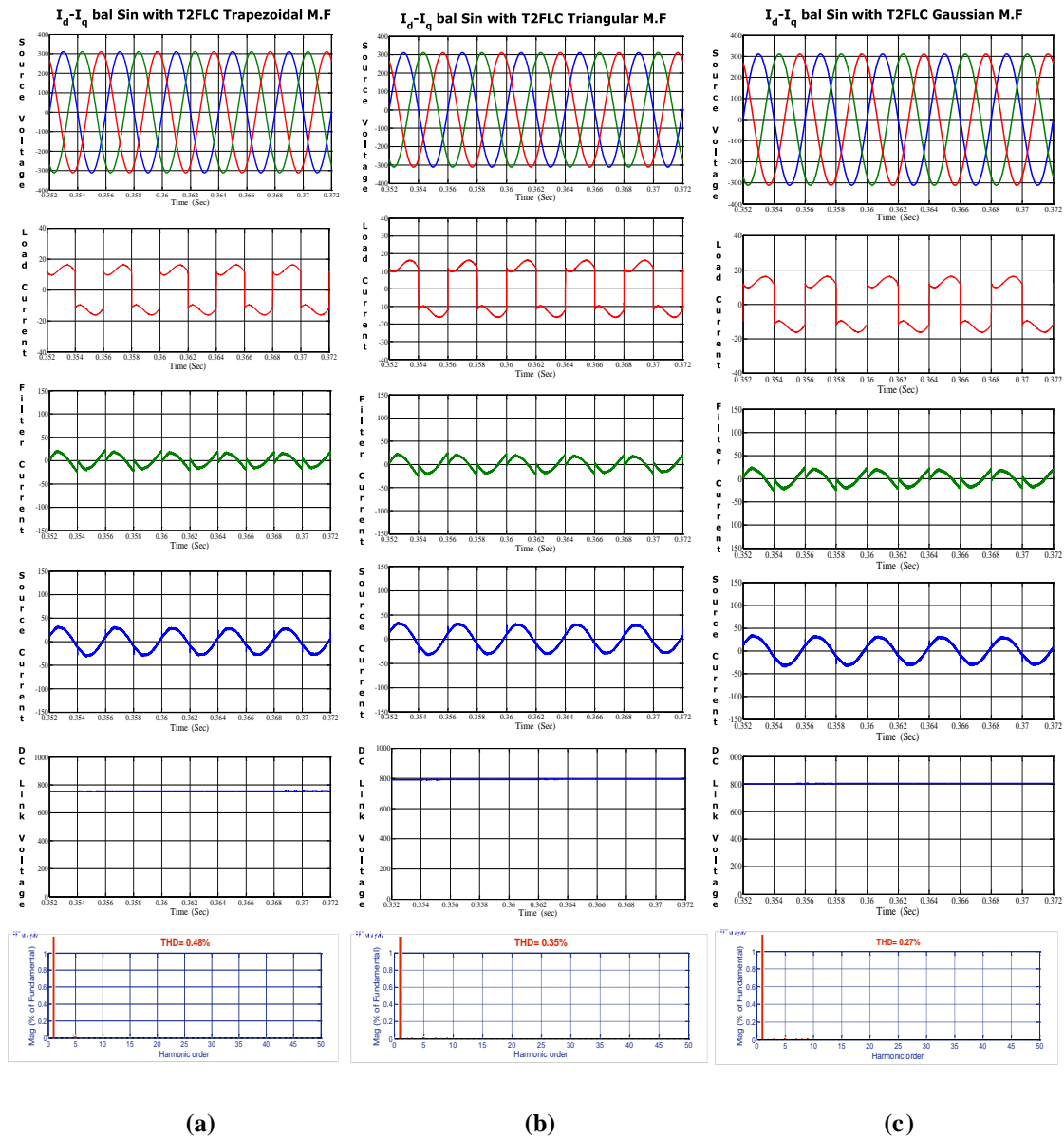


Fig. 4.8 SHAF response using I_d-I_q control strategy with **Type-2 FLC** under **balanced Sinusoidal** condition using **MATLAB**

(a) *Trapezoidal MF* (b) *Triangular MF* and (c) *Gaussian MF*.

(i) Source Voltage (ii) Load Current (iii) Compensation current (iv) Source Current with filter (v) DC Link Voltage (vi) THD of Source current

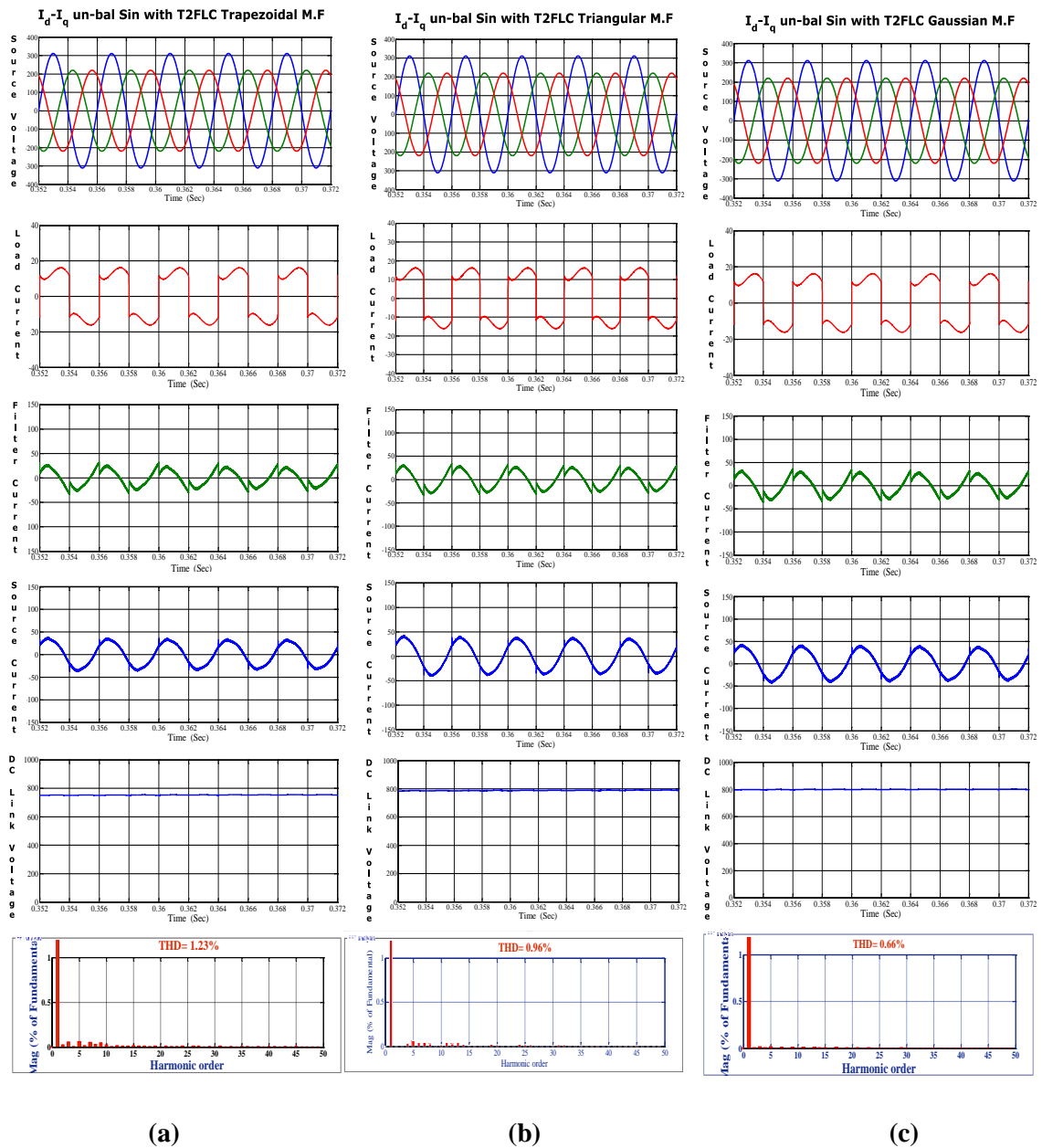
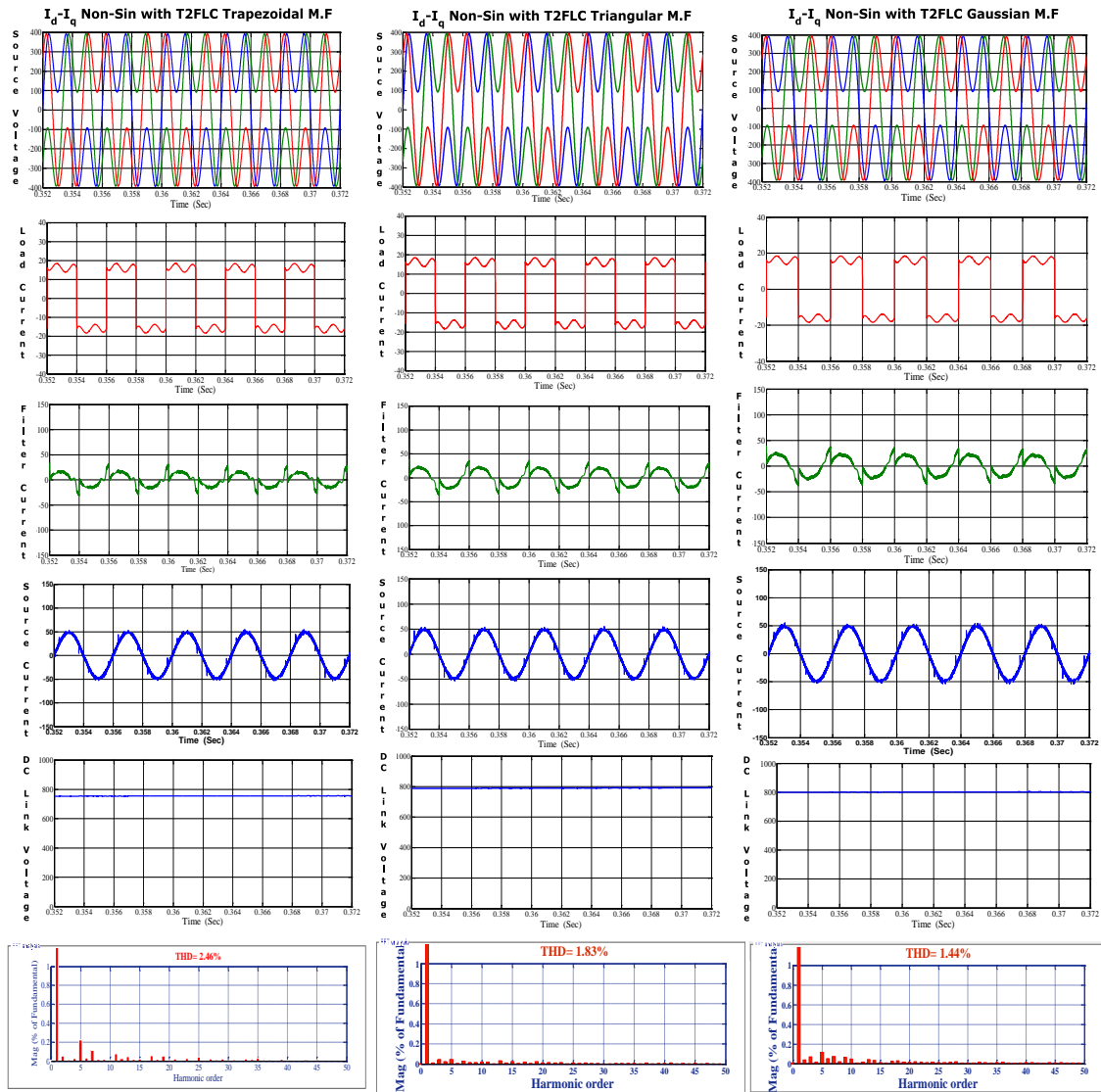


Fig. 4.9 SHAF response using I_d-I_q control strategy with **Type-2 FLC** under **Un-balanced Sinusoidal** condition using **MATLAB**

When the supply voltages are balanced and sinusoidal, I_d-I_q control strategy using Type-2 FLC, with all membership functions (Trapezoidal, Triangular and Gaussian), are converging to the same compensation characteristics. However, under unbalanced and non-sinusoidal conditions, the I_d-I_q control strategy using Type-2 FLC with Gaussian MF shows superior performance over the TYPE-2 FLC with other two MFs.



(a)

(b)

(c)

Fig. 4.10 SHAF response using I_d-I_q control strategy with **Type-2 FLC** under **Non-Sinusoidal** condition using **MATLAB**

(b) Trapezoidal MF (b) Triangular MF and (c) Gaussian MF.

(i) Source Voltage (ii) Load Current (iii) Compensation current (iv) Source Current with filter (v) DC Link Voltage (vi) THD of Source current

While considering I_d-I_q control strategy using Type-2 FLC with different Fuzzy MFs, SHAF is succeeded in compensating harmonic currents. It is observed that, quality of source current waveforms is extremely good and notches in the waveform are eliminated.

4.6 Comparative Study

Fig. 4.11 and Fig. 4.12 (bar graphs), illustrate the THD of source current for $p-q$ and I_d-I_q control strategies using PI controller, Type-1 FLC and Type-2 FLC with different Fuzzy MFs under various source voltage conditions (balanced, unbalanced and non-sinusoidal) respectively.

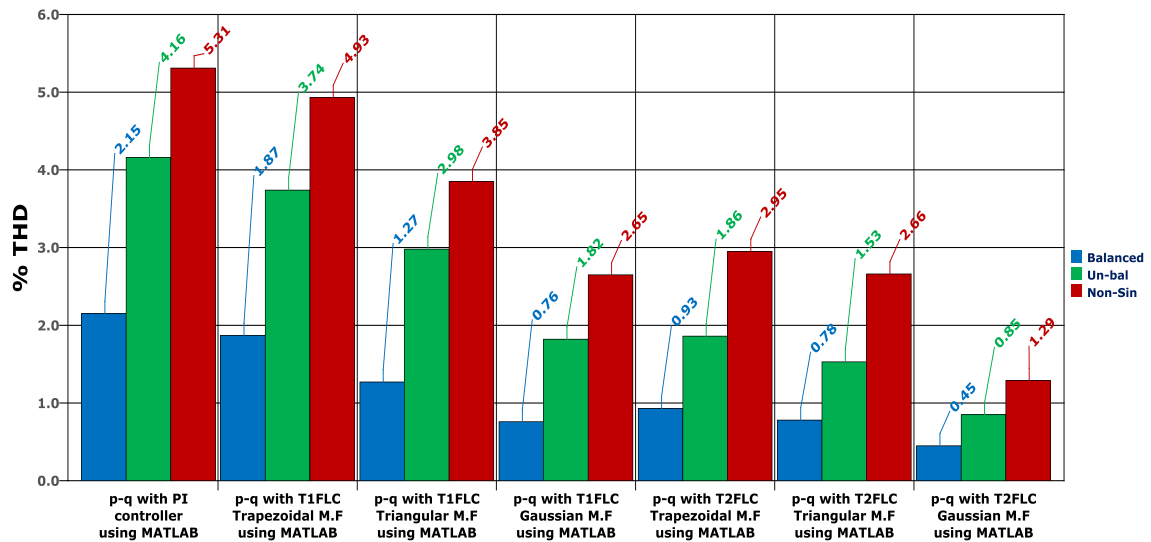


Fig. 4.11 The Bar Graph indicating the THD of Source Current for $p-q$ control strategy using PI controller, Type-1 FLC and Type-2 FLC with different Fuzzy MFs using MATLAB

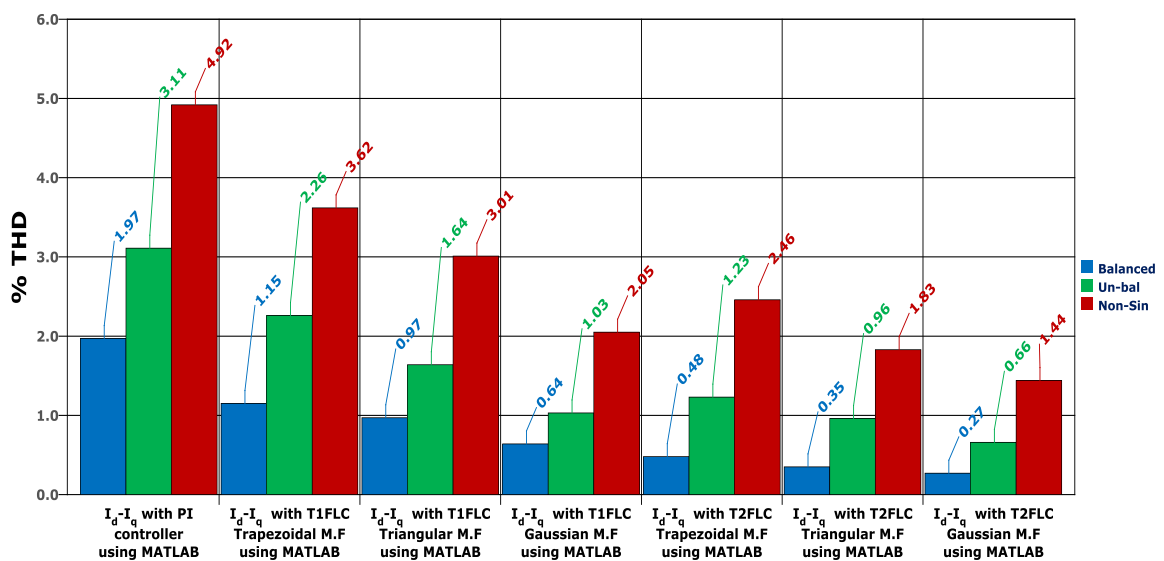


Fig. 4.12 The Bar Graph indicating the THD of Source Current for I_d-I_q control strategy using PI controller, Type-1 FLC and Type-2 FLC with different Fuzzy MFs using MATLAB

4.7 Summary

In this chapter Type-2 FLC based shunt active filter control strategies (p - q and I_d - I_q) with different Fuzzy MFs are developed to improve the power quality by mitigating the harmonics. The control scheme using three independent hysteresis current controllers have been implemented. The performance of the control strategies has been evaluated, in terms of harmonic mitigation and DC link voltage regulation. The proposed SHAF with different Fuzzy MFs (Trapezoidal, Triangular and Gaussian) is able to eliminate the uncertainty in the system and SHAF gains outstanding compensation abilities. The detailed simulation results using MATLAB/SIMULINK software are presented to support the feasibility of proposed control strategies.

The simulation results showed that, even if the supply voltage is non-sinusoidal the performance of Type-2 FLC based I_d - I_q control strategy with Gaussian MF showing better compensation capabilities in terms of THD compared to I_d - I_q theory with PI, Type-1 FLC with all MFs, and Type-2 FLC with Trapezoidal and Triangular MFs and also p - q theory with PI, Type-1 FLC and Type-2 FLC with all MFs. While considering I_d - I_q control strategy using Type-2 FLC with different Fuzzy MFs, SHAF is succeeded in compensating harmonic currents. It is observed that, quality of source current waveforms is extremely good and notches in the waveform are also eliminated.

The control approach has compensated the neutral harmonic currents and the dc bus voltage of SHAF is almost maintained at the reference value under all disturbances, which confirm the effectiveness of the controller. While considering the I_d - I_q control strategy using Type-1 FLC and Type-2 FLC and the p - q control strategy with Type-2 FLC, the SHAF has been found to meet the IEEE 519-1992 standard recommendations on harmonic levels, making it easily adaptable to more severe constraints such as highly distorted and/or unbalanced supply voltage.

Chapter - 5

Introduction to RT-LAB and Real-time implementation of Type-2 FLC based Shunt active filter control strategies

Introduction to RT-Lab

Evolution of Real-time simulators

RT-Lab Simulator Architecture

How RT-Lab Works

OP5142 configuration

Real-time results (Type-2 FLC with different Fuzzy MFs)

Comparative study

Summary

CHAPTER - 5

In the previous chapter, proposed Type-2 Fuzzy logic controller is discussed and simulation results are also presented. It is concluded that proposed Type-2 FLC based shunt active filter control strategies are suitable for mitigation of harmonics presented in the system even if the supply voltage is non-sinusoidal and/or distorted. So in this chapter, the proposed Type-2 FLC based shunt active filter control strategies are verified with Real-time digital simulator (OPAL-RT) to validate the proposed research.

This chapter is organized as follows: Section 5.1 introduces the role and advantages of using real-time simulation by answering three fundamental questions; what is real-time simulation? Why is it needed and how it works? Section 5.2 provides the details of Evolution of Real-Time Simulators, Section 5.3 provides the details of RT-Lab Simulator Architecture, Section 5.4 provides the details of how RT-LAB Works, Section 5.5 provides the details of OP5142 configuration. Real-time results of Type-2 FLC based p - q and I_d - I_q control strategies with different Fuzzy MFs using real-time digital simulator (OPAL-RT) are presented in sections 5.6 and 5.7. Section 5.8 provides the comparative study and finally Section 5.9 states all concluding remarks.

5.1 Introduction to RT-LAB

Simulation tools have been widely used for the design and enhancement of electrical systems since the mid twentieth century. The evolution of simulation tools has progressed in step with the evolution of computing technologies [132]. In recent years, computing technologies have upgraded dramatically in performance and become extensively available at a steadily decreasing cost. Consequently, simulation tools have also seen dramatic performance gains and there is a steady decrease in cost. Researchers and engineers now have access to affordable, high performance simulation tools that were previously too costly,

except for the largest manufacturers and utilities. RT-LAB [7, 50, 65, 98, 104, 132, 144-157], fully integrated with MATLAB/Simulink, is the open Real-Time Simulation software environment that has revolutionized the way Model-based Design is performed. RT-LAB's flexibility and scalability allow it to be used in virtually any simulation or control system application, and to add computing-power to simulations, where and when it is needed.

This simulator was developed with the aim of meeting the transient simulation needs of electromechanical drives and electric systems while solving the limitations of traditional real-time simulators. It is based on a central principle; the use of extensively available, user-friendly, highly competitive commercial products (PC platform, Simulink). The real-time simulator consists of two main tools; a real-time distributed simulation package (RT-LAB) [144] for the execution of Simulink block diagrams on a PC-cluster, and algorithmic toolboxes designed for the fixed time-step simulation of stiff electric circuits and their controllers. Real-time simulation [145] and Hardware-In-the-Loop (HIL) applications [146-148] are progressively recognized as essential tools for engineering design and especially in power electronics and electrical systems [149].

5.1.1 Why using real-time simulation?

a) Gaining time

- ↗ Allowing test engineers to gain time in the testing process.
- ↗ Find problems at an earlier stage in the design process.
- ↗ Proceeding to a device design while the actual system is not physically available.

b) Lowering cost

- ↗ Reduces enormous cost on testing a new device under real conditions.
- ↗ The real-time system could test many possible configurations without physical modification.
- ↗ Reduction of total cost over the entire project and system life cycle.

c) **Increasing test functionalities**

- ↪ Fake and test all possible scenarios that could happen in real life in a secure and simulated environment.
- ↪ High flexibility by being able to modify all parameters and signals of the test system at a glance.
- ↪ Automatic test script in order to run tests 24 hours a day, 7 days a week.

5.1.2 What is a real-time simulation?

Fixed-step solvers solve the model at regular time intervals from the beginning to the end of the simulation. The size of the interval is known as the step size: T_s . Generally, decreasing T_s increases the accuracy of the results while increasing the time required simulating the system [150].

Definition:

In a real-time system [151], we define the time step as a predetermined amount of time (ex: $T_s = 10 \mu s$, 1 ms, or 5 ms). Inside this amount of time, the processor has to read input signals, such as sensors, to perform all necessary calculations, such as control algorithms, and to write all outputs, such as control actuators.

How to define a time step

Inputs or Outputs highest frequency sampling consideration generally, decreasing the time step increases the accuracy of the results while increasing the time required to simulate the system. The rule of thumb is to have around 10 to 20 samples per period for an AC signal for a 1 kHz signal: $1/(20 * 1kHz) = 50 \mu s$

5.2. Evolution of Real-Time Simulators

Simulator technology has evolved from physical/analogue simulators (high-voltage direct current (HVDC) simulators & Transient Network Analysers (TNAs)) for Electromagnetic Transient (EMT) and protection & control studies, to hybrid TNA/Analogue/Digital

simulators capable of studying EMT behaviour, to fully digital real-time simulators, as illustrated in **Fig. 5.1**. Physical simulators served their purpose well. However, they were very large, expensive and required highly skilled technical teams to handle the tedious jobs of setting up networks and maintaining extensive inventories of complex equipment [150]. With the development of microprocessor and floating-point DSP technologies, physical simulators have been gradually replaced with fully digital real-time simulators. **Fig. 5.2** gives the details of speed, cost and size of RT-LAB Simulators

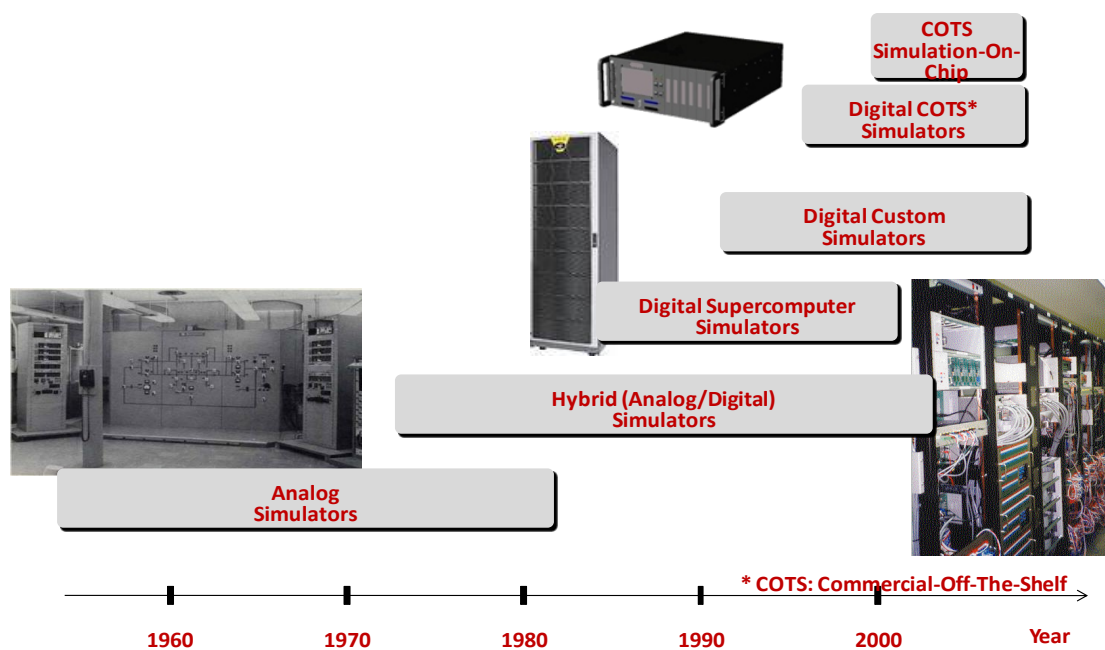


Fig. 5.1 Evolution of RT-LAB Simulator

COTS-based high-end real-time simulators equipped with multi-core processors have been used in aerospace, robotics, automotive and power electronic system design and testing for a number of years [6]. Recent advancements in multi-core processor technology means that such simulators are now available for the simulation of EMT expected in large-scale power grids, micro grids, wind farms and power systems installed in all-electric ships and aircraft. These simulators, operating under Windows, LINUX and standard real-time operating systems (RTOS), have the potential to be compatible with a large number of commercially available power system analysis software tools, such as PSS/E (Power System Simulator for

Engineering), EMTP-RV (Electro Magnetic Transients Program - Restructured Version) and PSCAD (Power Systems Computer Aided Design), as well as multi-domain software tools such as SIMULINK and DYMOLA. The integration of multi-domain simulation tools with electrical simulators enables the analysis of interactions between electrical, power electronic, mechanical and fluid dynamic systems.

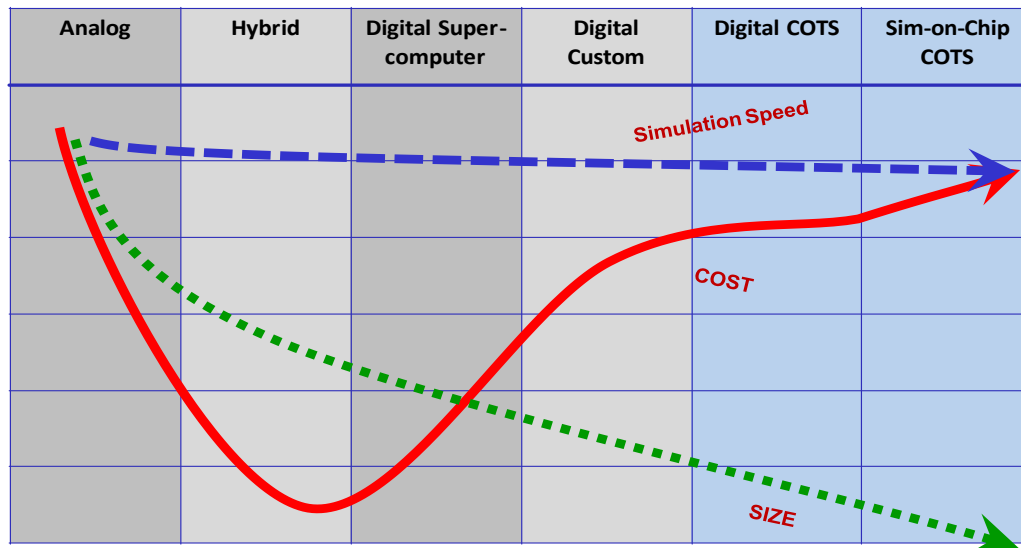


Fig. 5.2 Speed, cost and size of RT-LAB Simulators

The latest trend in real-time simulation consists of exporting simulation models to FPGA (Field-Programmable Gate Array). This approach has many advantages. First, computation time within each time step is almost independent of system size because of the parallel nature of FPGAs [152]. Second, overruns cannot occur once the model is running and timing constraints are met. Last but most importantly, the simulation time-step can be very small, in the order of 250 nanoseconds. There are still limitations on model size since the number of gates is limited in FPGAs. However, this technique holds promise.

5.3. RT-LAB Simulator Architecture

5.3.1. Block Diagram and Schematic Interface

The present real-time electric simulator is based on RT-LAB real-time, distributed simulation platform; it is optimized to run Simulink in real-time, with efficient fixed-step

solvers, on PC Cluster [153]. Based on COTS non-proprietary PC components, RT-LAB is a flexible real-time simulation platform, for the automatic implementation of system-level, block diagram models, on standard PCs. It uses the popular MATLAB/Simulink (Matrix Laboratory) as a front-end for editing and viewing graphic models in block-diagram format. The block diagram models become the source from which code can be automatically generated, manipulated and downloaded onto target processors (Pentium and Pentium-compatible) for real-time or distributed simulation.

5.3.2 *Inputs and Outputs (I/O)*

A requirement for real-time HIL applications is interfacing with real world hardware devices, controller or physical plant alike. In the RT-LAB real-time simulator, I/O interfaces are configured through custom blocks, supplied as a Simulink toolbox. The engineer merely needs to drag and drop the blocks to the graphic model and connect the inputs and outputs to these blocks, without worrying about low-level driver programming. RT-LAB manages the automatic generation of I/O drivers and models code so to direct the model's data flow onto the physical I/O cards.

5.3.2 *Simulator Configuration*

In a typical configuration (**Fig. 5.3**), the RT-LAB simulator consists of

- ✧ One or more target PCs (computation nodes); one of the PCs (Master) manages the communication between the hosts and the targets and the communication between all other target PCs. The targets use the REDHAT real-time operating system.
- ✧ One or more host PCs allowing multiple users to access the targets; one of the hosts has the full control of the simulator, while other hosts, in read-only mode, can receive and display signals from the real-time simulator.
- ✧ I/Os of various Types (analog in and out, digital in and out, PWM in and out, timers, encoders, etc).

The simulator uses the following communication links;

- ↳ Ethernet connection (100 Mb/s) between the hosts and target PCs.
- ↳ Ethernet connection between target nodes allowing parallel computation of models with low and medium step size (in msec range), or for free-running, on real-time simulation.
- ↳ Fast shared-memory communication between processors on the same motherboard (dual, quad or 8 processors)
- ↳ Fast IEEE 1394 (FireWire) communication links (400 Mb/s) between target PCs for parallel simulation of models with small step sizes (down to 20 μ s) and tight communication constraints (power systems, electric drive control, etc).

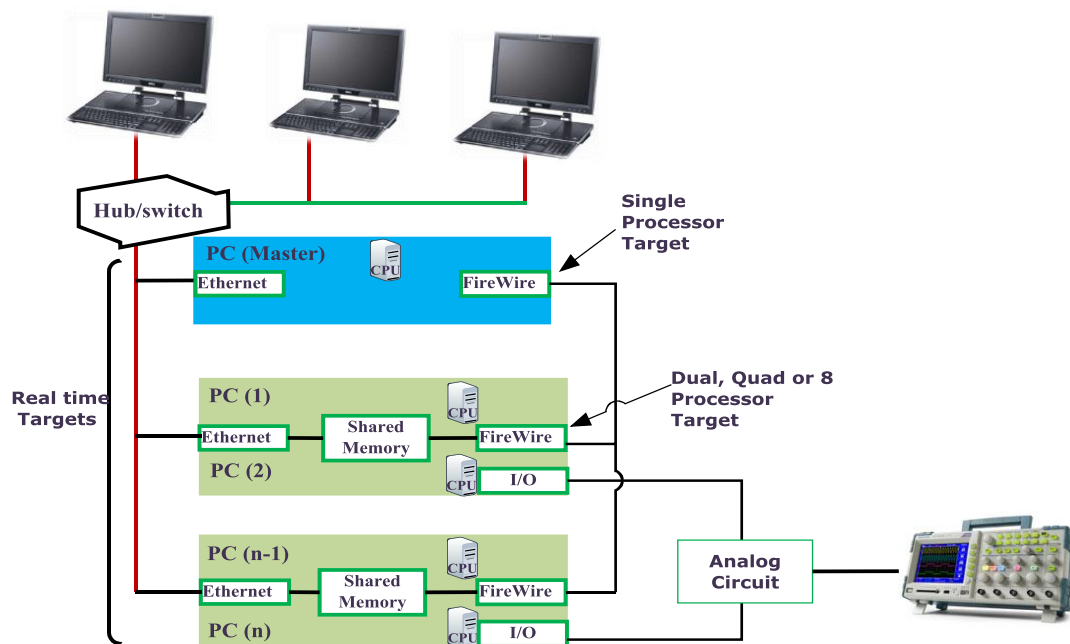


Fig. 5.3 RT-LAB Simulator Architecture

5.4 How RT-LAB Works

RT-LAB allows the user to readily convert simulink models, via Real-time workshop (RTW), and then to conduct Real-time simulation of those models executed on multiple target computers equipped with multi-core PC processors [147]. This is used particularly for HIL and rapid control prototyping applications [155, 156]. RT-LAB transparently handles

synchronization, user interaction, real world interfacing using I/O boards and data exchanges for seamless distributed execution

5.4.1 Single Target Configuration

In this configuration (**Fig. 5.4 and Fig. 5.5**), typically used for rapid control prototyping, a single computer runs the plant simulation or control logic. One or more hosts may connect to the target via an Ethernet link. The target uses QNX or Linux as the RTOS (real-time operating system) [157] for fast simulation or for applications where real-time performance is required. RT-LAB [7, 50, 65, 98, 104, 132], used Red Hat ORT which is the standard Red Hat distribution package with an optimized set of parameters to reach real-time performance enabling to reach model time step as low as 10 micro sec on multi-core processors.

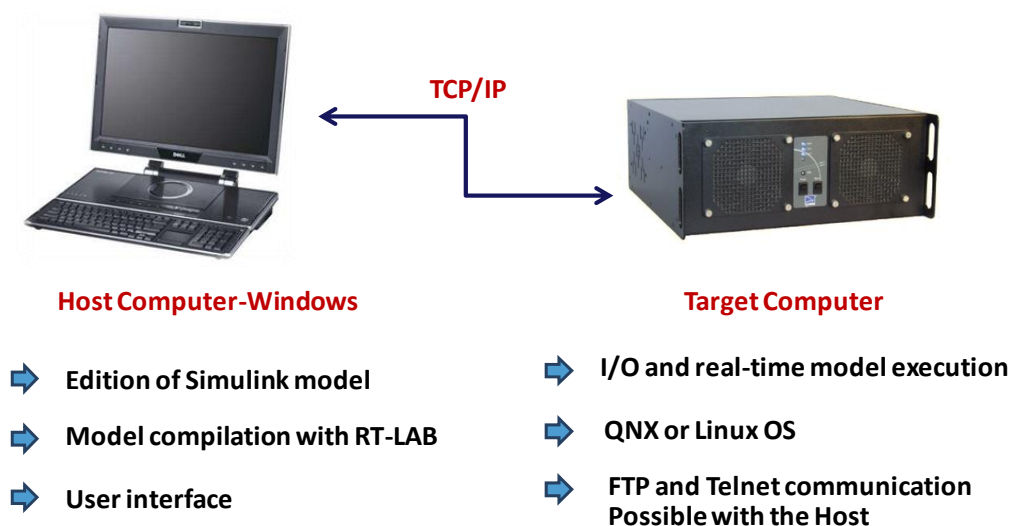


Fig. 5.4 RT-LAB Simulator with Single Target system

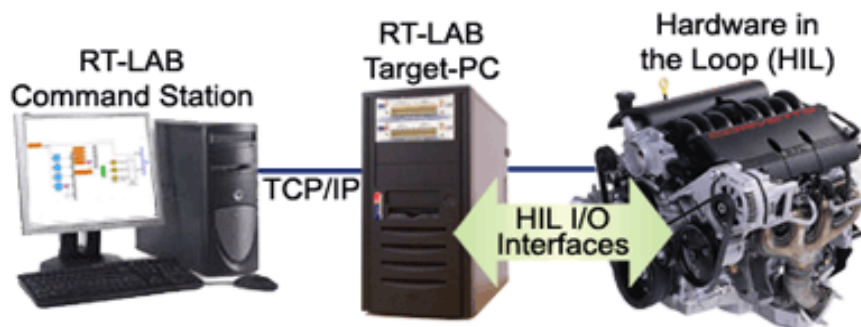


Fig. 5.5 RT-LAB Simulator with Single Target system and HIL

5.4.2 Distributed Target Configuration

The distributed configuration (**Fig. 5.6 and Fig 5.7**) allows for complex models to be distributed over a cluster of multi-core PCs [147] running in parallel. The target nodes in the cluster communicate between each other with low latency protocols such as FireWire, Signal wire or Infinite Band, fast enough to provide reliable communication for real-time applications.

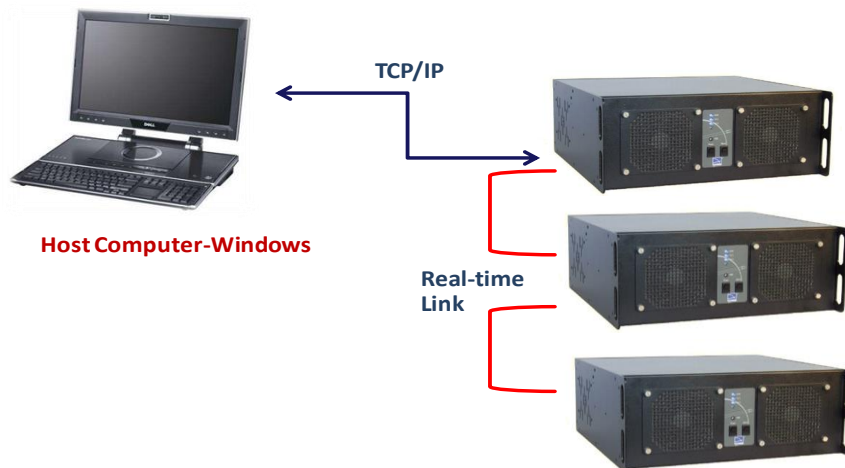


Fig. 5.6 RT-LAB Simulator with distributed target system

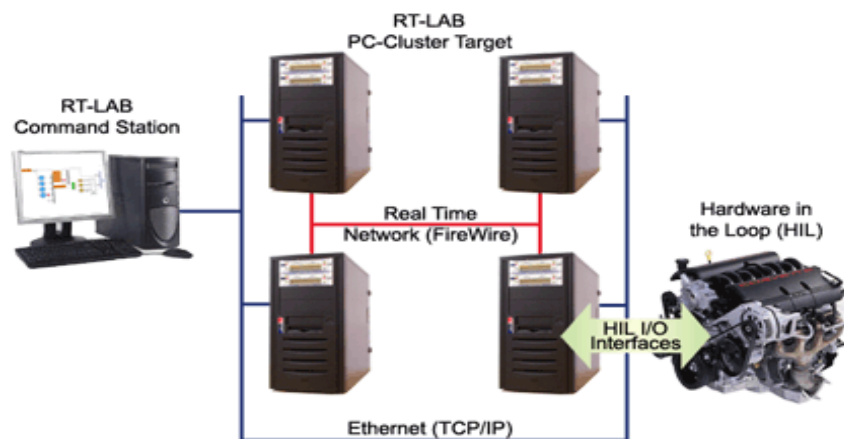


Fig. 5.7 RT-LAB Simulator with distributed target system and HIL

The real-time cluster is linked to one or more host stations through a TCP/IP (Transmission Control Protocol / Internet Protocol) network. Here again, the cluster of PCs can be used for Real-Time applications (using QNX or Red Hawk Linux), or fast simulation of complex systems (using QNX, Red Hawk or Windows). RT-LAB PC-cluster targets are

designed for flexible and reconfigurable mega-simulation [157]. The user can build and expand the PC-cluster as needed, then redeploy the PCs for other applications when the simulation is done. RT-LAB can accommodate up to 64 nodes running in parallel.

5.4.3 *Simulator solvers*

The RT-LAB electrical simulator uses advanced fixed time-step solvers and computational techniques designed for the strict constraints of real-time simulation of stiff systems. They are implemented as a Simulink toolbox called ARTEMIS [144] (Advanced Real-Time Electro-Mechanical Transient Simulator), which is used with the sim Power Systems. PSB (Power System Block set) is a Simulink toolbox that enables the simulation of electric circuits and drives within the Simulink environment. While PSB now supports a fixed-time-step solver based on the Tustin method, PSB alone is not suitable for real-time simulation due to many serious limitations, including iterative calculations to solve algebraic loops, dynamic computation of circuit matrices, un-damped switching oscillations, and the need for a very small step size which greatly slows down the simulation. The ARTEMIS solver uses a high-order fixed time-step integration algorithm that is not prone to numerical oscillations, and advanced computational techniques necessary for the real-time simulation of power electronic systems and drives such as:

- ↪ Exploitation of system topology to reduce matrices size and number by splitting the equations of separated systems.
- ↪ Support for parallel processing suitable for distributed simulation of large systems
- ↪ Implementation of advanced techniques for constant computation time.
- ↪ Strictly non-iterative integration.
- ↪ Real-time compensation of switching events occurring anywhere inside the time step, enabling the use of realistic simulation step sizes while ensuring a good precision of circuits with switches (GTO, IGBT, etc) [7, 50, 65, 98, 104, 132].

5.4.4 RT-LAB Simulation development Procedure

Electric and power electronic systems are created on the host personal computer by interconnecting:

- ↪ Electrical components from component model libraries available in the Power System Block-set (PSB).
- ↪ Controller components and other components from Simulink and its toolboxes that are supported by Real-Time-Workshop (RTW).
- ↪ I/O blocks from the simulator I/O tool boxes. The easy to use drag and drop Simulink interface issued at all stages of the process.
- ↪ These systems are then simulated and tuned off-line in the MATLAB/Simulink environment [144]. ARTEMIS fixed step solvers are used for the electric part and Simulink native solvers for the controller and other block-diagram parts. Finally, the model is automatically compiled and loaded to the PC-Cluster with RT-LAB simulation interface [145].

The simulator software converts Simulink and Sim Power Systems non-real-time models to real-time simulation by providing support for:

- ↪ **Model Distribution:** If a model is too complex to be computed within the time step, the simulator allows the model to be distributed over several processors, automatically handling the inter-processor communication through TCP/IP, FireWire or Shared Memory. Electric systems can be separated by using natural delay in the system (Analog-to-Digital conversion delays, filtering delays, transmission lines, etc).
- ↪ **Multi-rate Computation:** Not all the components in a system need to be executed at very small time steps. If the system can be separated into subsystems and executed at different update rates, cycles can be freed up for executing the subsystem(s) that need to be updated faster.

- ↳ **Specialized Solvers:** The simulator uses libraries of specialized solvers (ARTEMIS) and blocks that address many of the mathematical problems that arise when taking a model to real-time [140], such as new fixed step integrators that reduce the errors introduced when replacing a variable step integrator, and special tool box that compensate for errors introduced when events occur between time steps (RT-Events).
- ↳ **Software and Hardware Interfaces:** In addition to wide range of I/O Types and boards, the simulator includes a comprehensive application program interface (API) that allows signals in the model to be used in other on-line software for visualization and interaction.

5.5 PCI OP5142 configuration

The OP5142 (**Fig. 5.8**) is one of the key building blocks in the modular OP5000 I/O system from Opal- RT Technologies [144]. It allows the incorporation of FPGA technologies in RT-LAB simulation clusters for distributed execution of HDL (Hardware description language) functions and high-speed, high-density digital I/O in real-time models. Based on the highest density Xilinx Spartan-3 FPGAs, the OP5142 can be attached to the backplane of an I/O module of either a Wanda 3U- or Wanda 4U-based Opal-RT simulation system. It communicates with the target PC via a PCI-Express (Peripheral Component Interconnect - Express) ultra-low-latency real-time bus interface.

The OP5142 includes connectivity to up to four (4) 4U digital and/or analog I/O conditioning modules. This allows the incorporation of task-specific I/O hardware, such as high-speed analog signal capture and generation. Furthermore, FPGA [152] developers can incorporate their own functionality, using the System Generator for DSP toolbox or their favourite HDL development tool, through the PCIe interface without the need for connecting to the JTAG (Joint Test Action Group) interface. Configuration files can be uploaded and stored on the built-in Flash memory for instant start up. The PCI-Express port on the OP5142

adapter board allows the user to connect the distributed processors together and operate at faster cycle times than ever before. This real-time link takes advantage of the FPGA [152] power to deliver up to 2.5 Gbits/s full-duplex transfer rates. Table 5.1 Gives the description of OP5142 layout [7, 50, 65, 98, 104, 132].

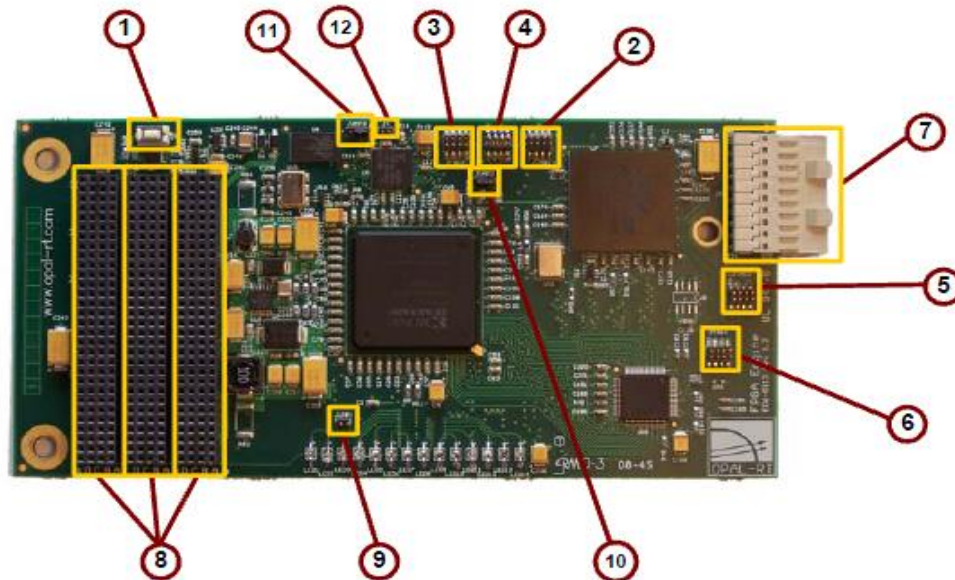


Fig. 5.8 OP5142 Layout

5.5.1 Key Features

Reconfigurability

The OP5142 platform FPGA [152] device can be configured exactly as required by the user. Integration with Simulink, the System Generator for DSP toolbox from Xilinx and RT-XSG from Opal-RT Technologies allows the transfer of Simulink sub models to the OP5142 FPGA processor for distributed processing. In addition, standard and user-developed functions can be stored on the on-board Flash memory for instant start-up. The OP5142 board is configurable on-the-fly using the PCIe bus interface and the RT-Lab design environments.

Performance

The OP5142 [7, 50, 65, 98, 104, 132], series products enable update rates of 100 MHz, providing the capability to perform time-stamped capture and generation of digital events for

high precision switching of items such as PWM I/O signalling up to very high frequencies, as I/O scheduling is performed directly on the OP5142 board [144].

Channel Density

- ↳ Up to 256 software-configurable Digital I/O lines for event capture/generation, PWM I/O and user functions;
- ↳ Up to 128 16-bit Analog I/O channels, simultaneous sampling at 1 MS/s per channel for digital-to-analog conversion and 400 kS/s for analog-to-digital conversion.

Table 5.1 - Description of components in OP5142 Layout (OPAL-RT)

Pin	Name	Description
1	S1	FPGA Engine manual reset
2	JTAG1	FPGA JTAG interface
3	JTAG2	CPLD JTAG interface
4	JUMP4	JTAG Architecture selection
5	JTAG3	PCIe Bridge JTAG interface
6	JTAG4	SerDes JTAG interface
7	JP1	PCIe & Synchronization bus and Power supply
8	J1/J2/J3	Backplane data, ID and I2C interface
9	JUMP1	Identification EEPROM write protection
10	JUMP2	FPGA configuration mode selection
11	JUMP3	Flash memory Write protection
12	J4	Flash memory forced programming voltage

1. **FPGA Engine manual reset:** This button is connected to the master reset signal of the OP5142 board. Pressing this button forces the FPGA reconfiguration, and then sends a reset signal to all OP5142 subsystems.

2. **FPGA JTAG interface:** This connector give access to the OP5142 JTAG chain. It is used to configure the flash memory with its default configuration file. The JTAG connection enables the user to program manually the reprogrammable components on the board and to debug the design using the Chip scope, through the System Generator for DSP “Chip scope” block. The use of this port is reserved for advanced users. In general, this port should not be used after the board is manufactured. Depending upon the “JUMP4” jumper presence, this interface may give access to either the FPGA and CPLD configuration, or only the FPGA one.
3. **CPLD JTAG interface:** If the “JUMP4” jumpers are set to the independent mode, this connector gives access to the CPLD JTAG configuration interface. The JTAG connection enables the user to program manually the reprogrammable components on the board. The use of this port is reserved for advanced users. In general, this port should not be used after the board is manufactured. If the jumpers are set to the shared mode, the CPLD and FPGA JTAG configuration are daisy-chained, and the “JTAG1” connector must be used instead of this one.
4. **JTAG architecture selection:** This connector enables the JTAG interface of the OP5142 CPLD and FGPA to be daisy-chained. For independent operation, place jumper between pins 6-8. For daisy chain operation, place jumpers between pins 1-2, 3-4, 5-6 and 7-8, and use the FPGA JTAG connector only.
5. **PCIe Bridge JTAG interface:** This connector give access to the PLX PCI-express bridge JTAG interface. It is used during manufacturing to configure the bridge with its default configuration, and should not be used by the user.
6. **SerDes JTAG interface:** This connector give access to the Texas Instrument Serializer - Deserializer JTAG interface. It is used during manufacturing to configure the chip with its default configuration, and should not be used by the user.

- 7. PCIe & Synchronization bus and Power Supply:** This port implements all data and power transfers that need to be done with the external world. It carries to the external PCI-express adapter:
- ↻ The synchronization pulse train to a RTSI (real-time system integration) connector;
 - ↻ Data communication packets to the PCI-express bus;
 - ↻ Power supply voltages.
- 8. Backplane Data, ID and I²C interface:** These three connectors are to be attached to the Wanda Backplane Adapter J1, J2 and J3 headers. They exchange all I/O-related data to the I/O module, including identification data, serial communication with I²C devices and user I/O dataflow.
- 9. Identification EEPROM write protection:** This header enables the write protection of the EEPROM (Electrically Erasable Programmable Read only Memory) located on the OP5142. EEPROM contains the board revision ID, and it always remains write-protected.
- 10. FPGA Configuration Mode selection:** This header enables the developer to select the way the OP5142 FPGA should be configured. The two options are (a) JTAG configuration, or (b) Slave parallel configuration (from the Flash memory). In normal use, the FPGA should always be configured using the Slave parallel feature. Note that pin #1 is on the left-hand side of the header (i.e. the “J”UMP side).
- 11. Flash Memory write protection:** This header is used to enable the developer to write some reserved sectors of the configuration flash memory. These sectors should never be used by the user.
- 12. Flash memory forced programming voltage:** This header provides a 12V supply voltage to the JUMP3 connector. JUMP3 is used to enable the developer to write some reserved sectors of the configuration flash memory. These sectors should never be used by the user. Note that pin #1 is on the left-hand side of the header (i.e. the “J”4 side).

5.5.2 Technical Specifications

Digital I/O

↵ Number of channels	256 input/output configurable in 1- to 32-bit
↵ Groups Compatibility	3.3V
↵ Power-on state	High impedance

FPGA

↵ Device	Xilinx Spartan 3
↵ I/O Package	fg676
↵ Embedded RAM available	216 Kbytes
↵ Clock	100 MHz
↵ Platform options	XC3S5000
↵ Logic slices	33,280
↵ Equivalent logic cells	74,880
↵ Available I/O lines	489

Bus

↵ Dimensions (not including connectors)	PCI-express x1
↵ Data transfer	2.5 Gbit/s

5.5.3 Analog conversion interface:

Two Types of analog conversion modules are available: the **OP5340** is a bank of analog-to-digital converters (**ADC**) and the **OP5330** is a bank of digital-to-analog (**DAC**) converters. The analog conversion banks must be placed onto an OP5220 passive carrier, thus providing an easy access to the modules on the front panel of the Wanda box. OP5330 and OP5340 [144] features are:

- ↵ Up to 16 analog Input (OP5340) or digital Output (OP5330) channels;
- ↵ One 16-bit ADC (OP5340) or DAC (OP5330) per channel;
- ↵ Accuracy of +/- 5mV;

- ↻ Simultaneous sampling on all channels eliminates skew errors inherent in multiplexed channels;
- ↻ Up to 500 kS/s update rate for every channel. Total throughput of up to 8 MS/s;
- ↻ Dynamic range of $\pm 16V$;
- ↻ Hardware configurable on-board signal conditioning and anti aliasing filter;
- ↻ On-board EEPROM memory for calibration parameters;
- ↻ Library of drag-and-drop Opal-RT RT-XSG blocks for Simulink

5.6 System Performance of Type-2 FLC based $P-Q$ Control Strategy with Different Fuzzy MFs using real-time digital simulator

Fig. 5.9, 5.10 and 5.11 gives the details of Source Voltage, Load Current, Compensation current, Source Current with filter, DC Link Voltage, THD of Type-2 FLC based $p-q$ control strategy with different Fuzzy MFs under balanced, un-balanced and non-sinusoidal supply voltage conditions using real-time digital simulator (OPAL-RT) hardware.

Initially the system performance is analysed under balanced sinusoidal conditions, during which the Type-2 FLC with all three MFs (Triangular, Trapezoidal & Gaussian) are good enough at suppressing the harmonics and the THD of $p-q$ control strategy using real-time digital simulator is 1.36%, 1.02% and 0.73% respectively. However, under un-balanced and non-sinusoidal conditions the Type-2 FLC with Gaussian MF shows superior performance. The THD of the $p-q$ control strategy using Type-2 FLC with Trapezoidal MF under un-balanced condition is 2.28% and under non-sinusoidal condition it is 3.31%. The THD of the $p-q$ control strategy using Type-2 FLC with Triangular MF under un-balanced is 1.87% and under non-sinusoidal condition it is 2.92%. The THD of the $p-q$ control strategy using Type-2 FLC with Gaussian MF under un-balanced condition is 1.25% and under non-sinusoidal condition it is 2.14% using real-time digital simulator.

p-q control strategy using Type-2 FLC with Trapezoidal, Triangular and Gaussian MFs under bal Sinusoidal with RTDS

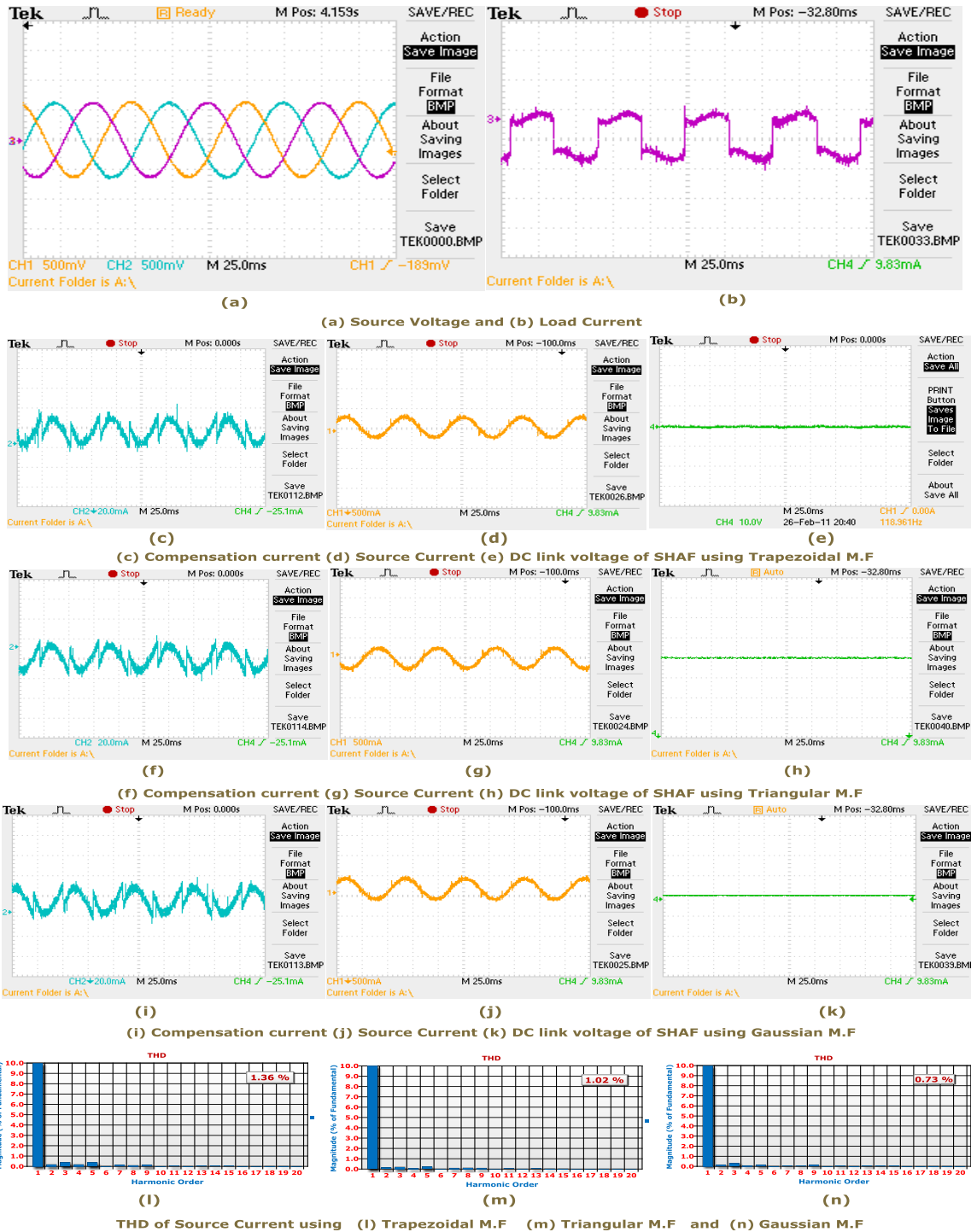
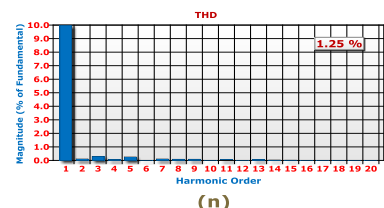
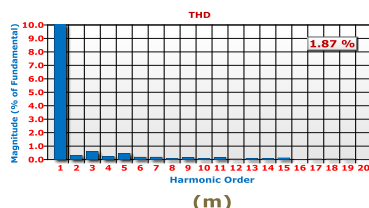
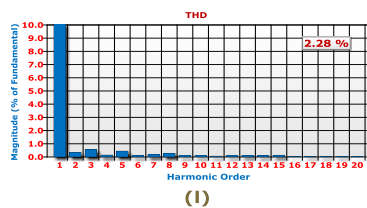
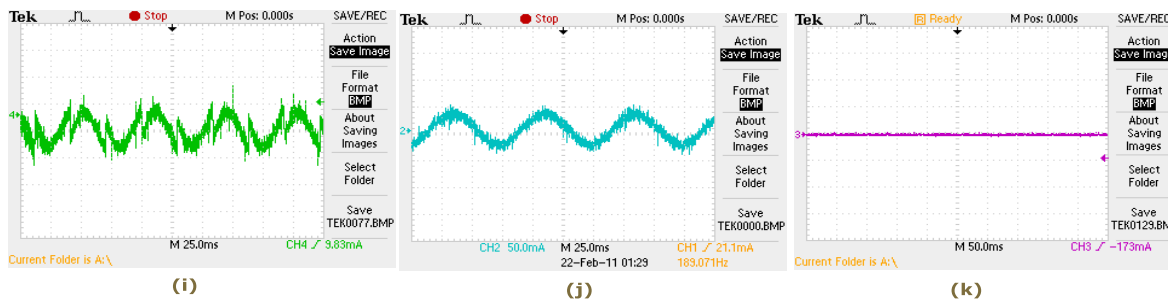
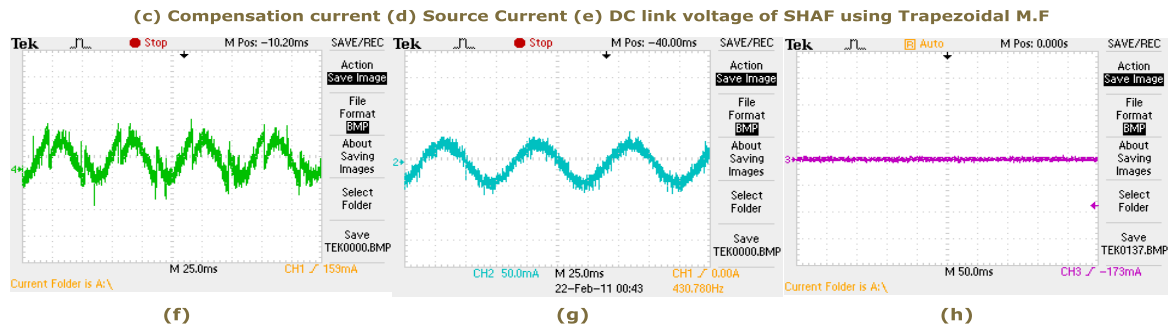
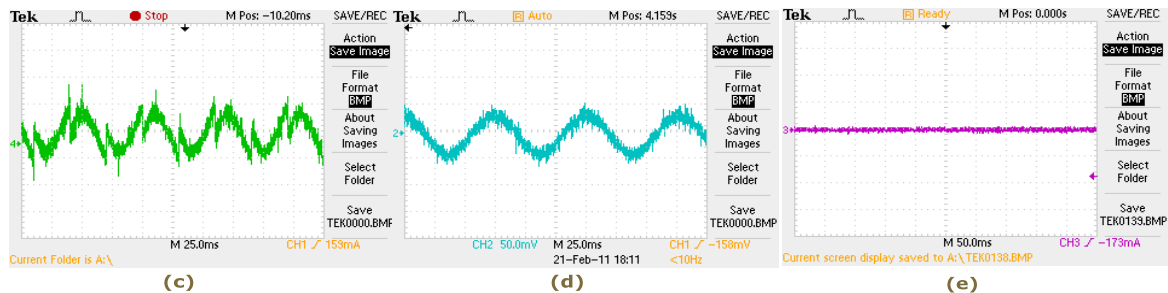
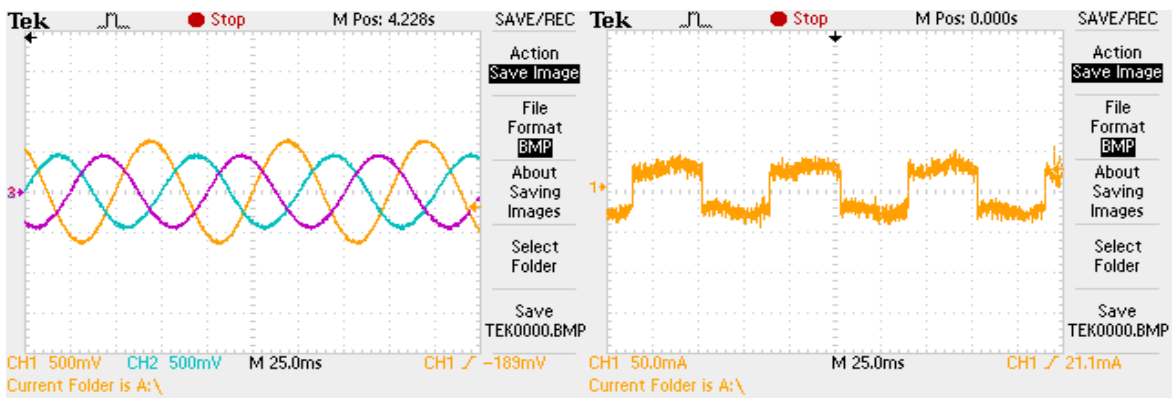


Fig. 5.9 SHAF response using *p-q* control strategy with Type-2 FLC (Trapezoidal, Triangular and Gaussian MF) under balanced Sinusoidal condition using real-time digital simulator

(a)Source Voltage (b)Load Current (Scale 30A/div) (c)Compensation current (Scale 20A/div) using Trapezoidal MF (d)Source Current (Scale 40A/div) with filter using Trapezoidal MF (e)DC Link Voltage using Trapezoidal MF (f)Compensation current using Triangular MF (g)Source Current with filter using Triangular MF (h)DC Link Voltage using Triangular MF(i)Compensation current using Gaussian MF (j)Source Current with filter using Gaussian MF (k)DC Link Voltage using Gaussian MF (l)THD of Source current with Trapezoidal MF (m)THD of Source current with Triangular MF (n)THD of Source current with Gaussian MF

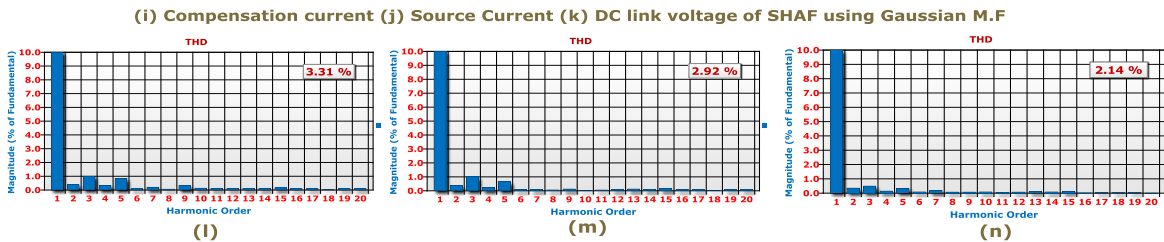
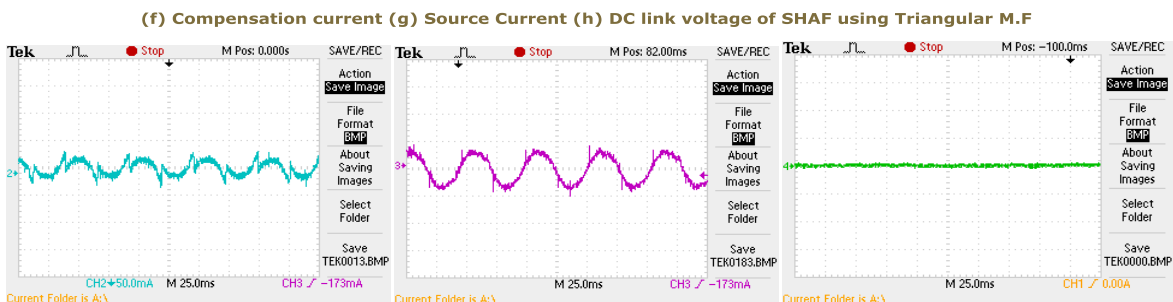
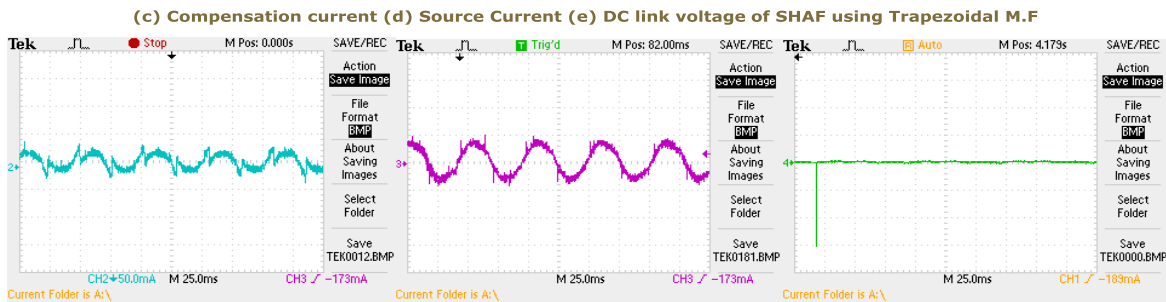
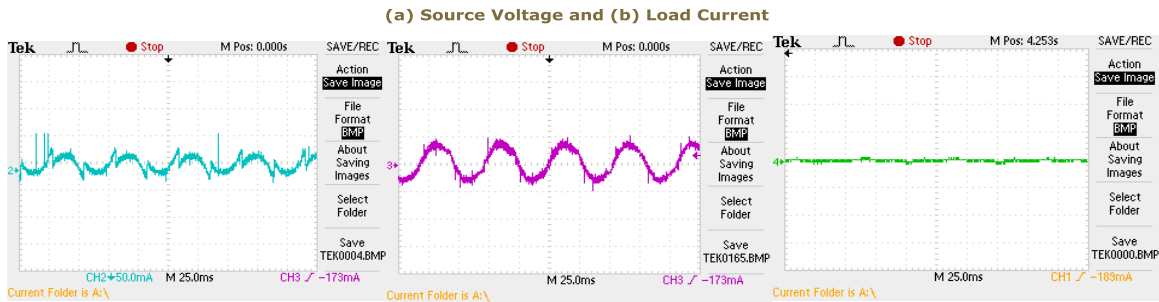
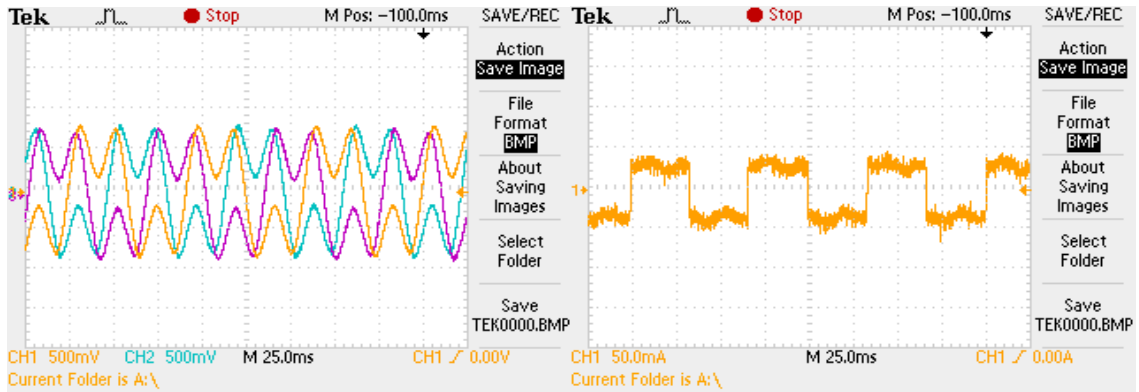
p - q control strategy with Type-2 FLC with Trapezoidal, Triangular and Gaussian MFs under Un-bal Sin condition with RTDS



THD of Source Current using (l) Trapezoidal M.F (m) Triangular M.F and (n) Gaussian M.F

Fig. 5.10 SHAF response using p - q control strategy with Type-2 FLC (Trapezoidal, Triangular and Gaussian MF) under un-balanced Sinusoidal condition using real-time digital simulator

p-q control strategy with Type-2 FLC with Trapezoidal, Triangular and Gaussian MFs under Non-Sinusoidal with RTDS



THD of Source Current using (l) Trapezoidal M.F (m) Triangular M.F and (n) Gaussian M.F

Fig. 5.11 SHAF response using p-q control strategy with Type-2 FLC (Trapezoidal, Triangular and Gaussian MF) under Non-Sinusoidal condition using real-time digital simulator

Even though, the $p-q$ control strategy using Type-2 FLC with different Fuzzy MFs is able to mitigate the harmonics, small amount of notches are observed in the source current. The main reason behind the notches is that the controller failed to track the current correctly and thereby APF fails to compensate completely. So to mitigate the harmonics perfectly one has to choose perfect control strategy. So to avoid the difficulties occur with $p-q$ control strategy, we have considered I_d-I_q control strategy with Type-2 FLC.

5.7 System Performance of Type-2 FLC based I_d-I_q Control Strategy with different Fuzzy MFs using real-time digital simulators

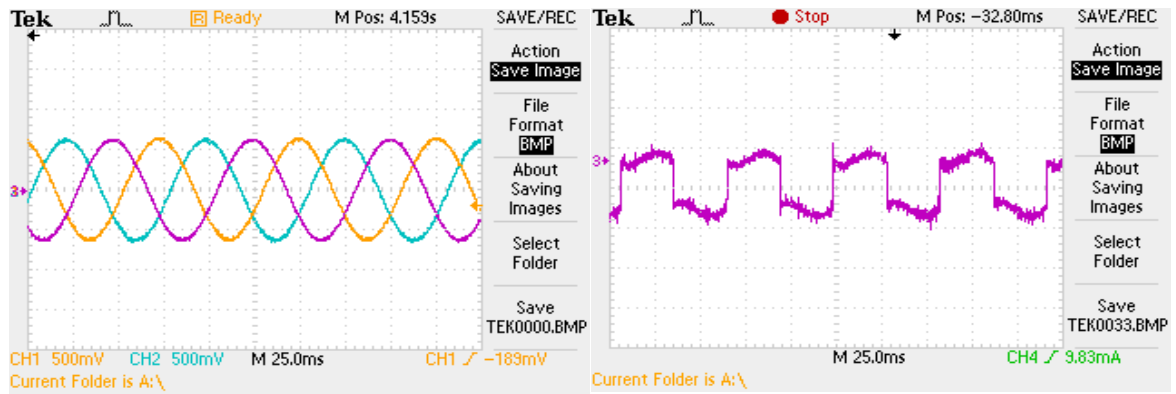
Fig. 5.12, 5.13 and 5.14 gives the details of Source Voltage, Load Current, Compensation current, Source current with filter, DC Link Voltage, THD of Type-2 FLC based I_d-I_q control strategy with different Fuzzy MFs using real-time digital simulator.

Initially the system performance is analysed under balanced sinusoidal conditions, during which the Type-2 FLC with all three MFs (triangular, trapezoidal and Gaussian) are good enough at suppressing the harmonics. The respective THDs of SHAF in real-time digital simulator are 0.66%, 0.52% and 0.43%.

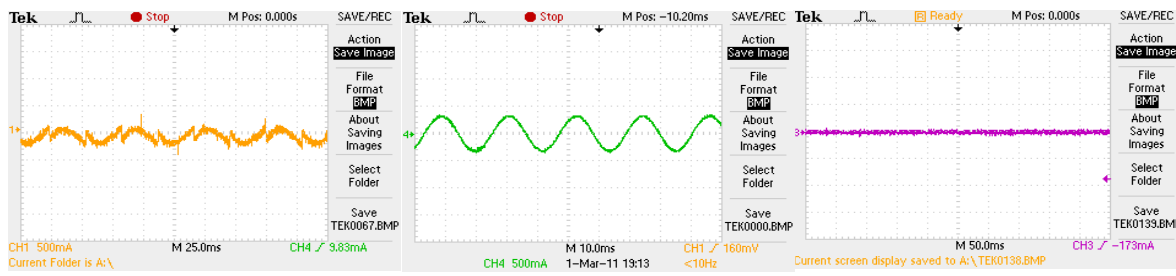
The THD of the I_d-I_q control strategy using Type-2 FLC with Trapezoidal MF under un-balanced condition is 1.38% and under non-sinusoidal it is 2.62%. The THD of the I_d-I_q control strategy using Type-2 FLC with Triangular MF under un-balanced is 1.17% and under non-sinusoidal it is 1.98%. The THD of the I_d-I_q control strategy using Type-2 FLC with Gaussian MF under un-balanced is 0.79% and under non-sinusoidal condition it is 1.63%. These are all obtained using real-time digital simulator.

While considering I_d-I_q control strategy using Type-2 FLC with different Fuzzy MFs, SHAF is succeeded in compensating harmonic currents. It is observed that, source current waveforms are very good; notches in the waveform are eliminated by using I_d-I_q control strategy with Type-2 FLC different Fuzzy MFs.

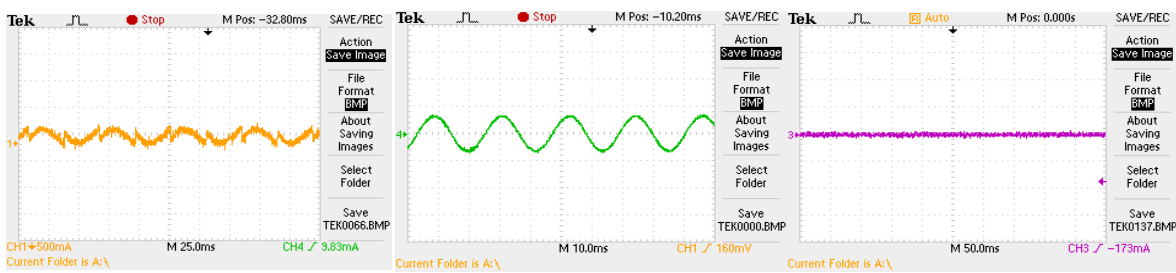
I_d - I_q control strategy using Type-2 FLC with Trapezoidal, Triangular and Gaussian MFs under balanced Sinusoidal



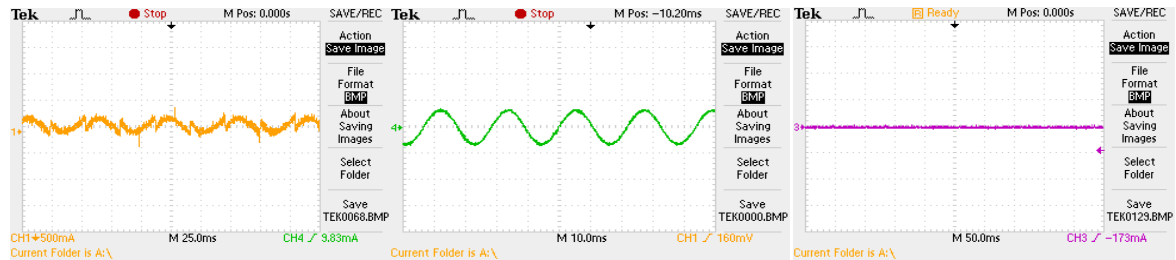
(a) Source Voltage and (b) Load Current



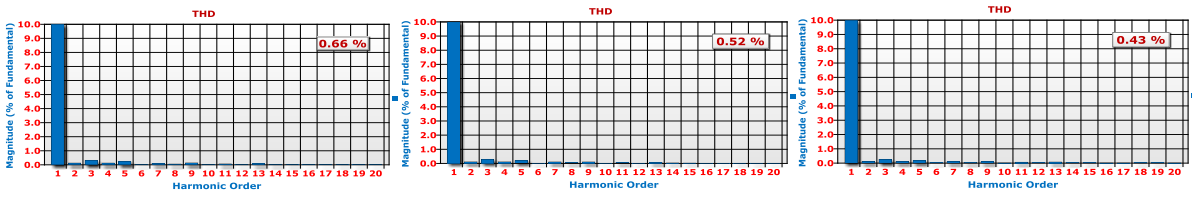
(c) Compensation current (d) Source Current (e) DC link voltage of SHAF using Trapezoidal M.F



(f) Compensation current (g) Source Current (h) DC link voltage of SHAF using Triangular M.F

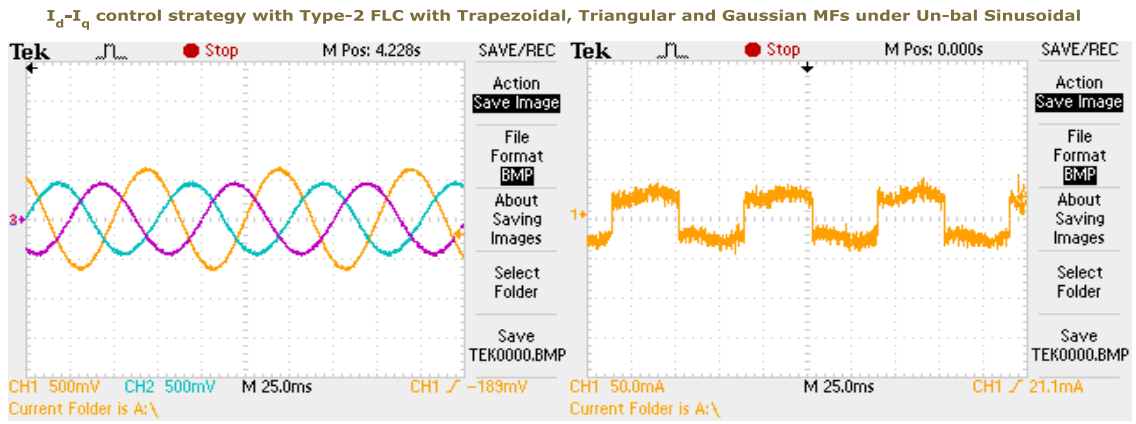


(i) Compensation current (j) Source Current (k) DC link voltage of SHAF using Gaussian M.F

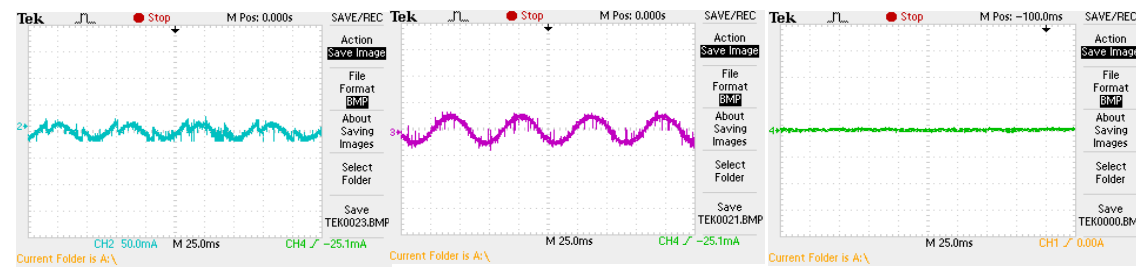


THD of Source Current using (l) Trapezoidal M.F (m) Triangular M.F and (n) Gaussian M.F

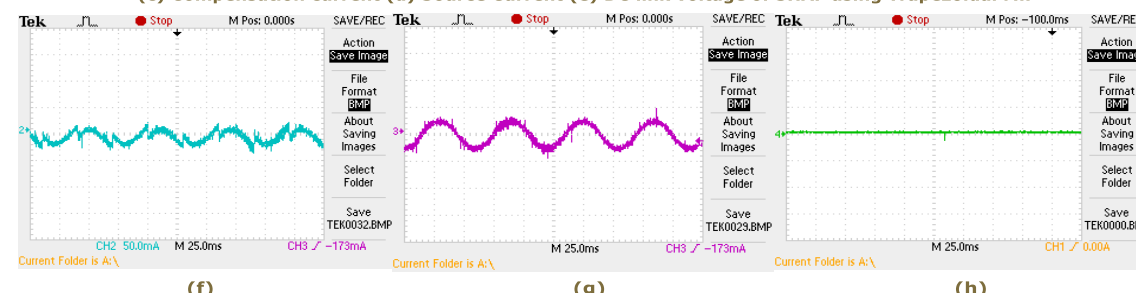
Fig.5.12 SHAF response using I_d - I_q control strategy with Type-2 FLC (Trapezoidal, Triangular and Gaussian MF) under balanced Sinusoidal condition using real-time digital simulator



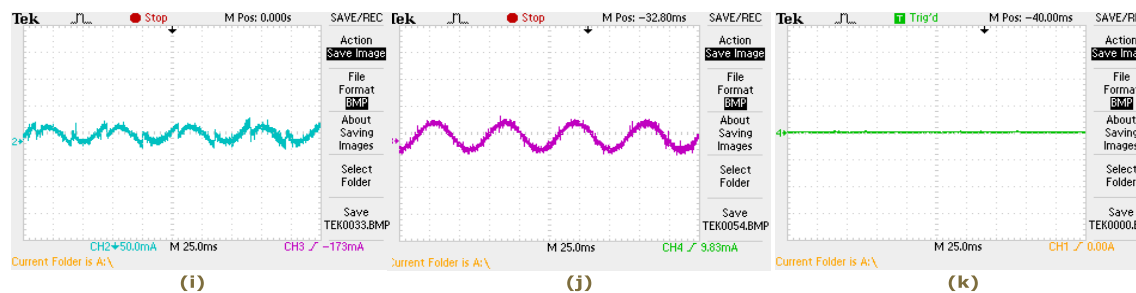
(a) Source Voltage and (b) Load Current



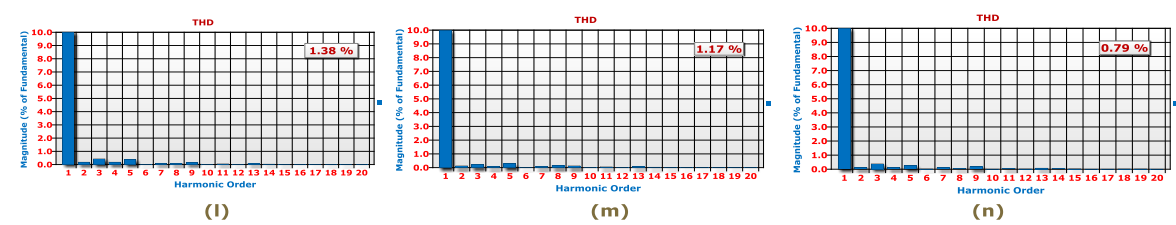
(c) Compensation current (d) Source Current (e) DC link voltage of SHAF using Trapezoidal M.F



(f) Compensation current (g) Source Current (h) DC link voltage of SHAF using Triangular M.F



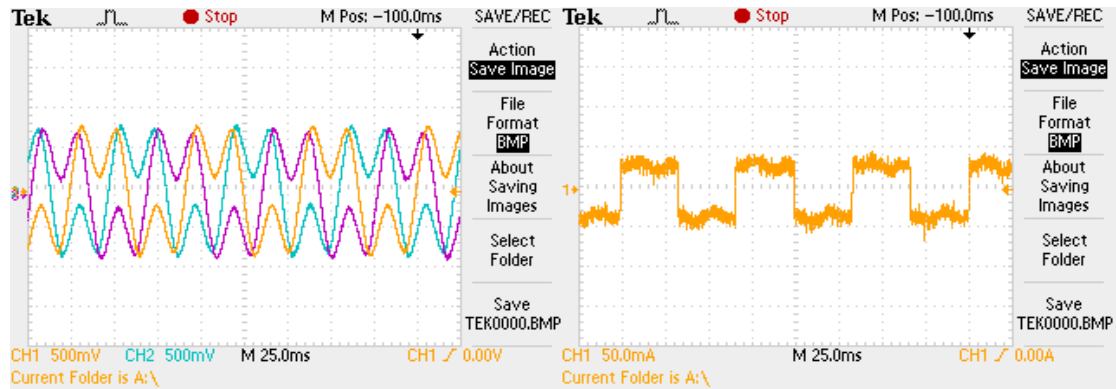
(i) Compensation current (j) Source Current (k) DC link voltage of SHAF using Gaussian M.F



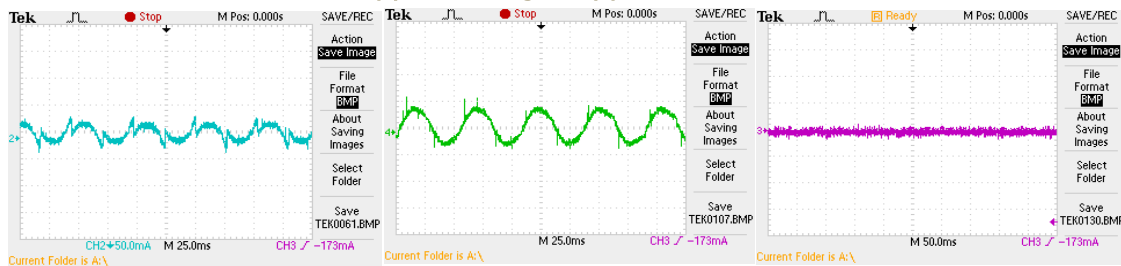
THD of Source Current using (l) Trapezoidal M.F (m) Triangular M.F and (n) Gaussian M.F

Fig. 5.13 SHAF response using I_d-I_q control strategy with Type-2 FLC (Trapezoidal, Triangular and Gaussian MF) under un-balanced Sinusoidal condition using real-time digital simulator

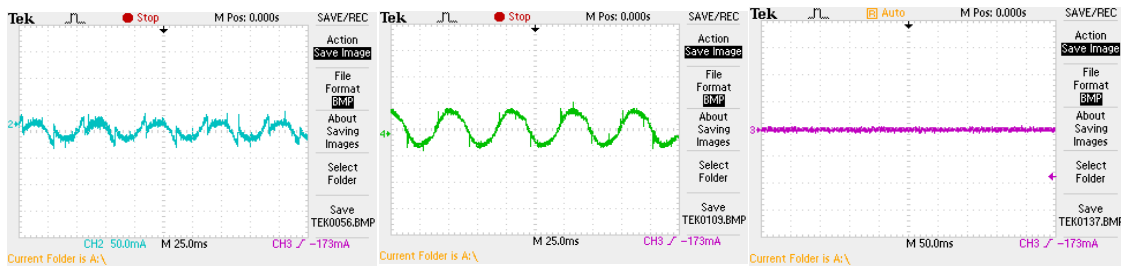
I_d-I_q control strategy with Type-2 FLC with Trapezoidal, Triangular and Gaussian MFs under Non-Sinusoidal with RTDS



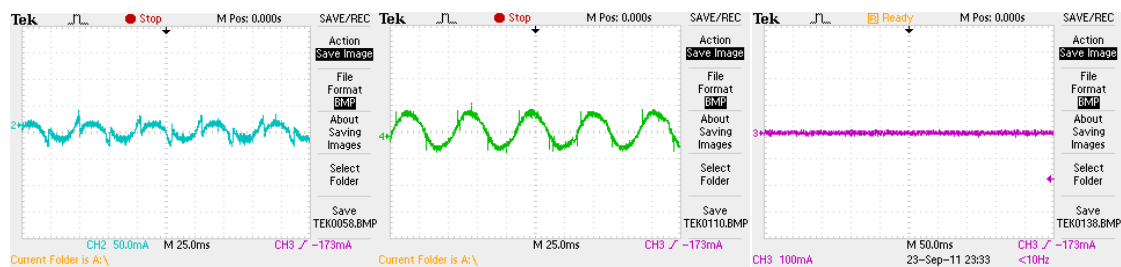
(a) Source Voltage and (b) Load Current



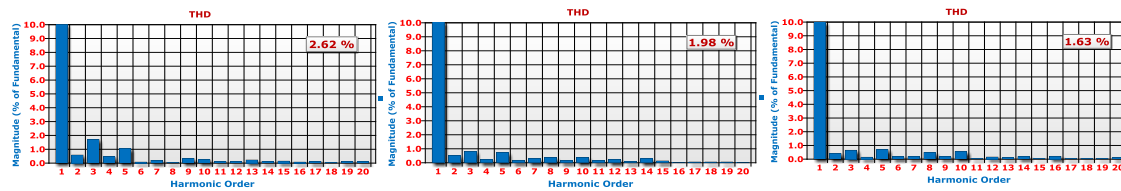
(c) Compensation current (d) Source Current (e) DC link voltage of SHAF using Trapezoidal M.F



(f) Compensation current (g) Source Current (h) DC link voltage of SHAF using Triangular M.F



(i) Compensation current (j) Source Current (k) DC link voltage of SHAF using Gaussian M.F



THD of Source Current using (l) Trapezoidal M.F (m) Triangular M.F and (n) Gaussian M.F

Fig. 5.14 SHAF response using I_d-I_q control strategy with Type-2 FLC (Trapezoidal, Triangular and Gaussian MF) under Non-Sinusoidal condition using real-time digital simulator

The Real-time implementation results showed that even if the supply voltage is non-sinusoidal the performance with I_d-I_q theory with Type-2 FLC comfortably outperformed the results obtained using $p-q$ theory with Type-2 FLC.

5.8. Comparative Study

Fig. 5.15 and Fig. 5.16 (bar graphs), clearly illustrate the THD of Source Current for $p-q$ and I_d-I_q control strategies using PI controller, Type-1 FLC and Type-2 FLC with different Fuzzy MFs using real-time digital simulator under various source conditions.

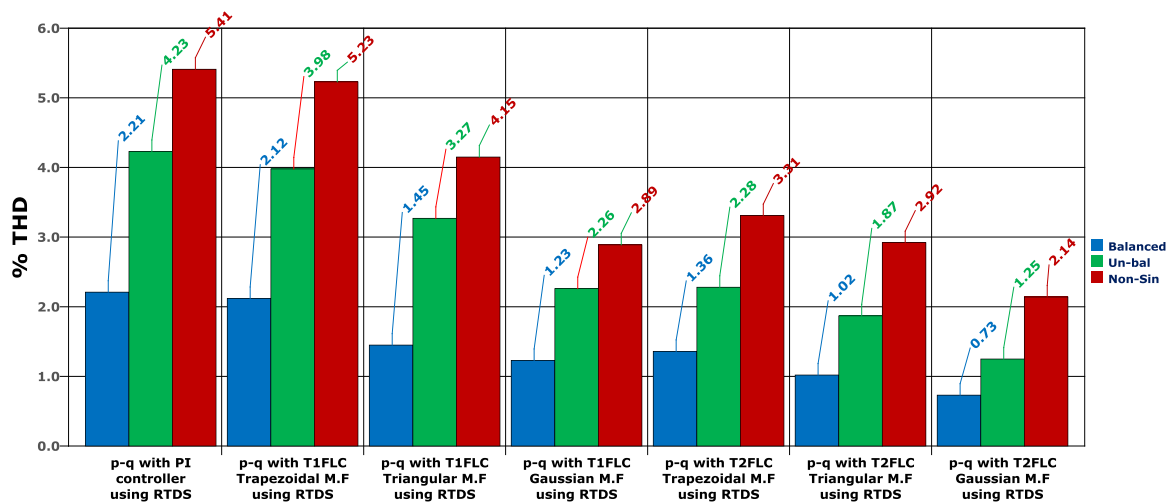


Fig. 5.15 The Bar Graph indicating the THD of Source Current for $p-q$ control strategy using PI controller, Type-1 FLC and Type-2 FLC with different Fuzzy MFs using real-time digital simulator

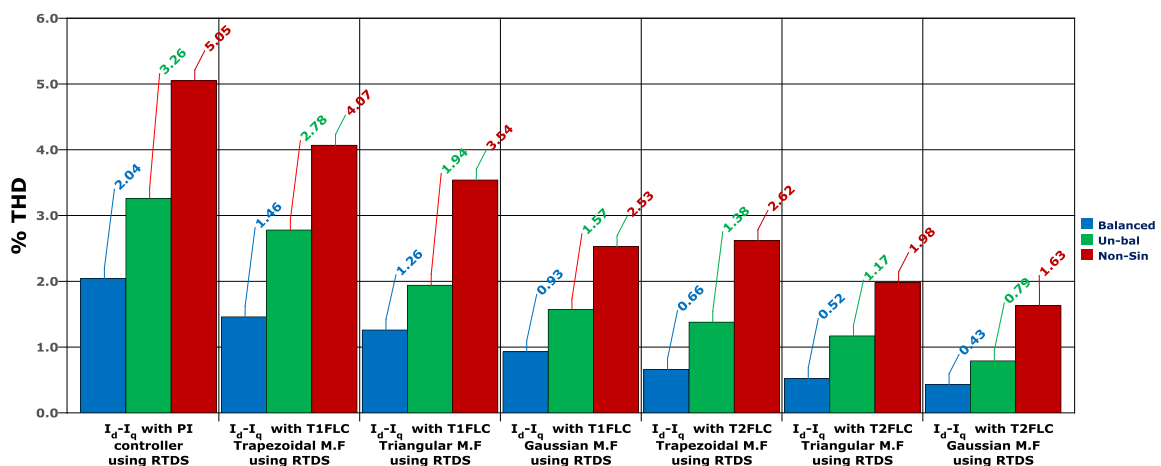


Fig.5.16 The Bar Graph indicating the THD of Source Current for I_d-I_q control strategy using PI controller, Type-1 FLC and Type-2 FLC with different Fuzzy MFs using real-time digital simulator

5.9. Summary

Modern power systems continue to evolve requiring constant evaluation of new constraints. Major studies will require the use of very fast, flexible and scalable real-time simulators. This chapter has introduced a specific class of digital simulator known as a real-time simulator. The latest trend in real-time simulation consists of exporting simulation models to FPGA. This approach has many advantages. First, computation time within each time step is almost independent of system size because of the parallel nature of FPGAs. Second, overruns cannot occur once the model is running and timing constraints are met. Last but most importantly, the simulation time-step can be very small, in the order of 250 nanoseconds. There are still limitations on model size since the number of gates is limited in FPGAs. However, this technique holds promise.

The Real-time implementation results showed that even if the supply voltage is non-sinusoidal the performance of Type-2 FLC based I_d-I_q theory with Gaussian MF showing better compensation capabilities in terms of THD compared to I_d-I_q theory with PI controller, Type-1 FLC (with all three MFs) and Type-2 FLC (Trapezoidal, Triangular MF) and also compared to $p-q$ theory with PI controller, Type-1 FLC (with all three MFs) and Type-2 FLC (with all three MFs).

While considering the I_d-I_q theory using Type-1 FLC and Type-2 FLC; and the $p-q$ control strategy with Type-2 FLC; the SHAF has been found to meet the IEEE 519-1992 standard recommendations on harmonic levels, making it easily adaptable to more severe constraints such as highly distorted and unbalanced supply voltage. The control approach has compensated the neutral harmonic currents and the dc bus voltage of SHAF is almost maintained at the reference value under all disturbances, which confirm the effectiveness of the controller.

Chapter - 6

Conclusions and Future Scope

Conclusions

Future scope

6.1 CONCLUSIONS

In this research work, our main objective being compensation of current harmonics generated due to the presence of non-linear loads in three-phase four-wire distribution system, the research studies presented in this thesis starts with an introduction to harmonics clearly specifying its description, causes and consequences. The role of passive power filters in harmonics elimination is discussed. But to avoid the inevitable drawbacks of passive filters, we moved towards the use of Active power filters (APFs). After comparing various APF configurations, we chose the three-phase four-wire capacitor midpoint Shunt APF VSI-PWM configuration for the modelling of shunt APF.

We have evaluated the performances of $p-q$ and I_d-I_q control strategies by comparing the THDs in compensated source currents and DC link voltage regulation under balanced, unbalanced and distorted/non-sinusoidal supply conditions. DC-link voltage regulation with the help of PI controller, Type-1 FLC and Type-2 FLC with different Fuzzy MFs (Trapezoidal, Triangular and Gaussian MF) to minimize the power losses occurring inside APF is studied. We had a discussion on various drawbacks encountered in conventional PI controller. The next research concentrated on the implementation of Type-1 FLC with different Fuzzy MFs (Trapezoidal, Triangular and Gaussian MF), this also suffers from several drawbacks resulting in severe deterioration of APF performance. Hence we have developed Type-2 FLC with different Fuzzy MFs; that could overcome the drawbacks observed in the PI and Type-1 FLC. Three-phase reference current waveforms generated by proposed scheme are tracked by the three-phase voltage source converter in a hysteresis band control scheme. The performance of the control strategies has been evaluated in terms of harmonic mitigation and DC link voltage regulation. The simulation (MATLAB) results are validated with real-time implementation on Real-time digital simulator (OPAL-RT).

The findings of the above investigations are summarized in the **Figs. 6.1, 6.2, 6.3 and 6.4**. **Fig. 6.1, Fig. 6.2, Fig. 6.3 and Fig. 6.4 (line graphs)**, Clearly illustrates the amount of THD of source current reduced from one controller to other controller for shunt active filter control strategies under various source conditions using MATLAB and Real-time digital simulator.

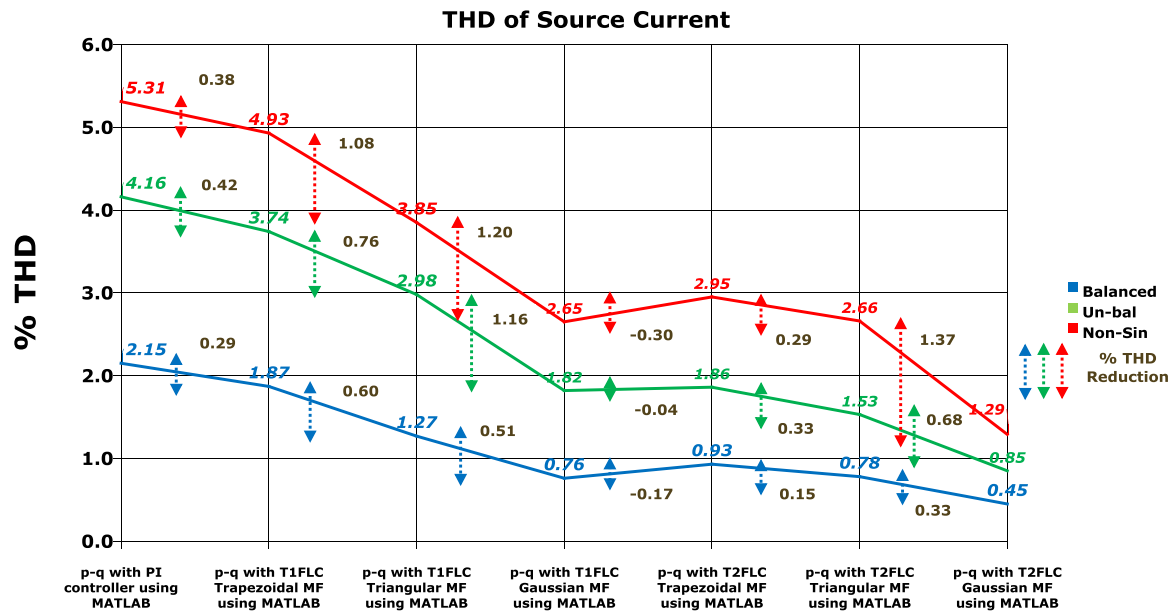


Fig. 6.1. The Line Graph indicating the amount of **THD reduced** for PI controller, Type-1 FLC and Type-2 FLC with different Fuzzy MFs using $p-q$ control strategy with **MATLAB**

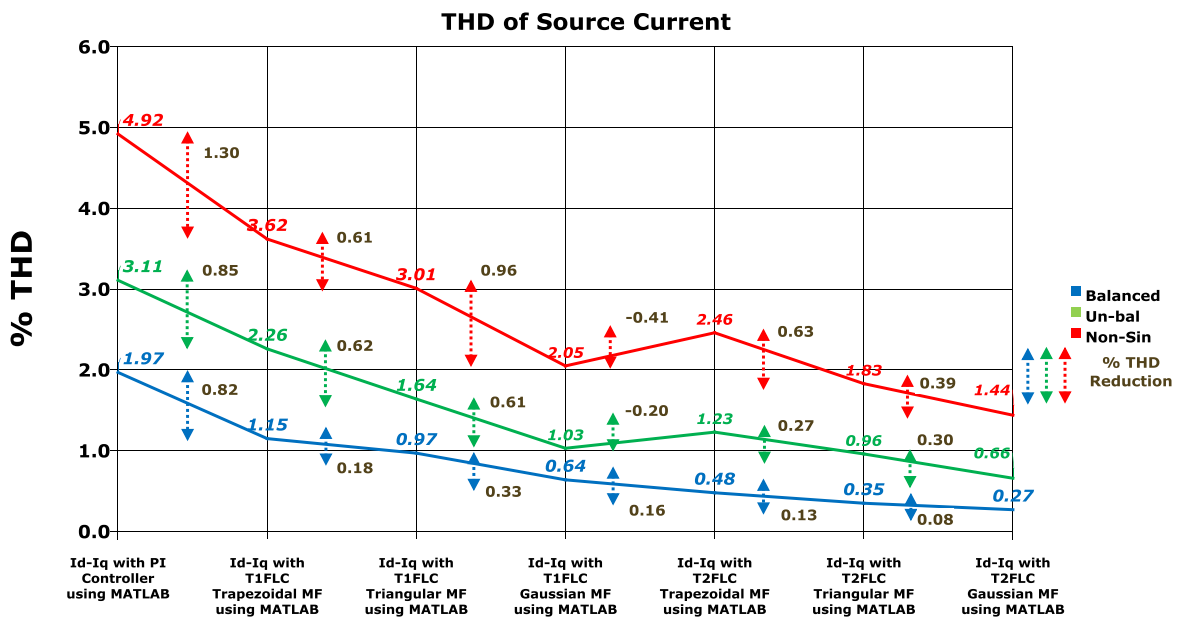


Fig. 6.2. The Line Graph indicating the amount of **THD reduced** for PI controller, Type-1 FLC and Type-2 FLC with different Fuzzy MFs using I_d-I_q control strategy with **MATLAB**

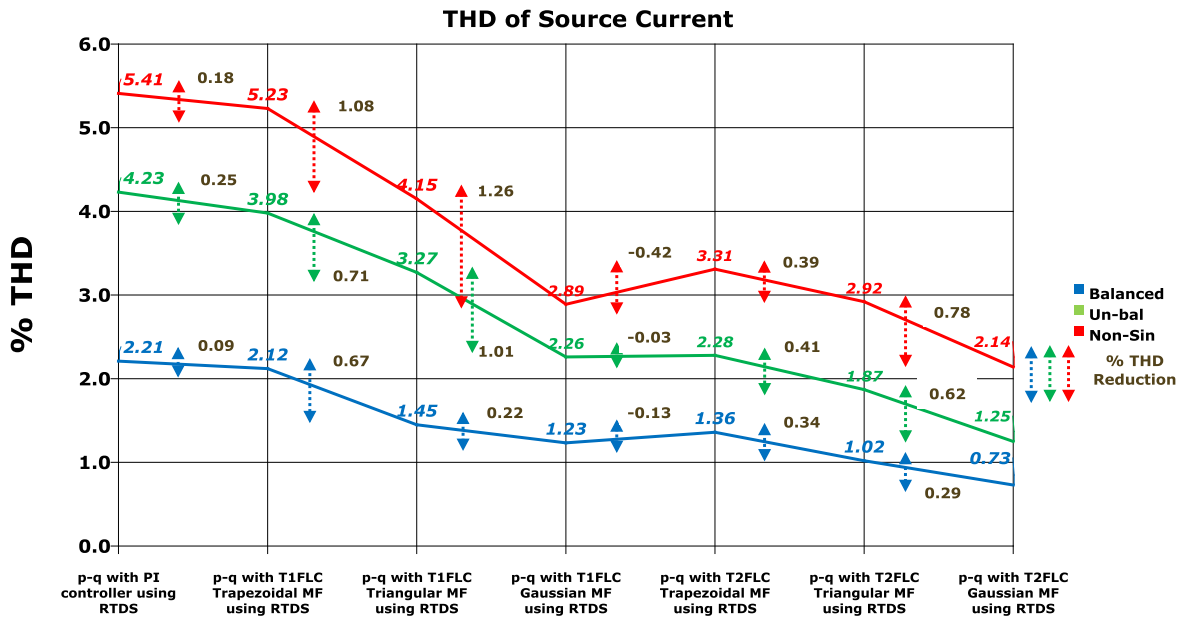


Fig. 6.3. The Line Graph indicating the amount of THD reduced for PI controller, Type-1 FLC and Type-2 FLC with different Fuzzy MFs using p - q control strategy with Real-time digital simulator

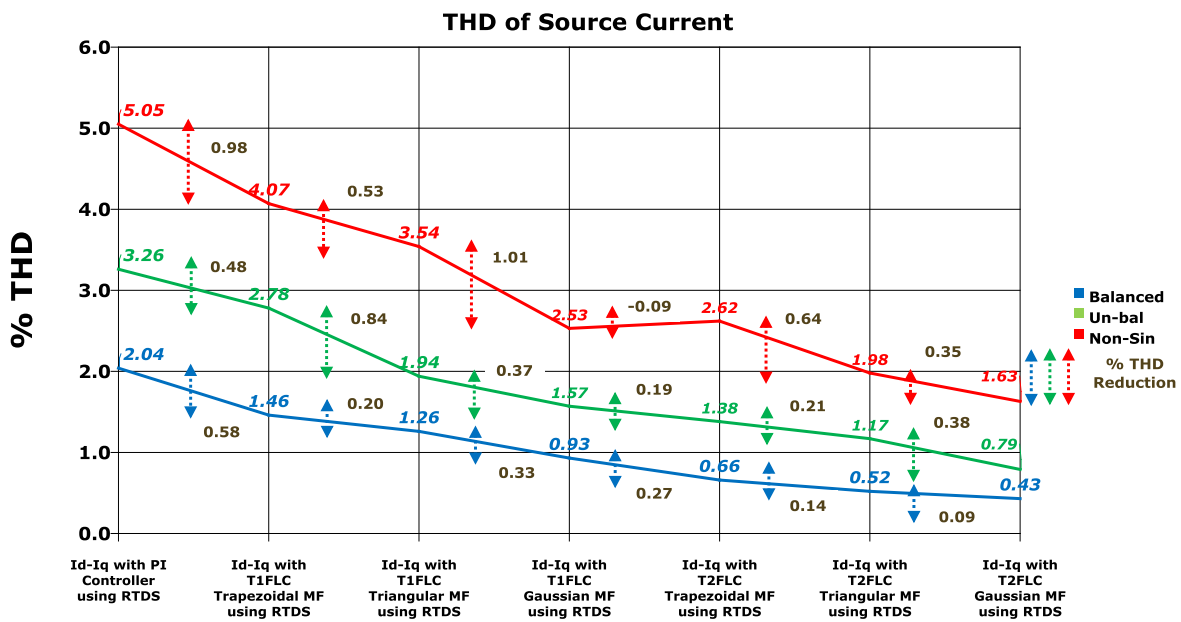


Fig. 6.4. The Line Graph indicating the amount of THD reduced for PI controller, Type-1 FLC and Type-2 FLC with different Fuzzy MFs using I_d - I_q control strategy with Real-time digital simulator

The investigations carried out in this research work yield the following important conclusions.

- ↳ It can be inferred from the simulation and real-time results of Chapter 2 that, $p-q$ control strategy yields inadequate results under un-balanced and/or non-sinusoidal source voltage conditions.
- ↳ Under unbalanced and/or non-sinusoidal condition, $p-q$ control strategy is not succeeded in compensating harmonic currents, notches are observed in the source current. The main reason behind the notches is that the controller failed to track the current correctly and thereby APF fails to compensate completely. So to avoid the difficulties occur with $p-q$ control strategy, we have considered I_d-I_q control strategy.
- ↳ The I_d-I_q scheme is the best APF control scheme for compensation of current harmonics for a wide variety of supply voltage and loading conditions. The THD in source current can also be lowered down satisfactorily below 5%, thereby satisfying the IEEE-519 standards on harmonic level. Simultaneously, it also compensates for excessive neutral current.
- ↳ Under un-balanced and/or non-sinusoidal conditions, PI controller is unable to maintain the DC link voltage constant (V_{dc} is nearer to 780V, but V_{dc-ref} is 800V) and it is unable to mitigate the harmonics completely and THD is close to 5%. The mitigation of harmonics is poor when the THD of source current is more. But according to IEEE 519-1992 standard, THD must be less than 5%. So to mitigate harmonics effectively, we have considered *Type-1 FLC* with different Fuzzy MFs.
- ↳ I_d-I_q control strategy using *Type-1 FLC* with different Fuzzy MFs, the SHAF is able to maintain the DC link voltage constant (V_{dc} is nearer to 790V, but V_{dc-ref} is 800V) and it is able to mitigate harmonics (THD is nearly equal to 2.5% to 3.5%) in a better way than that of $p-q$ control strategy using *Type-1 FLC* with different Fuzzy MFs (THD is nearly equal to 3% to 5%).

- ✦ Even though, the I_d-I_q control strategy using *Type-1 FLC* with different Fuzzy MFs is able to mitigate the harmonics but notches are present in the source current. So to avoid the difficulties occur with *Type-1 FLC* based $p-q$ and I_d-I_q control strategies with different Fuzzy MFs, we have considered *Type-2 FLC* with different Fuzzy MFs.
- ✦ The proposed *Type-2 FLC* based SHAF with different Fuzzy MFs is able to eliminate the uncertainty in the system) and SHAF gains outstanding compensation abilities. *Type-2 FLC* is able to maintain the DC link voltage constant (V_{dc} is nearer to 797V; which is almost equal to V_{dc-ref} 800V) and it is able to mitigate harmonics (THD is nearly equal to 1% to 2%) in a superior way than *Type-1 FLC* (THD is nearly equal to 2.5% to 5%).
- ✦ While considering the I_d-I_q control strategy using Type-1 FLC (Trapezoidal, Triangular and Gaussian MF) and Type-2 FLC (Trapezoidal, Triangular and Gaussian MF) and the $p-q$ control strategy with Type-1 FLC (Triangular and Gaussian MF) and Type-2 FLC (Trapezoidal, Triangular and Gaussian MF), the SHAF has been found to meet the IEEE 519-1992 standard recommendations on harmonic levels.
- ✦ PI controller, Type-1 FLC and Type-2 FLC based shunt active filter control strategies ($p-q$ and I_d-I_q) with different Fuzzy MFs (Trapezoidal, Triangular and Gaussian) are verified with Real-time digital simulator (OPAL-RT) hardware to validate the proposed research.
- ✦ The *Simulation and Real-time implementation results* showed that even if the supply voltage is un-balanced and/or non-sinusoidal the performance of SHAF using I_d-I_q theory with Type-2 FLC (Gaussian MF) showing better compensation capabilities in terms of THD compared to I_d-I_q theory with PI, Type-1 FLC (Trapezoidal, Triangular and Gaussian MF) and Type-2 FLC (Trapezoidal, Triangular MF) and also $p-q$ theory

with PI, Type-1 FLC (Trapezoidal, Triangular and Gaussian MF) and Type-2 FLC (Trapezoidal, Triangular and Gaussian MF). The control approach has compensated the neutral harmonic currents and the dc bus voltage of SHAF is almost maintained at the reference value under all disturbances, which confirm the effectiveness of the controller.

↳ *RT-Lab real-time simulation results* further confirm the results obtained from *MATLAB simulations* that is, I_d-I_q scheme is the best reference compensation current extraction scheme and *Type-2 FLC* based controller is most efficient out of all the other conventional (PI) and Type-1 FLC based controllers discussed in this thesis.

6.2 FUTURE SCOPE

This thesis efforts have been made improve the power quality of power system by mitigating the current harmonics and maintaining dc-link voltage constant using PI controller, Type-1 FLC and Type-2 FLC based shunt active filter control strategies ($p-q$ and I_d-I_q) with different Fuzzy MFs under various source voltage conditions. It has explored some good ideas and suitable solutions, but further investigation is necessary.

↳ In this research work, we have attempted to improve the power quality of power system by *mitigating the current harmonics* and *maintaining dc link voltage constant*.

Many applications require a compensation of a combination of **voltage and current based problems**, a few of them being interrelated. A **hybrid of active series and active shunt filters** is an ideal choice for such mixed compensation. Moreover, this hybrid of both APF's (also known as a **unified power quality conditioner, UPQC**) is also quite suitable for individual current or voltage based compensation. However, the rating, size, and cost of this UPQC is on the higher side, therefore, for few combinations of compensation such as voltage and current harmonics, other APFs (**active series and passive shunt**) are considered most suitable.

↳ The proposed shunt active filter has been operated by using two control strategies, namely *p-q* and *I_d-I_q control strategies*.

Applying the improved control strategies (**Perfect harmonic cancellation control strategy** and etc.) can still improve the power quality. So potential of proposed version could be explored by adopting different control strategies.

↳ The proposed shunt active filter has been operated by using three controllers, namely *PI controller, Type-1 FLC and Type-2 FLC with different Fuzzy MFs*.

Applying the improved controllers (**Neuro-Fuzzy** and etc.) can still improve the power quality. So potential of proposed version could be explored by adopting different controllers.

↳ In this research work, we had considered *Fuzzy Hysteresis current control scheme* for generation of gating signals to the devices of the APF.

Applying the improved switching techniques (**Adaptive Fuzzy hysteresis controller** and etc.) can still improve the output quality. So potential of proposed version could be explored by adopting different switching techniques.

↳ In this research work, we had considered *Mamdani* type of Fuzzy logic controller with **49 rules**; type of membership functions are *Trapezoidal, Triangular and Gaussian*; No. of membership functions are *seven*; Type of implication is *Mamdani Max-Min Operation* and Type of defuzzification method is *centroid of area method*.

Takai Sugeno Fuzzy logic controller is better than the Mamdani type of Fuzzy logic controller in the sense that it requires only **two numbers of Fuzzy sets, four rules** compared to seven Fuzzy sets, 49 rules used for the Mamdani type FLC. Hence, the TS FLC is a good aspirant for improving the performance of a system by eliminating the harmonics.

References

REFERENCES

- [1] H. Akagi, "New trends in active filters for power conditioning," *IEEE Trans. Ind. Appl.*, Vol. 32, No. 6, pp. 1312-1322, Nov./Dec.1996.
- [2] H. Rudnick, Juan Dixon and Luis Moran, "Active power filters as a solution to power quality problems in distribution networks," *IEEE power & energy magazine*, pp. 32-40, Sept. / Oct. 2003.
- [3] S. Bhattacharya and D. M. Divan, "Hybrid series active/parallel passive power line conditioner with controlled harmonic injection," *U.S. Patent 5 465 203*, Nov. 1995.
- [4] Bhim Singh, K. Al-Haddad, and A. Chandra, "A Review of Active Filters for Power Quality Improvement," *IEEE Trans. on Industrial Electronics*, Vol.46, No.5, Oct. 1999.
- [5] J. H. Choi, G. W. Park, and S. B. Dewan, "Standby power supply with active power filter ability using digital controller," in Proc. *IEEE APEC'95*, pp. 783–789, 1995.
- [6] Z. Li, H. Jin, and G. Joos, "Control of active filters using digital signal processors," in *Proc. IEEE IECON'95*, pp. 651–655, 1995.
- [7] Suresh Mikkili, A. K. Panda, "Real-time implementation of PI and Fuzzy logic controllers based shunt active filter control strategies for power quality improvement," *International Journal of Electrical Power and Energy Systems – Elsevier*, Vol.43, pp. 1114-1126, 2012.
- [8] A. Teke, L. Saribulut, M.Tumay, "A Novel Reference Signal Generation Method for Power Quality Improvement of Unified Power Quality Conditioner," *IEEE Transactions on Power Delivery*, Vol: 26, No: 4, pp. 2205–2214, 2011.
- [9] S. Saad, L. Zellouma, "Fuzzy logic controller for three-level shunt active filter compensating harmonics and reactive power," *Electric Power Systems Research*, Vol.79, pp.1337–1341, 2009.

- [10] Parmod Kumar, and Alka Mahajan, "Soft Computing Techniques for the Control of an Active Power Filter," *IEEE Transactions on Power Delivery*, Vol. 24, No. 1, Jan. 2009.
- [11] Fatiha Mekri, Benyounes Mazari, and Mohamed Machmoum, "Control and optimization of shunt active power filter parameters by fuzzy logic," *Can. J. Elect. Comput. Eng.*, Vol. 31, No. 3, Summer 2006.
- [12] P. Kirawanich, and Robert M. O'Connell, "Fuzzy Logic Control of an Active Power Line Conditioner," *IEEE Trans. on Power Electronics*, Vol. 19, No. 6, Nov. 2004.
- [13] S. K. Jain, P. Agrawal and H.O. Gupta, "Fuzzy logic controlled shunt active power filter for power quality improvement," *IEEE Proc. of Electric Power Applications*, Vol.149, No. 5, 2002.
- [14] A. Bhattacharya, and Chandan Chakraborty, "A Shunt Active Power Filter With Enhanced Performance Using ANN-Based Predictive and Adaptive Controllers," *IEEE Transactions on Industrial Electronics*, Vol. 58, No. 2, February 2011.
- [15] Maurizio Cirrincione, Marcello Pucci, and Gianpaolo Vitale, "A Single-Phase DG Generation Unit With Shunt Active Power Filter Capability by Adaptive Neural Filtering," *IEEE Transactions on Industrial Electronics*, Vol. 55, No. 5, May 2008.
- [16] Hsiung Cheng Lin, "Intelligent Neural Network-Based Fast Power System Harmonic Detection," *IEEE Transactions on Industrial Electronics*, Vol. 54, No. 1, Feb. 2007.
- [17] D. O. Abdeslam, P. Wira, J. Merckle, D. Flieller, and Y. A. Chapuis, "A Unified Artificial Neural Network Architecture for Active Power Filters," *IEEE Trans. on Industrial Electronics*, Vol. 54, No. 1, February 2007.
- [18] F. J. Alcantara, P. Salmeron, "A New Technique for Unbalance Current and Voltage Estimation with Neural Networks," *IEEE Trans. on Pow. Sys*, Vol. 20, No. 2, 2005.
- [19] J. R. Vazquez and P. Salmeron, "Active power filter control using neural network technologies," *IEE Proc. Electric Power Applications*, Vol. 150, No. 2, 2003.

- [20] S. M. R. Rafiei, Reza Ghazi, and H. A. Toliyat, "IEEE-519-Based Real-Time and Optimal Control of Active Filters Under Non-sinusoidal Line Voltages Using Neural Networks," *IEEE Transactions on Power Delivery*, Vol. 17, No. 3, July 2002.
- [21] Y. M. Chen, and R. M. O. Connell, "Active Power Line Conditioner with a Neural Network Control," *IEEE Transactions on Industry Applications*, Vol.33, No.4, 1997.
- [22] M. Rukonuzzaman and M. Nakaoka, "Single-phase shunt active power filter with harmonic detection," *IEE. Proc. Electric power Applications*, Vol. 149, No. 05, 2002.
- [23] A. C. Liew, "Excessive neutral currents in three-phase fluorescent lighting circuits," *IEEE Trans. Ind. Applicat.*, vol. 25, pp. 776–782, July/Aug. 1989.
- [24] T. M. Gruz, "A survey of neutral currents in three-phase computer power systems," *IEEE Trans. Ind. Applicat.*, vol. 26, pp. 719–725, July/Aug. 1990.
- [25] F. Z. Peng, G. W. Ott Jr., D. J. Adams, "Harmonic and reactive power compensation based on the generalized instantaneous reactive power theory for three-phase four-wire systems," *IEEE Trans. Power Electron.*, Vol. 13, No. 5, pp. 1174-1181, Nov. 1998.
- [26] Suresh Mikkili, A. K. Panda, "PI and Fuzzy Logic Controller based 3-phase 4-wire Shunt active filter for mitigation of Current harmonics with I_d - I_q Control Strategy," *Journal of power Electronics (JPE)*, vol. 11, No. 6, Nov. 2011.
- [27] A. Mansoor, W. M. Grady, P. T. Staats, R. S. Thallam, M. T. Doyle, and M. J. Samotyj, "Predicting the net harmonic currents produced by large numbers of distributed single-phase computer loads," *IEEE Trans. Power Delivery*, vol. 10, pp. 2001–2006, 1994.
- [28] Active Filters: Technical Document, 2100/1100 Series, *Mitsubishi Electric Corp.*, Tokyo, Japan, pp. 1–36, 1989.
- [29] A. H. Kikuchi, "Active power filters," in Toshiba GTR Module (IGBT) Application Notes, *Toshiba Corp.*, Tokyo, Japan, pp. 44–45, 1992.

- [30] S. A. Moran and M. B. Brennen, "Active power line conditioner with fundamental negative sequence compensation," *U.S. Patent 5 384 696*, Jan. 1995.
- [31] G. T. Heydt, "Electric Power Quality," *West Lafayette, IN: Stars in a Circle*, 1991.
- [32] D. D. Shipp, "Harmonic analysis, suppression for electrical systems supplying static power converters other nonlinear loads," *IEEE Trans. Ind. Applicat.*, vol. 15, pp. 453–458, Sept./Oct. 1979.
- [33] L. Rossetto and P. Tenti, "Evaluation of instantaneous power terms in multi-phase systems: Techniques, application to power-conditioning equipment," *Eur. Trans. Elect. Power Eng.*, vol. 4, no. 6, pp. 469–475, Nov./Dec. 1994.
- [34] L. S. Czarnecki, "Combined time-domain, frequency-domain approach to hybrid compensation in unbalanced non sinusoidal systems," *Eur. Trans. Elect. Power Eng.*, vol. 4, no. 6, pp. 477–484, Nov./Dec. 1994.
- [35] Abdelmadjid Chaoui, Fateh Krim, Jean-Paul Gaubert, Laurent Rambault, "DPC controlled three-phase active filter for power quality improvement," *International Journal of Electrical Power and Energy Systems*, vol.30, pp.476–485, 2008.
- [36] N. Zaveri, A. Chudasama, "Control strategies for harmonic mitigation and power factor correction using shunt active filter under various source voltage conditions," *Int. Journal of Electrical Power and Energy Systems*, vol.42, pp.661–671, 2012.
- [37] H. Akagi, kanazawa, and Nabae "instantaneous reactive power compensators comprising Switching devices without energy storage components" *IEEE Trans on Industry Applications*, Vol. Ia-20, No. 3, pp. 625-630, May/June 1984.
- [38] H. Akagi et al, "Instantaneous Power Theory and Applications to Power Conditioning," New Jersey. *IEEE Press/Wiley-Inter-science*, ISBN 978-0-470-10761-4, 2007.
- [39] H. Akagi, Y. Kanazawa, and A. Nabae, "Generalized theory of the instantaneous reactive power in three-phase circuits," in *Proc. IPEC Tokyo*, pp. 1375–1386, 1983.

- [40] A. Ferrero and G. S. Furga, "A new approach to the definition of power components in three-phase systems under non-sinusoidal conditions," *IEEE Trans. Instrum. Meas.*, vol. 40, pp. 568–577, June 1991.
- [41] H. Akagi and A. Nabae, "The p-q theory in three-phase systems under non-sinusoidal conditions," *Eur. Trans. Elect. Power Eng.*, vol. 3, no. 1, pp. 27–31, Jan./Feb. 1993.
- [42] Z. Zhou, Y. Liu, "Pre-sampled data based prediction control for active power filters," *International Journal of Electrical Power and Energy Systems*, vol.37; pp.13–22, 2012.
- [43] V. Soares, P. Verdelho and G. D. Marques, "An Instantaneous Active and Reactive Current Component Method for Active Filters," *IEEE Trans. Power Electron.*, Vol. 15, No. 4, pp. 660-669, 2000.
- [44] V. Soares et al. "Active Power Filter Control Circuit Based on the Instantaneous Active and Reactive Current $I_d - I_q$ Method," *IEEE Power Electronics Specialists Conference* pp. 1096-1101, 1997.
- [45] J. L. Willems, "Current compensation in three-phase power systems," *Eur. Trans. Elect. Power Eng.*, vol. 3, no. 1, pp. 61–66, Jan./Feb.1993.
- [46] Bhim Singh, P. Jayaprakash, D.P. Kothari, "New control approach for capacitor supported DSTATCOM in three-phase four wire distribution system under non-ideal supply voltage conditions based on synchronous reference frame theory," *International Journal of Electrical Power and Energy Systems*, vol.33; pp. 1109–1117, 2011.
- [47] P. Rodriguez, J. I. Candela, A. Luna, and L. Asiminoaei, "Current harmonics cancellation in three-phase four-wire systems by using a four-branch star filtering topology," *IEEE Trans. Power Electron.* Vol. 24, No. 8, pp. 1939-1950, Aug. 2009.
- [48] M.I.M. Montero, E.R. Cadaval, F.B. Gonzalez, "Comparison of control strategies for shunt active power filters in three-phase four wire systems," *IEEE Transactions on Power Electronics*, Vol. 22, no.1, pp. 229-236, 2007.

- [49] P. Salmeron, R.S. Herrera, "Distorted and unbalanced systems compensation within instantaneous reactive power framework," *IEEE Transactions on Power Delivery*, Vol.21, no.3, pp.1655-1662, 2006.
- [50] Suresh Mikkili and A. K. Panda, "Simulation and real-time implementation of shunt active filter I_d - I_q control strategy for mitigation of harmonics with different Fuzzy membership functions," *IET Power Electronics*, Vol. 5, No. 9, pp.1856 – 1872, 2012.
- [51] I. Holh, "Pulse width modulation - A survey," *IEEE Trans. on ind. Electronics*, Vol. 39, No. 5, pp. 410-4211, 1999.
- [52] A. Albanna, C.J. Hatziadoniu, "Harmonic analysis of hysteresis controlled grid-connected inverters," in proc. *IEEE/PES Power Systems Conference and Exposition (PSCE '09)* pp. 1 – 8, 2009.
- [53] A. Karaarslan, "Hysterisis control of power factor correction with a new approach of sampling technique," in proc. *IEEE 25th Convention of Electrical and Electronics Engineers in Israel*, pp. 765 – 769, 2008.
- [54] Fatiha Mekri , Mohamed Machmoum, Nadia Ait Ahmed, Benyounes Mazari, "A Fuzzy hysteresis voltage and current control of An Unified Power Quality Conditioner," in proc. *34th Annual Conference of IEEE IECON*, pp. 2684 – 2689, 2008.
- [55] H. Sasaki and T. Machida, "A new method to eliminate AC harmonic currents by magnetic flux compensation-considerations on basic design," *IEEE Trans. Power App. Syst.*, vol. PAS-90, pp. 2009–2019, Jan. 1971.
- [56] "Harmonic currents, static VAR systems," *ABB Power Systems*, Stockholm, Sweden, Inform. NR500-015E, pp. 1–13, Sept. 1988.
- [57] H. Akagi, S. Atoh, and A. Nabae, "Compensation characteristics of active power filter using multi series voltage-source PWM converters," *Elect. Eng. Japan*, vol. 106, no. 5, pp. 28–36, 1986.

- [58] S. Fukuda and M. Yamaji, "Design, characteristics of active power filter using current source converter," in *Conf. Rec. IEEE-IAS Annu. Meeting*, 1990, pp. 965–970.
- [59] C. K. Duffey and R. P. Stratford, "Update of harmonic standard IEEE- 519: IEEE recommended practices, requirements for harmonic control in electric power systems," *IEEE Trans. Ind. Applications*, vol. 25, pp. 1025–1034, Nov./Dec. 1989.
- [60] B. N. Singh, B. Singh, A. Chandra, K. Al-Haddad, "DSP based implementation of sliding mode control on an active filter for voltage regulation and compensation of harmonics, power factor and unbalance of nonlinear loads," *IEEE IECON '99*, Vol. 2, pp. 855 - 860, 1999.
- [61] F. Ferreira, L. Monteiro, J.L. Afonso, C. Couto, "A control strategy for a three-phase four-wire shunt active filter," *IEEE IECON*, pp. 411 – 416, 2008.
- [62] J. Dixon; J. Contardo; L. Moran, "DC link fuzzy control for an active power filter, sensing the line current only," in *proc. 28th Annual IEEE Power Electronics Specialists Conference (PESC '97)*, Vol: 2, pp. 1109 – 1114, 1997.
- [63] Mikkili. Suresh, A. K. Panda, S. S. Patnaik, S. Yellasiri, "Comparison of two compensation control strategies for shunt active power filter in three phase four-wire system" in *proc. IEEE PES Innovative Smart Grid Technologies (ISGT), Hilton Anaheim, CA, USA*, pp.1-6, DOI:10.1109/ISGT.2011.5759126, 2011.
- [64] A.D. Le Roux, J.A. Du Toit, J.H.R. Enslin, "Integrated active rectifier and power quality compensator with reduced current measurement," *IEEE Transactions on Industrial Electronics*, Vol. 46 No. 3, pp. 504 – 511, 1999.
- [65] Suresh Mikkili and A. K. Panda, "RTDS hardware implementation and simulation of SHAF for mitigation of harmonics using p-q control strategy with PI and Fuzzy logic controllers," *Frontiers of Electrical and Electronic Engineering– Springer*, Vol. 7, No.4, pp. 427–437, 2012.

- [66] W. V. Lyon, "Reactive power and unbalanced circuits," *Electrical world*, Vol. 75, No. 25, pp. 1417-1420, 1920.
- [67] C.I. Budeanu, "Puissances reactives et fictives," *Institute Romaine de energy*, pub. No. 2, Bucharest, 1927.
- [68] C. I. Budeanu, "The different options and Conceptions Regarding Active power in Non-sinusoidal systems," *Institute Romaine de energy, pub. No. 4, Bucharest, 1927.*
- [69] S. Fryze, "Wirk, Blind und Scheinleistung in Elektrischen Stromkreisen mit nicht-sinusformigen verlauf von strom and Spannung," *ETZ-Arch. Electrotech.*, Vol.53, pp. 596-599, 625-627, 700-702, 1932.
- [70] M. S. Erlicki and A. Emmanuel-Eigeles, "New Aspects of Power Factor Improvements Part – I – Theoretical basis," *IEEE Transactions on Industry and General Applications*, Vol. 1GA-4, pp. 441-226, 1968.
- [71] H. Sasaki and T. Machida, "New method to Eliminate AC Harmonic by Magnetic Compensation- Consideration on Basic Design," *IEEE Transactions on Power Apparatus and Systems*, Vol. 90, No. 5, pp. 2009-2019, 1970.
- [72] T. Fukao, Iida, and Miyairi, "Improvements of the Power Factor of Distorted Waveforms by Thyristor based Switching Filter," *Transactions of the IEE-Japan*, Part-B, Vol.92, No.6, pp.342-349, 1970.
- [73] L. Gyugyi and B. R. Pelly, "Static Power Frequency Chargers : Theory Performance and Application," *Wiley*, 1976.
- [74] F. Harashima, Inaba, and Tsuboi, "A Closed-loop Control System for the Reduction of Reactive Power required by Electronic Converters," *IEEE Transactions on IECEI*, Vol. 23, No. 2, pp. 162-166, 1976.
- [75] L. Gyugyi and Strycula, "Active Power Filters," in *Proc. of IEEE Industrial Application Annual Meeting*, vol. 19-C, pp. 529-535, 1976.

- [76] I. Takahashi, Fuziwara, and A. Nabae, "Universal Reactive Power Compensator," in *Proc. of IEEE Industrial Application Annual Meeting*, pp. 858-863, 1980.
- [77] I. Takahashi, Fuziwara, and A. Nabae, "Distorted Current Compensation System using Thyristor based Line Commutated Converters," *Transactions of the IEE-Japan, Part-B*, Vol.101, No.3, pp.121-128, 1981.
- [78] H. Akagi, Y. Kanazawa, and A. Nabae, "Principles and Compensation Effectiveness of Instantaneous Reactive Power Compensation Devices," in *meeting of the power semiconductor converters Researchers- IEE Japan*, SPC-82-16, 1982.
- [79] H. Akagi, Y. Kanazawa, and A. Nabae, "Generalized theory of the Instantaneous Reactive Power and its Applications," *Transactions of the IEE-Japan, Part-B*, Vol.103, No.7, pp.483-490, 1983.
- [80] E. Clarke, "Circuit Analysis of AC Power Systems," *Symmetrical and Related Components*, Wiley, 1943.
- [81] F.M. Uriarte, "Hysterisis Modeling by Inspection," in *proc. 38th North American Power Symposium*, pp. 187 – 191, 2006.
- [82] L.A. Zadeh, "Fuzzy sets," *Information and Control*, Vol. 8, pp. 338-353, 1965.
- [83] L.A. Zadeh, "Outline of a new approach to the analysis of complex systems and decision processes," *IEEE Transactions on Systems, Man, and Cybernetics*, Vol. 3, No.1, pp. 28-44, Jan. 1973.
- [84] E. H. Mamdani, "Applications of Fuzzy logic to approximate reasoning using linguistic synthesis," *IEEE Transactions on Computers*, Vol. 26, No. 12, pp. 1182-1191, 1977.
- [85] E. H. Mamdani, "Advances in the linguistic synthesis of Fuzzy controllers," *International Journal of Man-Machine Studies*, Vol. 8, pp. 669-678, 1976.
- [86] Jin Zhao, B. K. Bose, "Evaluation of membership functions for Fuzzy logic controlled induction motor drive," *28th Annual Conference of IECON*, vol.1, pp. 229 – 234, 2002.

- [87] B. K. Bose, "Modern Power Electronics and AC Drives," *Prentice Hall, Upper Saddle River, NJ*, 2002.
- [88] L. A. Zadeh, "Fuzzy logic," *Computer*, Vol.21, No. 4, pp. 83 – 93, 1988.
- [89] A. Kandel, "Fuzzy expert systems," *C.R.C Pres, Inc. Boca Raton, FL*, 1992.
- [90] C. C. Lee, "Fuzzy logic in control systems : Fuzzy logic controller – part 1," *IEEE Transactions on systems, Man and Cybernetics*, Vol. 20, No. 2, pp. 404-418, 1990.
- [91] C. C. Lee, "Fuzzy logic in control systems : Fuzzy logic controller – part 2," *IEEE Transactions on systems, Man and Cybernetics*, Vol. 20, No. 2, pp. 419-435, 1990.
- [92] B. Kosko, "Neural networks and Fuzzy systems: a dynamical systems approach," *Prentice Hall, Upper Saddle River, NJ*, 1991.
- [93] Fuzzy inference system [online], available:
<http://www.mathworks.in/help/toolbox/fuzzy/fp351dup8.html>
- [94] T.A. Runkler, "Selection of appropriate defuzzification methods using application specific properties," *IEEE Trans. on Fuzzy Systems*, Vol.5, No.1, pp. 72 – 79, 1997.
- [95] Defuzzification methods [online], available:
<http://www.mathworks.in/products/demos/shipping/fuzzy/defuzzdm.html>
- [96] Fuzzy inference system Editor [online], available:
<http://www.mathworks.in/products/fuzzy-logic/description3.html>
- [97] D. Dubois and H. Prade, "Fuzzy Sets and Systems: Theory and Applications," *Academic Press*, New York, 1980.
- [98] Suresh. Mikkili and A.K.Panda, "Real-time implementation of power theory using FLC based shunt active filter with different Fuzzy M.F.s," *IECON 2012 - 38th Annual Conference on IEEE Industrial Electronics Society , Montreal, QC, Canada*, pp. 702 – 707, 25-28 Oct. 2012.

- [99] L.A. Zadeh, "Toward a restructuring of the foundations of Fuzzy logic (FL)," *IEEE International Conference on World Congress on Computational Intelligence Fuzzy Systems*, Vol. 2, pp. 1676 – 1677, 1998.
- [100] L.A. Zadeh, "Fuzzy logic: issues, contentions and perspectives," *IEEE International Conference on Acoustics, Speech, and Signal Processing*, Vol. 6, 1994.
- [101] W. Pedrycz, F. Gomide, "The design of Fuzzy sets," *Fuzzy Systems Engineering: Toward human-centric computing, Wiley-IEEE Press eBook chapters*, pp.67–100, 2007.
- [102] A. Elmitwally, S. Abdelkader, M. Elkateb, "Performance evaluation of fuzzy controlled three and four wire shunt active power conditioners," *IEEE Power Engineering Society Winter Meeting*, vol.3, pp.1650 – 1655, 2000.
- [103] J.-S.R. Jang, C.-T. Sun, E. Mizutani, "Neuro-Fuzzy and Soft Computing," *Prentice-Hall, Englewood Cliffs, NJ*, 1997.
- [104] Suresh Mikkili, Anup Kumar Panda, "Types-1 and -2 Fuzzy logic controllers-based shunt active filter I_d – I_q control strategy with different Fuzzy membership functions for power quality improvement using RTDS hardware," *IET Power Electronics*, Vol. 6, Issue 4, pp. 818 – 833, April 2013.
- [105] W. Pedrycz, F. Gomide, "Operations and Aggregations of Fuzzy Sets," *Fuzzy Systems Engineering: Toward Human-Centric Computing, Wiley-IEEE Press eBook Chapters*, pp. 101 – 138, 2007 .
- [106] M. Kantardzic, "Fuzzy sets and Fuzzy Logic," *Data Mining: Concepts, Models, Methods, and Algorithms, Wiley-IEEE Press eBook Chapters*, pp. 414 – 446, 2011.
- [107] Soo. Yeong Yi and Myung Jin Chung, "Robustness of Fuzzy Logic Control for an Uncertain Dynamic System," *IEEE Transactions on Fuzzy Systems*, vol. 6, no. 2, 1998.

- [108] A. Celikyilmaz,; I. B. Turksen, “Uncertainty Modelling of Improved Fuzzy Functions With Evolutionary Systems,” *IEEE Transactions on Systems, Man, and Cybernetics, Part B: Cybernetics*, Vol. 38 ,No.4, pp. 1098 – 1110, 2008.
- [109] J. M. Mendel, “Uncertainty, Fuzzy Logic, and Signal Processing,” *Signal Proc. J.*, vol. 80, pp. 913-933, 2000.
- [110] L.A Zadeh, “From Fuzzy logic to Extended Fuzzy logic - A first step,” *IEEE Annual Meeting of the North American Fuzzy Information Processing Society*, pp.1–2, 2009.
- [111] R. Sepulveda, O. Castillo, P. Melin, A. Rodriguez-Diaz and O. Montiel, “Handling Uncertainties in Controllers Using Type-2 Fuzzy Logic,” in *Proc. IEEE FUZZ Conference*, pp. 248-253, Reno, NV, May 2005.
- [112] R. Sepulveda, O. Castillo, P. Melin, A. Rodriguez-Diaz and O. Montiel, “Experimental Study of Intelligent Controllers Under Uncertainty Using Type-1 and Type-2 Fuzzy Logic,” *Information Sciences*, vol. 177, pp. 2023-2048, 2007.
- [113] Oscar Castillo and Patricia Melin, “Recent Advances in Interval Type-2 Fuzzy Systems,” *Springer Briefs in Applied Sciences and Technology*, Vol. 1, DOI: 10.1007/978-3-642-28956-9, 2012.
- [114] M. Mizumoto and K. Tanaka, “Some Properties of Fuzzy Sets of Type-2,” *Information and Control*, vol. 31, pp. 312-340, 1976.
- [115] L. A. Zadeh, “The concept of a linguistic variable and its application to approximate reasoning, Parts 1, 2, and 3,” *Information Sciences*, vol. 8, pp. 199-249; vol. 8, pp. 301-357, vol.9, pp.43-80, 1975.
- [116] O. Castillo and P. Melin, “Type-2 Fuzzy Logic Theory and Applications,” *Springer Verlag*, Berlin, 2008.
- [117] N. N. Karnik and J.M. Mendel, “An Introduction to Type-2 Fuzzy Logic Systems,” *Univ. of Southern Calif., Los Angeles, CA.*, June 1998.

- [118] N. N. Karnik, J. M. Mendel and Q. Liang “Type-2 Fuzzy Logic Systems,” *IEEE Trans. on Fuzzy Systems*, vol. 7, pp. 643-658, Dec. 1999.
- [119] J. M. Mendel, “Uncertain Rule-Based Fuzzy Logic Systems: Introduction and New Directions”. NJ: *Prentice-Hall*, 2001.
- [120] J. M. Mendel, R. I. John and F. Liu, “Interval type-2 fuzzy logic systems made simple,” *IEEE Trans. on Fuzzy Systems*, vol. 14, pp. 808-821, December 2006.
- [121] Wu Dongrui; J. M. Mendel, “On the Continuity of Type-1 and Interval Type-2 Fuzzy Logic Systems,” *IEEE Trans. on Fuzzy Systems*, Vol. 19, No. 1, pp. 179 – 192, 2011.
- [122] Q. Liang and J. Mendel, “Interval type-2 fuzzy logic systems: Theory and design,” *IEEE Transactions Fuzzy Systems*, vol. 8, pp. 535–550, 2000.
- [123] J. Castro, Oscar Castillo, L. G. Martínez, “Interval Type-2 Fuzzy Logic Toolbox,” *Engineering Letters*, 15:1, EL_15_1_14, 2007.
- [124] J. Castro, O. Castillo and P. Mellin, “An type-2 fuzzy logic toolbox for control applications,” *Proc. IEEE FUZZ Conference*, pp. 61-66, London, UK, July 2007.
- [125] E. H. Mamdani and S. Assilian, “An experiment in linguistic synthesis with a fuzzy logic controller,” *International Journal of Man-Machine Studies*, Vol. 7, No. 1, pp. 1-13, 1975.
- [126] S. Coupland and R. I. John, “Geometric Type-1 and Type-2 Fuzzy Logic Systems,” *IEEE Trans. on Fuzzy Systems*, vol. 15, pp. 3-15, February 2007.
- [127] G. J. Klir and B. Yuan, “Fuzzy Sets and Fuzzy Logic: Theory and Applications,” *Prentice Hall*, Upper Saddle River, NJ, 1995.
- [128] L. A. Zadeh, “Knowledge representation in fuzzy logic,” *IEEE Transactions on Knowledge and Data Engineering*, Vol. 1, pp. 89-100, 1989.
- [129] L. A. Zadeh, “Fuzzy logic computing with words,” *IEEE Transactions on Fuzzy Systems*, vol. 2, pp. 103–111, 1996.

- [130] R. I. John and S. Coupland, "Type-2 fuzzy logic: a historical view," *IEEE Computational Intelligence Magazine*, vol. 2, pp. 57-62, February 2007.
- [131] H. Hagra, "Type-2 FLCs: a new generation of Fuzzy controllers," *IEEE Computational Intelligence Magazine*, vol. 2, pp. 30-43, February 2007.
- [132] Suresh. Mikkili, A. K. Panda, "Performance analysis and Real-time implementation of Shunt Active Filter Current Control Strategy with Type-1 and Type-2 FLC Triangular M.F," *European Trans. on Electrical Power - Wiley*, 2012. DOI: 10.1002/etep.1698.
- [133] R. R. Yager, "On a general class of fuzzy connectives," *Fuzzy Sets and Systems*, Vol. 4, pp. 235-242, 1980.
- [134] R. R. Yager, "A Characterization of the Fuzzy Extension Principle," *J. Fuzzy Sets and Systems*, vol. 18, pp. 205-217, 1986.
- [135] J. R. Aguero and A. Vargas, "Calculating function of interval type-2 fuzzy numbers for fault current analysis," *IEEE Trans. on Fuzzy Systems*, vol. 15, pp. 31-40, Feb. 2007.
- [136] D. Dubois and H. Prade, "Operations on Fuzzy Numbers," *Int. J. Systems Science*, vol. 9, pp. 613-626, 1978.
- [137] N.N. Karnik and J. M. Mendel, "Operations on Type-2 Fuzzy Sets," *Fuzzy Sets and Systems*, vol. 122, pp. 327-348, 2001.
- [138] J. M. Mendel, "Type-2 fuzzy sets and systems: an overview," *IEEE Computational Intelligence Magazine*, vol. 2, pp. 20-29, February 2007.
- [139] S. Coupland; R. John, "A Fast Geometric Method for Defuzzification of Type-2 Fuzzy Sets," *IEEE Transactions on Fuzzy Systems*, Vol. 16 ,No.4, pp. 929 – 941, 2008.

- [140] D. Dubois and H. Prade, "Operations in a Fuzzy-Valued Logic," *Information and Control*, vol. 43, pp. 224-240, 1979.
- [141] R. R. Yager, "On the Implication Operator in Fuzzy logic," *Information Sciences*, vol. 31, pp. 141-164, 1983.
- [142] A. Kaufman and M. M. Gupta, "Introduction to Fuzzy Arithmetic: Theory and Applications", *Van Nostrand Reinhold*, NY 1991.
- [143] L. X. Wang, "Adaptive fuzzy systems and control: design and stability analysis," *Prentice Hall*, 1994.
- [144] RT-LAB Professional [online], available: <http://www.opal-rt.com/product/rt-lab-professional>
- [145] Real time simulation [online], available : en.wikipedia.org/wiki/Real-time_Simulation
- [146] M. Papini and P. Baracos, "Real-time simulation, control and HIL with COTS computing clusters," *AIAA Modelling and Simulation Technologies Conference*, Denver, CO, August 2001.
- [147] C. Dufour, G. Dumur, J.N. Paquin, and J. Belanger, "A multicore pc-based simulator for the hardware-in-the-loop testing of modern train and ship traction systems," *13th Power Electronics and Motion Control Conference*, Poland, pp.1475–1480, 2008.
- [148] D. Auger, "Programmable hardware systems using model-based design," *IET and Electronics Weekly Conference on Programmable Hardware Systems*, London, pp. 1-12, 2008.
- [149] V. Q. Do, J.-C. Soumagne, G. Sybille, G. Turmel, P. Giroux, G. Cloutier, S. Poulin, "Hypersim, an Integrated Real-Time Simulator for Power Networks and Control Systems," *ICDS'99, Vasteras, Sweden*, pp 1-6, May 1999.
- [150] J Belanger, P Venne, JN Paquin, "The What, Where and Why of Real-Time Simulation," pp. 37-49.

- [151] Simon Abourida, Christian Dufour, Jean Bélanger, Vincent Lapointe, “Real-Time, PC-Based Simulator of Electric Systems and Drives,” *International Conference on Power Systems Transients – IPST* in New Orleans, USA, 2003.
- [152] M. Matar and R. Iravani, “FPGA Implementation of the Power Electronic Converter Model for Real-Time Simulation of Electromagnetic Transients,” *IEEE Transactions on Power Delivery*, Vol. 25, Issue 2, pp. 852-860, April 2010.
- [153] J. A. Hollman and J. R. Marti, “Real Time Network Simulation with PC-Cluster,” *IEEE Trans. Power Systems*, vol. 18, no. 2, pp. 563-569, 2008.
- [154] I. Etxeberria-Otadui, V. Manzo, S. Bacha, and F. Baltes, “Generalized average modelling of FACTS for real time simulation in ARENE,” *IEEE 28th Annual Conference of the Industrial Electronics Society (IECON 02)*, Vol. 2, pp.864-869, 2002.
- [155] J. F. Cecile, L. Schoen, V. Lapointe, A. Abreu, and J. Belanger, (2006) www.opalrt.com. [Online] available : <http://www.opalrt.com/technical-document/distributed-real-time-frame-work-dynamic-management-heterogeneous-co-simulations>
- [156] G. Sybille and H. Le-Huy, “Digital simulation of power systems and power electronics using the MATLAB/Simulink Power System Block set,” *IEEE Power Engineering Society Winter Meeting*, Singapore, Vol. 4, pp. 2973-2981, 2000.
- [157] J. Belanger, V. Lapointe, C. Dufour, and L. Schoen, “eMEGAsim: An Open High-Performance Distributed Real- Time Power Grid Simulator. Architecture and Specification,” *International Conference on Power Systems (ICPS'07)*, Bangalore, India, December 12-14, 2007.

List of Publications

(Journals and Conferences)

PUBLICATIONS

JOURNALS: - 10 - Articles published in International Journals

- 1) Suresh Mikkili, Anup Kumar Panda, “Types-1 and -2 Fuzzy logic controllers-based shunt active filter I_d - I_q control strategy with different Fuzzy membership functions for power quality improvement using RTDS hardware,” **IET Power Electronics**, Vol. 6, Issue 4, pp. 818 – 833, **April 2013**.
- 2) Anup Kumar Panda, Suresh Mikkili, “FLC based shunt active filter control strategies for mitigation of harmonics with different Fuzzy MFs using MATLAB and real-time digital simulator,” **International Journal of Electrical Power and Energy Systems – Elsevier**, vol. 47, pp. 313-336, **May 2013**.
- 3) Suresh Mikkili, Anup Kumar Panda, “Performance analysis and real-time implementation of shunt active filter current control strategy with type-1 and type-2 FLC triangular M.F,” **International Transactions on Electrical Energy Systems - John Wiley & Sons Ltd**, DOI: 10.1002/etep.1698, **2013**.
- 4) Suresh Mikkili, Anup Kumar Panda, “Real-time implementation of PI and fuzzy logic controllers based shunt active filter control strategies for power quality improvement,” **International Journal of Electrical Power and Energy Systems – Elsevier**, vol. 43, pp. 1114-1126, **Dec. 2012**.
- 5) Suresh Mikkili, Anup Kumar Panda, “RTDS hardware implementation and simulation of SHAF for mitigation of harmonics using p-q control strategy with PI and Fuzzy logic controllers,” **Frontiers of Electrical and Electronic Engineering– Springer**, Vol. 7, No.4, pp. 427–437, **Dec. 2012**.
- 6) Suresh Mikkili, Anup Kumar Panda, “Simulation and real-time implementation of shunt active filter I_d - I_q control strategy for mitigation of harmonics with different Fuzzy membership functions,” **IET Power Electronics**, Vol. 5, No. 9, pp.1856 – 1872, **Nov. 2012**.

- 7) Anup Kumar Panda, Suresh Mikkili, “Fuzzy logic controller based Shunt Active Filter control strategies for Power quality improvement Using Different Fuzzy M.F.s,” **International Journal of Emerging Electric Power Systems: be press (Berkeley Electronics press)**, Vol. 13: Issue. 05, Article 2, **Nov. 2012**
- 8) Suresh Mikkili, Anup Kumar Panda, “Real-Time Implementation of Shunt Active Filter P-Q Control Strategy for Mitigation of Harmonics with Different Fuzzy M.F.s,” **Journal of power Electronics (JPE) (KIPE- South Korea)**, Vol. 12, No. 5, , pp.821-829, **Sept. 2012.**
- 9) Suresh Mikkili, Anup Kumar Panda, “PI and Fuzzy Logic Controller Based 3-Phase 4-Wire Shunt Active Filters for the Mitigation of Current Harmonics with the Id-Iq Control Strategy,” **Journal of power Electronics (JPE) (KIPE- South Korea)**, Vol. 11, No. 6, pp. 914-921, **Nov. 2011.**
- 10) Suresh Mikkili, Anup Kumar Panda, “RTDS Hardware implementation and Simulation of 3-ph 4-wire SHAF for Mitigation of Current Harmonics with p-q and I_d - I_q Control strategies using Fuzzy Logic Controller,” **International Journal of Emerging Electric Power Systems: be press (Berkeley Electronics press)**, Vol. 12: No. 5, **Aug. 2011.**

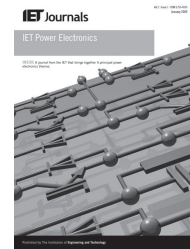
CONFERENCES: - 10 Articles presented in International Conferences

- 11) Suresh Mikkili, Anup Kumar Panda, “Real-time implementation of power theory using FLC based shunt active filter with different Fuzzy M.F.s,” **IECON 2012 - 38th Annual Conference on IEEE Industrial Electronics Society , Montreal, QC, Canada**, pp. 702 – 707, **DOI : [10.1109/IECON.2012.6388666](https://doi.org/10.1109/IECON.2012.6388666), 25-28 Oct. 2012.**
- 12) Suresh Mikkili, Anup Kumar Panda, “Fuzzy logic controller based 3-ph 4-wire SHAF for current harmonics compensation with id-iq control strategy using simulation and RTDS hardware,” **IEEE PEDS Singapore**, pp. 430-435, DOI: [10.1109/PEDS.2011.6147284](https://doi.org/10.1109/PEDS.2011.6147284), **07-10 Dec 2011.**
- 13) Mikkili Suresh, Anup Kumar Panda, S. S. Patnaik, S. Yellasiri, “Comparison_of_two_compensation_control_strategies_for_shunt_active_power_filter_in_three-phase_four-wire_system,”

IEEE PES Innovative Smart Grid Technologies (ISGT), Hilton Anaheim, CA, USA, pp.1-6, DOI:10.1109/ISGT.2011.5759126, 17 - 19 Jan. 2011.

- 14) Suresh Mikkili, Anup Kumar Panda, "Type-1 and Type-2 FLC based Shunt active filter I_d - I_q control strategy for mitigation of harmonics with Triangular MF," IEEE PEDES CPRI/IISC-Bangalore, pp.1-6, DOI: [10.1109/PEDES.2012.6484308](https://doi.org/10.1109/PEDES.2012.6484308), Dec. 16-19, 2012.**
- 15) Suresh Mikkili, Anup Kumar Panda, "Mitigation of Harmonics using Fuzzy Logic Controlled Shunt Active Power Filter with Different Membership Functions By Instantaneous Power Theory," IEEE SCES, MNNIT-ALLAHABAD, pp.1-6, DOI: [10.1109/SCES.2012.6199103](https://doi.org/10.1109/SCES.2012.6199103), 16-18, Marh 2012.**
- 16) Suresh Mikkili, Anup Kumar Panda, "PI controller based shunt active filter for mitigation of current harmonics with p-q control strategy using simulation and RTDS hardware," IEEE-INDICON, BITS-PILANI HYD, pp. 1-6, DOI: [10.1109/INDCON.2011.6139547](https://doi.org/10.1109/INDCON.2011.6139547), 16-18 Dec. 2011.**
- 17) Suresh Mikkili, Anup Kumar Panda, "Fuzzy logic controller based SHAF for current harmonics compensation with p-q control strategy using simulation and RTDS hardware," IEEE - INDICON, BITS-PILANI HYD, pp. 1-6, DOI: [10.1109/INDCON.2011.6139546](https://doi.org/10.1109/INDCON.2011.6139546), 16-18 Dec. 2011.**
- 18) Suresh Mikkili, Anup Kumar Panda, "Simulation and RTDS Hardware implementation of SHAF for current harmonics cancellation using I_d - I_q control strategy with PI and fuzzy controllers," IEEE ICPS- IIT MADRAS, pp. 1-6, DOI: [10.1109/ICPES.2011.6156669](https://doi.org/10.1109/ICPES.2011.6156669), 20-24 Dec 2011.**
- 19) Suresh Mikkili, Anup Kumar Panda, " I_d - I_q control strategy for mitigation of current harmonics with PI and fuzzy controllers," IEEE ICPS - IIT-MADRAS, pp. 1-6, DOI:[10.1109/ICPES.2011.6156668](https://doi.org/10.1109/ICPES.2011.6156668), 20-24 Dec 2011.**
- 20) Suresh Mikkili, Anup Kumar Panda, "PI and fuzzy controller based 3-ph 4-wire SHAF for current harmonics compensation using p-q control strategy," IET-SEISCON, pp. 299 – 303, DOI : [10.1049/cp.2011.0378](https://doi.org/10.1049/cp.2011.0378), 20-22 July 2011.**

Abstract
of
Publications
(Journals)



Types-1 and -2 fuzzy logic controllers-based shunt active filter I_d-I_q control strategy with different fuzzy membership functions for power quality improvement using RTDS hardware

Suresh Mikkili¹, Anup Kumar Panda²

¹Department of Electrical Engineering, National Institute of Technology-Goa, India

²Department of Electrical Engineering, National Institute of Technology-Rourkela, India
 E-mail: msuresh.ee@gmail.com; mikkili.suresh@nitgoa.ac.in

Abstract: This research paper proposes the shunt active filter (SHAF), which is used to improve the power quality of the electrical network by mitigating the harmonics with the help of Types-1 and -2 fuzzy logic controllers (Types-1 and -2 FLC) using different fuzzy membership functions (MFs). To carry out this analysis, active and reactive current (I_d-I_q) control strategy is chosen. Three-phase reference current waveforms generated by proposed scheme are tracked by the three-phase voltage source converter in a hysteresis band control scheme. The performance of the proposed control strategy has been evaluated in terms of harmonic mitigation and DC-link voltage regulation under various source conditions. To maintain DC-link voltage constant and to generate the compensating reference currents, the authors have developed Types-1 and -2 FLC with different fuzzy MFs (trapezoidal, triangular and Gaussian). The I_d-I_q control strategy with proposed Type-2 FLC is able to eliminate the uncertainty in the system and SHAF gains outstanding compensation abilities. The detailed real-time results using real-time digital simulator are presented to support the feasibility of proposed control strategy.

1 Introduction

Power quality (PQ) has been an important and growing problem because of the proliferation of non-linear loads such as power electronic converters in typical power distribution systems in recent years. Particularly, voltage harmonics and power distribution equipment problems result from current harmonics produced by non-linear loads [1]. The electronic equipment such as, computers, battery chargers, electronic ballasts, variable frequency drives and switched-mode power supplies, generate perilous harmonics and cause enormous economic loss every year. Problems caused by PQ have great adverse economic impact on the utilities and customers. Owing to that both power suppliers and power consumers are concerned about the PQ problems and compensation techniques [2].

Issue of Harmonics are of a greater concern to engineers and building designers because harmonics can do more than distort voltage waveforms, they can overheat the building wiring, causes nuisance tripping, overheat transformer units and cause random end-user equipment failures. Thus PQ has become more and more serious with each passing day. As a result active power filter (APF) gains much more attention because of excellent harmonic and reactive power compensation in two-wire (single phase), three-wire (three-phase without neutral) and four-wire (three-phase with neutral) ac power networks with non-linear loads.

The APF technology has been under research and development for providing compensation for harmonics, reactive power and/or neutral current in ac networks. Current harmonics are one of the most common PQ problems and are usually resolved by the use of shunt active filters (SHAF) [2].

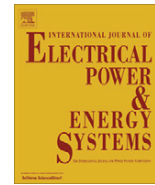
In this research paper, the performance of the SHAF current control strategy has been evaluated in terms of harmonic mitigation and DC-link voltage regulation. For extracting the three-phase reference currents for shunt APFs, we have developed SHAF instantaneous active and reactive current ' I_d-I_q ' control strategy. For regulating and maintaining the DC-link capacitor voltage constant, the active power flowing into the active filter needs to be controlled. To maintain DC-link voltage constant and to generate the compensating reference currents, we have developed Types-1 and -2 fuzzy logic controller (FLC) with different fuzzy MFs (trapezoidal, triangular and Gaussian). The proposed APF is verified through real-time digital simulator. The detailed real-time results are presented to support the feasibility of proposed control strategy.

When the supply voltages are balanced and sinusoidal, the two control strategies; instantaneous active and reactive power ($p-q$) control strategy and instantaneous active and reactive current (I_d-I_q) control strategy are converging to the same compensation characteristics but, when the supply voltages are distorted and/or un-balanced sinusoidal, these



Contents lists available at SciVerse ScienceDirect

Electrical Power and Energy Systems

journal homepage: www.elsevier.com/locate/ijepes

FLC based shunt active filter ($p-q$ and I_d-I_q) control strategies for mitigation of harmonics with different fuzzy MFs using MATLAB and real-time digital simulator

Anup Kumar Panda, Suresh Mikkili*

Dept. of Electrical Engineering, National Institute of Technology, Rourkela, India

ARTICLE INFO

Article history:

Received 21 January 2012
 Received in revised form 18 September 2012
 Accepted 1 November 2012

Keywords:

Harmonic compensation
 SHAF
 $p-q$ Control strategy
 I_d-I_q Control strategy
 Fuzzy logic controller
 Real-time simulator (OPAL-RT) Hardware

ABSTRACT

Problems caused by power quality have great adverse economical impact on the utilities and customers. Current harmonics are one of the most common power quality problems and are usually resolved by the use of shunt active filters (SHAFs). Control strategies ($p-q$ and I_d-I_q) for extracting the three-phase reference currents for shunt active power filters are compared, evaluating their performance under different source conditions. Three-phase reference current waveforms generated by proposed scheme are tracked by the three-phase voltage source converter in a hysteresis band control scheme.

The performance of the control strategies has been evaluated in terms of harmonic mitigation and DC link voltage regulation. The proposed SHAF with different fuzzy MFs (Trapezoidal, Triangular and Gaussian) is able to eliminate the uncertainty in the system and SHAF gains outstanding compensation abilities. The detailed simulation results using MATLAB/SIMULINK software are presented to support the feasibility of proposed control strategies. To validate the proposed approach, the system is also implemented on a real-time digital simulator (OPAL-RT) Hardware and adequate results are reported for its verifications.

© 2012 Elsevier Ltd. All rights reserved.

1. Introduction

The demand from the electricity customers for good quality [1] of power supply is ever rising due to the increase of sensitive loads. This is often a challenging task. The widespread use of adjustable-speed drives, static power converters such as single-phase and three-phase rectifiers and a large number of power-electronics based equipments cause distortion in the source currents [2]. The loads such as induction furnaces and motors increase the rating of the equipments used in the power system. Single phasing and unequal distribution of loads among three phases cause excessive neutral current to flow in the system. Though conventional load compensation using passive filters is simple to design and operate, it has drawbacks like resonance, overloading, and detuning. Moreover, it is not suitable for fast changing loads. The abovementioned problems are effectively alleviated by using a shunt active power filter (SHAF) [3]. The selection of control strategy for the SHAF plays a significant role to get the desired compensation characteristics. The two main control strategies for load compensation are instantaneous power and current ($p-q$ and i_d-i_q) control strategies [4].

In the i_d-i_q method [4–6] the angle ' θ ' is calculated directly from the main voltages which enables the method to be frequency inde-

pendent. As a result, a large number of synchronization problems with un-balanced and non-sinusoidal voltages are avoided.

Recently, fuzzy logic controllers [4,6] have received a great deal of attention in regards to their application to APFs. The advantages of fuzzy logic controllers over conventional controllers (PI) are that they do not require an accurate mathematical model, can work with imprecise inputs, can handle non-linearity, and are more robust than conventional PI controllers [4,6]. The Mamdani type of fuzzy logic controller, used for the control of an APF, gives better results when compared with PI controllers, but it has the drawback of a larger number of fuzzy sets and 49 rules.

Present paper mainly focused on the fuzzy logic controller with different membership functions (MF's) to analyse the performance of instantaneous power and current ($p-q$ and I_d-I_q) control strategies [4,7] for extracting reference currents of shunt active filters under different voltage conditions. PWM pattern generation based on carrier less hysteresis based current control is used for quick response. It is also observed that DC voltage regulation system valid to be a stable and steady-state error free system was obtained. Thus with fuzzy logic and (I_d-I_q) approaches a novel shunt active filter can be developed by using different MFs.

2. Instantaneous active and reactive power ($p-q$) theory

Instantaneous reactive power theory (or pq theory) was first proposed by Akagi and co-authors in 1984 [8], and has since been the subject of various interpretations and improvements. In this

* Corresponding author.

E-mail address: msuresh.ee@gmail.com (S. Mikkili).

Performance analysis and real-time implementation of shunt active filter Id-Iq control strategy with type-1 and type-2 FLC triangular M.F

Suresh Mikkili^{*,†} and A. K. Panda

Department of Electrical Engineering, National Institute of Technology, Rourkela, India

SUMMARY

This research article presents a novel approach based on an instantaneous active and reactive current component (i_d - i_q) theory for generating reference currents for shunt active filter (SHAF). Three-phase reference current waveforms generated by proposed scheme are tracked by the three-phase voltage source converter in a hysteresis band control scheme. The performance of the proposed control strategy has been evaluated in terms of harmonic mitigation and DC link voltage regulation under various source conditions.

In order to maintain DC link voltage constant and to generate the compensating reference currents, we have developed type-1 fuzzy logic controller (T1FLC) and type-2 FLC (T2FLC) triangular M.F. The SHAF with proposed type-1 and type-2 FLCs using triangular M.F is able to eliminate the uncertainty in the system. By using T2FLC triangular M.F, SHAF gains outstanding compensation abilities. The detailed simulation results using MATLAB/SIMULINK software are presented to support the feasibility of proposed control strategy. To validate the proposed approach, the system is also implemented on OPAL-RT (real-time) simulator, and adequate results are reported for its verifications. Copyright © 2012 John Wiley & Sons, Ltd.

KEY WORDS: shunt active filter; harmonic mitigation; type-1 fuzzy logic controller; type-2 fuzzy logic controller; triangular M.F; current control strategy; OPAL-RT simulator hardware

1. INTRODUCTION

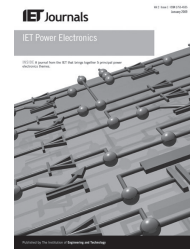
The concept of fuzzy systems [1] was introduced by Lotfi Zadeh in 1965 to process data and information affected by unprobabilistic uncertainty/imprecision. Soon after, it was proven to be an excellent choice for many applications since it mimics human control logic. These were designed to represent mathematically the vagueness and uncertainty of linguistic problems, thereby obtaining formal tools to work with intrinsic imprecision in different type of problems. It is considered as a generalization of the classic set theory. Intelligent systems based on fuzzy logic are fundamental tools for nonlinear complex system modelling.

With the development of type-2 fuzzy logic systems [2] and their ability to handle uncertainty, utilizing type-2 fuzzy logic controller (T2FLC) has attracted a lot of significance in recent years. It is an extension of the concept of well-known ordinary fuzzy sets, type-1 fuzzy sets. A type-2 fuzzy set is characterized by a fuzzy membership function, i.e. the membership grade for each element is also a fuzzy set in $[0, 1]$, unlike a type-1 fuzzy set [3], where the membership grade is a crisp number in $[0, 1]$. The membership functions of type-2 fuzzy sets are three dimensional and include a footprint of uncertainty (FOU), which is the new third dimension of type-2 fuzzy sets. The FOU provides an additional degree of freedom to handle uncertainties.

Power quality [4] problems have received a great attention nowadays because of their economical impacts on both utilities and consumers. The current harmonics is the most common problem of power quality, while voltage sags are the most severe. The advantages of FLC over conventional (PI)

^{*}Correspondence to: Suresh Mikkili, Department of Electrical Engineering, National Institute of Technology, Rourkela, India.

[†]E-mail: msuresh.ee@gmail.com



Simulation and real-time implementation of shunt active filter i_d-i_q control strategy for mitigation of harmonics with different fuzzy membership functions

S. Mikkili A.K. Panda

Department of Electrical Engineering, National Institute of Technology, Rourkela 769008, Orissa, India
 E-mail: msuresh.ee@gmail.com

Abstract: In this research study, the shunt active filter (SHAF) is used to improve the power quality of the electrical network by mitigating the harmonics with the help of different fuzzy membership functions (M.Fs) (trapezoidal, triangular and Gaussian). It is quite difficult to optimise the performance of power system networks using conventional methods, because of the complex nature of the systems that are highly non-linear and non-stationary. Three-phase reference current waveforms generated by the proposed scheme are tracked by the three-phase voltage source converter in a hysteresis band control scheme. The performance of the proposed control strategy has been evaluated in terms of harmonic mitigation and dc-link voltage regulation under various source conditions. The proposed SHAF with different fuzzy M.Fs is able to eliminate the uncertainty in the system and SHAF gains outstanding compensation abilities. The detailed simulation results using Matlab/Simulink software are presented to support the feasibility of the proposed control strategy. To validate the proposed approach, the system is also implemented on a real-time digital simulator hardware and adequate results are reported for its verification.

1 Introduction

The shunt active filter (SHAF) is an inverter driven to generate compensating currents that attenuate the harmonic components generated by the non-linear loads [1]. Therefore only the fundamental current component would be delivered by the mains supply. The performances of active filters depend on the inverter parameters, control method and the method for current reference determination. Owing to the proliferation of non-linear loads, such as power electronic converters in typical power distribution systems, the power quality [2] has become an important and growing problem. In particular, the voltage harmonics and power distribution equipment problems are the result of current harmonics produced by non-linear loads.

When the non-linear current passes through amenities of the electrical system and distribution transmission lines, additional voltage distortions will be produced because of the impedance associated with the electrical network. Thus, voltage and current waveform distortions will be developed when electrical power is generated, distributed and utilised. It is noted that non-sinusoidal current [3] results in many problems for the utility power supply company, such as: low-power factor, low-energy efficiency, electromagnetic interference, distortion of line voltage and so on.

It is well-known that when a neutral wire is overheated then excessive harmonic current will pass through the neutral line, which is three times that of the zero sequence current. Thus, a perfect compensator is necessary to avoid the negative consequences of harmonics. Although several control

strategies ($p-q$ and i_d-i_q) [4–6] have been developed, they still have contradictions with the performance of filters. When the supply voltages are balanced and sinusoidal, the two control strategies converge to the same compensation characteristics. However, when the supply voltages are distorted and/or unbalanced sinusoidal, these control strategies result in different degrees of compensation in harmonics. The $p-q$ control strategy is unable to yield an adequate solution when the source voltages are not ideal [7].

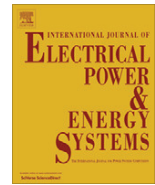
Recently, fuzzy logic controllers (FLC) [8] have received a great deal of attention for their application in active power filters (APFs). The advantages of FLC over conventional controllers are that they do not require an accurate mathematical model, can work with imprecise inputs, can handle non-linearity and are more robust than the conventional controllers. The Mamdani type of FLC is used for the control of an APF and it gives better results, but it has the drawback of a larger number of fuzzy rules.

The present paper mainly focused on the FLC with different membership functions (M.Fs) to analyse the performance of instantaneous real active and reactive current (i_d-i_q) control strategy [9] for extracting reference currents of SHAF under different source voltage conditions. PWM pattern generation based on carrier less hysteresis current control is used for quick response. In addition, the i_d-i_q method is used for obtaining reference currents in the system, because in this strategy, angle ' θ ' is calculated directly from the main voltages and enables operation to be frequency independent; thereby, this technique avoids a large number of synchronisation problems. It is also



Contents lists available at SciVerse ScienceDirect

Electrical Power and Energy Systems

journal homepage: www.elsevier.com/locate/ijepes

Real-time implementation of PI and fuzzy logic controllers based shunt active filter control strategies for power quality improvement

Suresh Mikkili*, A.K. Panda

Department of Electrical Engineering, National Institute of Technology, Rourkela, India

ARTICLE INFO

Article history:

Received 10 September 2011
 Received in revised form 8 June 2012
 Accepted 9 June 2012

Keywords:

Harmonic compensation
 SHAF (shunt active filter)
 p - q control strategy
 i_d - i_q control strategy
 PI controller
 Fuzzy logic controller

ABSTRACT

Instantaneous active and reactive power (p - q) and current (i_d - i_q) control strategies for extracting the three-phase reference currents for shunt active power filters are compared, evaluating their performance under different source voltage conditions with PI and fuzzy logic controllers in MATLAB/Simulink environment and also implemented using Real-Time Digital Simulator Hardware (RTDS Hardware). When the supply voltages are balanced and sinusoidal, then all control strategies with both controllers converge to the same compensation characteristics. However, when the supply voltages are distorted and/or unbalanced sinusoidal, these control strategies result in different degrees of compensation in harmonics. The p - q control strategy unable to yield an adequate solution when source voltages are not ideal. Extensive simulations are carried out with PI as well as fuzzy logic controller for both p - q and i_d - i_q control strategies by considering different voltage conditions and adequate results were presented. On owing i_d - i_q method with fuzzy logic controller gives away an out-standing performance under balanced, un-balanced and non-sinusoidal supply conditions. The detailed simulation and RTDS Hardware results are included.

© 2012 Elsevier Ltd. All rights reserved.

1. Introduction

Electrical power quality [1] has been, in recent years, an important and growing problem because of the proliferation of nonlinear loads such as power electronic converters in typical power distribution systems. Particularly, voltage harmonics and power distribution equipment problems result from current harmonics produced by nonlinear loads. Harmonics surfaced as a buzz word from 1980s which always threaten the normal operation of power system and user equipment. Highly automatic electric equipments, in particular, cause enormous economic loss every year. Owing both power suppliers and power consumers are concerned about the power quality problems and compensation techniques. Sinusoidal voltage is a conceptual quantity produced by an ideal AC generator built with finely distributed stator and field windings that operate in a uniform magnetic field. Since neither the winding distribution nor the magnetic field are uniform in a working AC machine, voltage waveform distortions are created, and the voltage-time relationship deviates from the pure sine function. The distortion at the point of generation is very small (about 1–2%), but nonetheless it exists. Since this is a deviation from a pure sine

wave, the deviation is in the form of an episodic function, and by definition, the voltage distortion contains harmonics [2].

It is noted that non-sinusoidal current results in many problems for the utility power supply company, such as: low power factor, low energy efficiency, electromagnetic interference (EMI), distortion of line voltage, etc. It is renowned that when neutral wire is overheated then excessive harmonic current will pass through the neutral line, which is three times that of zero sequence current. Thus a perfect compensator is necessary to avoid the consequences due to harmonics. Though several control techniques and strategies [3] have been developed but still performance of filter in contradictions; these became primarily motivation for the current paper.

Instantaneous active and reactive theory (p - q theory) was introduced by Akagi, Kawakawa, and Nabae in 1984 [4]. Since then, many scientists [5–8] and engineers made significant contributions to its modifications in three-phase four-wire circuits and its applications to power electronic equipment. The p - q theory [6] based on a set of instantaneous powers defined in the time domain. No restrictions are imposed on the voltage and current waveforms, and it can be applied to three phase systems with or without neutral wire for three phase generic voltage and current waveforms. Thus it is valid not only in the steady state but also in the transient state. p - q theory needs additional PLL circuit for synchronization so p - q method is frequency variant.

In i_d - i_q method [7] angle ' θ ' is calculated directly from main voltages and thus enables the method to be frequency

* Corresponding author.

E-mail addresses: msuresh.ee@gmail.com (S. Mikkili), akpanda.ee@gmail.com (A.K. Panda).

International Journal of Emerging Electric Power Systems

Volume 13, Issue 5

2012

Article 2

Fuzzy logic controller based Shunt Active
Filter control strategies for Power quality
improvement Using Different Fuzzy M.F.s

Anup Kumar Panda, *National Institute of Technology -
Rourkela, India*

Suresh Mikkili, *National Institute of Technology - Rourkela,
India*

Recommended Citation:

Panda, Anup Kumar and Mikkili, Suresh (2012) "Fuzzy logic controller based Shunt Active Filter control strategies for Power quality improvement Using Different Fuzzy M.F.s," *International Journal of Emerging Electric Power Systems*: Vol. 13: Iss. 5, Article 2.
DOI: 10.1515/1553-779X.2942

©2012 De Gruyter. All rights reserved.

Suresh MIKKILI, A. K. PANDA

RTDS hardware implementation and simulation of SHAF for mitigation of harmonics using p-q control strategy with PI and fuzzy logic controllers

© Higher Education Press and Springer-Verlag Berlin Heidelberg 2012

Abstract The main objective of this paper is to develop PI and fuzzy controllers to analyze the performance of instantaneous real active and reactive power (p-q) control strategy for extracting reference currents of shunt active filters (SHAFs) under balanced, unbalanced, and balanced non-sinusoidal conditions. When the supply voltages are balanced and sinusoidal, both controllers converge to the same compensation characteristics. However, if the supply voltages are distorted and/or unbalanced sinusoidal, these controllers result in different degrees of compensation in harmonics. The p-q control strategy with PI controller is unable to yield an adequate solution when source voltages are not ideal. Extensive simulations were carried out with balance, unbalanced, and non-sinusoidal conditions. Simulation results validate the superiority of fuzzy logic controller over PI controller. The three-phase four-wire SHAF system is also implemented on a real-time digital simulator (RTDS hardware) to further verify its effectiveness. The detailed simulation and RTDS hardware results are included.

Keywords harmonic compensation, shunt active filter (SHAF), p-q control strategy, PI controller, fuzzy logic controller, real-time digital simulator (RTDS hardware)

1 Introduction

Sinusoidal voltage is a conceptual quantity produced by an ideal alternating current (AC) generator built with finely distributed stator and field windings that operate in a

uniform magnetic field. Since neither the winding distribution nor the magnetic field are uniform in a working AC machine, voltage waveform distortions are created, and the voltage-time relationship deviates from the pure sine function. The distortion at the point of generation is very small (about 1% to 2%), but nonetheless it exists. Since this is a deviation from a pure sine wave, the deviation is in the form of an episodic function, and by definition, the voltage distortion contains harmonics [1].

When a pure sinusoidal voltage is applied to a certain type of load, the current drawn by the load is proportional to the voltage and impedance and follows the envelope of the voltage waveform. These loads are referred to as linear loads (loads where the voltage and current follow one another without any distortion to their pure sine waves) [2]. Examples of linear loads are resistive heaters, incandescent lamps, and constant speed induction and synchronous motors. In contrast, some loads cause the current to vary disproportionately with the voltage during each half cycle. These loads are defined as nonlinear loads, and the current and voltage have waveforms that are no sinusoidal containing distortions, whereby the 50-Hz waveform has numerous additional waveforms superimposed upon it, creating multiple frequencies within the normal 50-Hz sine wave. The multiple frequencies are harmonics of the fundamental frequency. Examples of nonlinear loads are battery chargers, electronic ballasts, variable frequency drives, and switching mode power supplies.

As nonlinear currents flow through a facilities electrical system and the distribution-transmission lines, additional voltage distortions are produced due to the impedance associated with the electrical network. Thus, as electrical power is generated, distributed, and utilized, voltage and current waveform distortions are produced. It is noted that non-sinusoidal current results in many problems for the utility power supply company, such as low power factor, low energy efficiency, electromagnetic interference (EMI), distortion of line voltage, etc. Eminent issues always arise

Received March 21, 2011; accepted March 13, 2012

Suresh MIKKILI (✉), A. K. PANDA

Department of Electrical Engineering, National Institute of Technology,
Rourkela, Orissa 769008, India
E-mail: msuresh.ee@gmail.com

Real-Time Implementation of Shunt Active Filter P-Q Control Strategy for Mitigation of Harmonics with Different Fuzzy M.F.s

Suresh Mikkili[†] and Anup Kumar Panda^{*}

^{†*}Dept. of Electrical Engineering, National Institute of Technology - Rourkela, Orissa, India

Abstract

This research article presents a novel approach based on an instantaneous active and reactive power component (p-q) theory for generating reference currents for shunt active filter (SHAF). Three-phase reference current waveforms generated by proposed scheme are tracked by the three-phase voltage source converter in a hysteresis band control scheme. The performance of the SHAF using the p-q control strategy has been evaluated under various source conditions. The performance of the proposed control strategy has been evaluated in terms of harmonic mitigation and DC link voltage regulation. In order to maintain DC link voltage constant and to generate the compensating reference currents, we have developed Fuzzy logic controller with different (Trapezoidal, Triangular and Gaussian) fuzzy M.F.s. The proposed SHAF with different fuzzy M.F.s is able to eliminate the uncertainty in the system and SHAF gains outstanding compensation abilities. The detailed simulation results using MATLAB/SIMULINK software are presented to support the feasibility of proposed control strategy. To validate the proposed approach, the system is also implemented on a real time digital simulator and adequate results are reported for its verifications.

Key words: Different fuzzy M.F.s (Trapezoidal, Triangular and Gaussian M.F's), Fuzzy logic Controller, Harmonic compensation, P-Q control strategy, Shunt active filter

I. INTRODUCTION

The shunt active filter (SHAF) is an inverter driven to generate compensating currents that attenuate the harmonic components generated by the nonlinear loads [1]. Therefore, only the fundamental current component would be delivered by the main supply. The performances of active filters depend on the inverter parameters, control method, and the method for current reference determination. Current reference can be obtained by using the band pass filters or the instantaneous power theory [2]. Band pass filters have the disadvantage in that they cause delay of the filtered signal. The instantaneous power theory, on the other hand, is based on complex voltage and current transforms and their inverse transforms. Furthermore, if the voltage source is distorted by harmonics the instantaneous power theory does not provide an accurate basis for active power filters; these become the primary

motivation for the current work.

The objective of this paper is to introduce an efficient controller (Fuzzy logic controller [3] with different membership functions (M.F's)) to obtain the dc link voltage constant and to mitigate the harmonics. The p-q method is used to obtain the current reference for the active power filter. The method for current reference determination is based on extracting the fundamental harmonic from a load current waveform without its phase shifting. In such way the current reference can be obtained simply by subtracting the fundamental harmonic from the measured load current.

The PI controller [4] requires precise linear mathematical models, which are difficult to obtain and may not give satisfactory performance under parameter variations, load disturbances, etc. Recently, fuzzy logic controllers have received a great deal of attention in regards to their application to APFs. The advantages of fuzzy controllers over conventional controllers are that they do not require an accurate mathematical model, can work with imprecise inputs, can handle non-linearity, and are more robust than conventional controllers. The Mamdani type of fuzzy controller, used for the control of an APF [5], gives better

Manuscript received Feb. 15, 2012; revised Jul. 18, 2012

Recommended for publication by Associate Editor Kyo-Beum Lee.

[†]Corresponding Author: msuresh.ee@gmail.com

Tel: +91 91 78 79 78 67, Fax: +91-661-2462999, N.I.T Rourkela

^{*}Dept. of Electrical Engineering, National Institute of Technology - Rourkela, India

International Journal of Emerging Electric Power Systems

Volume 12, Issue 5

2011

Article 5

RTDS Hardware Implementation and Simulation of 3-ph 4-wire SHAF for Mitigation of Current Harmonics with p-q and I_d-I_q Control Strategies using Fuzzy Logic Controller

Suresh Mikkili, *National Institute of Technology, Rourkela*
A.K. Panda, *National Institute of Technology, Rourkela*

Recommended Citation:

Mikkili, Suresh and Panda, A.K. (2011) "RTDS Hardware Implementation and Simulation of 3-ph 4-wire SHAF for Mitigation of Current Harmonics with p-q and I_d-I_q Control Strategies using Fuzzy Logic Controller," *International Journal of Emerging Electric Power Systems*: Vol. 12: Iss. 5, Article 5.

DOI: 10.2202/1553-779X.2758

Available at: <http://www.bepress.com/ijeeps/vol12/iss5/art5>

©2011 Berkeley Electronic Press. All rights reserved.

PI and Fuzzy Logic Controller Based 3-Phase 4-Wire Shunt Active Filters for the Mitigation of Current Harmonics with the I_d - I_q Control Strategy

Suresh Mikkili[†] and Anup Kumar Panda*

[†]* Dept. of Electrical Engineering, National Institute of Technology Rourkela, Rourkela, India

Abstract

Commencing with incandescent light bulbs, every load today creates harmonics. Unfortunately, these loads vary with respect to their amount of harmonic content and their response to problems caused by harmonics. The prevalent difficulties with harmonics are voltage and current waveform distortions. In addition, Electronic equipment like computers, battery chargers, electronic ballasts, variable frequency drives, and switching mode power supplies generate perilous amounts of harmonics. Issues related to harmonics are of a greater concern to engineers and building designers because they do more than just distort voltage waveforms, they can overheat the building wiring, cause nuisance tripping, overheat transformer units, and cause random end-user equipment failures. Thus power quality is becoming more and more serious with each passing day. As a result, active power filters (APFs) have gained a lot of attention due to their excellent harmonic compensation. However, the performance of the active filters seems to have contradictions with different control techniques. The main objective of this paper is to analyze shunt active filters with fuzzy and pi controllers. To carry out this analysis, active and reactive current methods (i_d - i_q) are considered. Extensive simulations were carried out. The simulations were performed under balance, unbalanced and non sinusoidal conditions. The results validate the dynamic behavior of fuzzy logic controllers over PI controllers.

Key Words: Fuzzy logic controller, Harmonic compensation, I_d - I_q control strategy, PI controller, Shunt Active power filter

I. INTRODUCTION

In recent years power quality [1] has become an important and growing problem due to the proliferation of nonlinear loads such as power electronic converters in typical power distribution systems. Particularly, voltage harmonics and power distribution equipment problems are the result of current harmonics [2] produced by nonlinear loads.

Eminent issues always arises in three-phase four-wire systems. It is well-known the that zero line may be overheated or causes a fire as a result of excessive harmonic current [3] going through the zero line three times or times that of three. Thus a perfect compensator is necessary to avoid the negative consequences of harmonics. Though several control techniques and strategies have been developed they still have contradictions with the performance of filters. These issues became the primary motivation for this paper.

In the i_d - i_q method from [4] the angle ' θ ' is calculated directly from the main voltages which enables the method to be frequency independent. As a result, a large number of syn-

chronization problems with un-balanced and non-sinusoidal voltages are avoided.

The PI controller in [5] requires precise linear mathematical models, which are difficult to obtain and may not give satisfactory performance under parameter variations, load disturbances, etc. Recently, fuzzy logic controllers have received a great deal of attention in regards to their application to APFs. The advantages of fuzzy controllers over conventional controllers are that they do not require an accurate mathematical model, can work with imprecise inputs, can handle non-linearity, and are more robust than conventional controllers. The Mamdani type of fuzzy controller from [6], used for the control of an APF, gives better results when compared with PI controllers, but it has the drawback of a larger number of fuzzy sets and 49 rules.

This paper focuses mainly on two controllers i.e., fuzzy and pi. In addition, a filter was developed with the instantaneous active and reactive current (i_d - i_q) method. This was then used to analyse the performance of the filter under different main voltages. This shows that the fuzzy controllers exhibit some superior performance over the PI controllers. To validate the current observations, extensive simulations were carried out and adequate results were obtained.

Manuscript received Nov. 15, 2010; revised Sep. 8, 2011

Recommended for publication by Associate Editor Kyo-Beum Lee.

[†] Corresponding Author: msuresh.ee@gmail.com

Tel: +91-78797867, Fax: +91-661-2462999, N.I.T Rourkela

* Dept. of Electrical Engineering, National Institute of Technology Rourkela, India